Orally Disintegrating Tablets: Formulation Development, Novel Engineering Solutions and Fixed Dose Combinations

Thomas James Dennison

Doctor of Philosophy

Aston University

November 2016

Aston University

Orally Disintegrating Tablets: Formulation Development, Novel Engineering Solutions and Fixed Dose Combinations

Thomas James Dennison

Doctor of Philosophy

2016

Thesis Summary

Orally disintegrating tablets (ODTs) are an attractive solid dosage form for patients who suffer from dysphagia, a difficulty in swallowing, which is particularly prevalent in paediatric and geriatric populations. ODTs and fixed dose combination (FDC) formulations are popular as they improve patient compliance and combination of the two has not previously been explored.

The requirement for ODTs to disintegrate rapidly whilst also being mechanically robust means that high drug loading is a significant challenge. An ODT formulation for the beta-lactam antibiotic flucloxacillin was developed at doses of 250 and 125 mg. ODTs were mechanically robust, however this limited disintegration to within 3 mins, with mannitol fragmentation being a major limitation.

Polymeric film coating was devised as a potential technique to enhance ODT mechanical properties. Due to high attrition during fluidisation a novel stationary coating technique was developed as a proof of concept. ODTs coated in this way, coupled with a post-coating curing step, demonstrated an increase in hardness of almost double and essentially zero friability. This novel coating technique could prove hugely beneficial in the formulation of high dose or poorly compactable drugs.

The application of ODTs for FDCs was tested with four model drugs: amlodipine (5 mg), atorvastatin (10 mg), isoniazid (50 mg) and rifampicin (75 mg). ODT formulations for single and FDCs showed rapid disintegration and good mechanical properties. Comparison of single and FDC dissolution profiles was performed using FDA recommended f_1 and f_2 testing. Bioavailability from ODTs was assessed using *in vitro* Caco-2 permeability and dissolution data and *in silico* physiologically based pharmacokinetic modelling. Bioequivalence was demonstrated between single and FDC for each drug in both fed and fasted states, whilst atorvastatin showed a positive food effect (enhanced peak plasma concentration and area under the curve), due to reduced metabolism by CYP3A4.

2

Acknowledgements

I would like to begin by thanking my supervisor Prof Afzal Mohammed for providing me with the opportunity to undertake this PhD and for his continued support, advice and expertise. His confidence and trust in me has undoubtedly allowed me to develop as a researcher and has grown the assurance that I hold in my own ability. Above all, his optimism and passion for this field of study has helped me on many occasions and for this I am extremely grateful. I would also like to thank my second supervisor Dr Raj Badhan for his contribution and knowledge and for being available whenever I needed help. I am very appreciative to the financial support supplied to me by the Medical Research Council and Viridian Pharma, without which this PhD would not have been possible.

I would also like to thank the technical team at Aston University, particularly Jiteen Ahmed and Christine Jakeman for their unwavering assistance and knowhow. I am also very grateful to Dr Michael Hofmann from the University of Birmingham for his contribution in micro-CT imaging. I would also like to extend my sincerest thanks to my colleagues within our research group: Jas Koner, Dr Affiong Iyire, Dr Eman Dahmash, Hamad Alyami, Ansarr Warraich and Habtom Ftuwi and to other members of the lab team, past and present. Getting to know you all over the past 4 years has been a pleasure.

Special thanks goes to my family. To my parents, you have been an incredible support over the past 4 years and long before. I would not have achieved this without the faith you have placed in me and I am eternally grateful for everything you have done for me; I couldn't have asked for anything more or anyone better as parents. To Charlie and Arch, thank you for always being there and for your patience, especially towards the end of this work. I am incredibly lucky and the past four years would have been unthinkable without you. To Lauren and Katy, Scott, Evie and George, thanks for your support and for always making me smile.

List of Contents

List of Abbreviations

API	Active pharmaceutical ingredient
AUC	Area under the curve
BP	British Pharmacopeia
C	Crospovidone
CLSM	Confocal laser scanning microscopy
C_{max}	Peak serum concentration
CS	Croscarmellose sodium
DOE	Design of experiments
EMA	European Medicines Agency
F	Bioavailability
f_1	Difference factor
f_2	Similarity factor
fa	Fraction dose absorbed
FaSSIF	Fasted-state simulated intestinal fluid
FDA	Food and Drug Administration
FDC	Fixed dose combination
FeSSIF	Fed-state simulated intestinal fluid
HPLC	High performance liquid chromatography
ICH	International Conference on Harmonisation
MCC	Microcrystalline cellulose
ODT	Orally disintegrating tablet
PEG	Polyethylene glycol
PVA	Polyvinyl acetate
Py	Apparent mean yield pressure
S	Starch
SSG	Sodium starch glycolate
t_{max}	Time to reach C_{max}
USP	United States Pharmacopeia
VMD	Volume median diameter
WHO	World Health Organization
XμCT	Microcomputed tomography

List of Tables

14

List of Figures

Publications List

Peer reviewed articles:

- Dennison TJ, Smith J, Hofmann MP, Bland CE, Badhan RK, Al-Khattawi A, Mohammed AR. (2016) Design of Experiments to Study the Impact of Process Parameters on Droplet Size and Development of Non-Invasive Imaging Techniques in Tablet Coating. PLoS ONE 11(8): e0157267

- Dennison TJ, Smith J, Badhan RK, Mohammed AR. (2016) Fixed Dose Combination Orally Disintegrating Tablets to Treat Cardiovascular Disease: Physiologically Based Pharmacokinetic Modelling to Assess Bioavailability. Drug Design, Development and Therapy. Submitted

- Ali Al-Khattawi, Affiong Iyire, Tom Dennison, Eman Dahmash, Clifford J Bailey, Julian Smith, Peter Rue, Afzal R Mohammed (2014) Systematic Screening of Compressed ODT Excipients: Cellulosic Versus Non - Cellulosic. Current Drug Delivery 11(4):486-500

Book Chapters:

- Tom Dennison, Ali AlKhattawi, David Terry and Afzal R Mohammed (2017) Developing medicines for children, with emphasis on the implications of the regulations and development process for the prescriber – Neonatal and Paediatric prescribing

- Tom Dennison, Ali AlKhattawi, David Terry and Afzal R Mohammed (2017) Extemporaneous Preparation of Medicines for Children - Neonatal and Paediatric prescribing

Oral Presentations:

- Non-Invasive Imaging Techniques to Assess Tablet Film Coat Quality after Optimisation of Droplet Size using Design of Experiments. *UK PharmSci, Glasgow, 2016*

Conference Proceedings:

- Dennison T, Smith J, Badhan RK, Mohammed AR. Investigating Disintegrants in a Simple Formulation for and Orally Disintegrating Tablet. *UKICRS Cork, April 2014.*

- Dennison T, Smith J, Badhan RK, Mohammed AR. A Quality by Design Approach Utilising Design of Experiments for Optimisation of Droplet Size for Tablet Film Coating. *From Drug Discovery to Drug delivery, Athens, November 2014.*

- Dennison T, Smith J, Hofmann M, Badhan RK, Mohammed AR. Design of Experiments for Optimisation of Droplet Size and its Effect on Film Coat Quality Studied Using Non-Invasive Imaging Techniques. *CRS, Seattle, July 2016.*

Chapter 1

Introduction

1.1   Paediatric Medicines

Over the past two decades there has been an effort to increase the number of prescription drugs designed for use in the paediatric population due to poor availability. There are many reasons for the lack of medicines that are labelled for paediatric use, which arise as a result of a significant paediatric knowledge gap. These include a lack of understanding of acceptable dosage form and size, volume of administration, taste and importantly safe dosage levels of both the active drug and all excipients included in a formulation. The lack of suitable medicines for the paediatric population means that unlicensed formulations are often prepared and administered by healthcare professionals. Improving understanding of the effect of medicines on children is of vital importance, however it is complicated by the requirement to protect the wellbeing of children in clinical trials and fears over ethical issues and causing harm [1].

The lack of paediatric approved medications has in the past resulted in missed opportunities for paediatrics to receive potentially useful or even lifesaving drugs. Conversely, the use of medicines in paediatrics, that only have evidence from adult studies, has, on occasion, had drastic consequences. Guidelines, first laid out by the FDA (Federal Drug Administration) and then the EMA (European Medicines Agency), have so far been successful in closing this knowledge gap and providing new, safe and suitable formulations for paediatrics. These guidelines describe both regulations and incentives in order to achieve this goal [2].

1.1.1   Legislation, Regulations and Incentives

The FDA has introduced numerous rules and regulations to promote the reporting of safety information and incentivise the conductance of studies for new paediatric therapeutics by offering extensions of market exclusivity. These include the 1994 Pediatric Labelling Rule, the 1997 Food and Drug Administration Modernization Act (FDAMA) and the1998 Pediatric Rule [3, 4]. The Best Pharmaceuticals for Children Act (BPCA) in 2002 extended the incentives program for 5 years, encouraging off-patent paediatric drug studies and requiring public transparency of study results [5]. The Pediatric Research Equity Act (PREA) of 2003 enforced mandatory studies for drugs and biologics, whilst the FDA Safety and Innovation Act (FDASIA) in 2012, extended previous

regulations to October 2017 and also required manufacturers to submit a Pediatric Study Plan (PSP) at an early stage of drug development [6].

Similarly, the European Medicines Agency (EMA) introduced the 2007 Paediatric Regulation to improve research into medicines for children, avoid needless risk to children and make authorised medications more accessible. It requires manufacturers to submit a drug development plan, known as a Paediatric Investigation Plan (PIP) in order for approval and offered a 6-month patent extension for new drugs upon PIP approval. Incentives for paediatric specific, older, off-patent drugs are also addressed. Other efforts include the European Paediatric Formulation Initiative's development of an online Safety and Toxicity of Excipients for Paediatrics (STEP) database, which includes input from research and industry [2, 7, 8].

1.1.2   Excipient Considerations

It is not just the active pharmaceutical ingredient (API) that is of concern in paediatric formulations. In order for a formulation to be successful a wide range of functional excipients are included, the choice of which will be determined by the dosage form and delivery method. Despite the traditional view that excipients are inert, no substance is completely free from toxicity. As excipients generally represent a substantial share of a formulation's composition, caution must be taken to select excipients that offer as little harm to the patient as possible. Due to differences in physiology, excipients which are safe in the adult population may offer a significant risk to paediatrics, due to pharmacokinetic differences altering their administration, distribution, metabolism and elimination when compared to adults. Safety concerns for paediatrics regarding commonly used excipients exist and include examples such as propylene glycol, benzyl alcohol and a selection of additive "E numbers", to name a few. With benzyl alcohol for instance, a commonly used preservative, its metabolism to hippuric acid which can be readily excreted, is reduced in neonates resulting in high toxicity [9, 10].

Published guidelines concerning the use of excipients in paediatric formulations [11] state that the selection of excipients for paediatric formulations should be done with special care and with consideration of different sensitivities between different age groups. The inclusion of any excipient in a formulation should be justified by its function

and should be included at the lowest possible concentration for the desired effect. Inclusion should also be reinforced using as much information from toxicological data, scientific guidelines, food legislation and literature as possible. Information about compatibility of excipients with the active and with other excipients should be disclosed. It is also agreed that any new excipient be examined in preclinical and clinical trials to ensure safety. No organisation, however, recommends the conductance of ADME studies over the entire paediatric age group, despite paediatrics being a target population [9, 12].

1.1.3   Considerations for Paediatrics

There are a number of reasons why formulations for adults are often not suitable for children. Infants experience rapid growth and development with different rates of growth of organs and maturation of active transport systems, metabolic pathways, and body systems. These differences mean that infants cannot be viewed as young adults as they often exhibit different responses to both active pharmaceutical ingredients (APIs) and excipients [13]. These include differences in pharmacokinetics, pharmacodynamics and adverse effects to different formulations. For example, pharmacokinetic differences between adults and paediatrics include gastric emptying rate and pH, gastrointestinal permeability and surface area for absorption [14]. Paediatric dose size changes from infancy to childhood, with doses calculated by body weight or surface area at older ages. As a result, paediatric formulations must be flexible enough and accurate enough to allow for this large dose range. A child's mental development will also determine their ability to tolerate different dosage forms, with many young children being unable to swallow conventional tablets or capsules. Indeed, the dosage must be in a form that can be accepted by a child or administered to that child by a caregiver [12, 15]. Palatability of oral medication is also crucial for paediatric compliance, since taste acceptance differs between adults and paediatrics and children will be less willing to tolerate a medicament they find to have an unacceptable taste [16].

1.1.4 Paediatric Relevant Dosage Forms

The oral route is the most favoured for long term dosing, with liquid formulations being the most popular and prevalent in the market due to dose flexibility and difficulties in swallowing tablets and capsules. Taste-masking oral formulations requires careful selection of excipients and can drive up costs, lead to long term instability and may not even be completely achievable (especially for bitter drugs). Although technologies such as encapsulation or complexation can be employed in taste masking they can be difficult to achieve and costly [17]. Selection of a suitable vehicle, most often water, can also present significant formulation challenges. Limitations of dose and volume due to drug solubility are also common issues, as is chemical, physical and microbial stability, which must be controlled for by the addition of antioxidants, buffers, suspending agents and preservatives [14]

Due to these limitations, a range of solid oral dosage forms suitable for children are available. Multiparticulates such as granules and pellets, for example, can be administered directly into the mouth or mixed with certain food or drink. These offer advantages such as ease of swallowing, dose flexibility and the possibility of drug combination, however incomplete ingestion (and therefore reduced dose), packaging and stability issues add complications [15]. Mini tablets are another popular innovation. These are 3 mm or smaller in diameter and can be produced using conventional tablet presses, limiting cost. Studies in young children indicate that they offer no risk of choking or aspiration and are fairly well accepted, although the ability to swallow increases with age. They also allow for flexible dosing and can be adapted to dispenser devices for ease of use and accuracy [18].

Orally disintegrating tablets (ODTs) are another suitable dosage form for paediatrics, which overcome dysphagia by disintegrating in the mouth upon contact with saliva. They can be produced by a variety of conventional and more specialised techniques. Production by direct compression offers the greatest ease and cost-effectiveness, however tablet performance is highly dependent on the API properties and taste masking for bitter drugs can be a complex necessity [19].

Chewable tablets and gums have also been developed for paediatrics. They do not require water, offer stability and ease of transport and are palatable. That said taste masking can prove difficult to achieve. Oral wafers are also suitable dosage forms for

children. These are small thin strips that adhere to the mucosa and dissolve, negating swallowing and avoiding the problem of spitting out. They benefit from containing small amounts of excipients, however have a limit for drug incorporation of around 50 mg and are also highly dependent on taste masking [20].

1.2   Orally Disintegrating Tablets

In recent years there has been increasing interest in orally disintegrating tablets (ODTs) as a preferable alternative to conventional solid oral dosage forms. ODTs rapidly disintegrate upon contact with saliva and the API disperses or dissolves. This rapid disintegration is of benefit to patients who experience dysphagia, a difficulty in swallowing that is particularly common amongst the elderly, paediatrics and patients suffering from a variety of disorders such as stroke or neurological problems. Difficulty in swallowing may also result from nausea, a lack of access to water, or from restricted-fluid-intake diets [19, 21, 22]. It has been estimated as much as 50% of the population suffer from dysphagia [23] resulting in serious problems with drug compliance and ineffective therapy.

ODTs may offer enhanced absorption and pharmacokinetic profiles and a faster onset of therapeutic effect [24]. Rapid dissolution in the mouth allows for absorption of some APIs from the oral cavity, pharynx and oesophagus and thus avoids, to some extent, gastric absorption. Pre-gastric absorption has the benefit of improved bioavailability and rapid systemic absorption (and thus high plasma levels) due to the avoidance of first-pass metabolism in the liver [25]. This has important implications for drugs that undergo significant hepatic metabolism, for instance and drugs that are inactivated by hepatic metabolism. Additionally, pre-gastric absorption of drugs that generate toxic metabolites, through hepatic and gastric metabolism, will be of benefit to the patient [26]. Conversely, prodrugs that require hepatic metabolic activation to their active form may not be suitable candidates for this technology.

Pharmaceutical companies see ODT technologies as attractive as they provide the opportunity for product differentiation and new dosage forms for drugs with which patent protection is expiring, in order to extend market exclusivity [27]. This increases revenue for the company, which is enhanced by the opportunity to sell to underserved patient populations. Consumers also benefit from a more convenient dosage form or dosing regimen [28]. Indeed, the interest in ODTs can be further understood by market studies showing that, once experienced, 70% of consumers would ask for ODTs from their doctor and purchase ODTs and 80% would prefer ODTs over regular tablets or liquid forms [29]. In addition to the ease of use, the pleasant mouthfeel of ODTs makes them favourable to patients [30].

There are a number of properties that a successful ODT must possess. Firstly, they must not require water for administration and must be able to disintegrate within a matter of seconds in contact with saliva. They must be able to tolerate the manufacturing process and handling without fracturing or fragmenting. They should be cost effective and allow for high drug loading if possible, although this is highly dependent on API properties. Preferably they should be unaffected by environmental conditions like temperature and humidity, so that conventional low-cost packaging can be used. Perhaps most importantly, they must have an agreeable taste that masks any unpleasant taste of the API or excipients, otherwise patient compliance will be detrimentally affected. Finally, the tablet must possess a pleasant mouth feel, with the tablet forming small particles after disintegration to avoid a gritty sensation [31-33].

1.3   Technologies Involved in ODT Manufacture

The interest in ODTs is exemplified by the 80 new patents that were filed for ODT technologies between the years of 1999-2010. A variety of techniques have been employed in the manufacture of ODTs, the main three being compression-based, moulding and freeze-drying, with compression technologies being by far the most favoured for drug production [19]. ODT properties will depend on the technology used for their production. The extent of drug loading is also dependent on the technology and as such APIs that require a high dose will be unsuitable for certain technologies [31]. The basic principles of each technology, including the benefits and challenges associated with each and the different classes of excipients involved, is discussed below, with an emphasis on direct compression.

1.3.1   Moulding

1.3.1.1 Compression Moulding

The moulding process involves moistening of a powder blend with a solvent before moulding the mixture into a tablet at low pressure. The moulded tablet then undergoes air drying to remove the solvent and thus volatile solvents, such as ethanol, are commonly used, although water is an option. Due to the low pressures (relative to that of conventional compression) used, the tablets formed are very porous which aids in disintegration. Powder sieving prior to moulding to reduce particle size can also be employed to enhance disintegration [34].

1.3.1.2 Heat Moulding

In addition to conventional moulding, heat moulding has been employed in the production of ODTs. This involves dissolving or dispersing the drug in a molten matrix followed by moulding. Using this technique a solution or suspension of drug, agar (as a binder) and sugar is poured into blister packaging and then solidified at room temperature before drying at 30°C under vacuum [35, 36].

1.3.1.3 No-Vacuum Lyophilisation

No-vacuum lyophilisation involves moulding a paste or slurry and then freezing to form a solid matrix. The solvent is then evaporated at a standard pressure resulting in a tablet with a partially collapsed matrix. This differs from standard lyophilisation in that evaporation occurs through the liquid phase to a gas, whereas with regular lyophilisation the solvent evaporates by sublimation. This method of drying improves the mechanical strength of the tablet by densifying the matrix [34, 37]. Depending on the solubility of the drug in the matrix, it may exist as either discrete particles or microparticles and may be fully or partially dissolved in the matrix [38].

1.3.1.4 Advantages and Challenges of Moulding

The dispersion matrix is generally comprised of water soluble sugars and this offers an advantage for moulded tablets as they facilitate a desirable rapid dissolution and pleasant taste. Compared to lyophilisation, moulding is easier and more adaptable to production on an industrial scale. Additionally, as mentioned, moulding produces highly porous tablets which aids in disintegration [35].

The high porosity of moulded tablets, however, compromises mechanical strength, with erosion and breakage through handling and opening of blister packets commonplace, with the confounding problem that hardening excipients, such as sucrose or polyvinyl pyrrolidone, will adversely affect disintegration rate. Tablets with sufficient mechanical strength and disintegration rates can be produced through the use of novel equipment and multi-step processes, however these are more complex and expensive [36, 37].

1.3.2   Freeze Drying/Lyophilisation

This process involves freezing the product and then subsequent removal of water by sublimation using a low pressure vacuum. The preparation is first poured into pre-formed blisters to form the tablet shape. Next, the blisters undergo controlled cryogenic freezing to control the size of the ice crystals that are formed and thus control pore size. The blisters are then sublimated using large scale freeze dryers to remove moisture. Finally,

the blisters are sealed using a heat-seal process for stability and protection [37]. This process forms the basis of a number of patented technologies such as Zydis, Quicksolv and Lyoc [31]. The tablets formed through this method are generally very light and highly porous and as a result disintegrate rapidly upon contact with the tongue, releasing the active drug. The process imparts a glossy amorphous structure to the diluent and sometimes to the API [33, 39].

Rapid disintegration of these highly porous and amorphous ODTs may also enhance absorption and hence bioavailability of the drug. Fast disintegration also imparts a pleasant mouth feel. Since this technology uses non-elevated temperatures it has the benefit of allowing for incorporation of thermo-labile drugs. The usefulness of freeze drying is limited however due to the high cost of machinery and processing and also the time involved in processing and handling. In addition, the tablets are fragile in standard blister packs and therefore more robust packaging is often required [32, 33, 37, 40, 41].

1.3.3   Mass Extrusion

This involves softening of an API excipient blend using a solvent mixture of water soluble polyethylene glycol and methanol, followed by extrusion, through an extruder or syringe, to form a cylindrical soft mass. The soft mass can then be divided into smaller segments using a heated blade [42]. This method can be used to form coated granules of bitter tasting drugs by crushing of the extrudate. These granules can then be compacted into ODTs through direct compression. This technology benefits by ease of preparation and a relatively low cost when compared to other methods [43].

1.3.4   Cotton Candy Process

This technology involves formation of a floss-like matrix of saccharides and polysaccharides. This is achieved by flash melting and spinning using a novel spinning technique. The sugar mixture is subjected to a temperature gradient of 180-250°C and spun at 3000-4000 rpm and then cooled rapidly upon leaving the system through an opening in the perimeter. The cotton-candy-like fibre produced is then milled and combined with the API and other excipients and compressed using conventional

equipment. The initial floss produced is in an amorphous state and in order to improve flowability it may be left to recrystallize. Recrystallization also improves mechanical strength and allows for higher drug loading [34, 44].

The cotton candy process is useful as it can accommodate high drug loading and infers good mechanical strength on the resultant tablet. It is limited however, in that due to the high temperatures employed this technology is not suitable for thermo-labile compounds. Additionally, multiple steps are involved using specialist equipment, which increases cost [44].

1.3.5   Granulation and Spray Drying

The vast majority of ODT patents are produced using compression technologies, as these are both simple and cost-effective. Granulation methods have been used in the production of ODTs, prior to compression of the granules into tablets [19]. Granulation is generally employed to improve the flow characteristics and homogeneity of the drug and excipient blend and may also improve compression characteristics [45].

1.3.5.1 Wet Granulation

Wet granulation is the most common method used in ODT production. To begin, a binder solution is added to a powder blend and mixed for a given time at a given speed, a process known as wet massing [45]. Granulating fluid often contains a volatile fluid such as ethanol that can be evaporated off. The use of a solvent in this way enhances the porosity and therefore disintegration of the finished tablet. The wet mass can be forced through a sieve or milled to produce wet granules which are then spread onto a tray and dried [19, 46].

1.3.5.2 Melt Granulation

Melt granulation is another common form of granulation used in ODT formation. This involves incorporation of a meltable hydrophilic waxy binder known as Superpolystate,

PEG-6-stearate with the powder blend. The mixture is heated above the Superpolystate melting point of 33-37°C and mixed using high shear mixers. This method increases both physical resistance of the tablet and aids in disintegration [33, 40].

1.3.5.3 Spray Drying

Spray drying involves the continuous transformation of a solution, slurry or emulsion to produce porous granules by drying using a hot medium. First the solution is atomised into fine droplets and the droplets are then mixed with a heated gas stream to evaporate the solvent. The dried granules are then separated from the gas stream and collected. The aqueous solution contains a particulate support matrix composed of both hydrolysed and non-hydrolysed gelatins as supporting agents, bulking agents such as mannitol, disintegrating agents such as sodium starch glycolate and an acidic or alkalinising agent such as citric acid/sodium bicarbonate to maintain the net charge of polypeptides. The polypeptide components included share the same charge and repel each other, and thus maintaining the net charge aids in disintegration [34, 36, 47].

Spray dried particles such as spray dried mannitol, erythritol or MCC have been shown to possess improved compactability as a result of increased plasticity conferred to the particles through the spray drying procedure. This improved plasticity is believed to be due to the increased deformity of the amorphous particles produced, in comparison to the original crystalline form. On the other hand, the shift towards an amorphous state may generate problems with stability with some excipients. The spherical particles formed through spray drying show improved flow characteristics and more readily rearrange in the tableting die, which again enhances compactability. Importantly, the thermostability of compounds should be considered when spray drying due to the high temperatures used [48, 49]

1.3.5.4 Advantages and Challenges of Granulation

As well as the usual benefits such as enhanced flowability, granulation offers advantages for ODT production. Both wet granulation and spray drying improve tablet porosity and as such can impart tablets with rapid dissolution. Due to the wax binder Superpolystate used in melt granulation, both physical strength and dissolution are enhanced [50].

On the other hand, these methods are more expensive than standard compression techniques and are more time consuming. In addition, wet granulation and spray drying are unsuitable for drugs susceptible to hydrolysis and may require the use of organic solvents [34].

1.3.6 Post-Compression Treatment

Due to certain limitations of compressed tablets, post compression technologies have been developed in order to improve ODT tablet properties, namely by improving the mechanical properties and the dissolution profile.

1.3.6.1 Sublimation

A common method for improving tablet dissolution rate is to improve porosity. Sublimation describes a process where volatile excipients such as urea, ammonium bicarbonate, naphthalene and urethane are added to the pre-compaction mix. These volatile ingredients are then removed after compaction through sublimation, resulting in a highly porous matrix. Typical dissolution times in the mouth for ODTs produced in this way are 10-20 s [32, 39].

1.3.6.2 Humidity Treatment

The mechanical strength of compressed tablets can be improved through moisture treatment after compression. The increased stability is due to liquid bridge formation upon moisture treatment and then formation of solid bridges upon drying. The liquid adsorbs onto the particles and forms a film into which the solid dissolves, eventually forming solid bridges upon drying [34].

1.3.6.3 Sintering

Sintering involves a process intended to improve mechanical strength of ODTs through sintering the tablet at 50-100°C and then re-solidifying by returning to ambient temperature. Disintegration times using this method can be rapid, with times between 3-60 s. Bulking agents, structure agents and binding agents are included in the initial mix. The structural mix should impart a porous structure to aid dissolution and commonly used agents include agar and albumin. Binding agents melt at the sintering stage and form bonds between granules, before re-solidifying as the temperature returns to ambient levels [34, 51]

1.3.6.4 Advantages and Challenges of Post Compression Treatment

The three common treatments described here each provide a different mechanism for improving either the strength or dissolution properties of ODTs. Typically, humidity treatment and sintering can improve the mechanical strength of lightly compressed tablets and sublimation increases the porosity of the tablet, enhancing disintegration rates [50].

These technologies do have limitations however. Importantly, all three treatments will require additional equipment and production costs, as well as an increased production time. Furthermore, humidity treatment will not be suitable for drugs vulnerable to hydrolysis, sintering will be unsuitable for thermo-labile compounds and sublimation will be unsuitable for drugs vulnerable to heat and volatile drugs [34].

1.4   Direct Compression

Direct compression describes compaction of a powder, after blending, into tablet form, using a conventional tablet press. Since only two operations are involved, direct compression is the most cost-effective and easiest technology for ODT production and is also attractive as it uses conventional equipment. The disintegration characteristics of directly compressed ODTs depends on the API, excipients and combination of excipients involved, such as disintegrants, water-soluble excipients and effervescent agents [35, 46]. Other directly compressed ODT properties are influenced by powder flow, compressibility and also dilution potential [52] and thus selection of suitable excipients is of paramount importance. Successful excipients for direct compression demonstrate good compressibility, flow and low moisture and lubricant sensitivity [53].

1.4.1   Advantages and Challenges of Direct Compression

In addition to their low cost and ease of production, directly compressed ODTs can be easily and rapidly produced and include readily available excipients. Since the process involves no water it is suitable for drugs that are susceptible to hydrolysis. Moreover, direct compression thus does not involve any drying steps and is suitable for drugs that are vulnerable to heat (thermo-labile), whose stability would otherwise be compromised. Direct compression also allows for the incorporation of high drug doses, which can be a serious limitation for ODTs produced using different technologies, in particular lyophilisation. Finally, directly compressed ODTs are mechanically strong and do not require expensive specialised packaging [31, 35, 46].

The major limitation of compression based ODTs is their relatively low porosity, as a result of the high pressures used to ensure tablet strength. This is important as uptake of water into ODTs is necessary for rapid disintegration and high porosity is necessary for this [54]. Directly compressed ODTs demonstrate good tablet hardness and have reasonable disintegration times. The disintegration time is however highly affected by both tablet size and hardness. Large, hard tablets disintegrate slowly and thus smaller, weaker tablets are more favourable. Consequently, ODT size can be a limitation and high friability and tablet rupturing are significant problems for ODTs that display satisfactory disintegration times. As a result, producing ODTs that rapidly disintegrate

whilst displaying sufficient mechanical strength is a major challenge [32, 39]. Finally, direct compression is not suitable for compounds that exhibit poor flowability, and specific excipients or granulation steps are needed to overcome this limitation [50].

1.4.2 Importance of Excipients

Since porosity is limited in directly compressed ODTs due to the high pressures involved, it is the careful selection of process parameters and excipients that determine dissolution time. In order to impart rapid dissolution three types of excipient are incorporated into a formulation, which operate by different mechanisms. These are disintegrants (superdisintegrants), water soluble excipients and effervescent agents [27]. Water soluble excipients improve the wettability of the tablet and improve water absorption. Amino acids have received interest in this respect, with studies into the use of amino acids to aid in disintegration with lyophilised tablets [19] and directly compressed tablets [55].

Superdisintegrants have received the most significant interest as excipients to achieve rapid disintegration in directly compressed ODTs. Superdisintegrants swell in contact with water and mechanically force the tablet apart. In addition, superdisintegrants such as crospovidone and croscarmellose sodium show wicking ability. Wicking describes uptake of water into the tablet through capillary action [19, 46]. This ability is especially advantageous for tablets with higher porosity, as wicking agents draw water into the pore space. Effective superdisintegrants also improve overall compressibility and compactability. Counter intuitively, it has been shown that more water-soluble superdisintegrants produce slower disintegration than less water-soluble superdisintegrants, due to the formation of a viscous water barrier upon swelling [32, 33]. Similarly, ODTs composed primarily of water soluble excipients, like sugar alcohol fillers, suffer from slower disintegration times as the soluble components on the outermost surface layer dissolve and form a concentrated viscous barrier that prevents further water absorption [56].

The amount of superdisintegrant added to formulations for directly compressed ODTs is generally low (typically 1-10%) and care should be taken to select the optimum concentration of superdisintegrant to ensure rapid disintegration. Disintegration

efficiency is governed by the force-equivalent concept, a combined measurement of disintegrating (swelling) force and water uptake. Crucially, superdisintegrants have critical concentrations, below which disintegration time Is slower and above which disintegration time remains constant or even increases, as a result of an increase in viscosity caused by gelling. Determination of an optimum superdisintegrant concentration is therefore important in limiting disintegration time, especially with disintegrants that display limited swelling ability [57]. Furthermore, sparing use of a superdisintegrant is beneficial as a combination of superdisintegrant with water soluble excipients and/or effervescent agents can augment disintegration ability [35].

1.4.3   Patented Systems

A number of different technologies for ODT production have been developed that incorporate compression, such as Orasolv, Durasolv, Flashtab and Wowtab [58]. Each of these systems uses other techniques prior to compression and tablets are therefore not produced purely by direct compression. Subsequently, development of effective ODTs from direct compression of a primary powder is an inviting prospect.

Orasolv and Durasolv are patented by Cima Labs Inc. and are similar in their production. Orasolv tablets contain taste-masked drug microparticles along with polyols as diluents, a disintegrant, an effervescent agent and also flavours, colours and lubricants. The tablets can incorporate drug in a range of 1 mg to 750 mg and are compressed at low force giving a tablet with poor hardness (6-25N) but rapid disintegration (10-40 s). As a result of low hardness, the tablets are contained in specialised aluminium blister packaging. Durasolv tablets have a similar formulation to Orasolv, including taste-masked drug microparticles but may not contain effervescent agents. They are compressed at higher forces than Orasolv tablets and can incorporate APIs in a range from 125 μg to 500 mg. These tablets disintegrate more slowly than the Orasolv technology, (10-50 s) but show an improved hardness (15-100N) and as a result the tablets can be contained in blister packaging or bottles [59-61].

Flashtab involves incorporation of a swelling agent and a super disintegrant, with the API being taste masked by direct coating. A highly water soluble sugar alcohol may be incorporated instead of the swelling agent, depending on the need. Excipients are first

granulated (wet or dry) and are then mixed with the coated drug, before compression into tablets with satisfactory mechanical integrity, that can withstand opening of blister packaging [60, 62].

Wowtab, developed by Yamanouchi Pharma, includes a mixture of high and low mouldable sugars that are granulated in a fluidised bed granulator along with other excipients and the API. The resultant granules are then mixed with lubricant and flavours and compressed using conventional equipment. The ODTs are then stored at controlled temperature and humidity before packaging into blisters or bottles. The technology benefits from rapid disintegration times (15-20 s) and sufficient strength to withstand manufacture, packaging, opening and handling [60, 63].

1.5 Excipients Suitable for Compressed ODTs

A large number of different excipients have been used in ODT formulations. The focus of this work is on directly compressed ODTs and, with this is mind, a list of excipients commonly used in ODTs formed by compression techniques is summarised in Table 1.1, along with their roles and their advantages and disadvantages. All excipients are compatible with direct compression and also granulation or moulding processes pre-compaction.

Table 1.1 Commonly used excipients in the production of ODTs by compression

Excipient	Role	Comment	Conc. Range (w/w)	Advantages	Disadvantages
Aspartame	Sweetener	Intense sweetening agent, sweetening power is 180-200 times that of sucrose; Slightly soluble in ethanol; Poor solubility in water	<1%	Masks unpleasant tastes; Intense sweetener, requiring very low concentrations	Incompatible with dibasic calcium phosphate, magnesium stearate and some sugar alcohols; Will not replace characteristics of sugars if sugar is removed
Calcium carbonate	Binder; Diluent	Odourless and tasteless powder or crystals; Insoluble in ethanol and water; Water solubility increased by ammonium salts or carbon dioxide	10-90%	Stable; Relatively non-toxic	May interfere with the absorption of other drugs from the GIT

Calcium phosphate	Diluent	Milled grade material is used in wet granulation and roller compaction and unmilled coarse grade is used in direct compression; Insoluble in ether, ethanol and water; Soluble in dilute acids	10-90%	Good flow properties; Good compaction; Non-hygroscopic and stable	Lamination and capping at high compaction forces; Requires lubricant; Unmilled has acidic surface, milled has alkaline surface; Incompatible with a number of drugs and excipients
Calcium sulphate	Diluent	Used as a dessicant due to hygroscopicity	10-90%	Non-toxic at excipient concentrations	May cake on storage; Incompatible with tetracycline antibiotics, indomethacin, aspirin, aspartame, ampicillin, cephalexin and erythromycin due to calcium salts
Citric acid monohydrate	Effervescent couple; Flavour enhancer	Odourless; Acidic taste; Crystalline	1-20%	Safe - found naturally in the body	Incompatibility issues
Colloidal silicon dioxide	Disintegrant; Adsorbent	Insoluble in organic solvents, water and acids; Forms a colloidal suspension in water; Hygroscopic but does not liquefy with water absorption	0.1-1%	Imparts good flow properties	

Croscarmellose sodium	Superdisintegrant	Odourless; Insoluble in water, ethanol, acetone and toluene; Rapidly swells to 4-8 times original volume; Promotes water absorption by wicking	2-5%	Stable; Rapid swelling; Can obtain good purity	Incompatible with strong acids or soluble salts of iron, zinc, aluminium and mercury; Ideally should not be combined with other hygroscopic materials
Crospovidone	Superdisintegrant; Binder	Larger particles disintegrate faster; Suggested as a replacement to MCC to aid in pelletisation; Hygroscopic;	2-5%	High capillary activity; High hydration capacity; Low tendency gel; Compatible with most organic and inorganic ingredients	Risk of metabolite phenylalanine in patients who suffer from phenylketonuria
Erythritol	Sweetener; Diluent	Non-hygroscopic; Zero calorie; Freely soluble in water; Slightly soluble in ethanol; Insoluble in ether and fats	10-90%	Stable; Good flowability; Cooling effect	Incompatible with strong oxidising agents and strong bases
Ethylcellulose	Water insoluble; Binder; Diluent; Taste masking agent	Can be dissolved in ethanol to form a binder; Slightly hygroscopic; Stable	5-80%	Tasteless; Free flowing; Stable	Produces hard tablets; Produces tablets with low friability; Incompatible with paraffin and microcrystalline wax

Fructose	Sweetener; Diluent	Hygroscopic; Sweeter than mannitol, and sorbitol	5-20%	Very sweet tasting; Imparts good crushing strength	Incompatible with strong acids or alkalis; Risk of reacting with amines, amino acids, peptides and proteins in the aldehyde form
Glucose	Binder; Sweetening agent	Water soluble; Low mouldability	5-20%	Sweet tasting; Stable; Forms strong compacts	Incompatible with a number of drugs; May cause browning (Maillard); Decomposition can occur with strong alkalis
Hydroxypropyl cellulose (HPC)	Binder	Increases viscosity; Soluble in water and polar organic solvents	2-6%	Acceptable flow characteristics	Compatibility with inorganic salts varies
Hydroxypropyl cellulose, low-substituted (L-HPC)	Binder; Diluent; Disintegrant	Number of different grades: LH-11 and LH-B1 used in DC	5-50%	Swells in water	Poor flowability; Insoluble in ethanol and ether
Hypromellose (HPMC)	Binder; Solubilising agent; Modified release agent	Wet granulation binder; Coating agent; Hygroscopic; Odourless and tasteless; Soluble in cold water; Insoluble in hot water, ethanol, ether and chloroform	2-80%	Stable	Incompatible with some oxidising agents; Does not complex with metallic salts or ionic organics

Lactose	Binder; Diluent	Susceptible to Maillard reaction; Milling improves compactability but is detrimental to flow	10-90%	Can be used with moisture-sensitive drugs; Odourless; Slightly sweet tasting; Suitable for spray drying to improve flow	May develop brown colouration (Maillard reaction) on storage; Many people are lactose intolerant
Magnesium stearate	Lubricant	Faint odour	0.2-5%	Stable	Incompatible with strong acids, alkalis, oxidising agents, iron salts, aspirin and some vitamins and alkaloid salts; Compromises disintegration and tablet strength
Maize starch gum (Dextrin)	Binder; Diluent	Slight odour; Insoluble in ethanol, chloroform and ether; Soluble in boiling water	5-50%	Non-toxic	Incompatible with strong oxidising agents
Malic acid	Effervescent acid; Acidifying agent; Flavouring agent	Is combined with an effervescent base and forms CO_2 in contact with water; Hygroscopic; Freely soluble in water and ethanol	1-20%	Masks bitter tastes; Slight apple flavour; Freely soluble in water	Combination with excipients and drugs with moisture content only, to prevent triggering a reaction
Maltitol	Binder; Diluent; Sweetener	Odourless; Water soluble; Relatively non-hygroscopic	10-90%	Non-cariogenic; Low glycaemic index so suitable for diabetics; Highly mouldable	Poor compactability

Maltodextrin	Binder; Diluent	Non-sweet, odourless; Slightly hygroscopic; Freely soluble in water, slightly soluble in ethanol	5-30%	No adverse effect on dissolution rate	Susceptible to browning (Maillard)
Maltose	Sweetener; Diluent	Odourless; 30% sweetness of sucrose	0.5-25%	Sweet taste; Highly mouldable	May react with oxidising agents; May brown (Maillard)
Mannitol	Sweetener; Diluent	Non-hygroscopic and may be used with moisture-sensitive ingredients; Occurs as crystalline powder or free-flowing granules; Stable in dry and aqueous states	10-90%	Mouth-feel; Cooling sensation; Sweet tasting	Poor compactability
Menthol	Flavouring agent	Soluble in ethanol; Normally sprayed onto granules	0.1-10%	Cooling sensation; Tendency to sublime and has been used to increase the porosity of granules	Incompatible with several compounds; Risk of hypersensitivity
Methyl cellulose	Disintegrant; Binder; Viscosity increasing agent	Low-medium viscosity grades used as binders, High viscosity grades used as disintegrants; Odourless and tasteless	2-10%	Stable	Incompatibility issues

Microcrystalline cellulose	Binder; Diluent	Strong binding; Good disintegration due to porosity and wicking; Variety of grades differing in method of manufacture, particle size, moisture and flow	5-15%	Hygroscopic; Good flowability; Good compactability due to plastic deformation	Practically insoluble in water, dilute acids and most organic solvents; Incompatible with strong oxidising agents
Polyvinylpyrollidone (PVP, povidone)	Disintegrant; Binder	Wet granulation binder; Very hygroscopic; Soluble in water, ethanol, acids, methanol, ketones and chloroform	0.5-90%	Shown to enhance dissolution of poorly soluble drugs	Forms adducts with some compounds
Silicic acid	Disintegrant	Used as a disintegrant for rapidly disintegrating granules	0.1-0.5%	Free flowing; Stable	Practically insoluble in water
Sodium Carbonate	Effervescent base; Diluent; Alkalising agent	Is combined with an effervescent acid and forms CO_2 in contact with water; Hygroscopic	2-10%	Rapid effervescence in presence of water and acid; Freely soluble in water	Requires combination with excipients and drug that possess low moisture contents, to prevent triggering a reaction
Sodium carboxymethyl cellulose	Disintegrant; Binder; Adsorbent	Insoluble in ether, acetone, ethanol and toluene; Forms colloidal solutions with water	0.1-90%	Absorbs significant amounts of water; Stable	Incompatibility issues; Lowers tablet hardness

Sodium lauryl sulphate	Surfactant; Lubricant	Smooth feel, bitter taste, faint fatty odour; Possesses some bacteriostatic action; Not hygroscopic; Insoluble in chloroform and ether	0.1-2%	Fairly stable; Compatible with mild acids	Incompatible with cationic surfactants, aluminium, lead and zinc; Precipitates with potassium salts; Moderately toxic, may cause skin irritation
Sodium starch glycolate	Superdisintegrant	Rapidly swells (300x volume); Disintegration efficiency unimpaired by hydrophobic excipients; Very hygroscopic	2-8%	Stable; Unimpaired by presence of hydrophobic excipients; Increased compaction pressure does not affect disintegration time	May cause caking if not stored in well-closed container; Disintegration times slower with high levels of soluble excipients; Interacts with glycopeptide antibiotics and basic drugs
Sodium stearyl fumarate	Lubricant	Sparingly soluble in water; Particles around 5-10 μm in diameter	0.5-2%	Non-toxic and non-irritant; Much more water soluble than magnesium stearate	Not as effective a lubricant as magnesium stearate
Starch	Binder; Disintegrant; Diluent	Insoluble in cold ethanol and cold water; Swells immediately in water (about 5-10%)	3-50%	Low concentrations 3-10% w/w can act as antiadherent and lubricant	Wheat proteins (gluten) unsuitable for celiacs

Xylitol	Sweetener; Taste masking agent; Diluent	Enhances product stability due to bacteriostatic and bactericidal action	0.5-25%	Non-cariogenic; Sweet taste; Cooling sensation; Enhances stability	Slightly hygroscopic; Incompatible with oxidising agents

1.6 Film Coating

1.6.1 History of Tablet Coating

The coating of tablets has a long history with its origins lying in sugar coating, a process borrowed largely from the confectionary industry. Despite the effectiveness of sugar coating in masking the taste of bitter tasting drugs, coating of tablets was a laborious task requiring great skill, with multiple steps that could take as longs as 5 days and resulted in large, heavy coated tablets. The resultant pressure to develop alternative coating methods manifested in the development of compression coating and film coating [64].

Compression coating received attention in the mid-twentieth century, promising far shorter lead times than sugar coating. The process involved tablet compression using one machine followed by transfer to a different machine that would compress coating material around the core. This process suffered from a variety of limitations, namely size and weight related, whilst significant drawbacks such as coat splitting due to core expansion, poor bonding between coat and core and low speed meant the techniques popularity did not endure [64].

Like compression coating, tablet film coating arose in the mid-twentieth century, largely due to the emergence of new materials, most importantly cellulose derivatives. Early film coating used organic based solvent coating solutions to avoid the risk of decomposition of active ingredients and benefited from greater ease of use. Significantly, the use of volatile organic solvents benefit from rapid evaporation and therefore their use provides a reduced risk of over wetting, which can cause substantial problems. Indeed, one of the major complications with using water as a coating solvent is its much greater latent heat of evaporation of 539 kcal/kg when compared to organic solvents such as ethanol at 204 kcal/kg [64-66]. Despite this however, there has been an increasing shift towards the use of aqueous based coatings due to a number of problems with organic solvents, to a point where now aqueous based coatings are much preferred. Most importantly, the use of organic solvents has been phased out due to toxicity concerns, including environmental pollution as well as safety concerns to operators and consumers, with ICH guidelines recommending the avoidance of organic solvents in pharmaceutical formulations [67-69]. This shift has also stemmed from escalating solvent costs, as well as technological advances and savings due to the removal of the need for solvent recovery systems [64, 70].

1.6.2   Applications and Objectives of Film Coating

Application of a film coat increases the cost, manufacturing time and complexity of drug production, and as such its use must be carefully considered. Clearly therefore, a film coating must provide a variety of applications and advantages, a number of which typically include [64, 66, 67, 71-74]:

- To mask the taste of a bitter drug
- To mask unpleasant odours
- To improve the stability of an API or excipient e.g. protection from light, moisture or oxidation
- To physically protect vulnerable cores
- To improve the aesthetics of inelegant cores e.g. by use of colours or glaze to provide a glossy sheen effect
- To provide product identity through the use of colours or logos. This extends to patient compliance and safety e.g. the use of different colours to avoid confusion for patients taking multiple medications
- To control drug release. This can be achieved in a number of ways depending on the requirement, for example:
    - For protection of an acid labile API from the gastric environment through the use of an enteric coating
    - For sustained release of the API in order to achieve a desired pharmacokinetic profile
    - For the purposes of different release technologies, such as osmotic pumps
- To form a barrier to coloured APIs that may stain
- To aid in swallowing of the dosage form
- To reduce the friction of the drug with packaging machinery
- To increase mechanical strength
- To segregate incompatible APIs, adjuvants and excipients by incorporation of one in the coat and the other in the core

With these numerous benefits of coating comes a complexity in coating techniques and processes and the materials required.

1.6.3 Conventional Coating Process

Polymeric film coats are thin coatings, usually 20-100 µm thick [75], that are generally applied to tablets using an atomisation spray process. Aqueous polymeric coats comprise of a coating polymer either dissolved or dispersed in water. Polymer dispersions exist as polymer spheres suspended in water, which importantly differ to polymer solutions in that viscosity is independent of polymer concentration, allowing for higher polymer concentrations. Atomisation of the coating solution is achieved using high pressure air. The coating fluid liquid sheet is first deflected away from the air stream, causing waves in the sheet that lead to formation of unstable ligaments, which break down further into fine droplets [76, 77]. Upon contact with the tablet, droplets impinge and spread across the surface. For polymer solutions a film is formed upon evaporation of the solvent, whereby the polymer chains interpenetrate, passing through a gel stage, followed by film formation with additional drying. The mechanism of film formation from polymeric dispersions is more complex; before polymer chains can interpenetrate polymer spheres must first coalesce, that is they must deform and fuse together, before a continuous film can form [78-80]. An important consideration in the film formation process is the minimum film forming temperature (MFT), above which film formation takes place. and is highly dependent on the polymer's glass transition temperature (T_g). It is recommended that coating temperatures around 10-20°C above the MFT are optimal [81].

Tablets are moved within the spray by mixing to ensure an even coating, and intermittently reside either within the spray path or outside of the spray path in drying zones. The two major techniques for this are drum or pan coating and fluidised bed coating, although pan coating is more common for tablet coating, whereas fluidised bed is more suited to coating of smaller objects such as granules. Pan coating involves the tablet cores being placed inside a rotating drum on an inclined axis, with tablets falling through the spray path from one or several atomisers. Perforated coating pans offer improved drying efficiency over conventional pans by passing drying air through the tablet bed. In fluidised bed coating, tablets are suspended and circulated by heated air from below, continuously passing through the spray path originating from atomisers placed either above or below the tablet bed, with the bottom spray technique being more popular. With either pan or fluidised bed coating, tablets are subject to a constant cycle of coating and drying, accumulating coating layers over time. Water evaporation from

fluidised bed systems is more efficient due to the greater extent of airflow [82, 83]. With either technique tablets are subjected to substantial mechanical stress which can lead to breakage or attrition. This problem is augmented during scale-up processes due to the greater weight of tablets used and increasing pan sizes. Tablet cores must therefore be mechanically robust enough to withstand these processes, with friability being a particularly important property to measure this ability and ideally cores should exhibit a friability of less than 0.1% [84].

1.6.4   Recent Tablet Coating Technologies

Despite the substantial evolution in sophistication of conventional coating processes and materials over the past half a century, new techniques for tablet coating have been developed. The various drawbacks of organic solvent based coatings have already been outlined. Despite the advantages of aqueous solutions, there are circumstances where their use is unsuitable, for example with APIs that are sensitive to water. Migration of water into the tablet core either during coating or storage and the energy needed to evaporate water are also drawbacks. New coating technologies are thus primarily concerned with dry coating [85].

The mechanisms concerning dry coating are similar to that of solvent based coating and generally involves pre-treatment of coating material, application of the coating material to the tablet and film formation. To soften the coating polymer and increase its adherence to the tablet surface, the coating material is often heated above its Tg before being applied to the tablet. Sintering and coalescence is then performed on the powder layers, followed by levelling and densification of the coating layer and finally hardening of the coating through a final cooling stage [86, 87].

Electrostatic dry coating involves application of a finely ground conductive ionic coating material to a tablet to which a strong opposite electrostatic charge has been applied. Film formation is then achieved through a curing step. Two variations of spraying units, Corona charging and Tribo charging units, exist for this application and differ by their charging mechanism [87]. Magnetically-assisted impaction coating is another example of a dry coating technology, where magnetic coating material is accelerated in a chamber using an alternating electromagnetic field, resembling a fluidised bed coater. Collision of particles with the tablet core and intra-particle collisions occur, resulting in attachment of coating material to the core. This technique is suitable for temperature sensitive

compounds since very little heat is generated [88-90]. A final example of a dry coating technology is hot melt coating whereby coating material is applied to the tablet core in a molten state. Hot melt coating using lipids is implemented for sustained drug release, which is the main application of this technique [91, 92]

1.6.5 Polymers for Film Coating

Polymers used for conventional film coating, that is coatings concerned with imparting improved appearance or mechanical properties for example, are generally water soluble. Due to their solubility they do not impede drug release and therefore are not useful in controlled release systems. These include cellulose based polymers and synthetic materials such as polyvinylalcohol-polyethylene glycol and polyvinylpyrrolidone-vinyl acetate copolymers. Cellulose derivatives are a major class of polymers used in convention film coating, the majority of which are in fact ethers, produced through reactions in alkaline solutions. HPMC, produced by the reaction between cellulose and methyl chloride is one such ether, with other examples including hydroxyethyl cellulose and HPC [79, 93]. The degree of substitution of hydroxyl groups and the molar substitution (which also includes the substitution of hydroxyl groups belonging to side chains), greatly influence the solubility and gel point of cellulose ethers. The use of HPMC is particularly prevalent in film coating procedures, due to a number of benefits such as solubility in both water and organic solvents. Furthermore, HPMC solutions are non-tacky, have relatively low viscosity and also have an established history of safe use [64].

Conversely, water insoluble polymers are used for controlled or sustained release coatings. Sustained release systems benefit from lower dosing frequency, which in turn enhances patient adherence. Due to the control over the pharmacokinetic profile of the API that these coatings can provide, plasma drug concentration can be maintained within a desired therapeutic window, and as such the risk of dangerously high plasma levels is reduced. Should the coating be compromised however, due to mechanical failure or concomitant alcohol consumption (with coats that are soluble in ethanol), there is a risk of dose dumping, where the entire drug dose is rapidly and unintentionally released, resulting in potentially devastating repercussions [79, 94-96].

Standard controlled release coatings work by delaying the rate at which intestinal fluid diffuses into the tablet core. Once the core has been exposed, either by coat erosion or

fluid penetration through the coating, the API then diffuses out from the core along a concentration gradient. The solubility of the drug is an important factor in its rate of release, with more water soluble APIs demonstrating faster release [97]. The diffusion of drug through the coat is also dependent on the coat density and thickness [98, 99]. One method for improving and further controlling the release rate of APIs (particularly, poorly water soluble APIs) from this type of coated dosage form is through the incorporation of hydrophilic material such as HPMC within the coating, which in contact with water forms pores within the coat that facilitate API release [100].

More sophisticated controlled release technologies have also been developed. Osmotic pump technology, for example, utilises a film coat (formed most commonly from cellulose acetate) containing a laser drilled orifice. The tablet core contains osmotic agents such as sodium or potassium chloride which generate an osmotic gradient, drawing in the intestinal fluid through the coating and resulting in an increased osmotic pressure within the core. The high pressure in the core then forces either dissolved or dispersed drug through the orifice, releasing the API into the gastro-intestinal tract [79, 101]. Another example of a sophisticated controlled release technology is that of enteric (delayed-release) coatings. This approach involves coating of the core with a weakly-acidic polymer, containing ionisable carboxylic acid groups. At the low pH of the stomach these polymers remain unionised and the coating remains intact; however, upon reaching the near neutral pH of the small intestine (around pH 6) the carboxylic acid groups ionise, causing the coating polymer to dissolve, whereby the API is released from the core. This system is particularly useful for acid-labile drugs or those, such as aspirin, known to cause irritation to the gastric mucosa [102, 103].

1.6.6   Coating Additives

Additives are often combined with coating polymers to improve film properties, alter film permeability or to aid in film formation. Plasticisers are used to improve the flexibility of brittle polymers films and thus reduce the potential for brittle fracture and also assist in aqueous based polymer sphere coalescence. Plasticisers work by weakening intermolecular forces between polymer chains and this is believed to occur through a combination of hydrogen bonding, dipole-dipole and dipole-induced-dipole interactions [87]. The choice and concentration of plasticiser has a major impact on the mechanical and adhesive properties of the polymer film and also on drug release [104-106]. Plasticisers should be non-volatile and thus contribute to the weight gain of a coated

tablet. It is also important that plasticisers are miscible with the coating polymer; in aqueous polymer dispersions this requires that plasticisers partition within the polymer spheres. The effectiveness of a plasticiser can be determined by its effect on T_g of the coating polymer, with more effective plasticisers causing greater decreases in T_g, reflecting the added flexibility imparted by the plasticiser [79, 107]. Three main types of plasticiser are commonly used which include: polyols, such as polyethylene glycols (PEGs), organic esters and oils/glycerides, such as castor oil [87].

Anti-adherents are a major additive for film coat polymer solutions and dispersions and are included to prevent substrate agglomeration during coating and storage. Talc is amongst the most common employed anti-adherents, although it must be included at very high quantities, which can lead to processing complications related to its sedimentation and subsequent clogging of the atomiser nozzle. This property may be attributed to its hydrophobic nature, a property which is also likely responsible for its tendency to reduce the dissolution rate of APIs [79, 108]. Its use also reportedly affects film mechanical and adhesive properties, and as a result, glyceryl monostearate has been suggested as a favourable alternative [109].

Surfactants can be added to improve droplet wettability and spreading ability on the tablet surface and are also used stabilise suspensions and emulsify poorly soluble plasticisers. Surfactants achieve this by lowering the surface tension of the polymer solution or dispersion. Droplet spreading, for example, is dependent on the surface tension between liquid-air and liquid-solid interfaces. Despite the low concentrations used surfactants can have pronounced effects on film coat properties and impact drug release [78, 79, 110].

Pigments are another important additive to film formulations and are used to improve the elegance and identification of coated dosage forms. Pigments such as titanium dioxide are also used to enhance the stability of light sensitive drugs. The pigments most commonly used are metal oxides and water insoluble lake dyes. Their use is complicated however, as they are known to significantly affect film permeability and mechanical properties and are also to prone to clog the spray nozzle [111, 112]. A number of other additives are also included in polymeric film coats including antioxidants, antimicrobials and sweeteners and flavours [87].

As discussed, film coatings offer one approach to modify solid-dosage forms, to offer enhancements or overcome problems. Similarly, combination of multiple APIs into a single formulation can offer a variety of benefits.

1.7 Fixed Dose Combinations

Fixed dose combinations (FDCs) involve the incorporation of two or more APIs into a single dosage form. These can include oral dosage forms such as tablets, capsules or liquids and parenteral forms including inhalation and intravenous or subcutaneous injections. Oral dosage forms comprise the vast majority of approved FDC formulations. Drug dose in FDCs can be increased or decreased, but must be maintained at a fixed ratio. There are a number of arguments behind combination of drugs into FDC form which broadly include compliance, efficacy and safety and financial benefits [113]. Indeed, the interest in FDCs in the pharmaceutical industry is steadily increasing, with the FDA approving 12 new FDC formulations in 2010 alone [114]. In certain therapeutic areas FDCs have been in use for over 50 years [115].

FDCs improve patient compliance due to simplification of the dosing regimen. Combination of medications into one form reduces the number of products required to take per day. Simplification of dosing to avoid confusion is particularly prevalent if two medications follow different dosing schedules, whereby doses can be adjusted to allow for once, or if necessary, twice daily dosing. FDCs thus offer greater ease of use to patients when compared to multiple medications, especially in patients who may also be being treated for other unrelated indications. This results in enhanced patient compliance and also drug efficacy, since the success of treatment is often highly dependent on consistent dosing [114]. It has been reported that FDCs reduce non-compliance to dosing regimens by 24-26% and are recommended for the treatment of chronic conditions, such as hypertension, where enhanced compliance translates into improved clinical outcomes [116].

Improved efficacy of FDCs may be achieved, as previously mentioned, through enhanced patient compliance, resulting in improved outcomes due to consistent dosing. Combination of drugs that have a synergistic activity is a popular strategy for improving treatment efficacy. Using this approach, the efficacy of a medication can be substantially improved without the need to increase the dosage levels and compromise safety, since the concurrent action of two drugs at well tolerated levels is greater than either drug alone [113]. Examples of such synergistic FDCs include glipizide/metformin in the treatment of diabetes, or artemether/lumefantrine to treat malaria. Bioavailability enhancement is another strategy by which FDCs can improve efficacy. This can be achieved by API combination, of which one inhibits the metabolism of the other. In some cases, efflux transport may also be inhibited. One such example is the combination of

lopinavir/ritonavir to treat HIV. Lopinavir is a substrate for CYP 3A4 and Pgp whereas ritonavir inhibits CYP3A4 and Pgp; inhibition of CYP3A4 and Pgp by ritonavir increases lopinavir plasma concentration and efficacy [117]. APIs are also combined to treat multiple indications in co-morbid disease states, such as amlodipine/atorvastatin treatment for hypertension and hyperlipidaemia, respectively, in cardiovascular disease. Finally, FDCs may also be employed where an API is included to counteract an adverse effect caused by the other. For example, the proton pump inhibitor famotidine can be combined with ibuprofen, to counteract gastric hyperacidity caused by ibuprofen [118].

FDCs are also attractive for business reasons, as they represent generally low-cost and low-risk ventures and offer the ability to extend market exclusivity past the expiration of patents. In the USA, if a FDC is deemed novel, non-obvious and useful then the FDA will allow patenting and enforce exclusivity by excluding competitors [119]. FDCs may also demand higher prices. Indeed, they can be highly lucrative, with 19 FDA approved products achieving sales in excess of $1 billion by the year 2014. Patients may also benefit financially since the number of prescriptions will be reduced [114].

A limitation of FDCs are that they offer little dosing flexibility due to their fixed drug ratio. In some cases, such as in the treatment of hypertension, FDCs should only be prescribed once management using a single medication has proven ineffective. This however does not always occur, raising concerns regarding patient exposure to unnecessary therapy [120]. Adverse side effects are common to many medicines and often the only way to determine whether a certain symptom is due to the medication is to stop treatment. Due to multiple drug inclusion in FDCs it is thus difficult to identify the active causing adverse side effects and the patient may also risk losing the benefits of a safe, beneficial drug [121]. FDCs are also limited by chemical and physicochemical incompatibilities between certain API combinations. This also extends to compatibility between API and excipients included in the formulation. Any incompatibilities should be investigated during early formulation development under stress conditions [122]. Drug interactions may alter the therapeutic effect, or similarly cause bioavailability issues, for example, in the case of the impaired bioavailability of rifampicin when combined with isoniazid in FDC formulations [123].

To avoid such issues with bioavailability and altered therapeutic effect it is favourable to perform *in vitro* assessment of FDCs.

1.8 In Vitro Intestinal Permeability

1.8.1 Different Techniques

Although advancements in drug delivery via alternative routes provide a vast array of administration options, the oral route remains the most popular for convenience and compliance reasons. Assessment and prediction of intestinal permeability of APIs is of vital interest in understanding the *in vivo* performance of oral dosage forms and in the drug discovery field its use is widespread during lead selection and optimisation. Drug absorption from the gastrointestinal tract is a crucial determinant of bioavailability and is governed by the physicochemical properties of the API. Permeability evaluation can be performed *in vitro* by various cell based, membrane based and excised tissue assays and by analysis of psychochemical properties. Each technique carries its own advantages and limitations which influence technique selection depending on the circumstance [124, 125].

1.8.2 Intestinal Absorption

For intestinal absorption a drug must traverse the epithelial cell membrane consisting of a phospholipid bilayer around 10 nm thick. Lipophilic tails confer a lipophilic core to the bilayer, whilst hydrophilic heads point outwards forming two adjacent hydrophilic surfaces. The hydrophilicity and hydrophobicity of an API will greatly influence its interaction with this bilayer and its ability to permeate as well as its transport pathway. This is conventionally measured by observing the distribution of a compound between a hydrophobic phase (usually octanol) and a water phase, referred to as the log of the partition coefficient (LogP), with LogP values above or below 0 indicating a lipophilic or hydrophilic compound, respectively. In general, lipophilic drugs offer enhanced absorption, however at LogP values above 5 permeability declines, due to sequestration of the highly hydrophobic compound within the membrane [126, 127]. Since the vast majority of drugs consist of weak acids or bases, the pH of the environment will also greatly influence permeability, since ionised forms are generally more water soluble and vice-versa. A drugs pKa is thus another important parameter when considering intestinal permeability [128].

Passive diffusion is the predominant mechanism for absorption of drugs through the intestinal epithelium. It follows Fick's law whereby the compound flux is driven by the

concentration gradient across the membrane, and is proportional to the diffusional area and drug permeability coefficient and is inversely proportional to the membrane thickness [129]. For unionised lipophilic compounds, passive diffusion occurs transcellularly, whereas polar and ionised molecules traverse paracellularly through intercellular tight junctions between adjacent epithelial cells [130]. Facilitated influx and efflux of compounds also occurs at both the apical and basolateral membrane of intestinal epithelial cells by ATP-binding cassette transporter proteins, such as P-glycoprotein (Pgp) and multidrug resistance-associated proteins [131]. Lastly, transcytosis and endocytosis are a mechanism by which larger compounds may be absorbed [132].

1.8.3   Cellular Models and Caco-2

Cell culture models are extensively used in the study of intestinal drug absorption. Cells are cultivated on permeable growth membranes, forming a monolayer by which transport across either the apical or basolateral membrane can be studied. They are superior to membrane models, such as the parallel artificial membrane permeability assay, in that they are characteristic of intestinal epithelial cells, being structurally and biologically similar and they express transporters and metabolic enzymes found *in vivo*. Cell models do possess a number of limitations however, suffering from high variability due to their polyclonal nature. Variations also stem from differences in culture conditions such as passage number, culture time, seeding density and culture media. Furthermore, they cannot represent the complexity of the intestine since they consist of only one cell type and do not offer high throughput due to long culturing times. Several different cell lines are employed for *in vitro* transport studies, including Caco-2, HT29-MTX, MDCK, TC7 and 2/4/A1 [133, 134].

The most popular cell line used in cellular models is the Caco-2 line. Caco-2 are an immortalised line of heterogeneous human epithelial colorectal adenocarcinoma cells, that differentiate to express features characteristic of mature polarised enteroctyes. They require extensive culture times of 21 days on porous transwell membrane inserts, although there have been efforts to develop protocols as short as 7 days [135]. Formation of confluent, differentiated and polarised cells, possessing tight junctions is most often assessed using transepithelial electrical resistance (TEER) measurements. Transport assays using Caco-2 cells yield apparent permeability coefficient (Papp) values, which give an indication of the permeability of a compound and can be compared to a vast

number of Papp values for different compounds in the literature. As well as passive permeability, Caco-2 cells can provide information on active transport of compounds, due to the presence of membrane transporters such as P-gp which is known to be highly expressed in these cells [133, 136].

To gain a further understanding of *in vivo* performance of FDCs, *in silico* tools offer a powerful approach to safely and rapidly investigate bioavailability and provide substantially more detail than cellular models can offer.

1.9 In Silico Pharmacokinetic Modelling

1.9.1 Modelling Background

The development of new drugs and drug delivery technologies has historically been plagued by high attrition, with a general rule of thumb that from 10,000 compounds only 1 will successfully make it to regulatory approval after an average of 15 years of study [137]. Pharmacokinetic modelling is a powerful tool employed to optimise drug discovery and reduce high attrition and the associated escalating costs [138]. For candidate identification and lead optimisation, consideration of drug metabolism and pharmacokinetics (DMPK) is crucial and encompasses the absorption, distribution, metabolism and excretion (ADME) properties of the compound [139]. Due to pharmacokinetic modelling, development failures due to poor pharmacokinetics have dropped from around 50% in 1990 to 10% [138].

The basis of any model involves the application of mathematical and statistical techniques to an existing data set in order to represent and predict the system being studied. Numerous models exist however none is perfect, each with their own strengths and limitations, and as such they are constantly being developed driven by theoretical considerations and new clinical information [138]. Methods to quantitatively predict pharmacokinetic outcomes involve simple models to predict certain parameters and increase substantially in complexity and sophistication, to physiologically based pharmacokinetic (PBPK) models, that are able to predict drug plasma concentration profiles. From plasma concentration time curves key clinically relevant information can be extrapolated, such as the peak plasma drug concentration, absorption kinetics and elimination. PBPK models have their roots in academic and toxicological applications, however in recent years it has been enthusiastically adopted for drug development and regulatory assessment. This is reflected by, and likely in part due to, a variety of open and commercially available user-friendly software packages that make PBPK modelling more accessible [140].

1.9.2 Modelling Approaches

Different modelling approaches have developed over time. The simplest of these is the classical empirical model, which draws upon existing *in vivo* drug plasma concentration profiles and aims to replicate them. These models require little theoretical understanding of the system and instead involves using a number of compartments with which the drug is instantaneously distributed, to describe ADME. Empirical models are most commonly

described by the sum of exponential terms representing the event in each compartment. Although these models can satisfactorily describe concentration-time profiles and derive information such as clearance parameters and even dosing regimens, they are limited in their extrapolation. This is a result of the simplicity of the system, with the descriptive parameters within each compartment lacking any physiological relevance [141].

Non-compartmental analysis is a model independent approach and was the most commonly used pharmacokinetic analysis tool before the dawn of modern computational power. A non-compartmental approach can determine certain pharmacokinetic parameters using calculations based on the area under the plasma concentration curve (AUC), which itself can be calculated using the trapezoidal rule. From the AUC, total body clearance, apparent elimination rate constant, mean residence time and apparent volume of distribution at steady state can be calculated [138, 142].

1.9.3 PBPK Modelling

Mechanistic pharmacokinetic PBPK models were first described in 1937 by Teorell [143] and developed during the 1960s and 1970s by Bischoff and Dedrick [144]. PBPK models are based on compartmental models but differ in complexity: instead of including a small number of compartments all organs and tissues are included as defined compartments. Another distinction is that compartmental models are primarily determined by clinical data whereas compartments in PBPK models are arranged anatomically and are connected to the vasculature, and therefore visualisation of the entire system as a whole is vital. PBPK models also demonstrate far greater complexity by including a vast range of drug independent variables. These include parameters such as age, ethnicity, genetics and disease states. Importantly, this means that PBPK models can be used to investigate potential differences in pharmacokinetics between different populations [145].

Compartments in PBPK models are designed based upon physiological information and its effect on ADME. The complexity may vary depending on the specific tissue or organ of interest. This approach is referred to as bottom-up, in that interactions between the drug and all included components are considered in order to predict the overall pharmacokinetic effect and make effective extrapolations. Each compartment is given a physiologically relevant volume and tissue partition coefficient and linked to the systemic circulation. Despite the discretion regarding the complexity of the model, at a minimum,

the route of administration, metabolism, excretion and storage sites of the drug must be considered for accurate ADME purposes. To aid in model design, a generic whole-body PBPK model (WB-PBPK) offering sufficient complexity is extensively used as a foundation for PBPK studies [146, 147]. WB-PBPK models comprise of 14 compartments that assume instantaneous and homogenous drug distribution. Basic perfusion rates are considered for all compartments, with the exception of dosing and target tissues, which are more complexly defined through introduction of rate-limiting factors, such as metabolising enzymes [138, 148].

As well as relevant systems data, when establishing a PBPK model compound-specific data is also included. This includes physicochemical properties and data on permeability and metabolism from *in vitro* and *in vivo* sources. A wealth of information is available for most drug compounds in the literature and publically available databases and can also be obtained by self-study, for example, by performing *in vitro* cell absorption assays. Provided a limited amount of drug physicochemical information is available, unknown information can even be predicted using ADME software, whilst for some compounds predefined compound profiles may be included in the software [138, 148].

1.10 Thesis Aims and Objectives

There is a global lack of medicines suitable for use in paediatrics and a drive by regulatory bodies to encourage research and development of new suitable products to meet this demand. Reformulation of off-patent drugs into paediatric friendly forms offers an opportunity to provide for this underserved population. The oral route of drug delivery is historically, and remains, the most popular. ODTs offer a novel approach to improve patient compliance and are particularly suitable to paediatrics, although they present a challenge in achieving desirable properties with high dose APIs. FDCs offer another method to enhance compliance due to ease of dosing. Combination of the two in the interests of increased compliance and drug efficacy has so far not been exploited. Of importance during reformulation studies is the demonstration of bioequivalence. PBPK modelling is increasingly employed for this as a powerful tool to predict drug pharmacokinetics by simulating clinical trials.

The overarching aim of the work in this thesis is to engineer solutions to formulate ODT's for high dose drugs and to study their application in the development of fixed dose combinations.

The objectives of the work include:

- To formulate an ODT for flucloxacillin sodium, a generic antibiotic, at doses representing high drug loading and the challenges it represents,
- To explore the use of polymeric film coating of ODTs to overcome formulation challenges,
- To investigate the formulation of FDC ODTs of model generic drugs at paediatrically relevant doses and predict their *in vivo* performance using a PBPK modelling approach.

Chapter 2

Development of a Flucloxacillin Orally Disintegrating Tablet

2.1 Introduction

Flucloxacillin is a narrow spectrum beta-lactam bactericidal antibiotic that shows resistance to hydrolysis by beta-lactamase (penicillinase) producing bacteria such as *Staphylococcus aureus* [149]. Flucloxacillin is indicated for the treatment of infections of the chest, ear, nose, throat, skin and soft tissue. In addition, it is also prescribed for the treatment of endocarditis, osteomyelitis, meningitis, enteritis and septicaemia. It exhibits its bactericidal activity through inhibition of cell wall synthesis, by preventing cross linkage of peptidoglycan polymer chains by binding to penicillin binding proteins. Cell lysis then proceeds via the action of bacterial derived autolytic enzymes [150-152].

Flucloxacillin can be administered intravenously, intramuscularly and orally. For oral administration, flucloxacillin is commercially available under a number of different trade names in the UK including *Floxapen*® (GSK), *Ladropen*® (Berk) and *Fluclomix*® (Ashbourne). These are available as capsules in flucloxacillin's sodium salt form at a dose of 250 mg or 500 mg, and also as powders for reconstitution with water, in sodium or magnesium salt form at 125 mg/5 ml. The oral dose for an adult is 250-500 mg every 6 hours, ½ adult dose every 6 hours for children aged 2-10 years and ¼ adult dose every 6 hours for children aged 1 month to 2 years [153]. Flucloxacillin sodium comes as a white or almost white, crystalline, hygroscopic powder, that is freely soluble in water.

ODTs are an increasingly popular oral dosage form which benefit from improved patient compliance and do not require water for administration, due to disintegration in the oral cavity. ODTs offer greater convenience over reconstituted liquids, which require refrigeration, and enhanced stability, with reconstituted liquids providing a shelf life of only two weeks. Manufacture of ODTs by direct compression is cost effective, offers ease of production involving minimal process steps and allows the use of conventional tableting equipment. Formulation of a directly compressed flucloxacillin ODT is thus an attractive prospect. One significant drawback is the well-recognised bitter, unpalatable taste of flucloxacillin and would be particularly problematic for a dosage form designed to disintegrate in the oral cavity. This is even more problematic when considering dosing children, who are especially unwilling to take bitter medicines [154]. This is evident in powder for reconstitution formulations, which contain an intense sweetener, saccharin sodium, as well as other sweeteners such as sucrose and sorbitol and a variety of flavours.

As mentioned previously, ODTs contain commonly used excipients that are often multifunctional. Correct selection of diluents and disintegrants are particularly important

in creating a successful solid dosage form that shows rapid disintegration, is stable and mechanically strong.

Mannitol is a commonly used excipient in ODT formulations, functioning primarily as a diluent. It is so favoured due to its semi-sweet taste, smooth mouthfeel and negative heat of solution which imparts a cooling sensation in the mouth. It is water soluble, shows good wetting properties and is non-hygroscopic [155]. Polyols show good water solubility and erode in contact with water at the tablet surface, as opposed to disintegration which involves mechanical breakup of the tablet core due to swelling or gas formation [156]. A limitation of mannitol however, is that it displays poor compressibility and compactability. Granulation of mannitol has been shown to improve compactability, by enhancing plasticity and altering particle size and specific surface area [157]. Many different grades of mannitol are commercially available, with smaller particle sizes generating tablets with greater tensile strength due to increased interparticulate bonding [158]

Microcrystalline cellulose (MCC) is one of the most popular excipients in modern tableting. This multifunctional excipient is employed most commonly as a diluent but can also be used to aid disintegration [159], as a binder [160] and has a low lubricant requirement due its low residual die wall pressure [161, 162]. Its popularity is primarily due to its high compactability which allows production of tablets with good hardness. This is due to hydrogen bond formation between MCC particles under compression, which is facilitated by significant plastic deformation which brings a large particle surface area into close contact [162]. The presence of moisture within MCC particles also facilitates hydrogen bonding by acting as a lubricant that aids slipping and flow [163]. Mechanical interlocking of MCC particles is also proposed as being important for formation of strong tablets [164, 165]. The ability of MCC to act as a disintegrant is due to high porosity that enables wicking. Water entry into tablets through capillary pores breaks hydrogen bonds between MCC particles [166]. MCC is partially crystalline (70%) and partially amorphous (30%) and consists of microcrystals and amorphous regions. A number of manufacturers provide different forms of MCC which differ in grade and quality, which may be due to differences in crystallinity [164]. MCC also possesses good flow properties[167].

Crospovidone is a synthetic, water-insoluble cross linked homopolymer of N-vinyl-2-vinylpyrollidone. Crospovidone is commonly employed as a tablet disintegrant and as a binder and has also been used as a solubilising excipient [168]. Crospovidone is most commonly used as a superdisintegrant in formulations prepared by direct compression

and granulation methods, with a typical concentration range of 2-5%. Exceeding this range can cause negative effects on powder flow, hardness and friability [169-171]. Different particle size grades of crospovidone are available, with larger grades reported to enhance flow, disintegration and dissolution, but suffer from lower tablet hardness and increased friability when compared with finer grades [171, 172]. Unlike other superdisintegrants, crospovidone promotes rapid disintegration through a number of mechanisms, namely swelling, wicking and to some extent deformation. The highly porous morphology of crospovidone particles promotes rapid water absorption into tablets and the generation of hydrostatic pressures through volume expansion, which mechanically forces the tablet apart. In contact with water, deformed crospovidone particles recover their original structure and swell to disrupt the tablet core. Due to the high density of crosslinks, crospovidone also benefits from the absence of gel formation when fully hydrated. It is this extensive cross-linking that make crospovidone water insoluble, despite being hydrophilic [173, 174].

This work follows formulation development of a high dose flucloxacillin ODT produced by direct compression. Initial development involved a placebo using mannitol as a major diluent and crospovidone as disintegrant and investigation into the effect of processing conditions. Disintegrant concentration was next investigated before incorporation of flucloxacillin. Inclusion of different disintegrants and disintegrant combinations and reduction of flucloxacillin dose was next explored, in order to improve disintegration. Further refinement involving inclusion of a binder, alteration of blending and lubricant was also carried out.

Sub-sections within this chapter of work show discrete studies which appropriately follow the previous study (based upon findings), with the ultimate aim of producing an ODT formulation that overcomes some of the inherent limitations related to ODTs.

2.2   Materials and Methods

2.2.1   Materials

Flucloxacillin sodium was purchased from Carbone Scientific (UK). D-mannitol, D-sorbitol and magnesium stearate were purchased from Sigma –Aldrich (UK). Polyplasdone XL-10 was obtained from ISP (Switzerland). Avicel PH102 (MCC) was obtained from FMC Biopolymer (USA). Primellose (croscarmellose sodium) and Primojel (sodium starch glycolate) were gifts from DFE Pharma (Germany). Polyplasdone XL-10 (crospovidone) was obtained from ISP (Switzerland). Aerosil 200 Pharma (colloidal silicon dioxide) was obtained from Evonik Industries (Germany).

2.2.2   Tablet Formation

Direct compression of tablets (500 mg) at a compaction force of 10 kN (1 ton) or higher was performed using an Atlas T8 automatic press (SPECAC, UK). A manual uniaxial hydraulic press (SPECAC, UK) was used for production of tablets below a compaction force of 10 kN. A 13mm round, flat faced die was used for tablet production. All tablets were produced under ambient conditions and tablet characterisation was carried out immediately post compression

2.2.3   Angle of Repose

Angle of repose was calculated using the procedure outlined in the British Pharmacopeia [175]. Approximately 20 g powder was poured through a funnel onto a vibration-free base. The funnel was placed approximately 2-4 cm from the peak of the powder cone, in order to minimise the impact of falling powder on the cone formation. The height (h) and the diameter (d) of the cone was measured in triplicate and used to calculate the mean angle of repose, using the equation:

$$tan\,(\alpha)\;=\;h\,/\,(0.5\,x\,d)$$

Angle parameters are given in Table 2.1. A flow rating of fair or better would be acceptable.

Table 2.1 Parameters for angle of repose to assess powder flow. A flow rating of fair or better shows acceptable flow for high speed tableting.

Angle of Repose (degrees)	Flow
25-30	Excellent
31-35	Good
36-40	Fair - aid not needed
41-45	Passable - may hang up
46-55	Poor - must agitate/vibrate
56-65	Very poor
>66	Very, very poor

2.2.4 Bulk and Apparent Particle Density and Porosity

Particle density was measured using a helium pycnometer (Multipycnometer, Quantochrome Instruments, UK) on pre weighed tablets whose volumes had been calculated, based on Archimedes displacement principle. Porosity was calculated using the equation [155]:

$$\varepsilon = 100(1 - \frac{\rho_d}{\rho_t})$$

Where ε is the porosity and where ρ_d and ρ_t are the bulk density and true density, respectively. Porosity was measured in triplicates at each compaction force.

2.2.5 Carr's Index and Hausner Ratio

Powder flow was also assessed by analysis of powder bulk and tapped densities. Approximately 20 g powder was added to a 250 ml volumetric cylinder and the bulk volume recorded. The cylinder was subjected to 5 taps, 10 taps, 500 taps and 1250 taps sequentially until the point that no change in density occurred and the tapped volume was recorded. The bulk density and tapped density were then calculated by: density =

mass of powder / volume. Powder flow was assessed using the values generated by the Carr's Index (Compressibility Index) and the Hausner ratio [176, 177]:

$$\text{Carr's Index} = \frac{(Tapped\ density - B\quad density)}{Tapped\ density} * 100$$

$$\text{Hausner Ratio} = \frac{Tapped\ density}{Bulk\ density}$$

Compressibility index and Hausner ratio parameters are given in Table 2.2. A flow rating of fair or better would be acceptable.

Table 2.2 Parameters for compressibility index and Hausner ratio for assessment of powder flow

Compressibility Index (%)	Flow	Hausner Ratio
≤10	Excellent	1-1.11
11-15	Good	1.12-1.18
16-20	Fair	1.19-1.25
21-25	Passable	1.26-1.34
26-31	Poor	1.35-1.45
32-37	Very poor	1.46-1.59
>38	Very, very poor	>1.6

2.2.6   Disintegration Time

The disintegration time was measured in vitro using US pharmacopeia monograph ([701] disintegration). The disintegration apparatus used was Erweka ZT3, Appartebau, GMBH (Germany) and 800 ml distilled water maintained at 37˚C was used as the disintegration media. Tablets were measured individually by placing in the basket rack and the time taken for the tablets to disintegrate without leaving any solid residue in the rack, recorded. Disintegration time was measured in triplicates at each compaction force.

2.2.7 Fourier Transform Infrared Spectroscopy

FTIR spectroscopy was performed on powders using a Nicolet IS5 FTIR spectrometer equipped with an iD5 attenuated total reflectance (ATR) diamond from Thermo Fisher Scientific (USA). A small sample of powder was placed on the lens and the FTIR spectra was measured in the 4000-500 cm^{-1} regions. Analysis was carried out using OMNIC Specta Software (USA).

2.2.8 Friability

Tablet friability was determined on 6 tablets using a friabilator from J. Engelsmann AG (Germany). Tablets were placed inside the drum and rotated at 25 rpm, for a total of 100 revolutions. Tablet dust was removed pre and post testing to remove excess powder that would contribute to tablet mass. Friability was calculated and expressed as % tablet weight loss from initial tablet weight.

2.2.9 Hardness and Tensile Strength Measurements

A tablet hardness tester model TBF 1000 (Copley Scientific, UK) was used to measure the radial crushing strength (hardness) of tablets in triplicates. This data was then used to calculate the tensile strength of the tablets using the equation [178]:

$$\sigma = \frac{2F_c}{\pi dt}$$

Where σ is the tensile strength, F_c is the force needed to crush the tablet, d is the tablet diameter and t the thickness of the tablet.

2.2.10 Heckel Analysis

Heckel analysis to measure the compaction characteristics of the powders was performed out-of-die using the Heckel equation [179]:

$$ln\,(1/(1-D) \;=\; KP \;+\; A$$

Where D is the relative density of the tablet at pressure P. Plotting $\ln(1/(1-D)$ against the applied pressure P yields a Heckel plot, where the gradient of the linear portion is represented as K and the intersect is A. $1/K$ is used to calculate the mean yield pressure (Py) which is the pressure at which plastic deformation of the powder occurs. Mean yield pressure is therefore inversely related to the ability of a powder to plastically deform [180].

2.2.11 Particle Size Distribution

Particle size distribution was carried out using a particle size analyser Helos/BF and dry disperser RODOS with feeder VIBRI/L from Sympatec (Germany). The lens measuring range for the instrument was 0 to 175 µm. Approximately 1 g powder was added to the feeder tray and the run commenced at a trigger condition of 2% Copt for 10 s with a powder dispensing pressure of 2 bar. Particle size distribution curves were electronically produced and the volume mean diameter (VMD) recorded.

2.2.12 Scanning Electron Microscopy (SEM)

A Cambridge Instruments Stereoscan 90 (UK) SEM was used to study tablet surface morphology. Tablet samples were prepared by sectioning thin vertical cross-sectional slices of punched tablets using a razor, which were then loaded onto a universal holder. The samples were coated with a layer of gold using a Polaron SC500 sputter coater (Polaron Equipment, UK) at 20 mA for 6 mins at low vacuum in the presence of argon gas.

2.2.13 Statistical Analysis

Using IBM SPSS statistics 20 software, one-way ANOVA was conducted on the data for both compaction force and dwell time factors. Post hoc analysis was performed using Tukey's method, to ascertain significant differences between different compaction forces and dwell times.

2.3   Studying the Effect of Compaction Force and Dwell Time Variation

In this study, tablets composed of a simple formulation containing mannitol (diluent), crospovidone (superdisintegrant) and Mg stearate (lubricant and anti-adherent), were assessed at a range of compaction forces and dwell times. The tablets were formulated based on the criteria of an *in vitro* disintegration time of less than 30 s, as stipulated by the FDA [181]. This differs from a desired disintegration time of less than 3 min, outlined by the European Pharmacopeia [182]. The tablets were required to possess sufficient mechanical strength to withstand storage and handling.

2.3.1   ODT Preparation

Tablets (500 mg) consisting of mannitol (94%), crospovidone (5%) and Mg stearate (1%) were produced by direct compression. Mg stearate was mixed with the powder for a short time to prevent over-mixing, as this is known to negatively impact its ability as a lubricant, decrease tablet hardness and increase drug disintegration time [183]. The powder mixture was compressed at forces of 10, 20, 30, 40, 50 and 60 kN at a dwell time of 30 s. Tablets of the individual excipients (500 mg) mannitol and crospovidone were produced in the same manner, at forces of 5, 10, 15, 20, 25, 30 and 50 kN and 5% w/v Mg stearate suspended in acetone was applied to both the upper and lower punch as an anti-adhesive.

2.3.2   Results

2.3.2.1   Tablet Characterisation

Tablet characterisation was performed at each stage of development to assess tablet properties and guide development. Tablet compressibility, compactability and tabletability analysis were initially performed to provide information on the major excipients and their suitability and shortcomings with regard to this dosage form. These are important characteristics and determine the success of producing a mechanically robust tablet.

2.3.2.1.1   Compressibility

The compressibility of a material is defined as its ability to reduce in volume under pressure during loading [46]. In the context of solid dosage forms this is important as compressibility is a determinant of tablet strength, with highly compressible powders having enhanced interparticulate bonding due to close particle proximity [184, 185]. Powder compression is accompanied by a concurrent reduction in porosity, another important consideration with respect to directly compressed ODTs. The rapid disintegration of ODTs is often due in part to high porosity and resultant high specific surface area. It is for this reason that lyophilised tablets provide such rapid disintegration [32, 54]. Thus it is important to form a balance between porosity and tablet hardness, to produce tablets with sufficient structural integrity, yet with the ability to disintegrate rapidly. This can be achieved through careful selection of excipients and alteration of process parameters, for example through modifying compaction force.

Powder compressibility was assessed at a range of pressures (Figure 2.1) by measuring tablet porosity using the out of die method. Compressibility increased as compaction force exceeded 10 kN, with porosity values at 20, 30, 40 and 50 kN ranging from 0.49 to 0.50 showing no statistically significant differences ($p > 0.05$). Powder compressibility unexpectedly decreased at the greatest compaction force of 60 kN, with a porosity of 0.53 ± 0.01, which was not deemed different to the porosity demonstrated at the lowest compaction force of 10 kN.
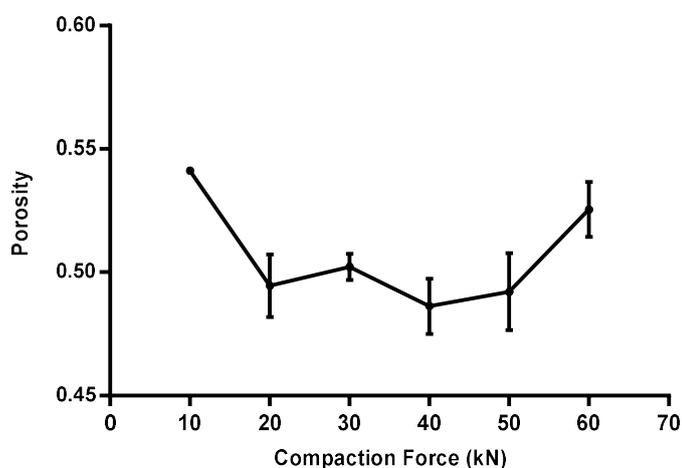
Figure 2.1 Porosity as a function of compaction force, showing compressibility of the powder mix. ODTs (500mg tablets) consisting of mannitol (94%), crospovidone (5%) and Mg stearate (1%) underwent direct compression at a range of forces with a dwell time of 30 s (mean ±SD, n=3).

2.3.2.1.2 Compactability

The compactability of a powder is its ability to yield and compact into a tablet with sufficient strength [186] and is assessed by plotting tensile strength against porosity [187]. Powder characteristics and compaction force are important factors in compactability, as bond formation through close contact under compression is necessary for formation of strong tablets [185]. Indeed, it is the ability of a powder to form strong particle-particle interactions (consolidate) under compression, that defines powder compactability. Ideally a mixture will exhibit high tensile strength, ensuring that the tablet formed is able to withstand storage and handling. For ODTs, high porosity is a key determinant of rapid disintegration times [42] and therefore powder compactability is of significant importance.

The compactability profile of the powder formulation is shown in Figure 2.2. Linear regression shows a general reduction in tensile strength with increased porosity. At 30 kN compaction force tablets demonstrated intermediate porosity and tensile strength and as such for this formulation 30 kN compaction force is suitable.
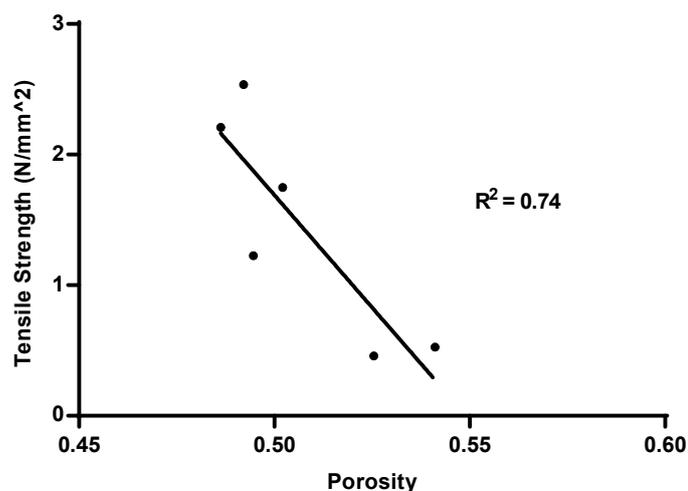
Figure 2.2 Tablet tensile strength (N/mm^2) against porosity to show compactability of the powder mixture. ODTs (500mg tablets) consisting of mannitol (94%), crospovidone (5%) and Mg stearate (1%) underwent direct compression at a range of forces with a dwell time of 30 s (mean ±SD, n=3).

2.3.2.1.3 Tabletability

Tabletability concerns the mechanical properties of a tablet upon compaction and is assessed by plotting tensile strength against compaction force [188]. Generally an increase in compaction force results in increased tablet crushing strength, exponentially at first and then plateauing at higher forces [189].

The data (Figure 2.3) shows a strong correlation between increases in tablet tensile strength with increased compaction force up to a compaction force of 50 kN, with non-linear regression giving an R^2 value of 0.99. This gave a maximum tablet tensile strength of 2.54 ± 0.15 N/mm^2. Tablet tensile strength dropped drastically to 0.46 ± 0.06 N/mm^2 at the highest compaction force of 60 kN. This drop in tensile strength was not statistically different than the tensile strength displayed by tablets at 10 kN compaction. This coincides with the increase in porosity at 60 kN.
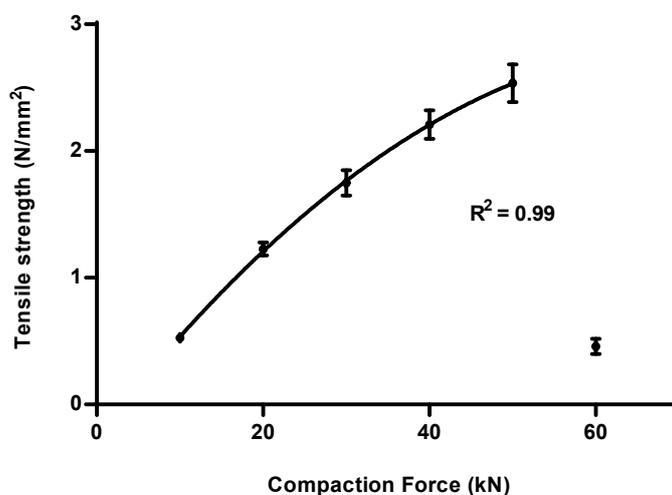
Figure 2.3 Tablet tensile strength (N/mm^2) against compaction force to demonstrate tabletability. ODTs (500mg tablets) consisting of mannitol (94%), crospovidone (5%) and Mg stearate (1%) underwent direct compression at a range of forces with a dwell time of 30 s (mean ±SD, n=3).

2.3.2.2   Heckel Analysis

To ascertain the mechanism of powder densification, Heckel analysis was performed on the excipients mannitol and crospovidone (Figure 2.4 and Figure 2.5, respectively). Heckel analysis is a tool for assessing the plasticity of a powder, that is, how readily a material will deform plastically under pressure. It gives a yield pressure value that is calculated from porosity data at a variety of compaction forces. A low yield pressure signifies high plasticity. Two techniques are commonly used in Heckel analysis, known as the out-of-die method and the in-die method. Since particles deform elastically under pressure, the out-of-die method provides a more accurate representation of powder compaction and consolidation, as elastic recovery after cessation of compression alters porosity [190].

Powders that deform plastically, as opposed to elastically, are known to produce stronger tablets and are associated with good compactability and reduced fragmentation [191]. Mannitol showed a high mean yield pressure of 2000.00 MPa, indicating poor plasticity, a value which was consistent with findings in the same lab [165]. In contrast, crospovidone appeared to behave more plastically, with a P_Y of 434.78 MPa and an R^2 value of 0.99.

90
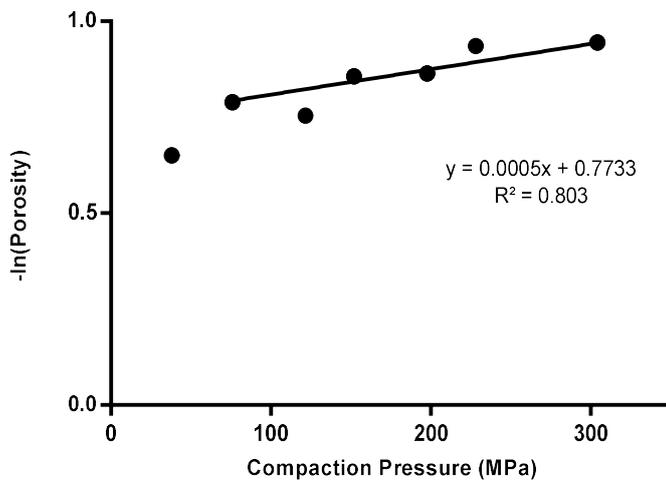
Figure 2.4 Heckel plot for mannitol using the out-of-die method, derived from relative density and compaction pressure. A gradient of the straight portion of the graph, 0.0005 corresponds to a Py (MPa) of 2000 (mean, n=3).
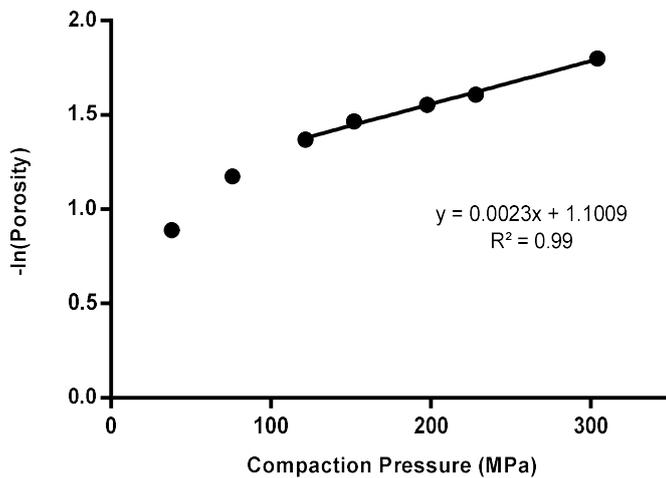
Figure 2.5 Heckel plot for crospovidone using the out-of-die method, derived from relative density and compaction pressure. A gradient of the straight portion of the graph, 0.0023, corresponds to a Py (MPa) of 434.78 (mean, n=3).

2.3.2.3 Friability

The extent of tablet friability is an important consideration during formulation of solid dosage forms. Tablet friability tests the likely percentage of the initial mass of a tablet lost as a result of chipping during transit. It is calculated by inflicting tablets to 100 cycles in a rotating drum. A weight loss greater than 1% is unacceptable, as stipulated by USP 29 [192]. Friability testing results are show in Figure 2.6. There is a linear decrease in tablet friability between 10 and 30 kN which plateaus thereafter, suggesting that at 30 kN, compaction force ceases to be the rate limiting factor for friability. As a result, to improve friability other approaches such as altering the excipient formulation or changing the procedure/technologies used for production should be explored.

2.3.2.4 Disintegration Time

Tablet disintegration time is of prime importance when formulating ODTs due to the requirement for rapid disintegration. Guidelines for ODTs require a disintegration of 3 mins or less, as stated by the European Pharmacopeia [182], whereas the FDA stipulate disintegration within 30 s [181]. All tablets displayed rapid disintegration within 30 s (Figure 2.6). Increasing compaction force had no effect on disintegration time. Disintegration time was therefore also unaffected by any changes in tablet porosity or hardness, suggesting that the choice of excipients determine rapid disintegration. This is likely primarily due to the wicking action and swelling ability of crospovidone. In addition, the high wettability and water solubility of mannitol and the good porosity displayed by the tablets will be important factors in rapid disintegration.
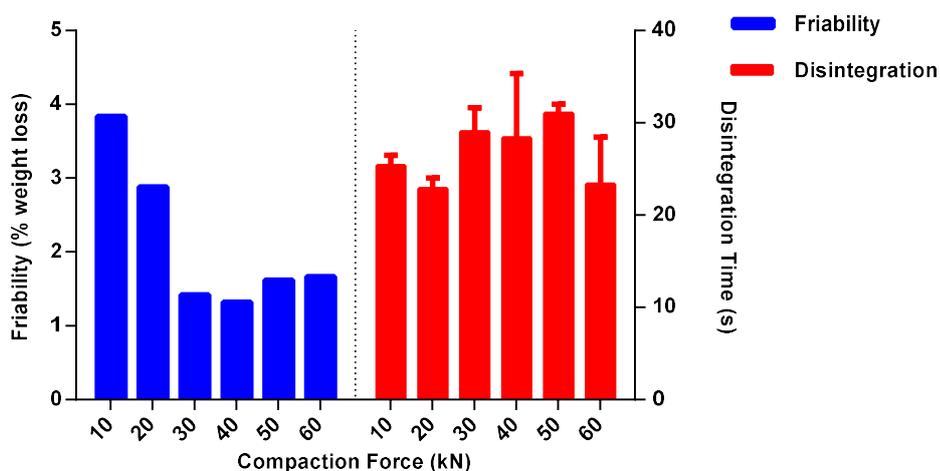
Figure 2.6 Friability (% weight loss) and disintegration time (s) against compaction force. ODTs (500mg) consisting of mannitol (94%), crospovidone (5%) and Mg stearate (1%) underwent direct compression at a range of forces with a dwell time of 30 s (mean ±SD, n=6).

2.3.2.5 Effect of Dwell Time

In order to test the effect of dwell time on tablet characteristics, tablets were produced at dwell times of 5, 10, 15 and 20 s. An intermediate compaction force of 30 kN was chosen, as this showed intermediate porosity and tensile strength when compared to tablets at other compaction forces. Tablet hardness, tensile strength, porosity and disintegration time were all measured.

The effect of dwell time on tablet characteristics is shown in Table 2.3. No difference (p>0.05) was seen with changes in dwell time for tablet hardness and disintegration time. Porosity however decreased as the dwell time increased past 5 s (p<0.05), after which no change was observed. High porosity is desirable to improve disintegration time. Since porosity was greatest at a 5 s dwell time and tablet hardness, tensile strength and disintegration time were not adversely affected, a shorter dwell time is preferable. Friability decreased after a dwell time of 5 s and remained constant from 10 to 20 s.

Table 2.3 Effect of dwell time on tablet characteristics ODTs (500mg tablets) consisting of mannitol (94%), crospovidone (5%) and Mg stearate (1%) underwent direct compression at 30 kN (3 tons) at a range of dwell times (mean ± SD, n=3).

Dwell Time (s)	Hardness (N)	Disintegration Time (s)	Porosity	Friability (%)
5	100.27 ± 4.03	23.00 ± 1.00	0.54 ± 0.01	2.32
10	102.87 ± 2.02	23.67 ± 1.53	0.49 ± 0.01	1.81
15	100.20 ± 0.85	25.00 ± 1.00	0.50 ± 0.01	1.77
20	101.10 ± 1.83	24.33 ± 1.53	0.49 ± 0.01	1.69

2.3.2.6 Tablet Morphology

Morphological analysis of tablets was performed using SEM (Figure 2.7). Tablets produced at a compaction force of 10 kN (low), 40 kN (intermediate) and 60 kN (high) were chosen for analysis. Tablets compacted at 60 kN had previously displayed unexpected porosity and hardness values.

At 10 kN the tablet shows porous structures and round edges, suggesting plastic deformation. At 40 kN the tablet appears less porous and the edges are sharper. This is consistent with the decrease in porosity seen when compaction force is increased past 10 kN. At 60 kN the particles no longer appear rounded, showing an elongated needle shaped morphology that was not apparent at lower compaction forces. This change seen at 60 kN is likely due to fragmentation of the powder mixture and may account for the observed changes in porosity and tablet hardness.
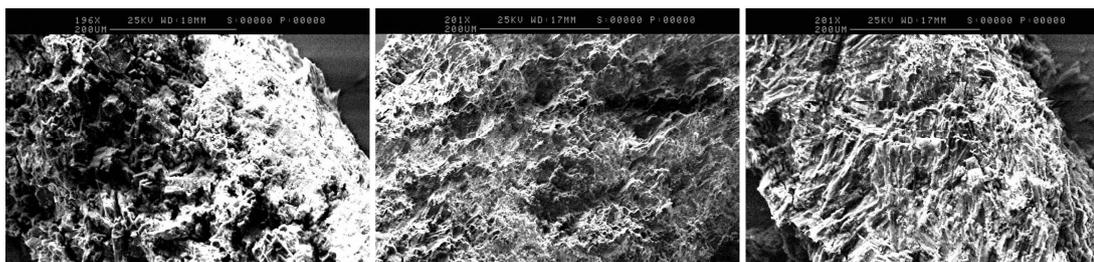
Figure 2.7 SEM 200x magnification of ODT tablet fragments. Tablets consisted of mannitol (94%), crospovidone (5%) and Mg stearate (1%) and were produced by direct compression at a dwell time of 30 s. The images show tablets compacted at a force of 10 kN, 40 kN and 60 kN respectively, from left to right.

2.3.3   Discussion

Overall, the disintegration time of tablets at all compaction forces was acceptable for ODTs at less than 30 s, as stated by the FDA. Only small changes in porosity were seen when the compaction force was altered, indicating that the porosity shown was an intrinsic characteristic of the powder mixture. Indeed, other groups have reported that hard crospovidone particles resist deformation in order to impart porosity to a tablet [193]. For further development of this formulation, it will be important to optimise the concentration of crospovidone. Superdisintegrants possess critical concentrations, below which disintegration time decreases and above which disintegration time stays consistent or may increase [57]. Optimising the concentration of crospovidone may therefore improve disintegration times and will also impact on the structural characteristics of the formulation.

The formulation showed good hardness, with tensile strength rising steadily up to a compaction force of 50 kN. Increased compaction force increases interparticular contact and promotes bond formation. Powders that deform plastically are associated with formation of better compacts. Fragmentation however, is also known to be an important mechanism of bond formation under compression. Particle fragmentation creates new surfaces and it is thus believed that fragmentation determines the number of bonds in a given cross-section; conversely, it is believed that deformation determines the strength of bonds [194]. At 60 kN there is a substantial drop in hardness, which coincides with an increase in porosity, likely due to fragmentation of the powder. Plastically deforming powders typically show mean P_y of 40-135 Mpa, whereas powders that primarily

consolidate by fragmentation show yield pressures in the range of 340-430 Mpa [186]. Both mannitol and crospovidone were shown to deform primarily by fragmentation. Indeed, mannitol has been shown to fragment under compaction, causing an increase in the population of small pores and decrease in large pores, with a concomitant increase in powder surface area [195]. The same group have reported an increase in tablet breaking force after mannitol fragmentation. Fragmentation of mannitol likely occurred at low compaction forces and therefore the spike in porosity at 60 kN is likely due to the more plastic crospovidone. Despite the increase in number of interparticulate bonds as a result of fragmentation, tensile strength decreases at 60 kN. This may be due to a drop in deformation of crospovidone particles upon fragmentation and an associated reduction in bonding strength. This reduction in bond strength can be seen by an increase in porosity, large reduction in tensile strength and also an increase in tablet volume, when compared to tablets compacted at 50 kN. All of this would suggest that strong bonding interactions are important in generating compacts for this formulation, and fragmentation of crospovidone at high compaction force is detrimental.

The main concern with this formulation is high friability, which exceeds 1% weight loss. This is likely due to the poor compactability and low plasticity of mannitol. Mannitol's needle shape is reported to be prone to fragmentation, resulting in a high die wall friction and poorly formed compacts with high friability [196, 197]. The use of different excipients with greater plasticity should therefore be investigated to improve friability. Incorporation of binders could be explored to improve compactability and friability, although at the detriment to disintegration time. Other diluents such as polyols and sugars have been incorporated into mannitol formulations to improve poor compactability and friability [48]. The incorporation of multiple diluents may therefore be another strategy for improving the friability of the tablets. Also, the addition of water-insoluble inorganic excipients should be considered, as these have been shown to impart good physical resistance, whilst not undermining disintegration times [35].

Dwell time was shown to have no effect on tablet hardness and disintegration time. An increase in porosity was seen at a dwell time of 5 s, which is favourable as this should aid in tablet disintegration. This was, however, associated with an apparent increase in friability. Despite this, since mass production of tablets would favour short dwell times and due to the other strategies that can be employed to improve friability, a 5 s dwell time would seem suitable for further formulation development.

2.4   Crospovidone as a Disintegrant

Crospovidone was included in a mannitol based, directly compressed ODT as a disintegrant/binder at a range of concentrations (1% to 5%) and compaction pressures (0.5 to 2 tons). The effect that incorporation of crospovidone had on tablet properties was investigated and the specific properties of crospovidone were also examined. Polypasdone XL-10 was the selected grade due to its small particle size [198], which it was hoped would improve tablet strength, as mannitol displays poor compaction properties.

Powder blends were prepared at a range of concentrations of crospovidone, see Table 2.4. Mannitol and crospovidone were blended for 5 mins, Mg stearate added and then mixed for a further 1 min. ODTs were compressed at a range of forces: 5 kN (0.5 ton), 10 kN (1.0 ton) and 20kN (2.0 ton) at a dwell time of 30 s. Target tablet weight was 500mg.

Table 2.4 Formulation of ODTs comprising mannitol as a diluent, increasing concentrations of crospovidone as a disintegrant and 1% Mg stearate as an antiadhesive and lubricant. Powder underwent direct compression at compaction forces of 0.5, 1 and 2 tons, with a dwell time of 30 s.

Crospovidone (% w/w)	Mg Stearate (% w/w)	Mannitol (% w/w)
0	1	99
1	1	98
2	1	97
3	1	96
5	1	94

2.4.1 Results

2.4.1.1 Powder Flow

The flowability of crospovidone was assessed (Table 2.5) by measuring the angle of repose and bulk and tapped densities to calculate the compressibility index and Hausner ratio. The angle of repose data indicates a good flow, whereas the compressibility index and Hausner ratio indicate poor flow. This is likely due to the small particle size of this grade of crospovidone (XL-10). An improvement in flow with grades of a larger particle size has been reported [198].

Table 2.5 Angle of repose, bulk density, tapped density, Hausner ratio and compressibility index of crospovidone (Polyplasdone XL-10), to show flowability. Flow ratings of fair or better are suitable for high speed tableting.

Angle of Repose	Bulk Density (g/cm3)	Tapped Density (g/cm3)	Hausner Ratio	Compressibility Index
31.22 ± 1.95 - Good	0.30 ± .00	0.44 ± .01	1.47 ± 0.04 - Very Poor	32.14 ± 1.77 - Very Poor

2.4.1.2 Particle Size Distribution

Particle size distribution data is shown in Table 2.6 and Figure 2.8. Polyplasdone XL-10 displayed a monomodal distribution with a slight negative skew, indicating that a small amount of the powder consisted of very small particles (X10 8.37 ± 0.18). The small average particle size, VMD 26.53 ± 1.03, would explain the poor flow seen with this powder

Table 2.6 Particle size distribution described using the polydispersity index and volume mean diameter (VMD) for Polyplasdone XL-10 using HELOS laser diffraction technique. Particle sizes are given in μm (Mean ± SD, n=3)

Particle Size Parameter	Polyplasdone XL-10 Particle Size (μm)
X10	8.37 ± 0.18
X50	22.4 ± 0.68
X90	50.67 ± 2.24
X99	84.48 ± 5.44
VMD	26.53 ± 1.03
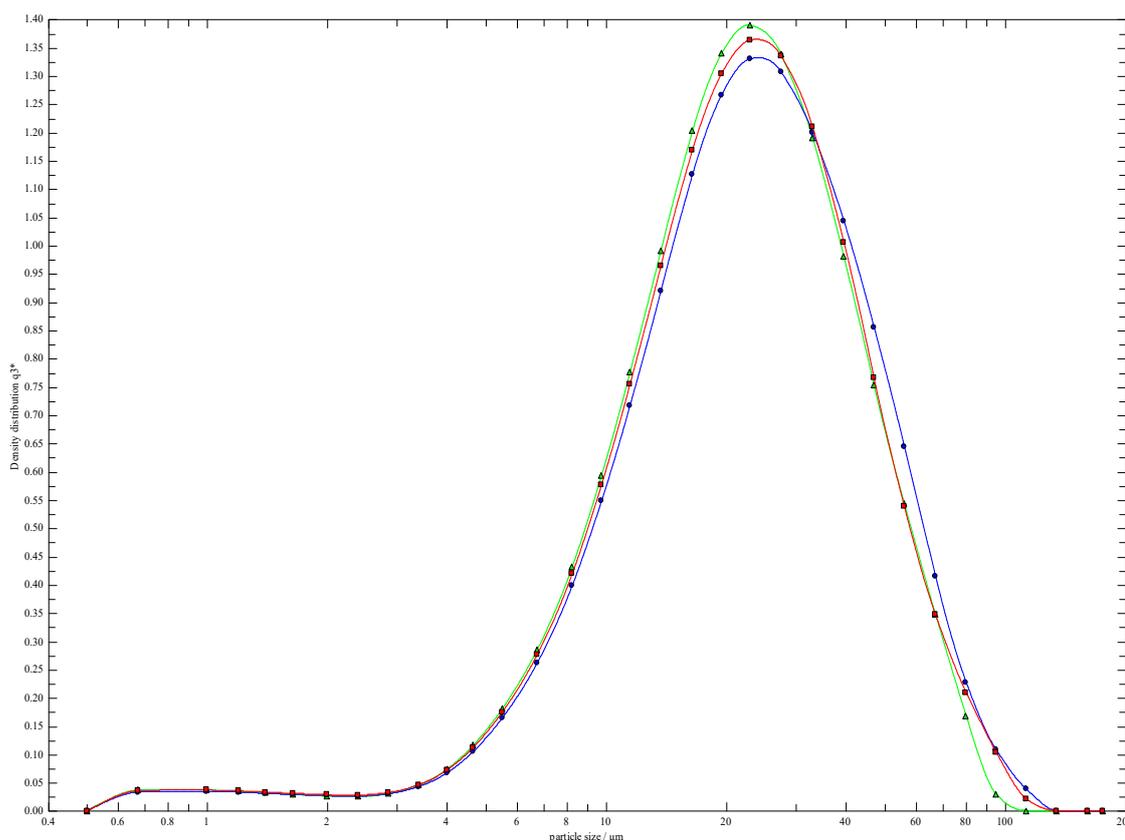
Figure 2.8 Particle size distribution of Polyplasdone XL-10 powder using HELOS laser diffraction technique (n=3)

2.4.1.3   Disintegration Time

Figure 2.10 gives the disintegration times of the mannitol based ODTs with increasing concentrations of crospovidone. The results for 0% crospovidone tablets have been excluded as they are drastically higher than those shown, with values for disintegration time of 872.67 ± 49.1, 762.33 ± 35.3 and 585.33 ± 44.12 s, with increasing compaction force, respectively. The disintegration time for all tablets containing crospovidone was within the 3 min margin as specified by the European Pharmacopoeia [199] and all tablets at the highest compaction force disintegrated within 30 s, as recommended by the FDA. Disintegration time was enhanced by increasing compaction force ($p < 0.05$) with most rapid disintegration shown at 2 tons ($p < 0.005$), as calculated by two-way ANOVA. No effect was seen with increase in crospovidone concentration, however the inclusion of crospovidone showed a drastic decrease in disintegration time ($p < 0.0001$).

2.4.1.4   Tablet Hardness

Tablet hardness (Figure 2.9) increased with increased compaction force at 1 ton ($p < 0.05$) and markedly at 2 ton ($p < 0.0001$), indicating that an increase in compaction force facilitates interparticulate bonding by bringing the particles closer together in contact. Crospovidone at a concentration of 5% produced significantly weaker tablets ($p < 0.0001$) when compared with the control and all other concentrations. Despite crospovidone's functionality as a binder, it appears that at higher concentrations this binding activity is compromised.
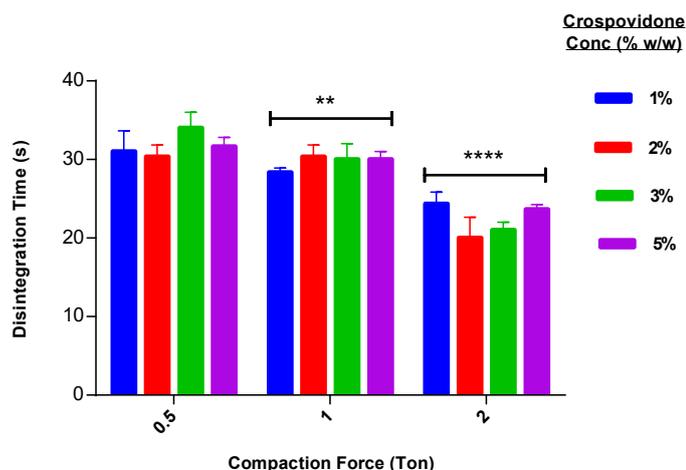
Figure 2.10 Disintegration time (s) as a function of compaction force. ODTs (500mg tablets) consisted of mannitol as a diluent, Mg stearate (1%) and crospovidone as a disintegrant at a range of concentrations up to 5%. Direct compression was performed at a range of compaction forces with a dwell time of 30 s (mean ±SD, n=3, ** ($P<0.01$) and **** ($P<0.0001$) compared to 0.5 ton
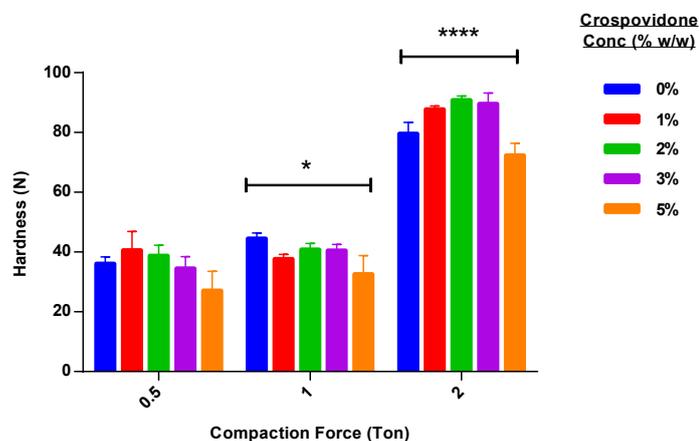
Figure 2.9 Tablet hardness (N) as a function of compression force. ODTs (500mg tablets) consisted of mannitol as a diluent, Mg stearate (1%) and crospovidone as a disintegrant at a range of concentrations up to 5%. Direct compression was performed at a range of compaction forces with a dwell time of 30 s (mean ±SD, n=3, * ($P<0.05$) and **** ($P<0.0001$) compared to 0.5 ton

2.4.1.5 Friability

Friability (Figure 2.11) generally showed a linear decrease with increase in compaction force, with R^2 values ranging from 0.98-0.75. All tablets were above an acceptable weight loss of 1%. There was no clear trend between crospovidone concentration and friability. At 0.5 ton however, 5% crospovidone produced tablets with dramatically higher friability of 8.54%.

2.4.1.6 Porosity

The results showed a decrease in porosity (Figure 2.12) with increased compaction force. Porosity decreased significantly at 1 ton ($p<0.0001$), with a less pronounced decrease when compaction force increased further to 2 ton ($p<0.005$). At concentrations of 0% and 1% crospovidone, the tablets displayed significantly lower porosity ($p<0.0005$). At higher concentrations of 2%, 3% and 5% porosity at 2 tons compaction the tablets showed the same level of porosity. Overall, the tablets containing 3% and 5% crospovidone showed a greater porosity than the 2% crospovidone tablets across all compaction forces. The established view that crospovidone enhances porosity is thus supported by the results shown here.
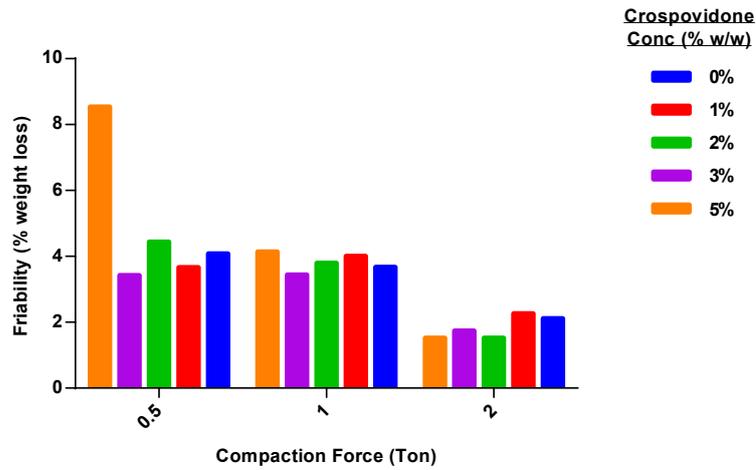
Figure 2.11 Friability (% weight loss) as a function of compression force. ODTs (500mg tablets) consisted of mannitol as a diluent, Mg stearate (1%) and crospovidone as a disintegrant at a range of concentrations up to 5%. Direct compression was performed at a range of compaction forces with a dwell time of 30 s (mean ±SD, n=6).
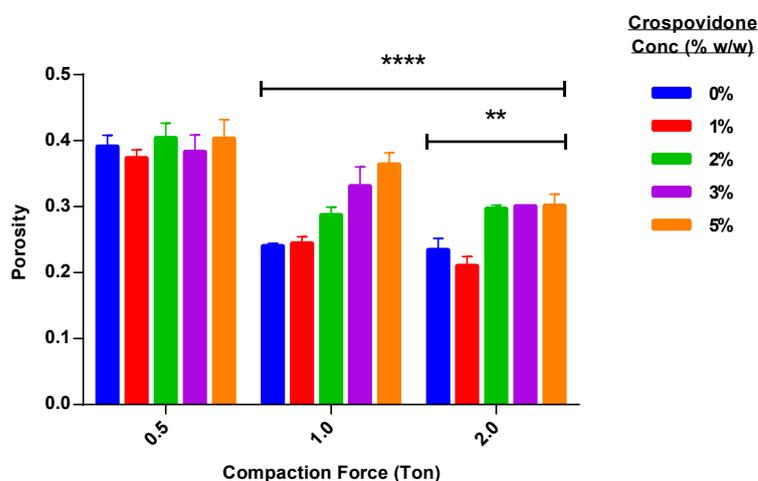
Figure 2.12 Compressibility profile comparing porosity against compression force. ODTs (500mg tablets) consisted of mannitol as a diluent, Mg stearate (1%) and crospovidone as a disintegrant at a range of concentrations up to 5%. Direct compression was performed at a range of compaction forces with a dwell time of 30 s (mean ±SD, n=3, **** (P<0.0001) compared to 0.5 ton, ** (P<0.01) compared to 1 ton

2.4.1.7 FTIR

FTIR spectra of Polyplasdone XL-10 (Figure 2.13) was consistent with the fingerprint region shown for crospovidone [158]. There is a strong absorption between 3700 and 2800 cm^{-1} due to high moisture content as liquid water absorbs strongly in this region, known as region A, due to its stretching vibrations [200]. High moisture content is reinforced by the carbonyl band at 1651.20 cm^{-1}, which is shifted from an expected value of 1667 to 1671.5 cm^{-1}, as a result of hydrogen bonding from the OH moiety [158, 201].
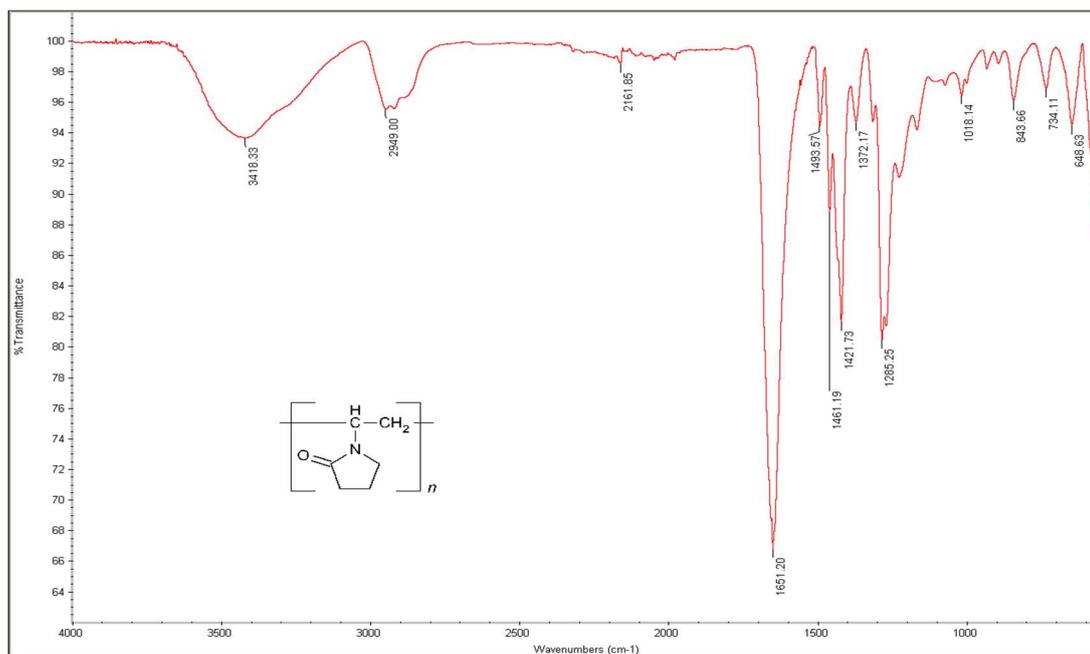
Figure 2.13 FTIR spectra for Polyplasdone XL-10, with the molecular structure of crospovidone also shown.

2.4.2   Discussion

Crospovidone shows poor flow as a result of cohesiveness due to a small particle size and this may necessitate the need for a glidant in formulations containing the disintegrant. Particle size of crospovidone is an important consideration since different grades convey different tablet properties [172]. Inclusion of crospovidone at as little as 1% w/w drastically improved disintegration time, demonstrating its exceptional ability as a disintegrant. Its propensity as a binder is also evident, as it improved tablet hardness upon inclusion and was optimal at concentrations of 2-3%. There was little difference in fact between tablets containing 2% and 3% crospovidone which also displayed optimal hardness and relatively high porosity. Beyond these concentrations tablet hardness and disintegration time suffers. The increase in porosity of tablets containing crospovidone is representative of its mechanism of disintegration by wicking. Similarly, a seemingly counterintuitive decrease in disintegration time with increased compaction force may be adequately explained by crospovidone's ability to swell, since a higher force can be exerted as a result of swelling when particles are less porous and packed tightly together. Finally, FTIR spectra appeared indicated the presence of water in the crospovidone powder possibly as a result of exposure to moisture in the air. A more anhydrous crospovidone powder may improve disintegration times.

Both mannitol and crospovidone demonstrated favourable properties for ODT formation, particularly a rapid disintegration and good hardness. Inclusion of flucloxacillin into this ODT formulation was next explored, and was expected to drastically alter ODT characteristics due the high doses used.

The next step of development involved including flucloxacillin in order to assess its influence over the ODT formulation developed thus far.

2.5   Incorporation of Flucloxacillin

A formulation for a 500 mg orally disintegrating tablet (ODT) containing 250 mg dose of the antibiotic flucloxacillin was designed (Table 2.7), for production via direct compression. Inclusion of mannitol as a diluent in preliminary studies inferred good disintegration times due to its high water solubility. Mannitol displays undesirable mechanical properties however, namely brittle fracture resulting in high friability. MCC (Avicel PH102) is a hugely popular binder/diluent and has been used in ODTs produced via direct compression. It benefits by enhancing aqueous penetration regardless of pore size, a trait which is very attractive for an ODT [202]. MCC has acceptable flow properties for high speed tableting [203] and it was hoped would improve the relatively poor flow exhibited by mannitol, which is cohesive as a result of its small size and morphology [158]. Mannitol showed poor compactability in preliminary studies with a tendency to fragment. Various polyols, have been used in combination with mannitol to improve its compactability properties [204] and sorbitol was explored here. Sorbitol also benefits from a sweet taste and cooling sensation in the mouth and is used as a sweetening agent and diluent in sugar-free powder for reconstitution formulations, however it does suffer from being hygroscopic [205]. In addition, colloidal silicon dioxide was included as a glidant, aspartame as an intense sweetener due to the bitter taste of the API and Mg stearate as an anti-adhesive and lubricant.

API and all excipients, with the exception of Mg stearate, were blended for 5 mins at which point Mg stearate was added and blending continued for a further 1 min. Compression was carried out at 30 kN at a dwell time of 5 s.

Table 2.7 Formulation of a 250 mg flucloxacillin ODT (500 mg). API and excipients are listed alongside their concentration % w/w. Powders underwent direct compression at a force of 30 kN with a dwell time of 5 s.

API/Excipient	% w/w
Flucloxacillin sodium	54.5
MCC	18.5
Mannitol	10
Sorbitol	10

Crospovidone	4
Aspartame	2
Colloidal silicon dioxide	0.5
Mg stearate	0.5

2.5.1   Results

2.5.1.1   Assessment of Flow

The flow properties of flucloxacillin sodium were investigated using angle of repose, Carr's index and Hausner ratio (Table 2.8). The mean angle of repose of 46.8˚ indicated poor flow. Both the compressibility index and the Hausner ratio demonstrate that flucloxacillin sodium has very, very poor flow properties. This is consistent with the literature [206], which reported very poor flow of the drug in powder form.

Table 2.8 Flow properties of flucloxacillin sodium powder, with data for angle of repose, Hausner ratio and compressibility index. Flow ratings of fair or better are suitable for high speed tableting.

Angle of Repose (degrees)	Hausner Ratio	Compressibility Index
46.83 ± 3.52	1.90 ± 0.15	47.27 ± 3.90

2.5.1.2   Particle Size Analysis

Analysis of particle size distribution was performed for the major diluents MCC and mannitol (Table 2.9). Crospovidone was also analysed, see section 2.4.1.2.

Table 2.9 Particle size distribution parameters for Avicel PH102 and mannitol, using HELOS laser diffraction technique. Particle sizes are given in μm (mean ± SD, n=3)

Particle Size Parameter	MCC (Avicel PH102) (µm)	Mannitol (µm)
X10	17.43 ± 0.08	6.88 ± 0.12
X50	59.96 ± 1.08	28.45 ± 0.65
X90	137.13 ± 1.92	68.48 ± 0.56
X99	170.26 ± 0.44	97.27 ± 0.93
VMD	69.90 ± 1.23	33.41 ± 0.50

2.5.1.3 Tablet Properties

Various tablet properties for the 250 mg flucloxacillin ODTs are shown in Table 2.10. Tablet mechanical properties were excellent, with very high values for hardness and tensile strength, and low friability. The high hardness is likely largely due to good compactability of MCC and the small particle size of mannitol which allows for a high surface area for interparticular bond formation. MCC particles are somewhat larger, which should enhance improve powder flow. Speed of disintegration was very slow for an ODT at 579.67 ± 8.50 s.

Table 2.10 Characteristics of 250 mg flucloxacillin ODTs. Tablets (500 mg) consisting of flucloxacillin sodium (54.5%), MCC (18.5%), Mannitol (10%), sorbitol (10%), crospovidone (4%), aspartame (2%), silicon dioxide (0.5%) and Mg stearate (0.5%) were directly compressed at a compaction force of 30 kN, with a dwell time of 5 s (mean ± SD, n=3; friability n=6).

Parameter	Mean ± SD
Disintegration time (s)	579.67 ± 8.50
Porosity	0.34 ± 0.03
Hardness (N)	210.83 ± 7.02
Tensile strength (N/mm^2)	3.78 ± 0.11
Friability (% weight loss)	0.25

Despite displaying good mechanical strength, the formulation containing 250 mg flucloxacillin suffered from very slow disintegration. Clearly disintegration time is important for an ODT and therefore increasing disintegration speed was highlighted as the next focus. The mechanism by which disintegration occurs for an ODT is determined by the disintegrants that are included in the formulation. A number of different disintegrants are available and commonly used, that work by a variety of mechanisms, with varying results depending on the formulation or process conditions. Crospovidone had only been investigated thus far and so use other disintegrants was next explored as a means to improve disintegration.

2.6 Investigation of Different Disintegrants

Disintegrants principally affect the rate of disintegration of ODTs produced by direct compression and must also impart good compactability [207]. In order to improve the rate of disintegration the effect of different superdisintegrants in differing concentrations was investigated. Due to the high cost of the API flucloxacillin sodium, placebo tablets were designed whilst maintaining the ratio of excipients, in order to mimic the flucloxacillin tablets as closely as possible. The placebo tablets were produced with a number of different disintegrants at concentrations of 2%, 4% and 8% w/w to determine optimal concentrations. The placebo formulation is shown in Table 2.11. The most commonly used superdisintegrants used in directly compressed tablets are crospovidone, croscarmellose sodium and sodium starch glycolate [208]. Starch is perhaps the most traditional disintegrant, which acts by swelling and may also aid disintegration by repulsion between particles [46]. All four of these disintegrants were included in the placebo formulation to assess their performance.

ODTs of the formulation shown in Table 2.11, were produced using the disintegrants crospovidone (C), croscarmellose sodium (CS), sodium starch glycolate (SSG) and starch (S). All excipients, except Mg stearate, were blended for 5 min, Mg stearate added and then mixed for a further 1 min. Powders were compressed at 30 kN with a 5 s dwell time

Table 2.11 Formulation of placebo tablets Excipient ratios have been maintained, however disintegrant concentrations have been set at 2%, 4% and 8%. The disintegrants used are crospovidone (C), croscarmellose sodium (CCS), sodium starch glycolate (SSG) and starch (S).

Disintegrant Placebo Formulation (% w/w)			
MCC	44	43	41
Mannitol	24	23.5	22.5
Sorbitol	24	23.5	22.5
Disintegrant	2	4	8
Aspartame	4	4	4
Colloidal Silicon Dioxide	1	1	1
Mg Stearate	1	1	1
Total (%)	100	100	100

2.6.1   Results

2.6.1.1   Porosity

Porosity was measured using the out-of-die method. Each of the four disintegrants tested (excluding starch) showed significantly different porosity ($p<0.001$) between groups (Figure 2.14). Changing the concentration of crospovidone had no effect on porosity. Croscarmellose showed no change in porosity between 2-4%, however at 8% an increase in porosity was observed ($p<0.05$) to 0.24 ± 0.01. SSG showed a small decrease in porosity at 4% ($p<0.005$) and then a large increase in porosity at 8% ($p<0.001$) to 0.53 ± 0.00. Overall croscarmellose containing tablets demonstrated the lowest porosity which increased as concentration increased. SSG imparted the highest porosity of all disintegrants, followed by crospovidone.

2.6.1.2 Tablet Hardness

Tablet hardness for all disintegrant placebos (Figure 2.15) was well above a required acceptable threshold of 60 N. As was seen with porosity, the choice of disintegrant impacted tablet hardness. Crospovidone formed the hardest tablets ($p<0.05$) at 8% (244.1 ± 10.8 N) and at 4% (240.2 ± 3 N), and hardness was comparable to that of CS and SSG at 2%. CS initially showed an increase in hardness with increased concentration, but then showed a large drop in hardness at 8% ($p<0.001$) to 174 ± 5.3 N, which was the poorest hardness overall. SSG showed good hardness at the lowest concentration, which fell at 4% ($p<0.001$) and showed no change at 8%. Starch on the other hand showed the poorest hardness ($p<0.05$) at the lowest concentration which improved at 4% ($p<0.05$), showing no change with an increase to 8% concentration. At 4% SSG, CS and starch all showed comparative hardness. Increase of disintegrant concentration past 4% had no effect on hardness, with the exception of CS which showed a substantial decrease.

2.6.1.3 Friability

All placebos displayed friability (Figure 2.16) below 1%, a maximum weight loss of 0.37% with starch. Indeed, starch showed the highest friability overall, with the least friable being SSG at a concentration of 8% showing just a 0.05% loss in weight.
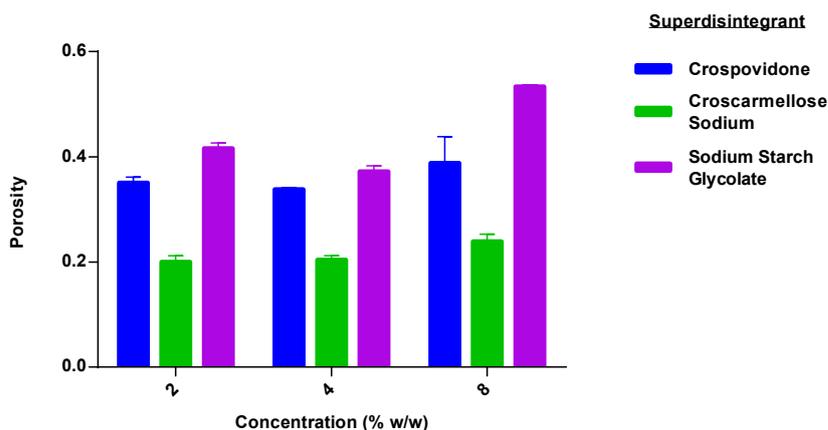
Figure 2.14 Porosity for all disintegrants against disintegrant concentration. ODTs (500 mg) consisting of MCC, mannitol, sorbitol, aspartame, silicon dioxide, Mg stearate and a disintegrant were directly compressed at a compaction force of 30 kN, with a dwell time of 5 s. Disintegrants C, CS, S and SSG were included at concentrations of 2%, 4% and 8%. Data for ODTs containing starch was not possible due to technical difficulties (mean ± SD, n=3).
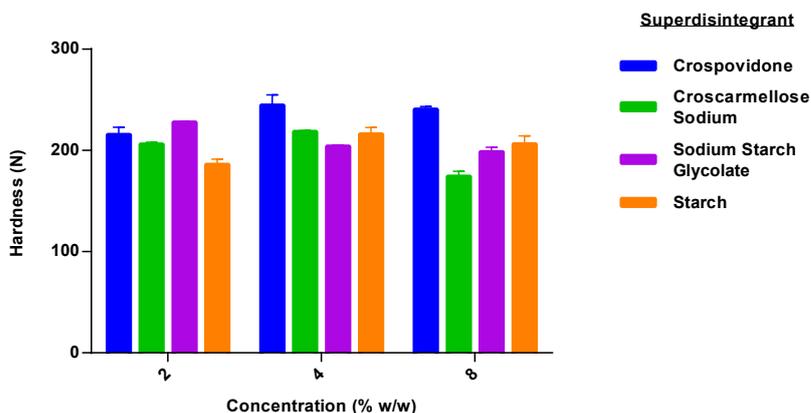
Figure 2.15 Hardness (N) against disintegrant concentration. ODTs (500 mg) consisting of MCC, mannitol, sorbitol, aspartame, silicon dioxide, Mg stearate and a disintegrant were directly compressed at a compaction force of 30 kN, with a dwell time of 5 s. Disintegrants C, CS, S and SSG were included at concentrations of 2%, 4% and 8% (mean ± SD, n=3)., (mean ± SD, n=3).
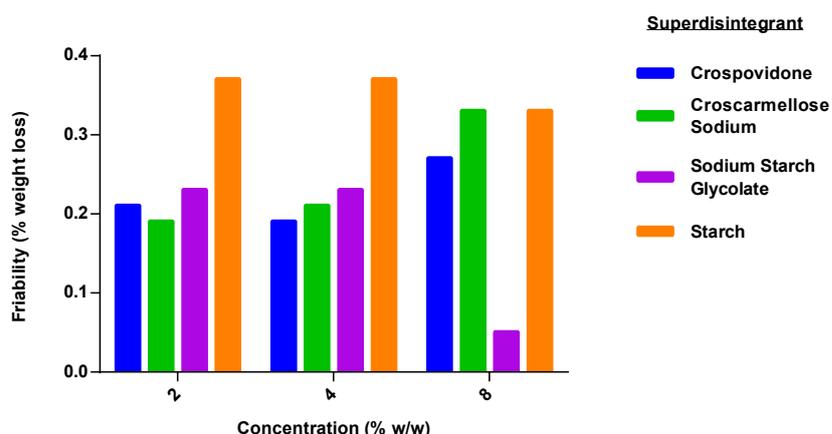
Figure 2.16 Friability (% weight loss) against disintegrant concentration. ODTs (500 mg) consisting of MCC, mannitol, sorbitol, aspartame, silicon dioxide, Mg stearate and a disintegrant were directly compressed at a compaction force of 30 kN, with a dwell time of 5 s. Disintegrants C, CS, S and SSG were included at concentrations of 2%, 4% and 8% (mean ± SD, n=6).

2.6.1.4 Disintegration Time

Choice of disintegrant was shown to affect disintegration time ($p<0.001$). None of the placebo tablets displayed disintegration within 3 mins (Figure 2.17). Crospovidone tablets showed the fastest disintegration time overall of 205.7 ± 11 s at 4%, which increased to 293.7 ± 24.9 s at 8% ($p<0.005$). At 2%, CS displayed the fastest disintegration ($p<0.05$), whilst the disintegration time of crospovidone was comparable to that of starch and SSG. CS showed a linear decrease in disintegration time ($p<0.005$) to 235 ± 9.6 s at 8%, suggesting that further increase in CS concentration may decrease disintegration time further. Similarly, SSG displayed a linear decrease in disintegration time ($p<0.001$) to an identical time to that of CS at 8%. Starch performed poorly as a disintegrant in comparison to the superdisintegrants crospovidone, CS and SSG, displaying times in the region of 10 mins.
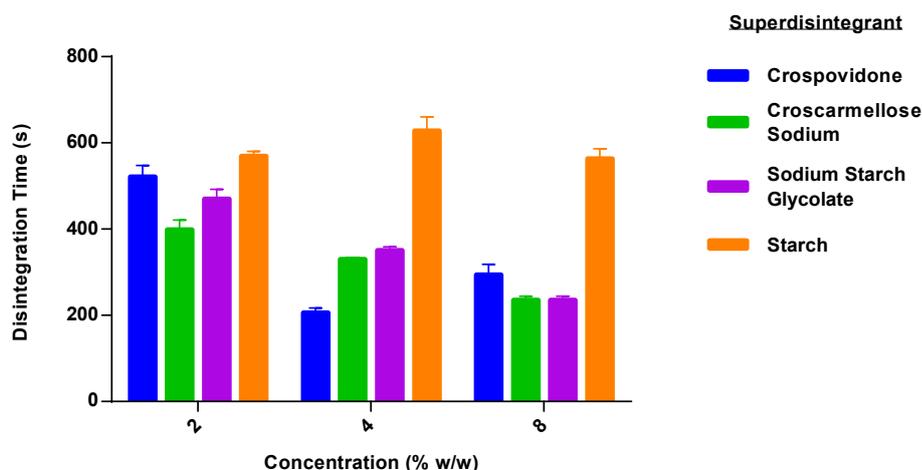
Figure 2.17 Disintegration time (s) against disintegrant concentration. ODTs (500 mg) consisting of MCC, mannitol, sorbitol, aspartame, silicon dioxide, Mg stearate and a disintegrant were directly compressed at a compaction force of 30 kN, with a dwell time of 5 s. Disintegrants C, CS, S and SSG were included at concentrations of 2%, 4% and 8% (mean ± SD, n=3).

2.6.2 Incorporation of Multiple Disintegrants

Disintegration times exceeded 3 mins for all disintegrants. In order to improve this, combinations of superdisintegrants were investigated, with evidence from the literature suggesting this may enhanced disintegration [42]. For example, Patil and Das [209] investigated varying combinations of crospovidone, CS and SSG when formulating Lamotrigine ODTs comprising mannitol and MCC as major diluents. They observed that a combination SSG and CS showed the most rapid disintegration. Similar findings have been reported when investigating combinations of superdisintegrants in the formulation of ODTs for the non-steroidal anti-inflammatory drug meloxicam [210] .

Superdisintegrants combinations were: crospovidone (4%) & CS (8%), crospovidone (4%) & SSG (8%), CS (8%) & SSG (8%), based upon the optimal concentrations observed previously. Other excipients were maintained in the same ratio as before.

2.6.2.1   Results – Disintegration Time and Hardness

Disintegration time for disintegrant combinations is shown in Figure 2.18. No improvement was seen with disintegrant combination compared to disintegrants alone. Combination of crospovidone and SSG showed the slowest disintegration of all combinations and disintegrants alone ($p < 0.05$). Combination of CS + SSG and C + CS was comparable to crospovidone alone. Combination of CS + SSG showed faster disintegration than the individual excipients CS and SSG alone ($p < 0.05$).

All of the combined disintegrant tablets showed good hardness (Figure 2.19) well above 150 N. Crospovidone containing ODTs were substantially harder than all other tablets ($p < 0.001$) at 244.1 ± 10.8 N. Addition of crospovidone to CS had no effect on tablet hardness. Similarly, addition of crospovidone to SSG gave an almost identical hardness of 198.1 ± 3.9 N when compared to SSG alone at 198.2 ± 5 N. When CS was added to SSG hardness decreased ($p < 0.05$), suggesting that tablet hardness in this case was dependent upon the weakest disintegrant.

Overall no improvement was seen with the incorporation of multiple disintegrants; tablet hardness fell markedly and disintegration time did not alter. ODTs containing crospovidone alone performed best and benefited from a lower optimum superdisintegrant concentration.
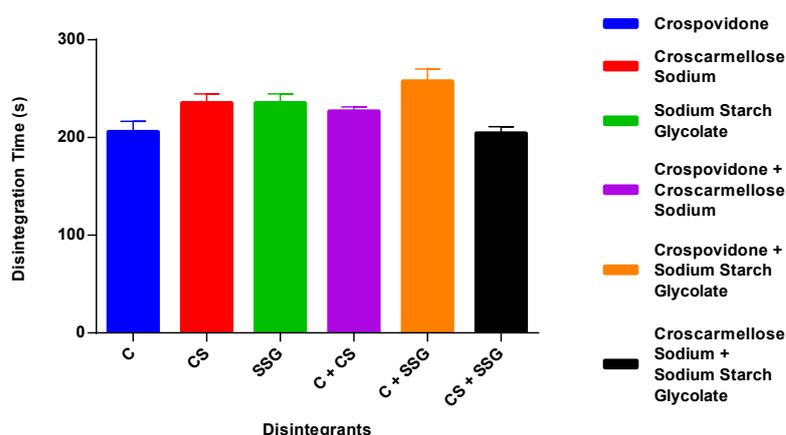
Figure 2.18 Disintegration time (s) against combinations of disintegrants at their optimum concentrations. ODTs (500 mg) consisting of MCC, mannitol, sorbitol, aspartame, silicon dioxide, Mg stearate and a disintegrant were directly compressed at a compaction force of 30 kN, with a dwell time of 5 s. Disintegrants C, CS and SSG were combined pairwise (mean ± SD, n=3).
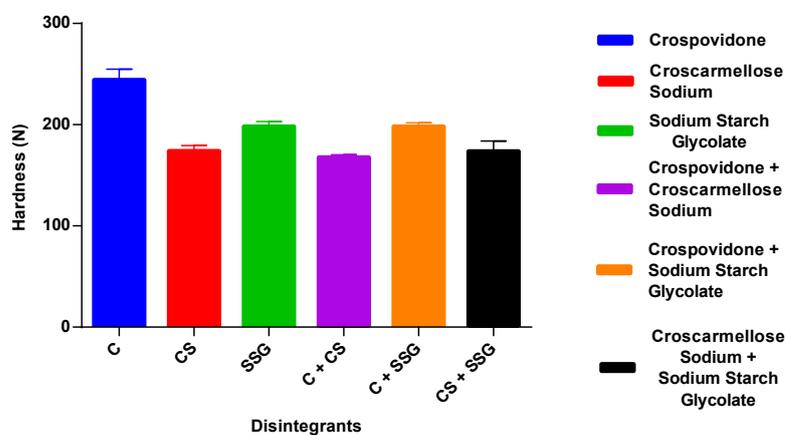
Figure 2.19 Hardness (N) against combinations of disintegrants at their optimum concentrations. ODTs (500 mg) consisting of MCC, mannitol, sorbitol, aspartame, silicon dioxide, Mg stearate and a disintegrant were directly compressed at a compaction force of 30 kN, with a dwell time of 5 s. Disintegrants C, CS and SSG were combined pairwise (mean ± SD, n=3).

2.6.3   Discussion

Despite showing good mechanical properties, all tablets disintegrated slowly (beyond 3 mins), with crospovidone at 4% performing best. Crospovidone also showed superior hardness and as such would likely perform well at lower compaction forces as an approach to improve disintegration time. CS performed poorly compared to SSG and crospovidone, with relatively low hardness coupled with low porosity. Despite CS and SSG displaying disintegration times at a concentration of 8% close to that of crospovidone at 4%, the superior mechanical properties displayed by crospovidone and its low optimum concentration, meant its use was continued in formulation development.

An optimum range of crospovidone between 4-6% has been reported in the literature [211-213]. The results suggest that disintegration times may be improved if CS and SSG concentrations are increased further, however it is known that past their optimum range formation of a viscous tablet outer layer impedes disintegration [214, 215]. Crospovidone has little tendency to gel and it is unclear why disintegration time decreases past its optimum range. Since crospovidone relies more heavily on rapid tablet wetting time (wicking) and less on its swelling ability compared to CS and SSG [215, 216], this increase in disintegration may be due in part to the insolubility of crospovidone when wetting time ceases to be a rate limiting factor. In order to increase disintegration speed, reduction of flucloxacillin dose to 125 mg was explored.

2.7   Reduction of Flucloxacillin Dose to 125mg

Reduction of the flucloxacillin dose to 125 mg was investigated as an approach to improve disintegration speed of the formulation. Reduction of the dosage could may offer additional benefits In addition, 125 mg solid oral dosage forms are currently not available presenting an opportunity for and ODT that would be suitable for administration to both adults and children aged 2-10 years alike; moreover, a further reduction of the dose may allow administration to even younger patients. Additionally, a dose reduction would ease taste masking of the drug.

The ratio of excipients was maintained as the original formulation (Table 2.7), although concentrations of aspartame and Mg stearate were maintained as these were at standard concentrations (Table 2.12). Powders were blended and compacted in the same manner as previously.

Tablet characterisation is summarised in Table 2.13. When compared to the 250 mg dose, the 125 mg ODTs showed significantly slower disintegration time ($p<0.001$) with increased hardness and tensile strength ($p<0.05$). Despite displaying improved hardness and tensile strength, friability remained at a similar level, possibly due to the greater mannitol content.

Table 2.12 Formulation of ODTs (500 mg) with a reduced dose of flucloxacillin sodium to 125 mg. Excipients concentration ratios have been maintained from 250 mg flucloxacillin dose tablets and are shown as % w/w.

125 mg Flucloxacillin ODTs	
	% (w/w)
Flucloxacillin Sodium	27.25
MCC	30.75
Mannitol	17.5
Sorbitol	17.5
Crospovidone	4
Aspartame	2

Colloidal Silicon Dioxide	0.5
Mg Stearate	0.5

Table 2.13 Properties of 125 mg flucloxacillin tablets. Data for 250 mg flucloxacillin tablets have also been included for ease of comparison. Powder underwent direct compression at a compaction force of 30 kN and a dwell time of 5 s (mean ±SD, n=3; friability n=6)

	Disintegration Time (s)	Hardness (N)	Tensile Strength (N/mm2)	Friability (% Weight Loss)
Flucloxacillin 125 mg	388.67 ± 14.29	294.80 ± 19.31	5.39 ± 0.35	0.23
Flucloxacillin 250 mg	579.67 ± 8.50	210.83 ± 7.02	3.78 ± 0.11	0.25

Despite a reduction at a 125 mg dose, disintegration time far exceeded 3 mins. Due to the complexity of the formulation it was not possible to determine the reasons behind the slow disintegration time. Consequently, a simplified formulation for 125 mg flucloxacillin tablets was investigated.

2.8 Effect of Varying Concentrations of MCC and Mannitol as Diluents in Flucloxacillin ODTs

Previous formulations for flucloxacillin ODTs comprising MCC, mannitol, sorbitol, crospovidone, Mg stearate and silicon dioxide showed excellent mechanical properties, but exhibited slow disintegration. Sorbitol has been shown to retard disintegration by decreasing the effectiveness of superdisintegrants [170] and was thus removed from the formulation. The effect of varying the concentrations of the major diluents, MCC and mannitol, was studied in order to optimise the formulation for faster disintegration. Silicon dioxide and aspartame were also removed from the formulation, to provide a clearer understanding of the combination of these two excipients and their compatibility with flucloxacillin sodium. MCC and mannitol were combined at different ratios to see the effect on tablet properties, see Table 2.14.

All excipients and drug, with the exception of Mg stearate, were blended for 5 mins. Mg stearate was then added and the powder was blended for a further 1 min. Direct compression was performed at a compaction force of 1 ton and a dwell time of 6 s.

Table 2.14 Formulation of 125 mg flucloxacillin sodium ODTs (500 mg), with varying ratios of MCC: mannitol. Concentrations of excipients and API are expressed as % w/w.

MCC: mannitol	3:1	2:1	1:1	1:2	1:3
	F1	F2	F3	F4	F5
Flucloxacillin sodium	27.25	27.25	27.25	27.25	27.25
MCC	50.00	44.50	33.38	22.25	16.75
Mannitol	16.75	22.25	33.38	44.50	50.00
Crospovidone	5.00	5.00	5.00	5.00	5.00
Mg st	1.00	1.00	1.00	1.00	1.00

2.8.1   Results

2.8.1.1   Disintegration Time

ODT characterisation is shown in Table 2.15. Disintegration time decreased when mannitol concentration was increased past an MCC: mannitol of 3:1 ($p<0.05$), with the exception of F3 (1:1) which did not show a significant reduction in disintegration when compared to F1, although F3 showed relatively high deviation. The performance for F2, F4 and F5 were similar, with the most rapid disintegration time seen with F4 at 138.33 ± 2.52 s. The improvement in disintegration time with increased incorporation of mannitol is likely due to the high water solubility of mannitol, as opposed to the insoluble MCC [158].

2.8.1.2   Hardness

Tablet hardness was compromised with increased mannitol concentration. Formulations F4 and F5 showed similar hardness ($p>0.05$), of 95.77 ± 5.74 N and 91.13 ± 3.19 N respectively. The strongest tablets ($p<0.001$) at 3:1 MCC: mannitol showed far superior hardness of 129.9 ± 4.40 N, demonstrating that inclusion of mannitol at even a low level was detrimental to tablet hardness.

2.8.1.3   Friability

Friability increased with increasing mannitol concentration, peaking at an MCC: mannitol of 1:2, before dropping at 1:3. Only formulations F1 and F2 displayed sufficiently low friability of less than 1%.

Table 2.15 Characterisation of ODTs containing 125 mg flucloxacillin where MCC: mannitol has been varied. ODTs compressed at 1 ton for 6 s (mean ± SD, n=3; friability n=6)

	Disintegration Time (s)	Hardness (N)	Friability %)
F1	180.33 ± 6.35	129.90 ± 4.40	0.59
F2	144.33 ± 5.86	109.00 ± 7.33	0.93
F3	148.00 ± 15.72	107.00 ± 5.62	1.31
F4	138.33 ± 2.52	95.77 ± 5.74	1.60
F5	139.67 ± 1.53	91.13 ± 3.19	1.16

2.8.2 Discussion

Increased mannitol concentration improved disintegration time, but mechanical properties were compromised due to brittle fracture of mannitol particles and poor compactability. Increased MCC concentration improved mechanical properties. A ratio of MCC: mannitol of 2:1 showed optimal properties, with good hardness, acceptable friability values and the most rapid disintegration, comparative to that of tablets with a greater mannitol content. This increased rate of disintegration was due to a drop in compaction force, optimisation of MCC and mannitol concentrations, reduction of flucloxacillin dose and also possibly to the omission of sorbitol. Sorbitol was included originally to counter poor mannitol compactability, however a low mannitol content and inclusion of MCC has allowed for production of strong tablets.

With the improvements in ODT performance shown, alteration of the blending process was hypothesised as a means to improve ODT characteristics.

2.9 Blending Alteration and Exclusion of Mg Stearate

At a ratio of 2:1 MCC: mannitol, ODTs demonstrated acceptable mechanical properties although disintegration times, despite showing improvement, were still longer than desired. The order of blending was explored to see the effect, if any, on tablet characteristics, potentially through coating or co-localisation of excipients.

Water insoluble lubricants like Mg stearate slow tablet wetting [217]. It is known that the inhibition of water penetration by Mg stearate is roughly proportional to its concentration [218]. It was believed that reduction of Mg stearate would improve disintegration for this formulation. The impact of Mg stearate on disintegration and hardness was therefore also examined by running another set of tablets in parallel where Mg stearate was not included.

A number of different blending orders were examined, with the theory that this would provide different excipient/API localisation within the powder blend and perhaps even some particle coating repercussions. The standard blend involved mixing API and excipients for 5 mins. Another variation involved blending of mannitol with flucloxacillin for 5 mins, then adding crospovidone and blending for 5 mins and then blending with MCC for 5 mins. Similarly, another variation involved using the same protocol, adding MCC first instead of mannitol. Lastly, ½ the MCC was blended with flucloxacillin for 5 mins, then crospovidone was blended for 5 mins, then mannitol for a further 5 mins, followed by the final ½ MCC for 5 mins. Mg stearate was or was not included as a final blending step for 1 min. Powders were compacted into tablets at a compression force of 1 ton with a dwell time of 6 s.

2.9.1 Results

Tablet characteristics are given in Table 2.16. Exclusion of Mg stearate greatly increased speed of disintegration ($p < 0.001$) as was expected, with the standard blend disintegrating in 75 s. In the absence of Mg stearate, no improvement in disintegration time was seen as a result of altered blending. In the presence of Mg stearate disintegration was slower when blending was altered, particularly when mannitol was added first. The effect of omission of Mg stearate on hardness was more complex, with a drop ($p < 0.05$) seen with the standard blend, an increase ($p < 0.05$) in hardness when mannitol was blended first and no change seen with MCC blended first. Blending order

had no impact on hardness when Mg stearate was included, however it did increase hardness in all cases in the absence of Mg stearate.

The improvement in disintegration time without Mg stearate was as expected. Initial blending of flucloxacillin with mannitol slowed disintegration, possibly due to a drop in tablet wettability. A particle interaction or coating effect may have meant that MCC particles were more exposed, causing a drop in tablet wettability. This would also explain how when MCC was added first, tablets gave comparable disintegration times when Mg stearate was not present. Why this is not true when Mg stearate was present is unclear, but could be due to an attenuation of the wettability of mannitol at the tablet surface, due to interaction with Mg stearate. It is difficult to ascertain any interaction of Mg stearate with crospovidone, since crospovidone was added at the same stage in each blending variation. Finally, an increase in tablet hardness as a result of changing blending order, in the absence of Mg stearate is encouraging since when MCC was added first and ½ first, disintegration time did not differ to the standard blend. An increase in blending time could therefore conceivably be employed to improve tablet hardness, for example if compaction force was lowered in order to achieve more rapid disintegration.

Table 2.16 Disintegration time and hardness values, for tablets containing flucloxacillin sodium (27.25%), MCC (44.5%), mannitol (22.25%), crospovidone (5%) and Mg stearate (1%) with altered blending orders. Powders were compacted into tablets at a compression force of 1 ton with a dwell time of 6 s. Differences between blend variations and the standard blend were assessed and any significance reported (*p<0.05, **p<0.01, ****p<0.0001, mean ± SD, n=3).

		Disintegration time (s)		Hardness (N)	
		Mean ± sd	Significant?	Mean ± sd	Significant?
1% Mg st	Standard blend	144.33 ± 5.86		109.00 ± 7.33	
	Mannitol first	243.67 ± 4.73	Yes****	98.67 ± 2.45	No
	MCC first	167.00 ± 11.27	Yes*	110.07 ± 6.62	No
No Mg st	Standard blend	75.00 ± 2.00		97.77 ± 4.05	
	Mannitol first	105.67 ± 18.50	Yes*	112.83 ± 4.54	Yes**
	MCC first	80.67 ± 9.50	No	109.60 ± 0.46	Yes**
	MCC 1/2 first, 1/2 last	85.67 ± 9.87	No	110.23 ± 2.27	Yes**

2.10 Conclusion

Despite several formulation development steps flucloxacillin containing ODTs were not quite able to fulfil the requirements of rapid disintegration (<30 s) whilst maintaining sufficient mechanical strength (>60 N), including low friability (<1%). Despite the benefits of mannitol, its tendency to fragment at low compression hinders the production of mechanically strong tablets with the concomitant problem of high friability. Investigating different disintegrants and disintegrant combinations revealed that crospovidone alone conveyed the most rapid disintegration. From initial placebo development, the inclusion of flucloxacillin retarded disintegration and lowering of the dose not only improved ODT properties but could allow for administration to paediatrics once formulation development is complete. A blend of MCC and mannitol at a ratio of 2:1 as major diluents was shown to be effective at lowering disintegration time within 3 min, whilst presenting good hardness values and friability below 1% for ODTs containing a 125 mg dose of flucloxacillin.

A number of challenges in formulation development remain. For example, although not included, flucloxacillin sodium exhibited poor flow due to a bi-modal particle size distribution with a large proportion of fines (data not shown), which was overcome through use of granulated flucloxacillin sodium. Use of PEG as an alternative water-soluble lubricant also showed some promise (data not shown) although it is likely that other well-established more water-soluble lubricants such as sodium stearyl fumerate would be more useful in further development. Use of a different grade of crospovidone, with a larger particle size, was also investigated as a means to improve disintegration and showed early promise (data not shown). Taste-masking remains a major problem and despite preliminary work to explore solutions for this (not included) this requires attention. Further development should include alteration of ODT shape, from a round flat faced geometry to a shape with softer edges, such as caplet or lozenge forms, in order to address the high friability across the majority of formulations.

Chapter 3

Film Coating of Directly Compressed ODTs

3.1   Introduction

Historically sugar coating was the primary form of tablet coating, derived from technology used in the confectionary industry and, although still used today, has been replaced largely by polymeric film coating processes [78]. This technique has the advantage of being able to control drug release, through careful selection of polymers and combinations of polymers, at varying thickness [98]. Additionally film coating using polymers constitutes a considerably lower increase in tablet weight, is single stage as opposed to multiple stage and is rapid in comparison to sugar coating [46]. Polymeric film coating is commonly employed for the design of drugs that disintegrate at target locations along the gastro-intestinal tract, for example, by optimising for enzymatic degradation [98].

Polymeric films are most commonly applied through spray atomisation. Spray atomisation involves dissolving the polymer in a solvent and atomisation by passing the solution through a nozzle under pressure, to form fine droplets. There are three general equipment types for film coating by spray atomisation; these are standard coating pans, perforated coating pans and fluidised bed systems. Coating pans are composed of a metal drum rotated at a specified speed. Tablets are placed inside and hot air is blown over the tablet surface to dry. Perforated pan beds work much in the same way, however they allow for better air flow and more efficient drying. Fluidised bed spray coating involves suspending tablets in an airflow that is heated to aid drying. Atomised solution is then sprayed onto the solution, either from above or below. Fluidised bed spray coating is more efficient when compared to pan coating as tablets can be suspended and coated simultaneously. This technique is also more commonly used in the laboratory in comparison to pan coating [219, 220]

During spraying droplets impinge and disperse across the tablet surface, forming a film after solvent evaporation [65]. The rate of solvent evaporation is critical in film formation and thus both the selection of solvent and the processing conditions are important considerations. Furthermore, the wettability of the solvent-polymer droplets on the tablet surface is dependent on the wettability of the droplet itself and also the tablet; therefore the surface properties of the tablet must also be considered[46, 78]. Traditionally highly volatile organic solvents were preferred, however mammalian, human and ecotoxicological data has shifted the focus towards aqueous-based suspension systems. This is important as solvents commonly constitute 80-90% of the total mass in batch processes [69]. As a result, various polymeric film forming agents are available

commercially that are suitable for suspension in water. Furthermore, a significant problem with the use of organic solvents is the increase in viscosity with increased polymer concentration which limits spreadability and thus limits the concentration of polymer that can be used. Aqueous based systems eliminate spreading problems when solvents rapidly evaporate and relative polymer concentration increases. The equipment used for aqueous based polymeric dispersion is the same as that used with organic solvents and only the processing parameters require modification [78].

Film coating of orally disintegrating tablets (ODTs) has not been explored in the literature and could offer advantages for conventional directly compressed tablets. Preliminary studies investigating mannitol based ODTs identified tablets that displayed rapid disintegration (<30 s) and good hardness and tensile strength values, although suffered from high friability. It was believed that this issue could potentially be addressed by addition of a film coat. It is has been shown that addition of a film coat can increase tablet hardness [221, 222]. Another important consideration for ODTs is taste, as disintegration of the tablet in the mouth exposes the API to the patient's taste buds. Due to flucloxacillin's unpleasant bitter taste sweeteners and flavours are incorporated into available dosage forms.

Mannitol based ODTs containing crospovidone as a disintegrant were used as a model for development of a film coating that could provide the benefits of improved friability, hardness and tensile strength. Despite the addition of an outer layer to the tablet it was paramount that speed of disintegration would not be adversely affected.

Kollicoat IR, BASF, Germany, consists of a polyvinyl alcohol-polyethylene glycol graft copolymer (PVA-PEG graft copolymer), in a 3:1 ratio which has been designed for use as an instant release film coating. It is soluble in water and reduces water surface tension, which is important for aqueous based solutions since it allows for easy spraying and facilitates good tablet surface wetting. Kollicoat IR rapidly disintegrates in water and shows excellent flexibility, which negates the need for addition of plasticisers [223]. The film coat claims to have many favourable qualities when compared to more traditional water soluble polymers such as hydroxypropyl methyl cellulose (HPMC). In the context of rapid disintegration, inclusion of Kollicoat IR at even low concentrations has been shown to significantly improve drug release rates of very slow releasing ethylcellulose based coatings, by increasing the rate and extent of water uptake. In one study, in contrast to HPMC, addition of PVA-PEG to the ethycellulose based coating did not result in flocculation of the colloidal coating, resulting in consistent release rates [224].

Kollicoat IR was selected as a model film coat polymer for investigations into proof of concept for the application of a film coat to directly compressed ODTs. Preliminary work focussed on developing a protocol and process conditions that would produce a good uniform film coat whilst avoiding process complications such as poor adhesion and twinning.

3.2 Materials and Methods

3.2.1 Materials

Flucloxacillin sodium was purchased from Carbone Scientific (UK). D-mannitol, sodium lauryl sulphate (SLS), D-sorbitol, magnesium stearate, Tween 80, PEG 400, PEG 1000 and eosin Y were purchased from Sigma-Aldrich (UK). Polyplasdone XL-10 (crospovidone) was obtained from ISP (Switzerland). Kollicoat IR (polyethylene glycol polyvinyl alcohol copolymer) was purchased from BASF (Germany). Tween 20 was purchased from Fischer BioReagents (UK). Avicel PH102 (MCC) was obtained from FMC Biopolymer (USA). Aerosil 200 Pharma (colloidal silicon dioxide) was obtained from Evonik Industries (Germany).

3.2.2 Film Coating

Kollicoat IR aqueous solutions at various concentrations (% w/w) were prepared by addition of powder to ultrapure water and left until fully dissolved using a magnetic stirrer for 30 mins at room temperature. Process parameters were determined through preliminary trials and are shown in Table 3.1. The same conditions were used for coating of all tablets unless otherwise stated. A preheating stage was included to enhance water evaporation from the tablet surface. The fan speed was kept lower for this stage to limit the extent of tablet attrition but at the same time still ensure uniform heating. Film coating was performed using a Caleva Process Solutions Mini Coater Drier 2 (Caleva, UK) fluidised bed spray coater.

Table 3.1 Process conditions for tablet film coating using a fluidised bed spray coater. Tablet batch size of 12.

Parameter	Value
Preheat	
Air temperature (°C)	60
Fan (m/sec)	10.00

Time (min)	10
Spraying	
Air temperature (°C)	60
Spray air pressure (bar)	2.00
Liquid flow rate (ml/min)	0.625
Fan (m/sec)	15.00
Time (min)	40
Drying	
Air temperature (°C)	60
Fan (m/sec)	15.00
Time (min)	5

3.2.3 Tablet Formation

Direct compression of tablets (500 mg) at a compaction force of 10 kN (1 ton) or higher was performed using an Atlas T8 automatic press (SPECAC, UK). A manual uniaxial hydraulic press (SPECAC, UK) was used for production of tablets below a compaction force of 10 kN. A 13mm round, flat faced die was used for tablet production. All tablets were produced under ambient conditions and tablet characterisation was carried out immediately post compression

3.2.4 Disintegration Time

The disintegration time was measured in vitro using US pharmacopeia monograph ([701] disintegration). The disintegration apparatus used was an Erweka ZT3 disintegration bath (Erweka GmbH, Germany) using 800 ml distilled water maintained at 37°C as disintegration media. Tablets were measured individually by placing in the basket rack and the time taken for the tablets to disintegrate without leaving any solid residue in the basket, recorded. Disintegration time was measured in triplicates at each compaction force.

3.2.5 Friability

Tablet friability was determined on 6 tablets using a friabilator from J. Engelsmann AG (Germany). Tablets were placed inside the drum and rotated at 25 rpm for mins, for a total of 100 revolutions. Excess tablet dust that would contribute to tablet mass was removed pre and post testing. Friability was calculated and expressed as % tablet weight loss from initial tablet weight.

3.2.6 Tablet Hardness Measurements

Tablet hardness apparatus (Schleungier 4M, Switzerland) was used to measure the radial crushing strength (hardness) of tablets in triplicate. Hardness was recorded in Newtons (N).

3.3   Film Coating Mannitol Based ODTs

The suitability of a polymeric film coating for an ODT was tested on mannitol based ODTs from previous studies for which there was existing data. Disintegration time, hardness and tablet friability were recorded for ODTs coated with increasing concentrations of Kollicoat IR. Additionally, the weight change in tablets pre and post coating was recorded, to monitor the success of the coating procedure and compare this to any changes in tablet characteristics.

3.3.1   Materials and Methods

Mannitol (94% w/w) based ODTs, consisting of a disintegrant crospovidone (5% w/w) and Mg stearate (1% w/w) as a lubricant and anti-adhesive were chosen as they had been previously studied and demonstrated rapid disintegration. ODTs were blended for 5 mins, before addition of Mg stearate followed by further mixing for 1 min. Compression was performed at 3 tons and a dwell time of 6 s.

3.3.2   Results

3.3.2.1 Tablet Hardness

A Kollicoat IR film coat improved tablet hardness at 20% and 25% aqueous solution. Initially tablet hardness (Figure 3.1) was compromised with the addition of Kollicoat IR, dropping to 88.8 ± 4.43 N at 5% solution ($p<0.05$), but rose linearly to an improved hardness when compared to controls ($p<0.05$), of around 115 N. Tablet hardness declined at the highest concentration of coat solution, to a level comparable to that of non-coated tablets.

3.3.2.2 Disintegration Time

Coating of tablets had no effect on disintegration time (Figure 3.2) at any Kollicoat IR concentration. All disintegration times were within a desired time of 30 s.

3.3.2.3 Friability

Friability (Figure 3.3) vastly reduced with increase in concentration of film Kollicoat IR. Non-coated tablets displayed a weight loss of 1.46%, whereas at the highest concentration of Kollicoat IR, weight loss was only 0.04%. It is important to note that weight loss caused by tablet attrition in the fluidised bed environment will have occurred during the film coating process and as such total weight loss will have been higher than the values shown here.
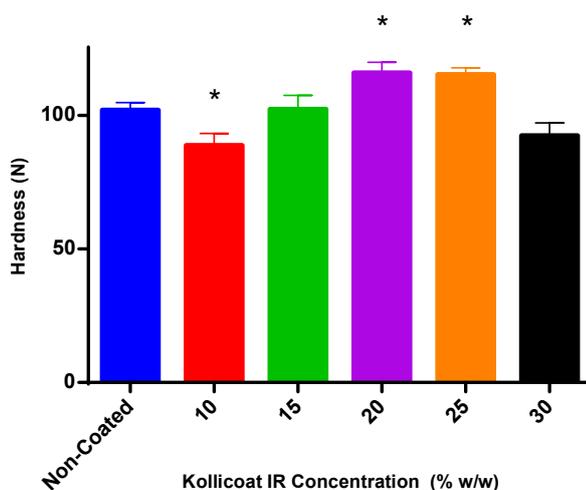
Figure 3.1 Hardness (N) of ODTs film coated with increasing concentrations of Kollicoat IR solution. ODTs (500mg tablets) consisting of mannitol (94%), crospovidone (5%) and Mg stearate (1%) underwent direct compression at a compaction force of 3 tons and a dwell time of 6 s (mean ±SD, n=3, * P<0.05 compared to non-coated)
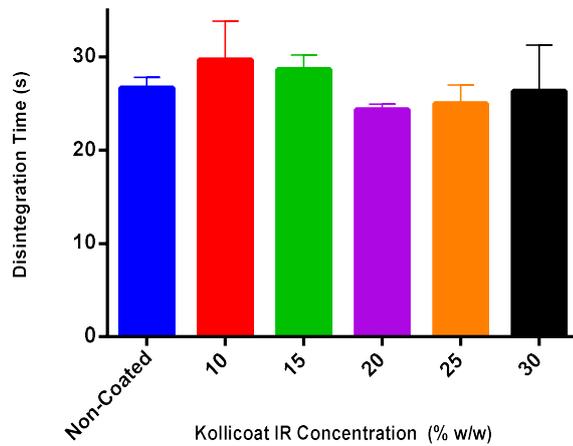
Figure 3.2 Disintegration time (s) of ODTs film coated with increasing concentrations of Kollicoat IR solution. ODTs (500mg tablets) consisting of mannitol (94%), crospovidone (5%) and Mg stearate (1%) underwent direct compression at a compaction force of 3 tons and a dwell time of 6 s (mean ±SD, n=3).
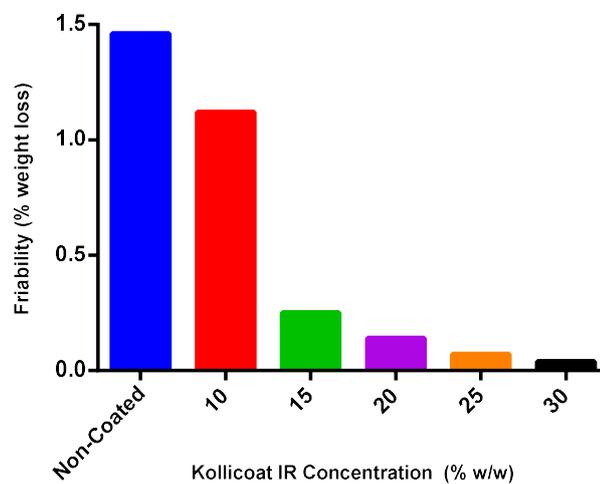
Figure 3.3 Friability (% weight loss) of ODTs film coated with increasing concentrations of Kollicoat IR solution. ODTs (500mg tablets) consisting of mannitol (94%), crospovidone (5%) and Mg stearate (1%) underwent direct compression at a compaction force of 3 tons and a dwell time of 6 s (mean, n=6).

138

3.3.2.4 Mass Changes

To estimate the extent of tablet attrition and weight loss during coating, tablets were put through the film coat process using the same process conditions, in the absence of spray solution, to provide a 'worst case' tablet weight loss as a result of the process. The change in tablet weight post film coating is shown in Figure 3.4. Non-coated tablets demonstrated a weight loss of 1.97%; interestingly, the weight loss was even greater (2.26%) in tablets coated with 10% Kollicoat IR, possibly due to variation in weight loss and only a very small increase in weight due to the film coat. Alternatively, the weight loss and poor hardness at 10% could be as a result of tablet over-wetting which affected mechanical properties. From concentrations at and exceeding 15%, weight gain was observed in a stepwise manner with increased concentration, to a maximum increase of 3.19% at 30% concentration.
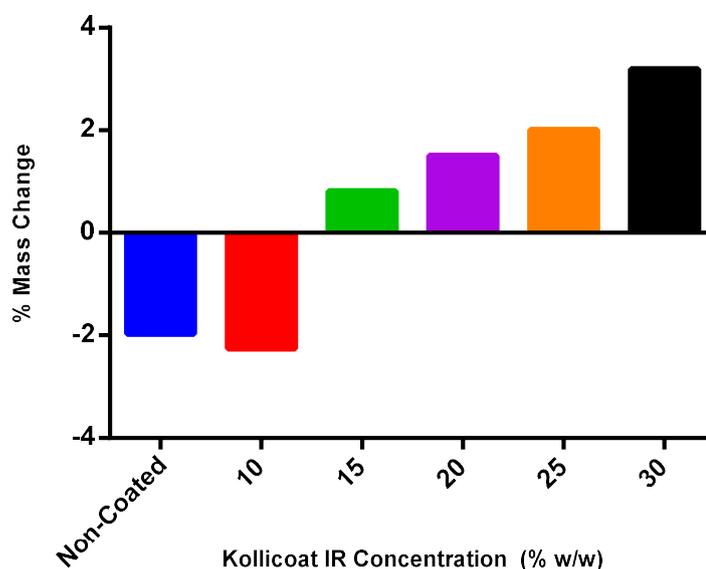
Figure 3.4 Mass change (%) of ODTs film coated with increasing concentrations of Kollicoat IR solution. ODTs (500mg tablets) consisting of mannitol (94%), crospovidone (5%) and Mg stearate (1%) underwent direct compression at a compaction force of 3 tons and a dwell time of 6 s (mean, n=12).

3.3.3   Discussion

Application of Kollicoat IR as a film coating was shown to be beneficial in improving desirable characteristics for ODTs. At concentrations of 20% and 25% hardness improved and friability decreased significantly. Crucially, disintegration time was not impacted by the presence of the film coat. Kollicoat IR may therefore be suitable for use as a coating for ODTs, with the view of improving the mechanical characteristics of the tablet, whilst not impeding disintegration. This is complicated however, due to the tablet weight loss from attrition during fluidisation. Weight loss will likely be at less than the 2% reported here, however, since the coat is being continuously applied and therefore improvement of mechanical characteristics will evolve throughout the process. Nevertheless, the literature recommends very low tablet friability, of around 0.1%, for film coating [220]. In order to apply film coating to friable ODTs would thus require a change in approach. Rounded and spherical tablets are recognised as offering greater intra-tablet coating uniformity [225, 226], whilst a more rounded geometry would likely reduce friability [227]. For these reasons, rounded tablet geometries are favoured for coating purposes.

Since the addition of a film coat did not retard disintegration the possibility that a film coating could instead enhance disintegration was explored. Surfactants are widely used in the chemical industry and are often used as wetting agents. Wetting agents can be used to lower the surface tension at a liquid-solid interface, enhancing spreadability of the liquid and thus improving wettability at the tablet surface [228]. Improving tablet wetting is a popular approach for enhancement of disintegration [229, 230]; the addition of wetting agents to a film coat to increase tablet wettability was thus explored.

3.4 Improving Disintegration Time of Flucloxacillin ODTs with a Film coat

The application of a Kollicoat IR film coat to flucloxacillin (125mg) ODTs was investigated to see the effect on tablet characteristics. A 20% (w/w) concentration solution was maintained from previous work with mannitol based placebo ODTs, based on favourable performance and good liquid flow during coating when compared to higher concentrations. The inclusion of a wetting agent to Kollicoat IR coatings, with the hypothesis that it may improve disintegration times by enhancing tablet surface wetting, was explored. A surfactant, sodium lauryl sulphate (2% w/w) was chosen as the wetting agent, due to its extensive inclusion in pharmaceutical dosage forms. Inclusion of SLS (2% w/w) into the tablet core was also investigated as a means to improve disintegration time.

3.4.1 Materials and Methods

The ODTs were composed of flucloxacillin sodium (27.25% w/w, 125 mg), mannitol (66.75% w/w), crospovidone (5% w/w) and Mg stearate (1% w/w) and were compressed at both 1 ton and 3 tons with a dwell time of 6 s. All excipients and API were blended for 5 mins, with the exception of Mg stearate, which was blended for 1 min as a final blending stage. The film coating parameters were maintained as per Table 3.1. The tablets containing SLS were produced in the same way, however for these tablets, mannitol concentration was reduced to 64.75% to allow for 2% SLS.

3.4.2 Results

3.4.2.1 Disintegration Time

Disintegration time (Figure 3.5) was not affected by the application of a 20% Kollicoat IR film coat. Addition of 2% SLS to the film coat for tablets compacted at 1 ton slightly reduced the disintegration time when compared to both the control and the 20% Kollicoat IR alone ($p < 0.05$), with a time of 163.67 ± 4.93 s. Increasing compaction force retarded disintegration ($p < 0.001$), with tablets compacted at 3 tons disintegrating around 90 s more slowly. Given the poor performance of tablets and coated tablets compacted at 3 tons, addition of SLS at this compaction force was not explored.

3.4.2.2 Tablet Hardness

Tablet hardness (Figure 3.6) was significantly higher when compaction force was increased to 3 tons (p<0.0001), with non-coated tablets displaying a hardness of 184.90 ± 4.42 N. Addition of a film coat at this force compromised hardness, with a reduction to 138.97 ± 3.07 N (p<0.0001). No change in hardness was observed for coated tablets compacted at a force of 1 ton. Furthermore, no significant effect was seen with addition of 2% SLS to the film coat.

3.4.2.3 Friability

Tablet friability (Figure 3.7) was reduced with increased compaction force and in both cases presence of a film coating essentially negated weight loss, dropping to around 0.001%, constituting chipping of the film coat itself. Addition of SLS had no impact on friability.
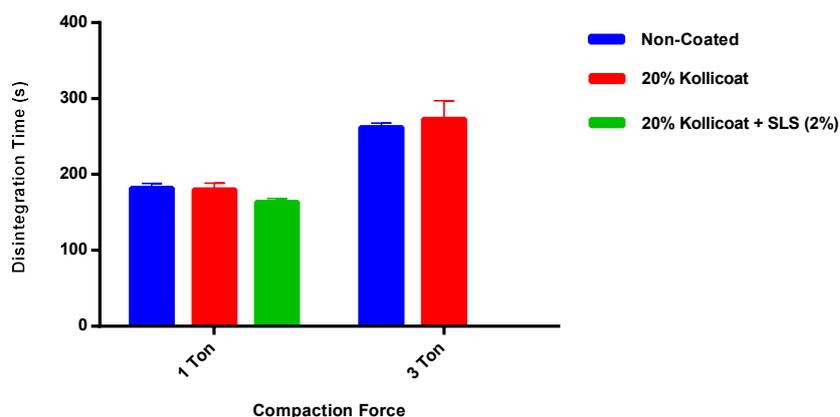
Figure 3.5 Disintegration time (s) of flucloxacillin (125mg) ODTs compacted at 1 ton and 3 tons. Tablets were coated with a 20% solution of Kollicoat IR with and without the surfactant SLS (2%). ODTs (500mg tablets) consisting of flucloxacillin sodium (27.25%), mannitol (66.75%), crospovidone (5%) and Mg stearate (1%) underwent direct compression with a dwell time of 6 s (mean ±SD, n=3).
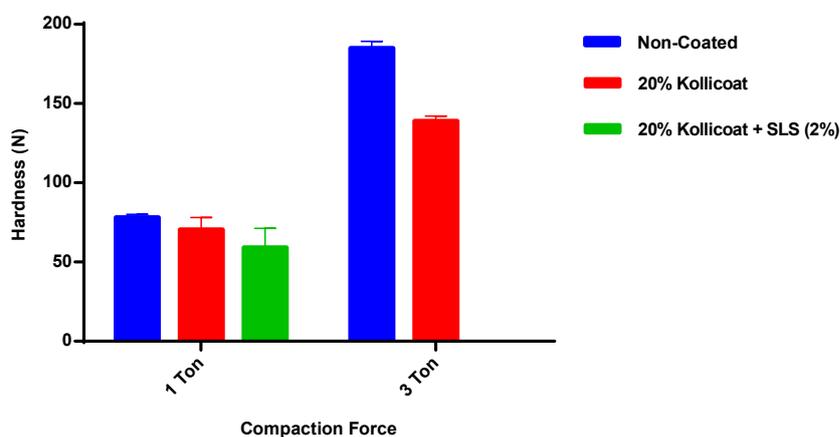
Figure 3.6 Hardness (N) of flucloxacillin (125mg) ODTs compacted at 1 ton and 3 tons. Tablets were coated with a 20% solution of Kollicoat IR with and without the surfactant SLS (2%) ODTs (500mg tablets) consisting of flucloxacillin sodium (27.25%), mannitol (66.75%), crospovidone (5%) and Mg stearate (1%) underwent direct compression with a dwell time of 6 s (mean ±SD, n=3).
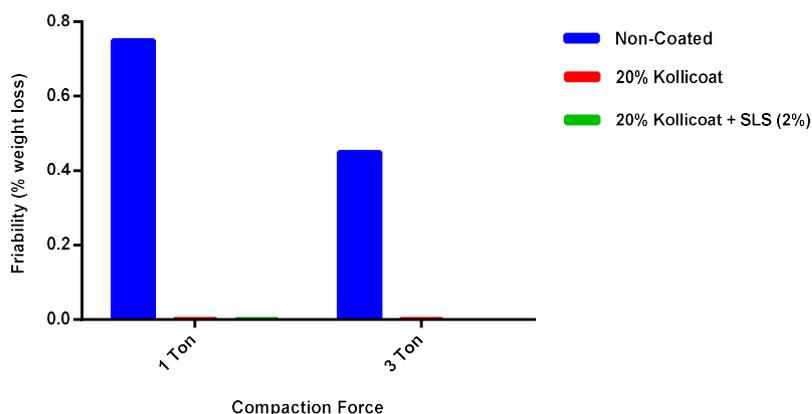
Figure 3.7 Friability (% weight loss) flucloxacillin (125mg) ODTs compacted at 1 ton and 3 tons. Tablets were coated with a 20% solution of Kollicoat IR with and without the surfactant SLS (2%) ODTs (500mg tablets) consisting of flucloxacillin sodium (27.25%), mannitol (66.75%), crospovidone (5%) and Mg stearate (1%) underwent direct compression with a dwell time of 6 s (mean ±SD, n=6).

3.4.2.4 Incorporation of SLS into the Tablet Core

To assess any effect of inclusion of a wetting agent into the tablet core, SLS (2% w/w) was incorporated into the formulation at the expense of a 2% reduction in mannitol concentration. Table 3.2 shows the effects on disintegration time, hardness and friability of addition of the wetting agent SLS into the table core of flucloxacillin (125mg) tablets. Despite being aimed at improving disintegration time, SLS impeded disintegration by 25 s. No effect was seen on tablet hardness, yet friability increased markedly to over 2%.

144

Table 3.2 Disintegration time (s), hardness (N) and friability comparison between flucloxacillin (125mg) tablets (500mg), with (2% SLS) and without (control) SLS. ODTs (500mg tablets) consisting of flucloxacillin sodium (27.25%), mannitol, crospovidone (5%) and Mg stearate (1%) underwent direct compression at a compaction force of 1 ton and a dwell time of 6 s. SLS was included into the tablet core at the expense of a 2% reduction in mannitol concentration to 64.75% (mean ±SD, n=3).

	Control		2% SLS		
	Mean	SD	Mean	SD	Significant?
Disintegration Time (s)	182.33	5.69	207.33	6.43	Yes**
Hardness (N)	78.10	1.99	73.97	5.23	No
Friability (%)	0.75		2.08		

3.4.3   Discussion

Addition of the wetting agent SLS to the Kollicoat IR film coat caused a slight increase in disintegration time. At 1 ton compression, SLS compromised the mechanical strength of film coated tablets when compared with uncoated tablets and similarly there was no change in friability. The subtle increase in hardness with film coating of mannitol based ODTs was not seen with tablets containing flucloxacillin, and in fact a decrease was seen in tablets compressed at 3 ton. Weakening of tablets compressed at higher force may be adequately explained due to changes in tablet surface characteristics such as roughness, porosity or wettability affecting interfacial bonding between the coating polymer and the tablet surface, resulting in compromised coating adhesion [222, 231].

The results hint at the possibility for improvement of mechanical properties and enhanced disintegration of an ODT through the application of a film coating. A wide variety of surfactants are used in oral dosage forms [232], which can be classified by their hydrophile-lipophile balance (HLB) [233]. Surfactants with higher HLB numbers (more hydrophilic) are more suitable as solubilising agents, whereas those with low HLB numbers function better as anti-foaming agents. HLB numbers in the range of 7-9 are indicative of good wetting and spreading agents and thus surfactants in this range hold potential for further development [46]. Surfactants in this range consisting primarily of

fatty-acids such as polyethylene glycol (PEG), sorbitan laurate and lecithin, are generally well tolerated [234-237].

3.5   Investigating Different Surfactants to Enhance Disintegration

Previous work showed that film coating could be employed as a method for improving mechanical properties, namely hardness and friability. Addition of SLS (2%) to the film coat solution showed a small but significant decrease in disintegration time and therefore more surfactants were chosen to test their effect on disintegration.

Micellar solubilisation is a commonly used technique to improve the solubility of poorly soluble drugs [238, 239]. Micelles form when surfactants reach a critical concentration, known as the critical micelle concentration (CMC). Due to this ability it was decided to include surfactants at, above and below their CMC, in order to determine if addition of surfactant in the film coat would also improve the solubility of a poorly soluble drug, such as ibuprofen. For many surfactants CMC values are often available from the literature or manufacturer. Commercial surfactants however contain surface active impurities that alter the CMC. The true CMC for the impure sample can be determined using the dye micellisation method [240]. At CMC hydrophobic dyes can become incorporated inside the hydrophobic centre of the micelle, which causes a shift in the wavelength maximum (λmax) of the dye [241], by which the CMC can be determined.

Tween (polysorbate) is a commonly used non-ionic surfactant, consisting of partial fatty acid esters of sorbitol copolymerised with PEG. They are highly hydrophilic, being used widely as an emulsifier for oil-in-water preparations. So popular is their use that Tween 80 is the most commonly used surfactant in parenteral preparations approved by the FDA. Polysorbate is regarded as generally non-toxic, however there have been some reports of hypersensitivity reactions when administered topically and intra-muscularly [158, 242]. PEG is classified as a plasticising agent, solvent, diluent and lubricant [158] and has also been reported to reduce the surface tension of water by acting as a surfactant [243], although this is not generally recognised. Due to their high hydrophilicity, PEGs are usually used in the manufacture of many commercial surfactants, typically PEG ethers, where they are coupled with hydrophobic molecules. PEGs have been employed as poor surfactants or cosurfactants on their own [244], particularly the lower weight PEGs such as PEG 400. Despite this however, CMC values are difficult to obtain from the literature, with only scattered reports [245, 246], casting doubt on whether or not micellar formation occurs. Here CMC value determination was attempted for a lower weight PEG (400) and a higher weight PEG (8000). In addition to its wetting ability and high hydrophilicity, PEG is employed in film coats as a polishing material and has been shown to increase film coat water permeability [158].

3.5.1 Materials and Methods

3.5.1.1 ODT Preparation

Tablets (500 mg) consisting of (w/w) MCC (47%), mannitol (23.5%), D-sorbitol (23.5%), crospovidone (4%), silicon dioxide (1%) and Mg stearate (1%) were produced by direct compression. All excipients were blended for 5 mins and then Mg stearate was added and the powder mixture blended for a further min. Tablets were compacted at a force of 30 kN and a dwell time of 6 s. This formulation was selected as it would show sufficiently slow disintegration time to highlight any effect of addition of surfactant to the film coat solution.

3.5.1.2 CMC Determination by Dye Micellisation Method

CMC was determined by the method used by Patist, Bhagwat [241]. A 0.019mM eosin Y dye solution was made using ultrapure water. Using this, a range of solutions from 0.002mM to 10mM for Tweens and 0.004mM to 50mM for PEGs were prepared and added in triplicate to a 96-well plate and left overnight, protected from direct light. Eosin Y in water absorbs maximally at 518nm and shifts to a maximum absorbance of 542nm when within micelles. By plotting dye absorbance as a function of surfactant concentration and then extrapolating the linear portion of the curve, the intercept with the absorbance at zero surfactant concentration yields the CMC. As such, absorbance spectra were read at 542nm at 25°C using a Multiskan GO Microplate Spectrophotometer (UK).

3.5.1.3 Preparation of Coating Solution

Kollicoat IR (20% w/w) coating solutions were used. Tweens were added at concentrations of ½ CMC, CMC and 10x the calculated CMC values. PEGs were added at concentrations of 0.02mM, 0.04mM and 0.4mM, to mimic the concentration range of Tweens.

3.5.2   Results

3.5.2.1 CMC Determination

CMC determination was carried out for Tween 20 and 80 and PEG 400 and 8000. The results for Tween 20 and Tween 80 are shown in Figure 3.8 and Figure 3.9 respectively. PEG 400 and PEG 8000 are shown in Figure 3.10 and Figure 3.11. For the Tween surfactants it was possible to calculate the CMC values, and these correlated well with the reported values by Patist, Bhagwat [241]. The PEG was not successful however; the PEG 8000 seemed to indicate micelle formation, however the curve did not plateau and therefore it was not possible to extrapolate from this a reasonable estimation of the CMC. Similarly, PEG 400 did show increased absorbance with increased concentration, however this was less defined and was not in a classic sigmoidal manner. As a result, it was decided to include the PEG at levels similar to that of Tween, in which the CMC could be calculated. Although it was not possible to state that PEGs would be included below, at and above CMC, including PEG in concentrations similar to that of Tween would allow us to compare the surfactants ability to affect disintegration time. The surfactant Span 20 was also tested (not shown here), although this gave similar results to PEG 8000 and was discontinued. Despite the failure of CMC determination for PEGs, the results for PEG 8000 in particular suggest it does form micelles and thus may warrant classification as a surfactant, despite lacklustre support for this in the literature.
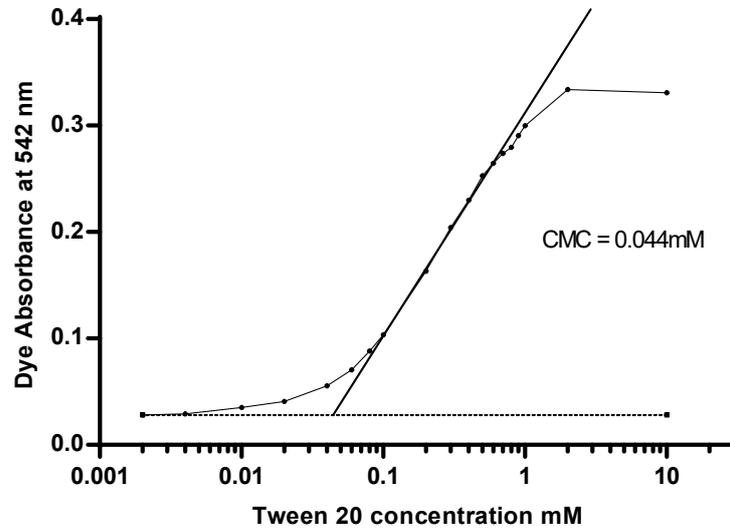
Figure 3.8 CMC determination of Tween 20 (0.044mM) by dye micellisation method (absorbance at 542nm, 25°C). Eosin Y in water in absence of surfactant (0.019mM) is displayed by a dashed line).
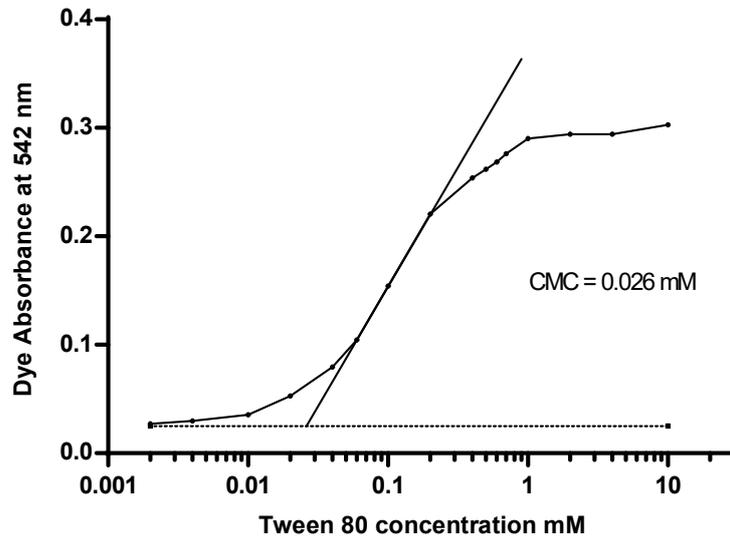
Figure 3.9 CMC determination of Tween 80 (0.026mM) by dye micellisation method (absorbance at 542nm, 25°C). Eosin Y in water in absence of surfactant (0.019mM) is displayed by a dashed line).
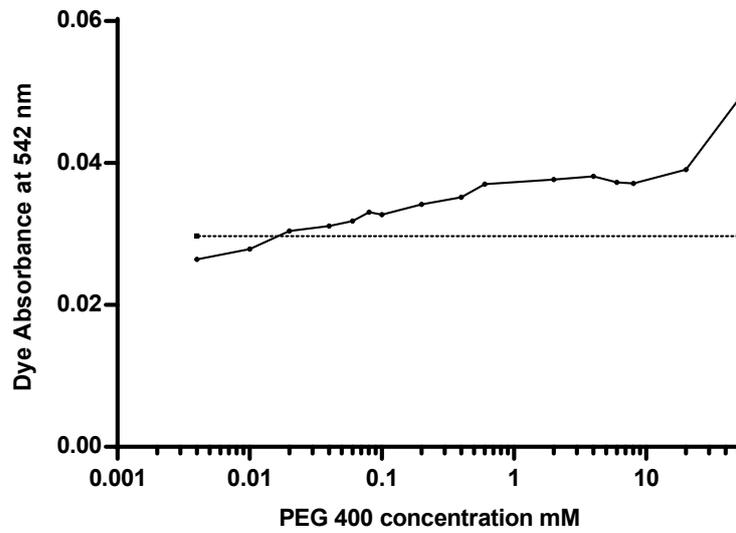
Figure 3.10 CMC determination of PEG 400 by dye micellisation method (absorbance at 542nm, 25°C). Eosin Y in water in absence of surfactant (0.019mM) is displayed by a dashed line).
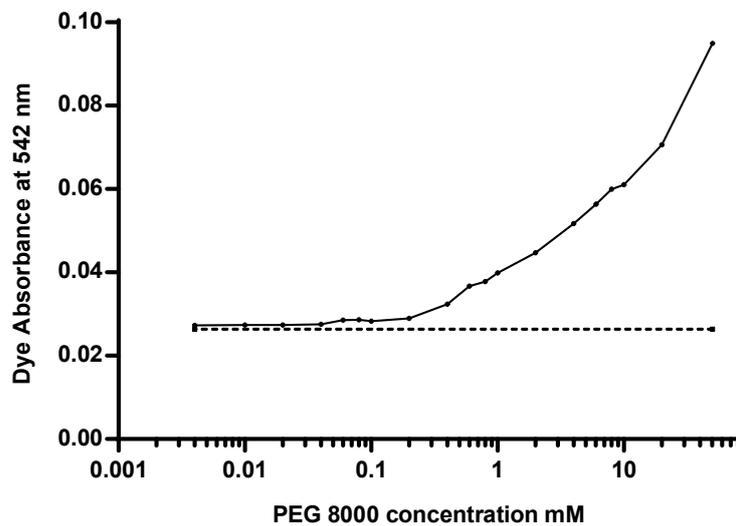
Figure 3.11 CMC determination of PEG 8000 by dye micellisation method (absorbance at 542nm, 25°C). Eosin Y in water in absence of surfactant (0.019mM) is displayed by a dashed line).

3.5.2.2 Surfactant Incorporation

Tablets coated with Kollicoat IR and a range of surfactants were tested for disintegration time and hardness. The results in Figure 3.12 do not show any decrease in disintegration time for any of the coated tablets when compared to the non-coated, with the majority showing that coating slowed disintegration. Only PEG 8000 and Tween 80 showed no change in disintegration time, at concentrations of 0.04 and 0.4mM, and ½ CMC and 10x CMC, respectively.

Hardness values for coated and non-coated tablets are shown in Figure 3.13. Addition of a coat had varying effects on tablet hardness, with some coats showing an increase in hardness and others a decrease; only Tween 80 at ½ and 10x CMC showed no significant difference compared to non-coated tablets. No obvious pattern in the data could be discerned. The greatest hardness was shown by tablets coated with Kollicoat IR and PEG 400 at 0.4mM, which showed an increase in hardness of 16.3%; Kollicoat IR alone showed a hardness increase of 9.2%. Similar increases in tablet hardness have been reported with coating of tablets with a hydroxypropyl methylcellulose coating formulation containing PEG 400 as a plasticiser and SLS as a surfactant [247]. It is unclear as to the effect of added surfactant from the results, although it is further suggested here that application of a film coat can enhance tablet hardness.
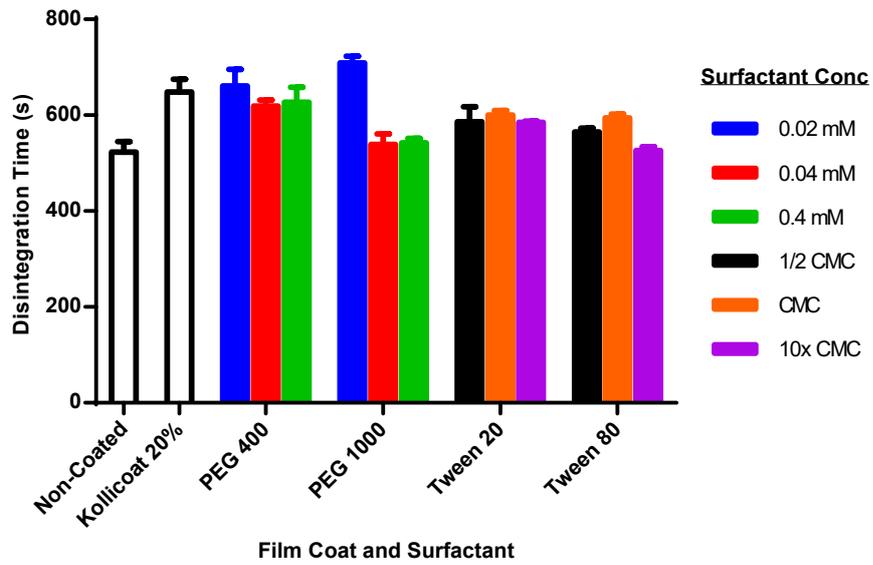
Figure 3.12 Disintegration time for film coated tablets (Kollicoat IR, 20% w/w) containing different surfactants at a range of concentrations. Tablets consisting of MCC (47%), mannitol (23.5%), D-sorbitol (23.5%), crospovidone (4%), silicon dioxide (1%) and magnesium stearate (1%) were produced by direct compression at 3 tons, 6 s dwell time (mean ±SD, n=3).
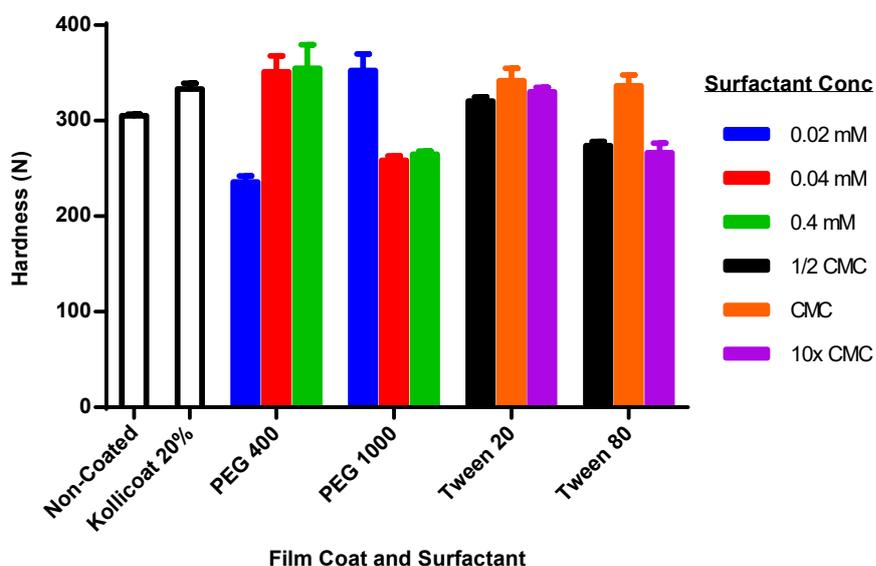
Figure 3.13 Hardness for film coated tablets (Kollicoat IR, 20% w/w) containing different surfactants at a range of concentrations. Tablets consisting of MCC (47%), mannitol (23.5%), D-sorbitol (23.5%), crospovidone (4%), silicon dioxide (1%) and magnesium stearate (1%) were produced by direct compression at 3 tons, 6 s dwell time (mean ±SD, n=3).

3.5.3 Discussion

CMC determination of PEG 400 and 8000 was unsuccessful, although it did suggest that PEG does show some surfactant behaviour. PEG 8000 in particular appeared to indicate micelle formation, although this does not plateau at such low concentrations. None of the results obtained show an improvement in disintegration time with addition of a surfactant, and in fact a marked increase in disintegration time was often observed. Since the success of ODTs often depends on a balance between disintegration speed and acceptable mechanical properties (including friability), even a small enhancement of tablet hardness (a maximum here of 16.3%) could make the difference between pass or failure.

3.6   Bi-layer Coating of Tablet Cores

Coating of tablet cores using Kollicoat IR combined with a surfactant had a mixed impact on disintegration time and hardness. The failure of surfactant to enhance disintegration may be due to its low concentration compared to, and interaction with, the coating polymer. As such, it was decided to segregate the coating polymer and surfactant by applying them as distinct coating layers (Figure 3.14). A surfactant coating solution, consisting of PEG as a film forming agent and plasticiser and Tween 80 as a surfactant was applied as a single discrete layer. A separate layer consisting of Kollicoat IR was also applied. Each film coat layer was tested as both an external layer and an internal layer. In addition, as an alternative to a surfactant coating, another PEG-based coating containing starch as a disintegrant was also tested. It was believed that swelling of starch in contact with water would aid in breaking of the film coat. Furthermore, combination of Tween 80 with starch as a single layer was also investigated. Film coating was applied to both hard tablet cores and weaker tablet cores.

3.6.1   Materials and Methods

Hard tablet cores consisting of (w/w) MCC (47%), mannitol (23.5%), D-sorbitol (23.5%), crospovidone (Kollidon CL, 4%), silicon dioxide (1%) and Mg stearate (1%) were produced by direct compression at 3 tons, 6 s dwell time. Weak cores consisting of Pearlitol Flash (99.6% w/w) and Mg stearate (0.4% w/w) were produced by direct compression at 1.6 ton, 6 s dwell time. Film coats containing a surfactant, a disintegrant or a combination of both were formed using PEG-8000 (10% w/w) as a film forming agent and plasticiser. The surfactant Tween 80 was included at 0.5% w/w and starch 1500 was included at 5% w/w as a disintegrant. The different film coat formulations are shown in

		C1	C2	C3	C4	C5	C6	C7	C8	C9
Inner layer	Kollicoat IR (20% w/w)			✓			✓			✓
	Tween 80 (0.5% w/w)	✓	✓					✓	✓	

	C1	C2	C3	C4	C5	C6	C7	C8	C9
Starch 1500 (5% w/w)				✓	✓		✓	✓	
Outer layer Kollicoat IR (20% w/w)		✓			✓			✓	
Tween 80 (0.5% w/w)			✓						✓
Starch 1500 (5% w/w)						✓			✓

Table 3.3.

Figure 3.14 Schematic of a bilayer coating (shaded regions) around a tablet core

Table 3.3 Different film coat formulations C1-9 (coating 1-9), described as either an inner layer or an outer layer. Tween 80 and starch 1500 are in a 10% w/w PEG 8000 aq solution.

		C1	C2	C3	C4	C5	C6	C7	C8	C9
Inner layer	Kollicoat IR (20% w/w)			✓			✓			✓
	Tween 80 (0.5% w/w)	✓	✓					✓	✓	
	Starch 1500 (5% w/w)				✓	✓		✓	✓	
Outer layer	Kollicoat IR (20% w/w)		✓			✓			✓	
	Tween 80 (0.5% w/w)			✓						✓
	Starch 1500 (5% w/w)						✓			✓

3.6.2 Results and Discussion

3.6.2.1 Coating of Hard Tablet Cores

Hard-core coated tablets were tested for disintegration time and hardness, Figure 3.15 and Figure 3.16, respectively. Disintegration was slowed by coating with Kollicoat IR and no improvement was seen with C1-C9, with C6, C7 and C8 demonstrating significantly slower disintegration time (P<0.05). Tablet hardness was improved by coating with Kollicoat IR alone, showing an increase from 305.07 ± 1.60 to 333.10 ± 6.13 N when compared with the uncoated tablets. Significant decreases in tablet hardness were seen with all other film coats, with the exception of C2.
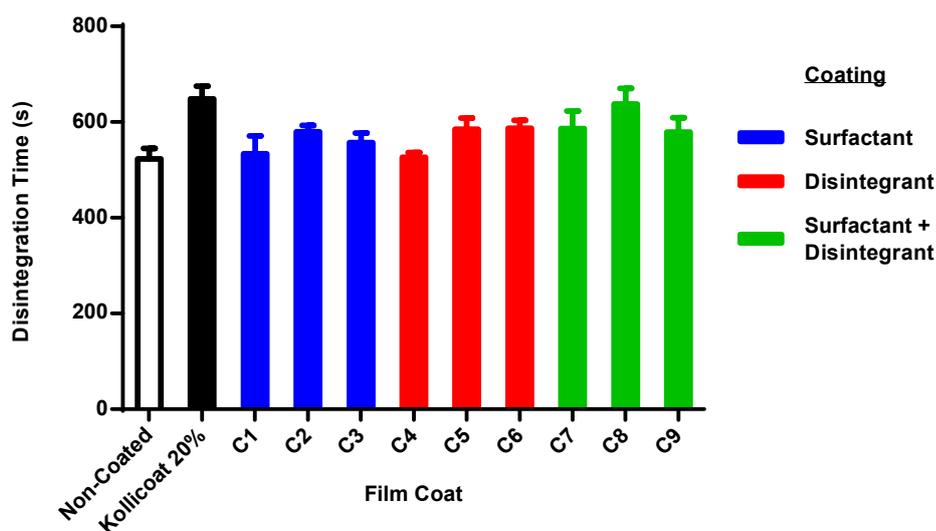
Figure 3.15 Disintegration time of hard tablet cores coated with a surfactant, a disintegrant or a surfactant and a disintegrant, with or without an additional Kollicoat IR (20% w/w) layer. Tablets consisting of MCC (47%), mannitol (23.5%), D-sorbitol (23.5%), crospovidone (4%), silicon dioxide (1%) and magnesium stearate (1%) were produced by direct compression at 3 tons, 6 s dwell time (mean ±SD, n=3).
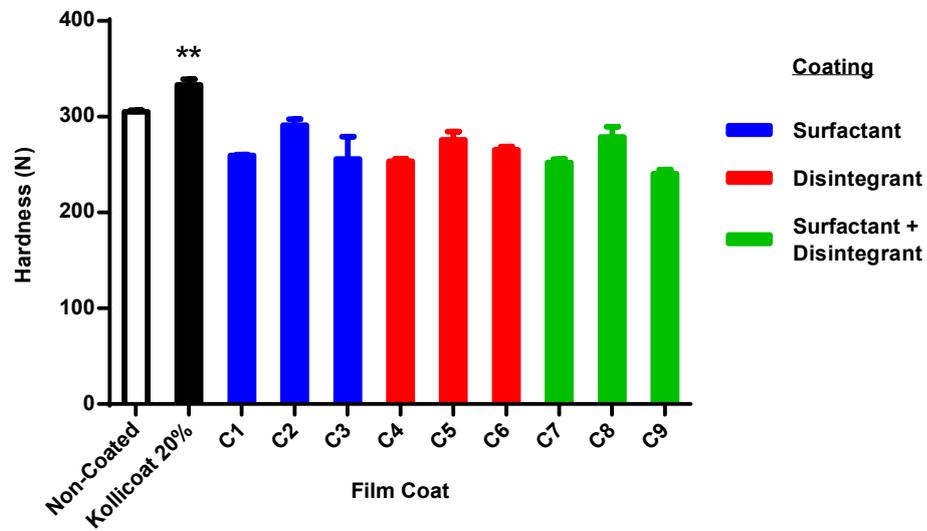
Figure 3.16 Hardness of hard tablet cores coated with a surfactant, a disintegrant or a surfactant and a disintegrant, with or without an additional Kollicoat IR (20% w/w) layer. Tablets consisting of MCC (47%), mannitol (23.5%), D-sorbitol (23.5%), crospovidone (4%), silicon dioxide (1%) and magnesium stearate (1%) were produced by direct compression at 3 tons, 6 s dwell time (mean ±SD, n=3, ** $P<0.01$ compared to non-coated)

3.6.2.2 Coating of Weak Tablet Cores

The addition of a surfactant layer alone and also as an inner layer with Kollicoat IR as an outer layer (C1 and C2, respectively) appeared to lower disintegration time (Figure 3.17) by around 5 s (15%) when compared to non-coated control, although this was not significant (P>0.05). This was however significant when compared to coated controls. When Kollicoat IR was applied as an inner layer, disintegration time rose. Applying coating layers consisting of disintegrant, surfactant or a combination of disintegrant and surfactant had no beneficial effect on disintegration time and in general slowed disintegration. C2 and C6 (Kollicoat IR containing coats) show decreased disintegration time when compared to Kollicoat IR alone.

Hardness values (Figure 3.18) did not demonstrate the same variability as disintegration times. No changes in hardness were seen with any of the film coated tablets.
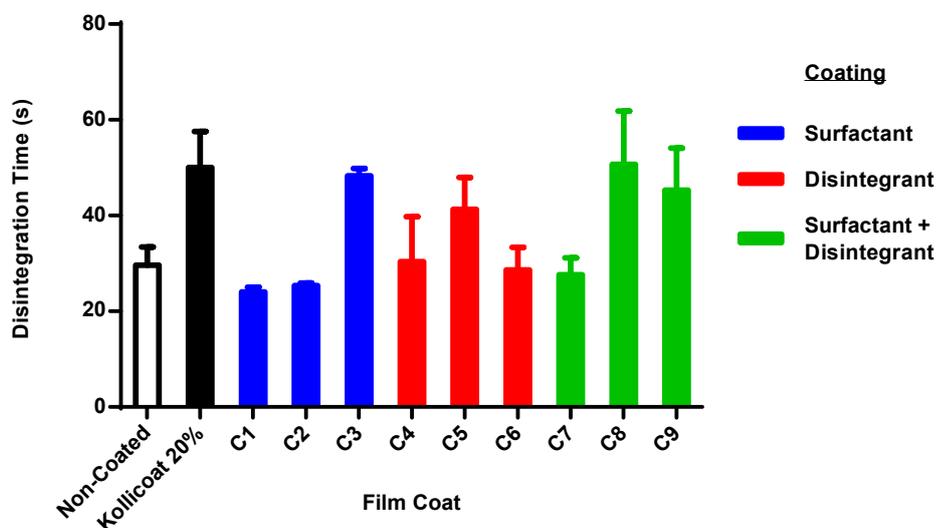
Figure 3.17 Disintegration time of soft tablet cores coated with a surfactant, a disintegrant or a surfactant and a disintegrant, with or without an additional Kollicoat IR (20% w/w) layer. Tablets consisting of Pearlitol Flash (99.6%) and magnesium stearate (0.4%) were produced by direct compression at 1.6 ton, 6 s dwell time (mean ±SD, n=3).
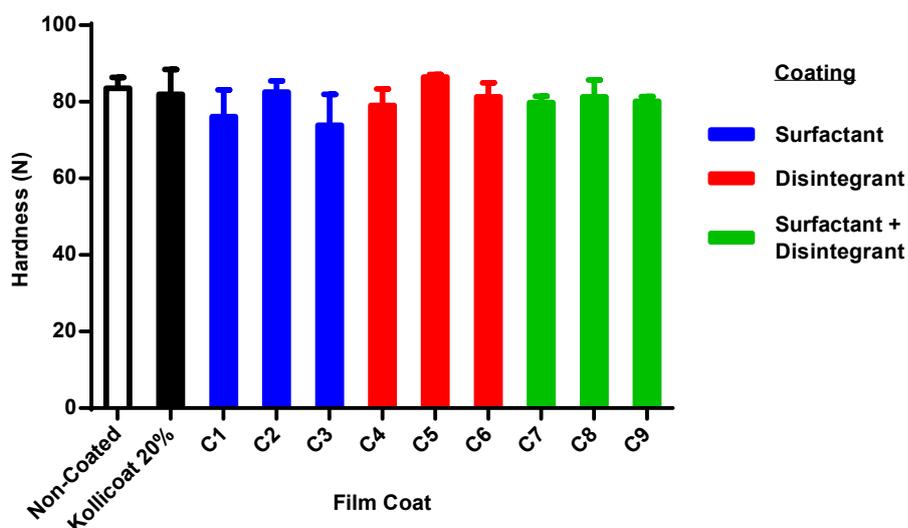
Figure 3.18 Hardness of soft tablet cores coated with a surfactant, a disintegrant or a surfactant and a disintegrant, with or without an additional Kollicoat IR (20% w/w) layer. Tablets consisting of Pearlitol Flash (99.6%) and magnesium stearate (0.4%) were produced by direct compression at 1.6 ton, 6 s dwell time (mean ±SD, n=3).

3.6.3   Discussion

Bilayer coating was not successful in enhancing disintegration compared to non-coated controls. When comparing to coated controls however, improvements were seen in disintegration time to the detriment of hardness (with hard cores), and improvements in disintegration and hardness values in some weak cores. Despite no improvement in disintegration compared to non-coated cores, several variations of bilayer coatings were able to show similar disintegration times, whilst simultaneously not compromising hardness. Furthermore, more favourable results were seen with weak cores, potentially due to greater porosity and thus wettability through capillary action. Weak cores however would ideally require a specialised coating that improved both disintegration time and mechanical properties.

Despite not being demonstrated here, based on previous work it was hypothesised that improvement of tablet hardness by applying Kollicoat IR as a film coat could be employed for weak tablet cores. Coating of weak cores would be suitable for APIs that have a poor compactibility profile and thus form weak compacts and for ODTs, since these are inherently weak due the necessity for rapid disintegration. The problem with this however

is that coating through conventional techniques requires tablets with very low friability due to the high contact process.

3.7   Stationary Film Coating: A Novel Approach for Application of Polymeric Film Coatings to Weak Cores

Poorly compactable drugs form weak compacts and suffer from undesirable mechanical properties [248, 249]. Similarly, ODTs often also display poor mechanical properties due to their requirement for rapid disintegration in the mouth [250]. To produce an ODT that simultaneously displays rapid disintegration and good mechanical strength is a significant challenge.

The two main techniques for application of a polymeric film coat, fluidised bed and pan coating, require robust tablets, with friability not exceeding 0.3% and ideally below 0.1% [220]. Thus, coating of weak cores to improve mechanical strength is not applicable using these techniques. To avoid substantial weight loss through fluidisation a novel approach for stationary film coating of weak cores was theorised. This would involve the tablet to be remain stationery during the coating process so that contact with surfaces within the coating chamber and other tablets is eliminated.

3.7.1   Materials and Methods

3.7.1.1 ODT Preparation and Coating

Aqueous solutions of Kollicoat IR (20% w/w) were used in the developmental stage. Weak cores consisting of 99% (w/w) Pearlitol Flash and 1% (w/w) Mg stearate were used for coating. Total tablet weight was 500 mg and tablets were directly compressed at 1 ton for 6 s. The fluidised bed coater was modified for stationary coating of tablets. Film coat solution was pumped at a low rate of 2 rpm or a high rate of 4 rpm, where stated.

3.7.1.2 Confocal Microscopy

Confocal microscopy was performed on a CLSM TCS SP5 II System (Leica Microsystems GMBH, UK) using a 10x dry objective. Riboflavin monophosphate sodium was used as a fluorescent dye (0.5% w/w) in the film coat solution, as described by Ruotsalainen, Heinämäki [251] and scanned at a wavelength of 458 nm. Maximum projection images were used to analyse the surface morphology based on the intensity of the fluorescence of pixels within each plane. Maximum projection images were also

rotated to provide a transverse view of the film coating to reveal film coat thickness, the morphology of the outer coating surface and also the tablet-core interface.

3.7.2   Development Pathway

In fluidised bed systems coating solution is sprayed from above onto tablets using an atomisation nozzle, whilst heated air from below the tablet bed suspends and dries the tablets within the coating chamber. For stationary coating, weak cores were initially tested on a fixed, perforated platform (Figure 3.19) that was inserted inside the fluidisation chamber. Hardness values for these tablets were 57.43 ± 16.26 N coated, around a 70% increase when compared to uncoated tablets which displayed hardness of 34.19 ± 3.20 N.

Despite a considerable increase in hardness values, the data showed high variance. Furthermore, quality of the film coat was very poor, with extensive peeling of the film coat from a high proportion of tablets which was attributed to tablet over-wetting [252]. Another significant issue was scattering of tablets due to the high pressure atomising air from above (tablets had to be contained within a ring), meaning that drying was impeded. As a result of over wetting and peeling, the successful yield was low.
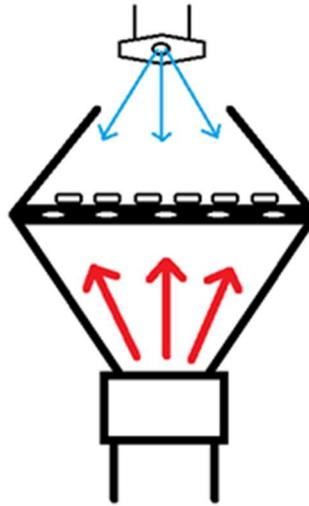
Figure 3.19 Schematic of modifications made to the film coater. A perforated platform was placed within the coating chamber so that the tablets would be stationary during coating. Heated air flow is shown in red and film coat solution spray is shown in blue.

It was concluded that incomplete drying of tablets during coating had led to over wetting. Both the heat inside the chamber and the air flow over the tablets are important for efficient water evaporation. To improve this, tablets were held in place by vacuum so that a strong air flow over tablets could be applied without the tablets scattering. Tablets were placed on top of a new perforated platform within the coating chamber and held in place by vacuum (Figure 3.20). Numerous trials with this modified setup were necessary for optimisation of the process and process parameters. Although improvements in coating quality were seen, the yield remained low due to poor adhesion of the coat to the tablet surface and subsequent peeling of the coat from the tablet. This was attributed to the heated air from below flowing around the inner cone and not over the tablet surface.
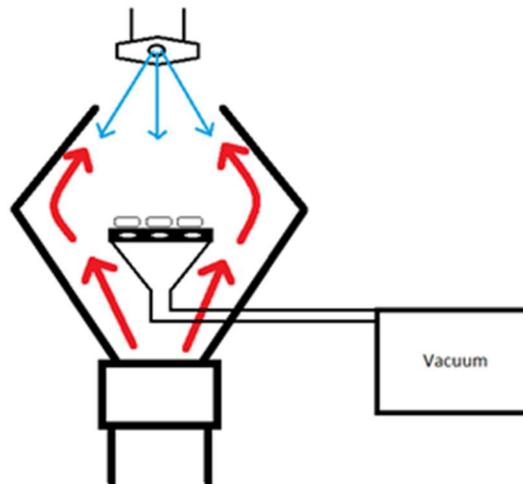
Figure 3.20 Schematic of modifications made to the film coater. A separate funnel with a perforated platform was placed inside the coating chamber. This was attached to a vacuum to hold the tablets fixed in place during coating. Heated air flow is shown in red and film coat solution spray is shown in blue.

Through modification of the coating chamber it was possible to redirect the air flow (Figure 3.21) over the tablet surface, instead of directly escaping from the top of the coating chamber, to improve drying. This modification bore an immediate improvement in film coat adhesion and a greater yield. Several runs optimising the process parameters saw improvements in hardness to around 55 N. Addition of a curing step (45°C overnight) increased tablet hardness as high as 66.65 ± 10.22 N. The addition of extra heated air from above was also tested, showing similar hardness values of 62.58 ± 8.66 N. Through the modification of a generic fluidised bed system, hardness values of coated tablets were effectively doubled (from 34.19 ± 3.20 N for uncoated tablets).
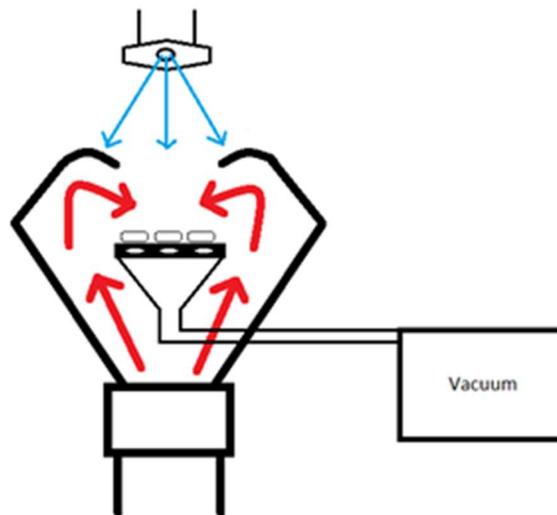
Figure 3.21 Schematic of modifications made to the film coater. The opening to the top of the chamber was modified to redirect air flow back towards the tablet platform. Heated air flow is shown in red and film coat solution spray is shown in blue.

The ability of this modified system was tested on model formulations containing a poorly compressible and compactable drug, metformin HCl [253, 254] and a drug that displays good compressibility and compactability and poor water solubility, ibuprofen [255, 256]. The tablets (500 mg) consisted of 10-50% API, 49-89% Pearlitol Flash and 1% Mg stearate w/w. Tablets (500 mg) containing a flucloxacillin sodium dose of 68 mg (equivalent to 62.5 mg Flucloxacillin), 85.4% Pearlitol Flash and 1% Mg stearate were also coated and tested. The results for hardness are displayed in Figure 3.22 and Figure 3.23.
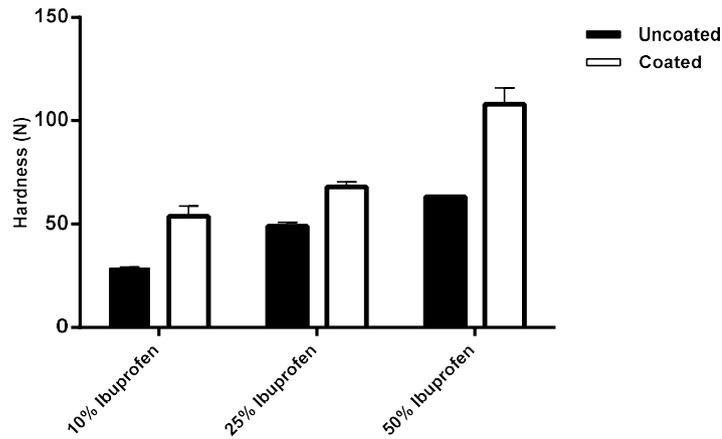
Figure 3.22 Hardness values for ibuprofen tablets at varying concentrations (% w/w) before and after stationary coating with 20% w/w Kollicoat IR. Tablets (500 mg) consisting of API, 1% Mg stearate and Pealitol Flash as a diluent were produced by direct compression, 1 ton, 6 s dwell time (n=3, mean ± sd).
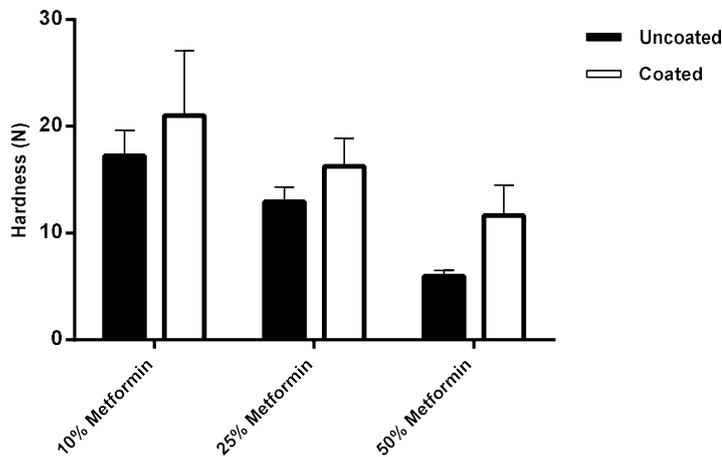
Figure 3.23 Hardness values for metformin HCl tablets at varying concentrations (% w/w) before and after stationary coating with 20% w/w Kollicoat IR. Tablets (500 mg) consisting of API, 1% Mg stearate and Pealitol Flash as a diluent were produced by direct compression, 1 ton, 6 s dwell time (n=3, mean ± sd).

Ibuprofen tablets showed substantial increases (p<0.001) in hardness after coating, rising to as high as 107.90 ± 8.00 N for 50% ibuprofen coated tablets. An increase in hardness of coated metformin tablets was only present at 50% metformin concentration. The more modest effect seen with metformin tablets may be due to the soft cores being more susceptible to over wetting when compared to the stronger ibuprofen cores and given metformin's high water solubility [257], a problem that may be overcome by improved drying efficiency. Nevertheless, the results from this small study serve as a convincing proof of concept.

For the flucloxacillin tablets, hardness increased by 23% from 66.3 ± 7.48 N to 81.56 ± 7.96 N. Both the coated and uncoated ODTs disintegrated within 2 mins 41 s, which is within the European Pharmacopeial limit of 3 mins [34]. Actual disintegration time is anticipated to be shorter as the USP test does not take into account the physiological conditions of the mouth [258].

3.7.3   Confocal Laser Scanning Microscopy

Confocal Laser Scanning Microscopy (CLSM) was employed to analyse the coating surface characteristics, coating thickness and tablet-coating interface. Several variations of tablet/coating were used in order to determine the effect of the process conditions, tablet characteristics and the stationary coating method. Soft cores and hard cores were coated for 40 min using the stationary method at a low pump rate to ensure a smaller droplet size for efficient drying and smooth coating surface (see chapter 4). Tablets coated using the stationary method were flipped half way through the coating period for coverage on both faces. Hard cores were coated using conventional fluidisation, one set at the regular pump rate for 40 mins whilst the other was coated at the same low pump rate conditions, but required coating for 90 mins for sufficient thickness. Individual images of the top face of the coated tablets were taken at sequential planes of focus to provide a non-invasive 3-D representation of the film coating. These images were compressed into a single maximum projection image (Figure 3.24). The images taken at multiple planes also allowed for 3-D projection of the surface based on the intensity of the fluorescence of pixels within each plane (Figure 3.25), allowing analysis of the surface morphology of the film coat. Maximum projection images were also rotated to provide a transverse view of the coating (Figure 3.26), similar to a cross-section, allowing comparison of the thickness of the film coating, the morphology of the outer coating surface and also the tablet-core interface.
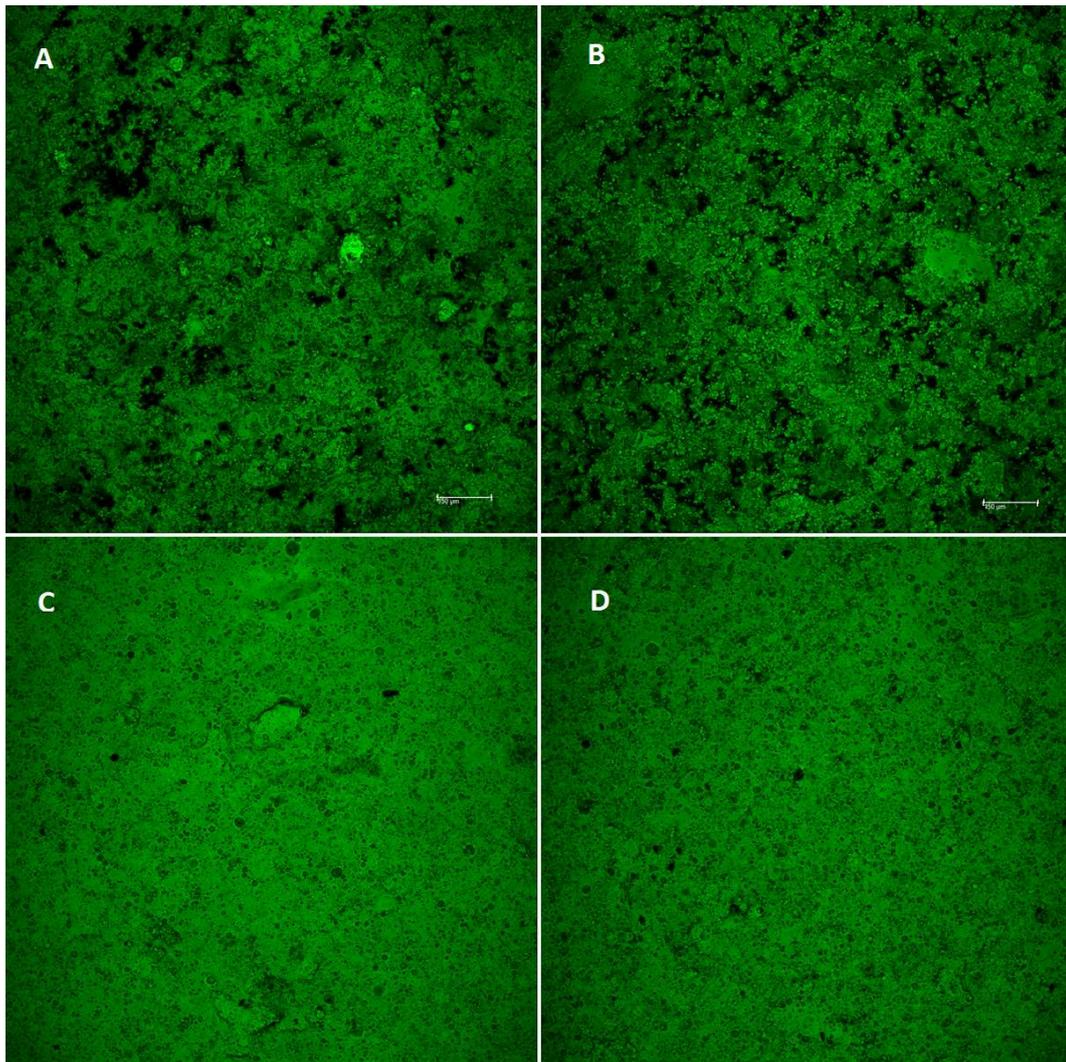
Figure 3.24 Maximum projections of the top surface of fluorescently coated tablets, providing information on the roughness and uniformity of the coating. Film coat consisting of Kollicoat IR 20% w/w and riboflavin 5'-monophosphate sodium 0.5% w/w as a fluorescent dye. Hard fluidised tablets coated at a higher pump rate (A), hard fluidised tablets coated at a low pump rate (B), hard stationary tablets (C) and weak stationary tablets (D) coated at a low pump rate.
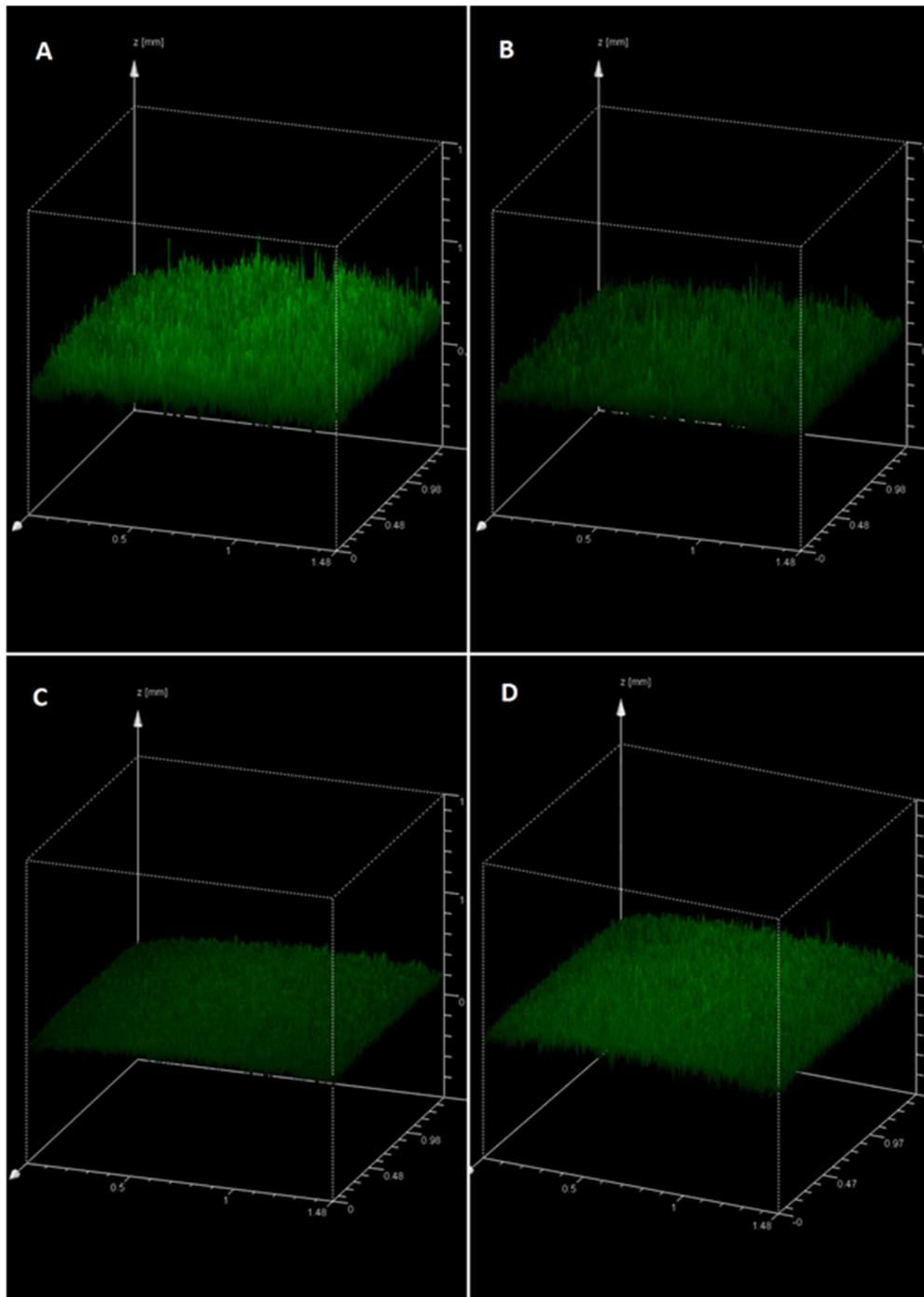
Figure 3.25 3D CLSM image showing fluorescence intensity at each image layer, providing a visual representation of surface morphology. Film coat consisting of Kollicoat IR 20% w/w and riboflavin 5'-monophosphate sodium 0.5% w/w as a fluorescent dye. Hard fluidised tablets coated at a higher pump rate (A), hard fluidised tablets coated at a low pump rate (B), hard stationary tablets (C) and weak stationary tablets (D) coated at a low pump rate.
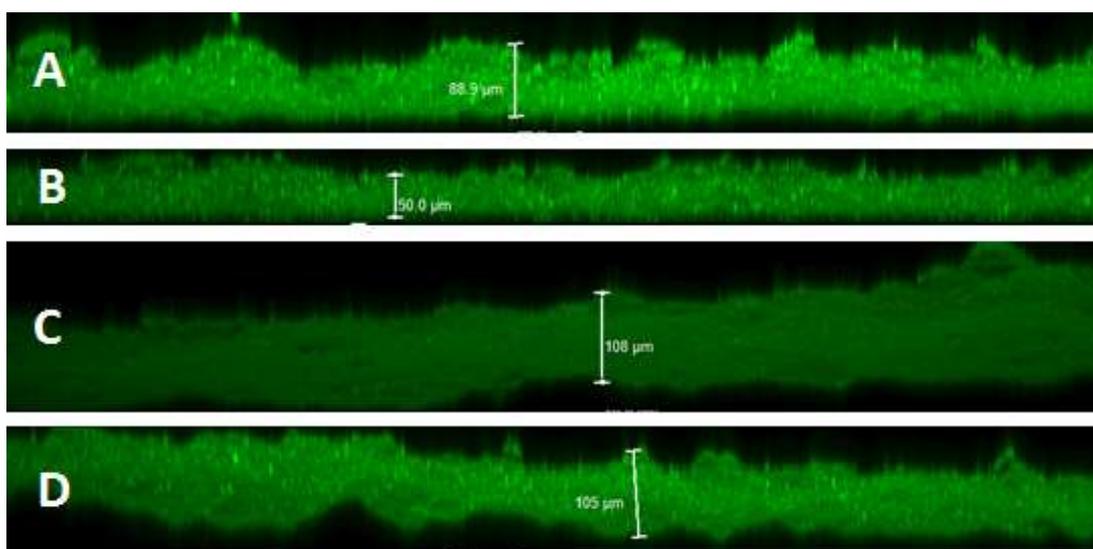
Figure 3.26 Transverse view of a maximum projection image, showing coating thickness, the morphology of the tablet surface (top) and the coating-core interface (bottom). Film coat consisting of Kollicoat IR 20% w/w and riboflavin 5'-monophosphate sodium 0.5% w/w as a fluorescent dye. Hard fluidised tablets coated at a higher pump rate (A), hard fluidised tablets coated at a low pump rate (B), hard stationary tablets (C) and weak stationary tablets (D) coated at a low pump rate.

A clear difference can be seen between the film coats produced by fluidisation and those produced by stationary film coating. Figure 3.24 and Figure 3.25 suggest that the fluidised coats have a rougher surface. The fluidised coats also appear to have a less complete and homogenous covering, with many dark patches apparent on the fluidised tablets indicating pores or a lack of coating coverage. It was necessary to coat the hard fluidised tablets at the lower pump rate for significantly longer (90 mins, as opposed to 40 mins) in order to produce a film with adequate thickness. At the lower pump rate, stationary tablets are sat within the plume of the spray, receiving a constant exposure to the film coat solution. When this low spray rate is applied to the fluidised environment, contact between the tablet and the coating solution is much less frequent. Despite more than doubling the coating time for the fluidised tablets at the low pump rate, the thickness was only roughly half that of the stationary (Figure 3.26), at around 50 µm compared to 100-110 µm, respectively, suggesting that the novel stationary method can produce a thicker coating in a shorter period of time. If accurate, the reduction in both financial and time costs could be substantial.

One concern over the stationary coating method, visible in Figure 3.26, is the unevenness of the tablet-core interface when compared to the smooth tablet-core interface of the fluidised tablets. This can likely be attributed to over wetting of the tablet surface and subsequent leaching of the coating solution into the tablet, or local disintegration at the tablet surface. Over wetting may also result in poor adhesion of the film coat solution to the tablet surface and pore formation between the tablet core and the coat. In either case, avoidance of over wetting through improving drying would likely provide insight into the root of this problem and may result in a smooth coating-core interface.

3.7.4 Discussion

Stationary coating provides a novel technique to improve the mechanical characteristics of weak cores and could aid in the development of ODTs and solid dosage forms of poorly compressible and compactable drugs. The evidence here suggests that coating in this way may also improve the quality and uniformity of the film coating. This method may also benefit from quicker coating times, thus saving time and reducing cost. There are of course limitations to this novel approach that demand attention, namely the requirement to manually flip the tablets during the coating process to coat both faces. Similarly, although tablet edges were coated the quality and consistency of this was not investigated here. To resolve both of these issues may require a radical new approach to provide even coating of stationary dosage forms; conversely, this may also be achieved through simply using tablets of a more rounded geometry, coupled with enhancing the spreadability of the coating polymer solution. Furthermore, problems likely resulting from over wetting would necessitate improved drying. With the potential various benefits and despite the limitations described here, as a proof of concept, stationary film coating was able to impart substantial mechanical strength onto weak tablet cores, a feat otherwise not possible with conventional coating methods due to the high tablet attrition they cause.

3.8   Conclusion

The ability to improve the mechanical strength of tablets, including both crushing strength and friability, was demonstrated by application of an instant release film coating. The effect on disintegration time with incorporation of other excipients into the film coat, namely surfactants and disintegrants, in either a single layer or bilayer was inconclusive. Regardless of this however, it was shown that a coating could be applied to a tablet without hindering either disintegration or hardness, whilst offering the various advantages of a coating, significantly in this case, the reduction of tablet friability to a negligible level. The limitation of weak cores of poorly compactable drugs to lose substantial weight through the fluidised bed coating process was addressed by the development of a novel stationery coating technique. Modification of the existing fluidised bed apparatus through use of a vacuum system to hold the tablets in place and redirection of the air flow inside the coating chamber overcame the complications of tablet scattering and over-wetting, respectively. Furthermore, weak tablets containing poorly compactable drugs coated using this technique followed by a curing stage displayed enhanced hardness and a satisfactory finish and thus formed a proof of concept for this novel approach. Several limitations for this new technique were prevalent and require addressing, most importantly the ability to rotate the tablets automatically during the process to ensure complete and uniform coating and further improvement of the drying process. Despite these concerns, the potential to improve the mechanical properties of weak tablets by stationary coating is, prior to this work, unexplored and could open up new possibilities in solid oral dosage form development.

Chapter 4 – Design of Experiments to Study the Impact of Process Parameters and
Development of Non-Invasive Imaging Techniques in Tablet Coating

175

Chapter 4

Design of Experiments to Study the Impact of Process Parameters and Development of Non-Invasive Imaging Techniques in Tablet Coating

Chapter 4 – Design of Experiments to Study the Impact of Process Parameters and Development of Non-Invasive Imaging Techniques in Tablet Coating

4.1 Introduction

The atomisation of a liquid stream into a fine spray is utilised in a variety of industries for a range of applications, including the pharmaceutical industry, where it is most notably employed for tablet film coating [79, 259]. During the atomisation process individual droplets evolve from a liquid stream with a concurrent increase in surface area to mass ratio of the liquid [260]. In principle, for atomisation to occur it is necessary to generate a high relative velocity between the liquid stream and the surrounding air or gas [261, 262]. The ratio of the flow rates of the atomising air and the liquid stream, known as the atomisation to liquid flow ratio (ALM), is considered an important parameter in determining droplet size [263, 264]. Various reports highlight the dependency of droplet size on both atomisation pressure and liquid flow rate (pump rate) [265, 266] and both have been recognised as critical process parameters (CPPs) for coating processes [267]. Viscosity is also known to significantly influence droplet size during atomisation [268, 269], with higher viscosity liquids forming larger droplets during atomisation.

Twin-fluid atomisation is a complex and multivariable process that, despite significant efforts, is still not well understood and remains difficult to predict [268]. The general agreed mechanism involves an initial sheet formation of the liquid stream after exiting the nozzle, followed by a breakup into stretched liquid ligaments and then droplet formation [76, 77, 259, 270]. A more recent and complex two-stage instability mechanism comprises the formation of an initial shear instability forming waves on the liquid surface and then a Raleigh-Taylor instability at the wave crests, forming ligaments that stretch and further break up into droplets [268, 271-273]. Unfortunately for tablet film coating, few studies have been undertaken using non-Newtonian (viscous) fluids [274].

Production of a high quality tablet film coat depends upon multiple factors such as the formulation [275], equipment [276] and process parameters [277, 278]. The importance of droplet size on coating efficiency and quality has been reported, [270, 279, 280] with small droplets responsible for a more homogenous or even distribution of coating solution on the tablet surface [281, 282]. More rapid water evaporation due to the greater volume to surface area ratio of small droplets [283-285] leads to greater coating efficiency [286]. Over-wetting, which can result in defects such as poor adhesion of coating polymer to the tablet surface, peeling, twinning, picking and sticking and tablet erosion [79, 287], is thus less prevalent with smaller droplets. Tablet defects, particularly poor adhesion can harm film functionality and negatively impact on the mechanical properties provided by a film coat. Typical droplet sizes in fluidised bed coating range

between 20 and 100 µm, with coating efficiency reportedly being optimal below 10 µm, although this may run the risk of spray-drying of droplets before they reach the tablet surface [286, 288]. To date no studies have investigated the direct impact of droplet size on tablet film coat using micro scale imaging. Revealing the micro scale morphology of the coat in this way could provide information on coat quality as well as the interaction of the coat with the tablet core.

The aim of this study was to investigate and identify the differences in tablet film coats produced from either small or large droplets using micro imaging techniques. To produce droplets of a known size a design of experiments (DOE) approach was implemented to evaluate the impact of three CPPs: atomisation pressure, pump rate and polymer concentration on droplet size during atomisation of a film coat solution from a twin-fluid external mixing nozzle. The generated model was then exploited to reveal the process conditions required to achieve droplets of a desired size. The hypothesis that small droplets would create films that were more even and homogenous was then tested non-invasively using confocal microscopy (CLSM) and X-ray microcomputed tomography (XµCT). CLSM has been used previously for imaging of film coatings [251, 289, 290] and XµCT has been used to study tablet microstructure [291], particle coating [292] and tablet coat visualisation [251, 293], although common radiopacifying agents to improve contrast have not previously been included. Both imaging techniques provided qualitative and quantitative information that revealed differences in coat characteristics depending on the droplet size used.

4.2 Materials and Methods

4.2.1 Materials

D-mannitol, D-sorbitol, magnesium stearate, bismuth(III) oxide and barium sulphate were purchased from Sigma –Aldrich (Poole, UK). Polyplasdone XL-10 (crospovidone) was obtained from ISP (Switzerland). Avicel PH102 (MCC) was obtained from FMC Biopolymer (Philadelphia, USA). Aerosil 200 Pharma (colloidal silicon dioxide) was obtained from Evonik Industries (Essen, Germany). A coating polymer Kollicoat IR (BASF, Germany) and a fluorescent dye riboflavin 5′-monophosphate sodium salt (Sigma-Aldrich, Pool, UK) were obtained for film coating work.

4.2.2 Viscosity Measurements

Viscosity measurements of Kollicoat IR solutions were performed on a Brookfield LVDV-I+ viscometer (Massachusetts, USA) using spindle 1 (for concentrations of 12.5% w/w and below) and spindle 2 (for 20% w/w) at 100rpm, 25°C.

4.2.3 Tablet Formation

A formulation consisting of MCC (47% w/w), mannitol (23.5% w/w), sorbitol (23.5% w/w), crospovidone (4% w/w) and silicon dioxide (1% w/w) was blended for 5 mins followed by addition of magnesium stearate (1% w/w) and further blending for 1 min. Direct compression of tablets (500 mg) at a compaction force of 30 kN and 6 s dwell time was performed using an Atlas T8 automatic press SPECAC® (Slough, UK). A 13mm round, flat faced die was used for tablet production. All tablets were produced under ambient conditions.

4.2.4 Film Coating and Apparatus

Suspensions of Kollicoat IR (BASF. Germany) were prepared using ultrapure water. The suspensions were pumped and atomized using a Mini Coater Drier-2 (Caleva Process Solutions Ltd., Dorset, UK) comprising a 1/8 JJAU-SS air-actuated external mixing

atomising nozzle (Spraying Systems Co., Wheaton, IL, USA). Film coating conditions were determined from the results obtained from the DOE study to obtain desired droplet sizes. In all cases, fluidization air was provided at a velocity of 16 m/s and a temperature of 60°C. Assuming a linear correlation between coating time and film coat thickness for solutions of the same polymer concentration, large droplet coating was performed for 2.5x longer to achieve a similar coating thickness between the two droplet sizes.

4.2.5 Droplet Size Analysis

Real-time measurement techniques offer the advantage of measuring droplet size ranges and droplet dimensions more accurately [251, 294]. Real-time droplet size measurements using laser diffraction was performed on a Spraytec System (Malvern Instruments Ltd, Malvern, UK), to record droplet size distribution under different conditions. In order for the laser to access the spray path the fluidisation chamber was removed and the spray gun was placed 8 cm above the path of the laser beam. The measuring distance to the nozzle was set at 8.5 cm. Each sample was measured in a continuous mode for one min, with particle size distribution measured once per s. Kollicoat IR solutions were used for droplet size analysis.

4.2.6 Design of Experiments (DOE)

4.2.6.1 CQA and CPP Selection

Critical quality attribute (CQA) and CPP selections were based on reports from the literature concerning the importance of droplet size on coating quality and parameters effecting droplet size during atomisation, discussed earlier. CPP selection was also determined by the limitations of the experimental setup, namely removal of the coating chamber. Droplet volume median diameter (VMD) was selected as a CQA and a range of 20-100 µm chosen based on typical droplet size range during coating and the risk of spray drying at lower droplet sizes. Pump rate, atomisation pressure and viscosity/polymer concentration were chosen as CPPs. Appropriate CPP ranges were founded on the equipment ranges and preliminary work with the apparatus and coating polymer. The atomisation pressure range was set at 1-2 bar and pump rate at 1-4 rpm

(corresponding to a flow rate of 10-40 ml/hour). Kollicoat IR concentrations (w/w) were set at 5%, 12.5% and 20% corresponding to a viscosity of 0.99, 3.10 and 15.00 mPa.s respectively.

4.2.6.2 Experimental Design

Modelling of the atomisation process was performed using MODDE 10 software (Umetrics, Sweden). A quadratic process model using response surface modelling optimisation with a central composite face-centred design was chosen. This required 17 runs, including 3 centre points. These ranges were used to set low, medium and high levels for each parameter, see Table 4.1. Medium levels were used for the centre point measurements and were run in triplicate. All experimental runs are shown in Table 4.2.

Table 4.1 Low, medium and high levels for CPPs. The medium level for each CPP was used for centre point measurements.

	Low	Medium	High
Pump Rate (rpm)	1	2.5	4
Atomisation Pressure (bar)	1	1.5	2
Kollicoat IR Concentration (% w/w)	5	12.5	20

Table 4.2 Randomised experimental runs for DOE study, including 3 centre points. Experiment number 14 (greyed out) was eventually removed from consideration

Experiment Number	Run Order	Pump Rate (rpm)	Pressure (bar)	Concentration (% w/w)
13	1	2.5	1.5	5
16	2	2.5	1.5	12.5
6	3	4	1	20
11	4	2.5	1	12.5
2	5	4	1	5
8	6	4	2	20
7	7	1	2	20
3	8	1	2	5
15	9	2.5	1.5	12.5
1	10	1	1	5
14	11	2.5	1.5	20
12	12	2.5	2	12.5
9	13	1	1.5	12.5
5	14	1	1	20
10	15	4	1.5	12.5
17	16	2.5	1.5	12.5
4	17	4	2	5

4.2.7   Confocal Scanning Laser Microscopy (CLSM)

Confocal microscopy was carried out on a CLSM TCS SP5 II System (Leica Microsystems GMBH, UK) using a 10x dry objective. Riboflavin monophosphate sodium was used as a fluorescent dye (0.5% w/w) in the film coat solution, as described by Ruotsalainen, Heinämäki [251] and scanned at a wavelength of 458 nm. Maximum projection images were used to analyse the surface morphology based on the intensity of the fluorescence of pixels within each plane. Maximum projection images were also rotated to provide a side view of the film coating to reveal film coat thickness, the morphology of the outer coating surface and also the tablet-core interface.

4.2.8   X-Ray Microcomputed Tomography (XµCT)

XµCT was performed using a Skyscan 1172 high- resolution micro-CT (Bruker, Belgium). Samples were placed in a Perspex tube and separated by polystyrene spacers. Samples were scanned using an Al/Cu filter, at a pixel size of 6.79 µm, a source voltage of 89 kV, current of 112 µÅ and rotated through 360° at increments of 0.64°. Projections were reconstructed using NRecon software (Skyscan, Version 1.5.11) to produce non-invasive cross-sections of the tablets at sequential z planes.

4.2.9   Film Coat Water Content

Film coat sections (around 5 mg) were analysed for water content by thermogravimetric analysis (TGA). A PerkinElmer Pyris 1 TGA (Massachusetts, USA) was used to heat samples from 50-150°C (holding for 5 min at 100°C) and % weight loss measured as film coat water content.

4.2.10 Image Analysis

Porosity measurements of XµCT reconstructions were performed using two separate methods. Bruker-MicroCT CT-Analyser (CTAn, Bruker, Belgium) was used to provide porosity measurements of the coating using the 5 outermost reconstructions in the z-plane, calculating porosity using the porosity plug-in. ImageJ (National Institutes of Health, USA) was used to process the reconstructions by adjusting the image threshold by applying the Huang threshold and subsequent binarisation, followed by measuring the porous area fraction at a set ROI of the coating. Fluorescent coat porosity was measured in the same way as XµCT using the ImageJ method. Film coat thickness at the top and bottom tablet surface for fluorescent coats was performed using ImageJ, starting with image processing through initial contrast adjustment, followed by binarisation, hole filling and despeckling to produce one complete binary section. The local thickness plugin for ImageJ, based upon the algorithm developed by Hildebrand and Rüegsegger [295], was used to measure film coat thickness; this involves fitting spheres within the binary layer and the film coat thickness at any point measured as the diameter of the largest sphere at that point. Surface roughness of the coat was

represented by the root mean square (RMS) of the valleys and peaks of the coating, otherwise put as the standard deviation in individual film coat thickness values [296]. Heat maps were generated using the HeatMap From Stack ImageJ plugin by Samuel Péan [297].

4.3 Results and Discussion

A model of the atomisation process was generated from the droplet size data. Model optimisation revealed the parameters required to produce droplets of a given size and this informed the choice of process conditions for tablet coating. Before coating, however, the model required verification and validation.

4.3.1 DOE

4.3.1.1 Model Verification and Validation

A residuals normality plot was used to identify any outliers, resulting in the exclusion of one of the data points from the total 17. The quadratic model generated was fitted against the data and the response is shown in the summary of fit plot (Figure 4.1), which provides information on the strength and robustness of the model. The R^2 value of 0.977 signified a low variation in the response (droplet size) and strong fit between the data and the model. The Q^2 value of 0.837, ideally >0.5, demonstrated a high predictive power, allowing for confident prediction of the effect of changing process parameters on droplet size and process optimisation. The model also demonstrated a strong score for validity of 0.736, far exceeding the required value of >0.25. Similarly the value obtained for reproducibility of 0.967 significantly surpassed the requisite value of 0.5, indicating good experimental control and low pure error.

For further model validation a lack of fit plot and ANOVA were employed to compare the model error and pure error. In the lack of fit plot (Figure 4.1) the first bar shows standard deviation (SD) due to lack of fit or model error (SD-LoF) and the second bar shows the SD of the pure error (SD-pe). The final bar shows the SD of pure error * the critical F-value (SD-pePsqrt(F(crit)), at the p = 0.05 level of significance. The SD-LoF is much lower than SD-pePsqrt(F(crit), indicating a good fit. The ANOVA shows a very low variance of P <0.00001 due to the regression model, whereas the variance due to residuals and replicate errors was insignificant at a P value of 0.348. The results obtained for both lack of fit and ANOVA validate the model by demonstrating low error due to the model and a low level of pure error in the experimental setup, indicating good control over the experiment.

4.3.1.2 Regression Model Equations and Factor Effects

The regression model equation was based upon the correlation coefficients and their effect on droplet size. The values were determined from the effects plot (Figure 4.1), where the coefficient for each significant response was scaled and centred to allow for interpretation. Either a positive or negative effect on droplet size is judged significant if the confidence interval crosses the origin, with insignificant effects excluded from the model, giving the regression model equation:

$$Y_1 = 31.89 + 11.05\,X_1 - 10.28\,X_2 + 14.25\,X_2^2 + 14.29\,X_3^2 + 4.60\,X_2X_3 - 10.63\,X_1^2$$

Where: $Y_1 = Droplet\ size,\ X_1 = Concentration,\ X_2 = Pressure,\ X_3 = Pump\ Rate$
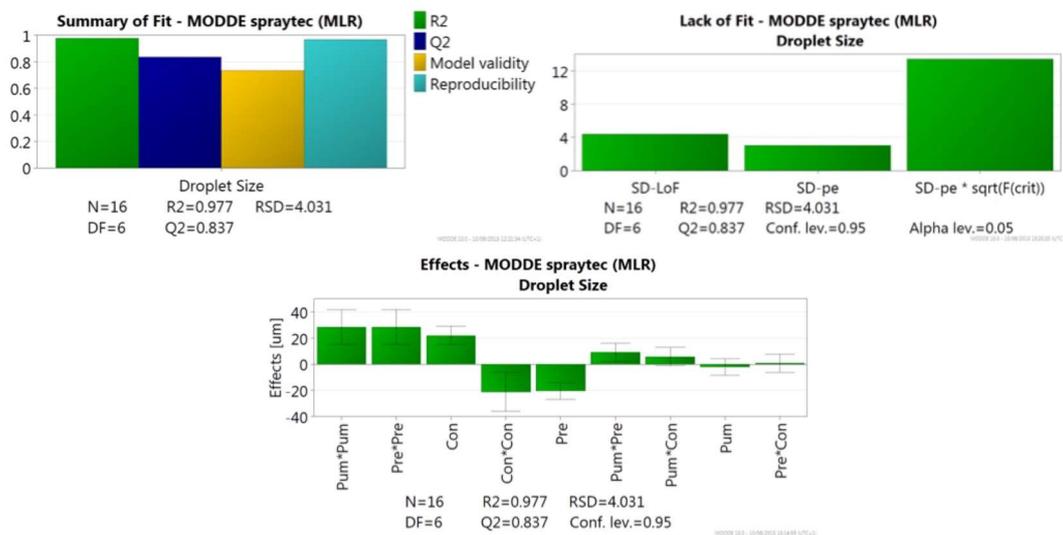
Figure 4.1 Summary of fit plot showing model fit (R^2), predictability (Q^2), model validity and reproducibility. The model has been fitted using RSM. Lack of Fit plot showing standard deviation (SD) due to lack of fit (SD-LoF), SD of pure error (SD-pe) and SD of pure error * the critical F-value (SD-pePsqrt(F(crit)). Effects plot for the three factors: pump rate (Pum), concentration of Kollicoat IR suspension (Conc) and atomisation pressure (Pre). Factors are ordered in terms of impact on droplet size. Confidence interval bars are included for each factor.

The derived regression model equation describes a complex process with linear and/or quadratic relationships for all parameters with droplet size. The most significant factor that showed a linear effect on droplet size is concentration (X_1), followed by the atomisation pressure (X_2). When the concentration of Kollicoat IR is increased there is an increase in droplet size; conversely, an increase in atomisation pressure leads to a reduction in droplet size. No significant linear relationship between pump rate and droplet size was seen. All three factors also had a significant quadratic relationship with change in droplet size, with pump rate and atomisation pressure showing very similar values for their coefficients. An interaction between pump rate and pressure (X_2X_3) was also detected, a finding made possible by DOE.

More detailed information on the effect that changes in each factor had on droplet size is shown in the Main Effects Plot, Figure 4.2. The plot for the interaction between pump rate and atomisation pressure is also shown in Figure 4.2. A clear trend can be seen with an increase in concentration causing an increase in droplet size and an increase in atomisation pressure causing a decrease in droplet size, with the effect of pump rate being more complex. All three plots show a characteristic curved quadratic shape. The increase in droplet size seen with increased Kollicoat IR concentration peaked around the 12.5% centre point, with little change seen at 20%. The relationship seen with increasing pump rate is complex, with the plot forming a clear U shape and the smallest droplets forming approximately between 2 and 3 rpm. The interaction plot between pump rate and atomisation pressure demonstrates finer droplet formation at high pressure. Notably, the difference in droplet size at low and high pump rates is different depending on the atomisation pressure; at low pressure there is a decrease in droplet size from around 77 to 65 µm, whereas at high pressure there is an increase in droplet size from around 47 to 54 µm. This behaviour of a decrease in droplet size with increased flow rate at low pressure and an increase in droplet size with increased flow rate at high pressure is in line with that described for external mix twin-fluid atomisers by Suyari and Lefebvre [294]. They attributed this behaviour to the fact that at low pressure the atomisation equipment operates in a simplex pressure-swirl mode, whereas at high pressure it operates in a simplex-airblast mode. In pressure-swirl mode the increase in liquid flow rate is analogous to an increase in liquid injection pressure; in simplex-airblast mode, due to the high air pressure the increase in flow rate lowers the ALM, thus lessening the atomisation ability. The increase in droplet size seen at the lowest flow rate

may similarly be explained by the low flow rate being equivalent to a low liquid injection pressure, resulting in a liquid sheet at the nozzle exit that is more stable and resistant to breakup.
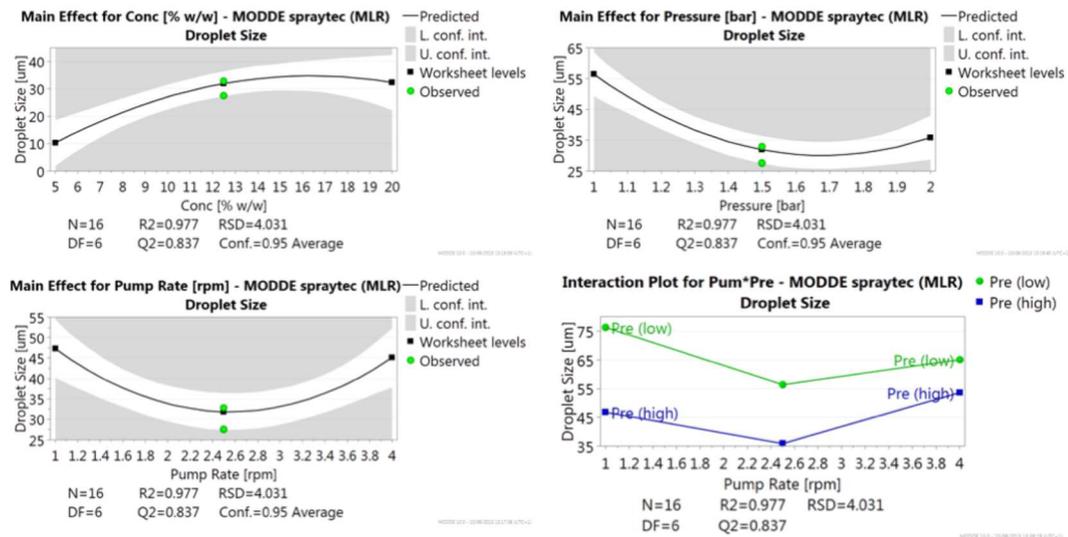
Figure 4.2 Main Effect Plots for concentration, atomisation pressure and pump rate on droplet size. Bottom right, Interaction Plot for the interaction between pump rate and atomisation pressure. The two lines show atomisation pressure at the low level

The response contour plots, Figure 4.3, give a visual representation of changes in droplet size over the parameter ranges, allowing for optimisation of the process conditions. The plots indicate that in order for very fine droplet formation the major limiting factor is the polymer concentration, since at the mid and high polymer concentrations droplet sizes do not fall below 30 µm unlike at the low polymer concentration.
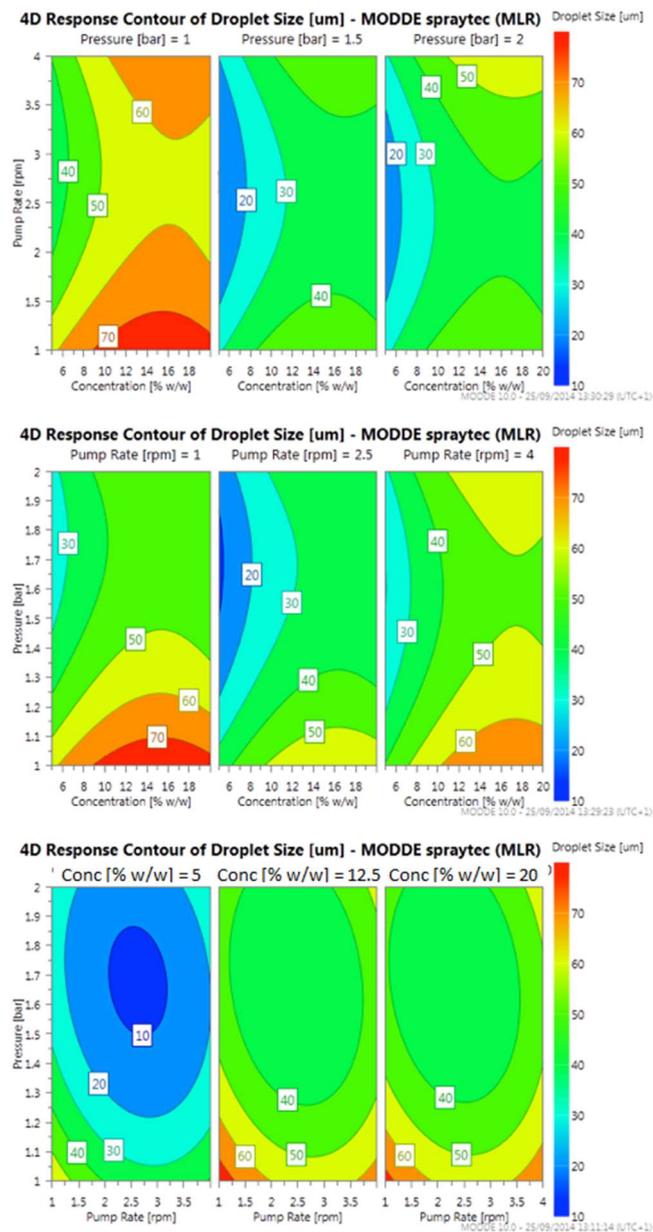
Figure 4.3 Response contour plot with respect to fixed levels of atomisation pressure, pump rate and polymer concentration.

4.3.2   Film Coating

The DOE atomisation model allowed for coating of tablets with either large or small droplets. A small droplet VMD of 20 μm and a large droplet VMD of 70 μm were chosen to show the effect of droplet size on the film coat. The conditions to produce droplet sizes as close to these as possible were determined by optimisation of the model using

MODDE software. Polymer concentration was set at 8.49% (w/w) (corresponding to a viscosity of 1.73 mPa.s) for both droplet sizes in order for droplet properties to remain consistent, with the exception of VMD. The predicted droplet sizes and the process conditions required to achieve these are shown in Table 4.3.

Table 4.3 Processing conditions for production of small and large droplets

Predicted droplet VMD (µm)	Pump rate (rpm)	Atomisation pressure (bar)	Polymer concentration (% w/w)	Coating time (min)
21.0	2.56	1.68	8.49	80
69.3	1	1	8.49	200

4.3.3 Film Coat Imaging

Qualitative analysis of the tablet coatings was performed non-invasively using XµCT and CLSM, to examine the effect of droplet size. Processing of the images yielded quantitative information for film coat thickness and porosity, providing a greater comparison between large and small droplet coating quality.

4.3.3.1 Confocal Microscopy

Maximum projection images of the film coated tablets at different droplet sizes are shown in Figure 4.4. A marked difference can be seen between the two batches. The film coatings of 20 µm droplets are clearly more uniform and complete when compared to the 70 µm droplet coatings. Dark spots in these images indicate areas of low or no coating (pores); the smaller droplet size coated tablets (1 A and 1 B) appear to have a much more complete coating, with fewer dark spots visible when compared to the larger droplet size. Furthermore, the smaller droplet coated tablets display a more consistent texture and colour, with the larger droplets forming patches of increased intensity of fluorescence indicating poor homogeneity. Unlike the small droplet coatings, in the large droplet coatings droplet outlines are visible, most apparent in the 25x magnification (2 B). This would suggest a greater water content for the large droplet coats through

insufficient water evaporation, however TGA analysis showed no significant difference (P=0.31) in water content between small and large droplet coatings, with values of 2.68±0.03% and 2.51±0.14% respectively.
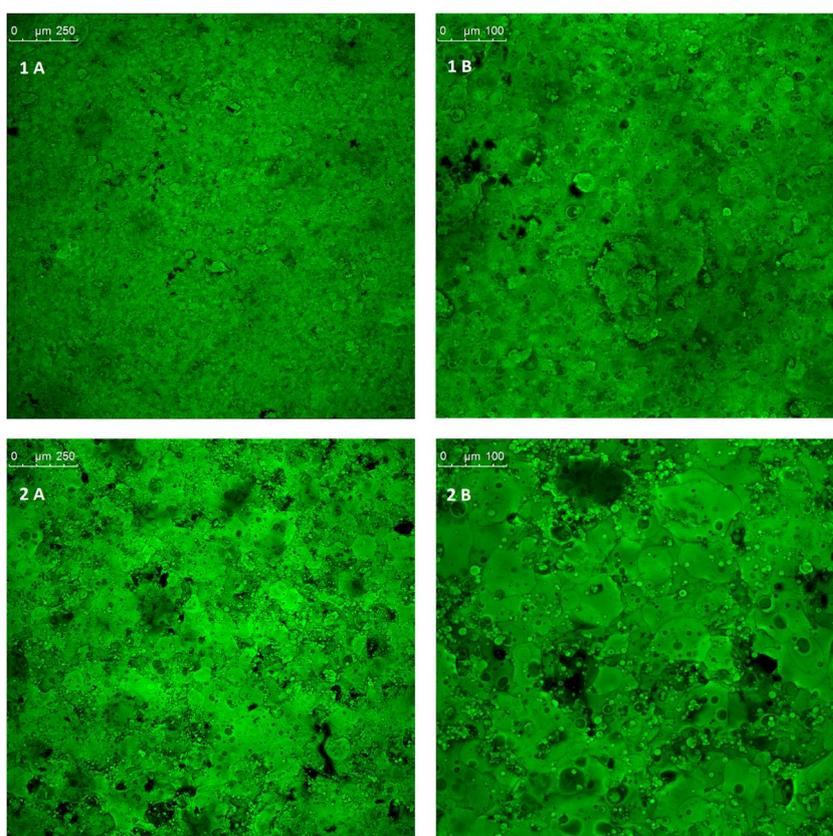
Figure 4.4 Maximum projection images of the film coat surface, providing a visual representation of surface morphology and film coat uniformity. Aqueous film coat consisting of Kollicoat IR 20% w/w and riboflavin 5'-monophosphate sodium 0.5% w/w as a fluorescent dye. Tablets coated by fluidised bed coating method at defined droplet sizes: 20μm (1) and 70 μm (2). Images were taken at 10x (A) and 25x (B) magnification.

Pixel fluorescence intensity of images at sequential planes was used to generate a 3D projection (Figure 4.5) of the coating to provide a representation of the surface roughness. These images indicate a thicker coating with large droplets and complement the maximum projection images by showing a rougher surface for the tablets coated with

large droplets (2). A transverse view of the maximum projection images can be seen in Figure 4.6 and gives a non-invasive cross-section of the film coat and the coat-core interface. Since film coat thickness was assumed to be largely dependent on the solid content of the film coat and this was corrected for by coating time, no difference in coating thickness was expected between large and small droplet coatings. Small droplet coatings however are much thinner when compared to the large droplet coatings, with the differences actually being in a similar magnitude as the difference in coating time (2.5x). This may be due to a higher porosity seen with the large droplet coatings.
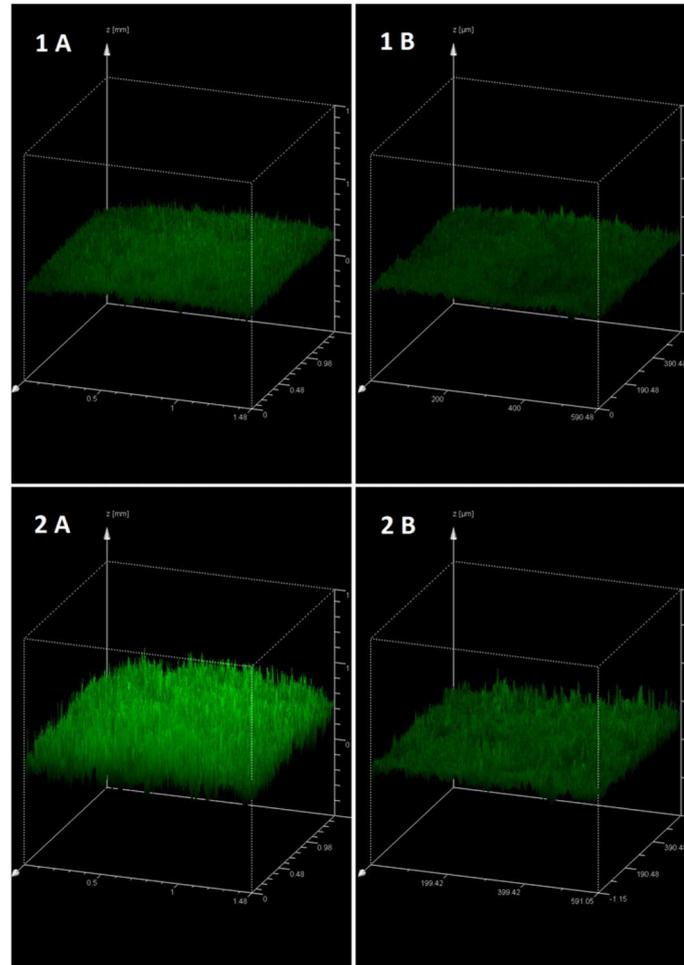
Figure 4.5 3D CLSM image showing fluorescence intensity at each image layer, providing a visual representation of surface morphology. Film coat consisting of Kollicoat IR 20% w/w and riboflavin 5'-monophosphate sodium 0.5% w/w as a fluorescent dye. Tablets coated by fluidised bed coating method at defined droplet sizes: 20µm (1) and 70 µm (2). Images were taken at 10x (A) and 25x (B) magnification.
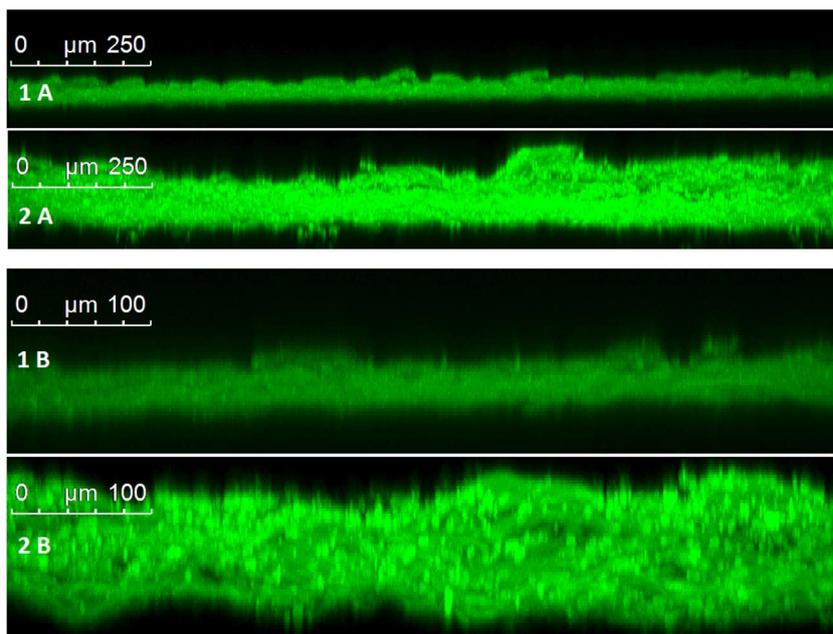
Figure 4.6 Transverse view of maximum projection images showing the film coat thickness and morphology. Film coat consisting of Kollicoat IR 20% w/w and riboflavin 5'-monophosphate sodium 0.5% w/w as a fluorescent dye. Tablets coated by fluidised bed coating method at defined droplet sizes: 20µm (1) and 70 µm (2). Images were taken at 10x (A) and 25x (B) magnification.

The images obtained by CLSM suggest that small droplets have produced a thinner, more compact coat that is more homogenous, complete and smooth. This can be attributed to the more efficient evaporation of small droplets due to their greater surface area to volume ratio. These findings are significant since the differences seen between the coats may impact upon the overall tablet properties.

4.3.3.2 Micro-CT

XµCT was used to complement confocal data to assess film coat quality and characteristics. Imaging of the tablet core alone was not possible due to low radiopacity shown by the tablet core excipients and Kollicoat IR, as measured using an aluminium step wedge to compare against aluminium standards. Barium sulphate ($BaSO_4$) and bismuth(III) oxide (Bi_2O_3) were tested as contrast materials for incorporation into both

the tablet core and the polymer coating to increase radiopacity. $BaSO_4$ has been used extensively in orthopaedic surgery as a radiopacifier in bone cement to monitor the healing process after fixation of artificial joints [298]. Bi_2O_3 is similarly considerably used as a radiopacifier component of dental cement for peri-/postoperative assessment [299]. XμCT reconstructions in Figure 4.7 and Figure 4.8 show transverse views of the entire tablets. Addition of either contrast material increased radiopacity enough for successful imaging. The distribution of the contrast material within the tablet core was initially not homogenous, with clumps visible in the reconstructions where contrast material had been blended with the rest of the formulation. Co-processing of the contrast material with the formulation by milling then vastly improved homogeneity of the tablet core. Contrast material inclusion in the coat similarly increased radiopacity for successful imaging. Increasing contrast material concentration in the film coat produced sharper, more defined images, as shown in Figure 4.8, B and D.
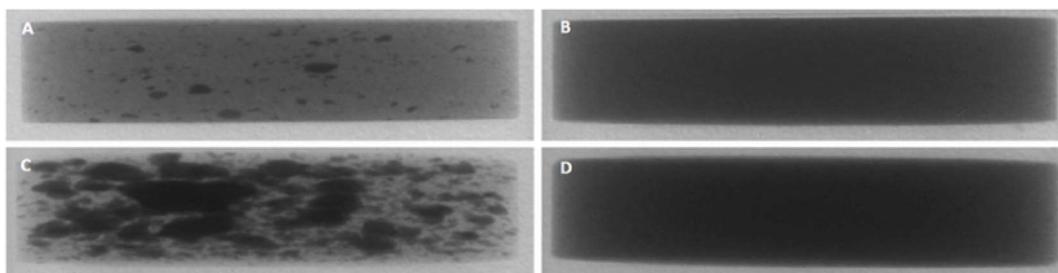
Figure 4.7 Transverse view of XμCT reconstruction of placebo tablets (13mm) containing contrast material in the core. Contrast material Bi_2O_3 is included at 5% w/w and 10% w/w (milled), A and B respectively. $BaSO_4$ is included at 10% w/w and 20% w/w (milled), C and D respectively.
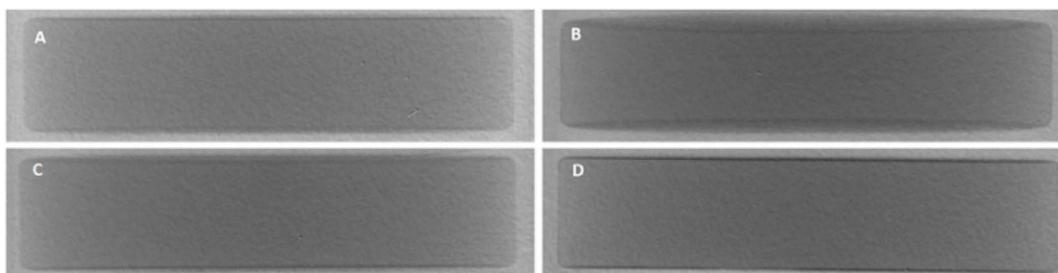
Figure 4.8 Transverse view of XµCT reconstruction of placebo tablets (13mm) containing contrast material in the coat. Contrast material Bi_2O_3 is included at 1% w/w and 2.5% w/w, A and B respectively. $BaSO_4$ is included at 2% w/w and 5% w/w, C and D respectively.

To determine the effect of droplet size on film coat Bi_2O_3 (2.5% w/w) was added to the coating solution. Bi_2O_3 was chosen as contrast material since $BaSO_4$ demonstrated similar radiopacity but at a higher concentration. The parameters for obtaining the defined droplet sizes caused issues with effective coating with contrast material. At the higher pump rate of 2.56 rpm, Bi_2O_3 was readily pumped and atomised. The lower pump rate of 1 rpm necessary for large droplet production proved more challenging and required reduction in the coating solution pumping length, due to the increased transit time of the insoluble bismuth oxide.

Figure 4.9 shows the XµCT maximum projections of the top tablet surface, coated with either large or small droplets. The surface images for the small droplet coating complement the confocal data by showing a homogeneous, uniform coating. Similarly, the surface of the large droplet coating shows large droplet artefacts on the coating surface and poor homogeneity. These differences are particularly clear in the heat map images.
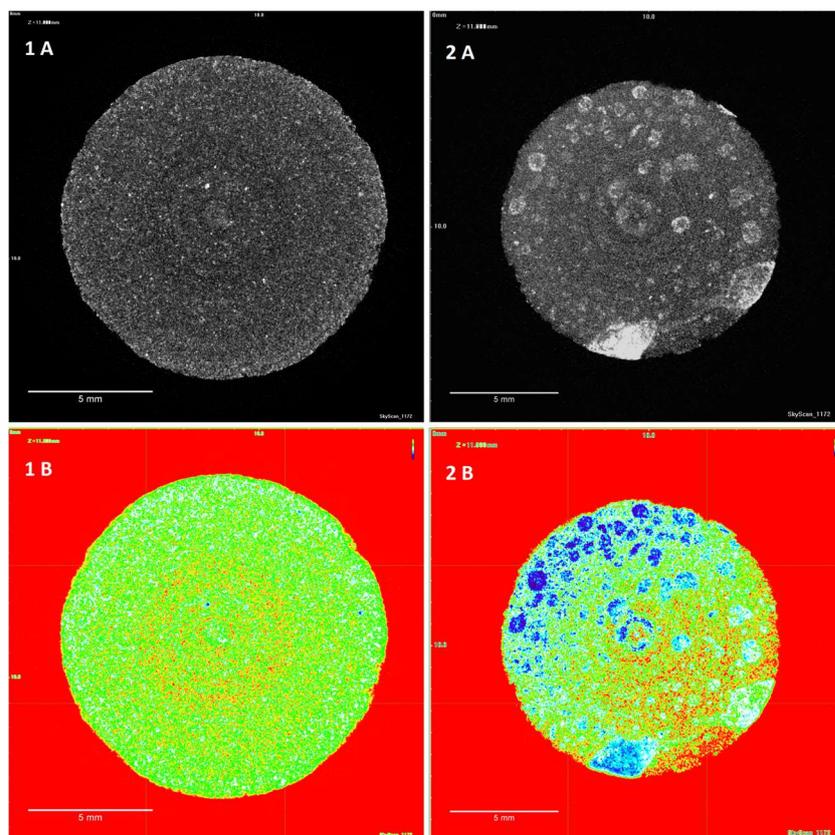
Figure 4.9 Maximum projection and heat map images of the tablet surface of XμCT reconstructed film coated tablets of either large or small droplet size. Placebo tablets were coated with Kollicoat IR and bismuth oxide (2.5% w/w). Droplet size coatings of 20μm (1) and 70 μm (2) are shown in maximum projections (A) and heat maps (B). Heat maps demonstrate coat uniformity, with blue areas and red areas representing high and low intensity of radiopacity, respectively.

4.3.3.3   Film Coat Thickness and Porosity

Analyses of film coat porosity for XμCT reconstructions were performed using two different techniques. Film coat porosity, thickness and roughness analysis was also performed for fluorescent coatings. Porosity measurements were used as an indication of film coat uniformity, with lower porosity representing a more concise coating. The results for the XμCT reconstructions are shown in Table 4.4. Both techniques for film coat porosity assessment show similar results and similar deviation. Large droplet coated tablets showed approximately double the coating porosity of 44.3±7.1% and

32.8±6.7% compared to the small droplet coating porosity values of 21.4±4.1% and 16.4±3.3% respectively, using each technique.

The results for the fluorescent coatings, shown in Table 4.5, show a similar trend, with large droplet coatings having double the porosity of small droplet coatings at 30.0±6.0% and 15.1±3.2% respectively and showing comparable values with the XμCT reconstructions. The film coat thickness measurements show that large droplet coatings are substantially thicker at 114.2±18.1μm compared to small droplet coatings at 48.4±8.1μm, as was visible from the transverse views of the maximum projection images. The greater surface roughness values for the large droplet coated tablets were not deemed significant ($P > 0.05$).

Table 4.4 Surface porosity measurements of film coatings analysed by XμCT. Porosity has been measured using either the CTAn or ImageJ technique.

Coating Porosity of XμCT Scans by Two Methods		
	Droplet Size	Mean (%)
CTAn	Small (20 μm)	21.4 ± 4.1
	Large (70 μm)	44.3 ± 7.1
ImageJ	Small (20 μm)	16.4 ± 3.3
	Large (μm)	32.8 ± 6.7

Table 4.5 Porosity, thickness and roughness measurements of fluorescent coatings. Maximum projection images were analysed using ImageJ. Coatings produced by large and small droplets are compared.

Film Coat Thickness and Porosity Measurements for Fluorescent Coatings			
	Porosity (%)	Thickness (μm)	Roughness - RMS (μm)
Small	15.1 ± 3.2	48.4 ± 8.1	6.6 ± 2.4
Large	30.0 ± 6.0	114.2 ± 18.1	12.8 ± 6.2

4.4   Conclusion

DOE successfully generated a robust model capable of predicting the impact that altering process parameters had on droplet size. All three CPPs under investigation were verified as having a significant impact on droplet size contributing to a complex atomisation process. This approach provided a wealth of information and insight into the process in a short time and allowed for droplet size optimisation that would not have been easily achieved otherwise.

Film coat characterisation by CLSM and XµCT provided complementary qualitative and quantitative information. Small droplets were shown to produce a more complete and concise film coating, and are expected to benefit from enhanced stability as a result of lower porosity and be less at risk to detrimental over-wetting. The increased thickness of large droplet coatings may be as a result of greater porosity of these coatings. The incorporation of a commonly used radiopaque contrast material for XµCT imaging of a film coat was designed to overcome a major limitation of XµCT, that is poor contrast between tablet and coating materials [293]. The wider implications could extend beyond coating, for example with inclusion of contrast materials into tablet cores for non-invasive analysis of internal tablet structure by XµCT. Another application could be to study homogeneity, not only within tablet cores but also powders.

Chapter 5

Fixed Dose Combination Orally Disintegrating Tablets to Treat Tuberculosis: Physiologically Based Pharmacokinetic Modelling to Assess Bioavailability

5.1   Introduction

Recognised as one of humankind's oldest diseases, with evidence of cases dating back more than 5000 years [300], tuberculosis (TB) remains a major cause of morbidity and mortality. Today there are an estimated 9.6 million TB cases worldwide, with the disease claiming 1.5 million deaths in 2014 alone [301]. Since 2000 the incidence of TB has fallen by 18%, at an average rate of 1.5% per year, with effective treatment within this time frame saving an estimated 43 million lives [301].

TB is an infectious disease caused by the aerobic bacterium *Mycobacterium tuberculosis* (MTB) [302]. Transmission occurs through aerosolisation of the bacterium into droplet nuclei by coughing, sneezing or talking [303]. Inhalation of the organism into the alveoli leads to respiratory infection that, if spreads, causes extrapulmonary tuberculosis, which can involve any organ system in the body [304]. Pulmonary tuberculosis, the most common presentation, is avoided in most cases of exposure through mucociliary clearance [305], or failing that through the successful activity of phagocytic alveolar macrophages, resulting in symptomless latent tuberculosis [306]. Around 5% of TB infections progress to the active form of the disease within two years, with about 10% of latent cases reactivating at some point later in life [303, 307-309]. TB outcome is dependent on a multitude of factors, most prominent of which is the immunocompetence of the individual [310], itself dependent on various intrinsic and extrinsic factors such as the hosts genetics and nutritional state, respectively [311, 312].

Clinical manifestation of TB depends on the site of infection. Pulmonary TB, historically referred to as consumption or pthisis, classically manifests as severe wasting [312], as well as cough, haemoptysis, chest pain, dyspnoea, malaise, fatigue, low-level fever and night sweats [313, 314]. Extrapulmonary TB can include the same symptoms as pulmonary TB, with a wide range of additional symptoms based upon the site of infection, such as meningitis (CNS), lymphadenitis (lymphatic), arthritis (skeletal) and haematuria (renal) [315, 316].

Various social, environmental and biological risk factors determine the risk of TB contraction [317]. Risks for infection and progression to disease are distinctly different; infection risk involves extrinsic factors including social and behavioural risks (alcohol, smoking and pollution), source infectiousness and proximity (including overcrowding and length of exposure), whereas risk of progression to disease is endogenous to the host [318]. Immunosuppressive conditions accelerate progression to active disease, with HIV

being especially potent [319, 320]. Impaired immune response as a result of malnutrition is also known to increase the risk of TB [321, 322], whilst a strong socioeconomic association with the disease exists, with the poorest experiencing the greatest risk [323]. Children also present an increased susceptibility to TB development, which is greater still before the age of 2 and after age 10 [324]. Other risk factors for progression to disease include diabetes, alcohol, smoking and indoor air pollution [318].

Isoniazid and rifampicin form the basis of front-line treatment for TB [301], with both drugs included in the WHO Model List of Essential Medicines [325] and Essential Medicines for Children [326]. Isoniazid (Biopharmaceutics Classification System (BCS) class I/III [327, 328]) is a pro-drug that requires activation by catalase-peroxidase enzyme (KatG), which is endogenous to MTB [329]. The drug inhibits the synthesis of mycolic acids, essential components of the bacterial cell wall [330, 331] and at therapeutic doses is bactericidal against actively growing intra and extra cellular MTB [332]. Rifampicin (BCS class II [333, 334]) also displays a bactericidal effect on MTB, by inhibition of transcription through high-affinity binding to the β-subunit of bacterial DNA-dependent RNA polymerase [75, 335]. Rifampicin is highly effective against TBM through its ability to readily diffuse into tissues, cells and bacteria [336]. The tendency of rifampicin to degrade substantially when combined with isoniazid in acidic media is a well-recognised complication when considering combination of the two drugs in solid oral-dosage forms [337-339]

The first-line recommended oral drug regimen for treatment of drug susceptible TB involves isoniazid, rifampicin, pyrazinamide and ethambutol for 2 months, followed by isoniazid and rifampicin for 4 months, with the regimen altering due to drug or multi-drug resistance [340]. Treatment for extrapulmonary TB does not differ, except in some cases where duration of therapy is extended [341]. Recommended doses for treatment of children differ compared to adults [342]. Fixed dose combinations (FDCs) are recommended for TB treatment of both adults and children [340, 342], however FDCs currently on the market do not correspond to appropriate doses for children [341]. FDCs for TB treatment have not been shown to alter efficacy, drug resistance or adverse effects or events when compared to single-dose [341]. Furthermore, whilst FDCs have not provided evidence for improvement of treatment outcomes, their use simplifies TB therapy, with some evidence for an increase in patient satisfaction [343].

In order for a new generic formulation to be approved it needs to demonstrate bioequivalence with a reference branded product. A bioequivalent drug will display

comparable bioavailability and thus *in vivo* performance (efficacy and safety) [344]. Bioequivalence can be assumed in the absence of clinical trials, if there is no significant difference in the rate and extent to which the active pharmaceutical ingredient (API) becomes available within the systemic circulation, when compared with the reference product [345]. Bioequivalence testing may also be applied in the assessment of FDCs [344]. For immediate release formulations bioequivalence can be determined by comparison of *in vitro* dissolution profiles using FDA recommended difference factor (f_1) and similarity factor (f_2) testing, for biowaiver applications [345, 346]. Comparison testing is not deemed necessary if test products display greater than 85% dissolution within 15 min, given that the API falls within BCS class I or III (although class III carries stricter requirements) [344]. The extension of biowaivers to BCS class II compounds is topic of much discussion [347-349].

Pharmacokinetic modelling and simulation has become an established tool over the past 20 years to predict drug pharmacokinetics in humans and assess the effect of intrinsic and extrinsic factors on drug exposure. Physiologically based pharmacokinetic (PBPK) models define tissues and organs as compartments, with parameters based upon decades of knowledge of body fluid dynamics [350, 351]. PBPK models consider ADME processes throughout all compartments to estimate the pharmacokinetic profile of a drug at a target tissue or organ [351, 352]. As such, PBPK models have become a powerful tool for prediction of oral drug absorption (to the systemic circulation) through integration of common *in-vitro* drug-specific information, with systems based data [138, 148]. PBPK modelling is often exploited for prediction of oral drug absorption, to study formulation changes [353, 354] or FDCs [355] whilst there is a significant effort to apply PBPK modelling to investigations into bioequivalence [356-358].

An FDC ODT for isoniazid and rifampicin could potentially increase patient compliance and be particularly beneficial in developing areas with little to no access to water. The use of a paediatric relevant dose would be valuable given the current lack of support and the widely reported and supported applicability of ODTs to enhance compliance in paediatric populations [33, 250, 359, 360], including patients as young as 6 months old [361]. Similarly, improved clinical outcomes from FDCs, due primarily to improved adherence as a result of reduced pill burden, are well documented [362-364].

This work describes the development and characterisation of an isoniazid and rifampicin FDC ODT targeted at paediatrics. Single dose and fixed dose drug dissolution from ODTs in biorelevant media and permeability data from *in-vitro* Caco2 cell monolayers

was used to predict drug pharmacokinetics through simulated clinical trials. This allowed for comparison of bioavailability of each API from single and combination formulations.

5.2   Materials and Methods

5.2.1   Materials

Isoniazid and rifampicin was purchased from Molekula Ltd (UK). PEARLITOL® Flash (mannitol-starch copolymer) was obtained from Roquette Pharma (France), with Avicel PH-102 micro-crystalline cellulose (MCC) and sodium stearyl fumerate (SSF) supplied by FMC BioPolymer (USA).

Biorelevant FaSSIF/FeSSIF/FaSSGF Instant Powder was purchased from biorelevant.com (UK). Sodium hydroxide, sodium chloride, sodium phosphate and glacial acetic acid for biorelevant media were obtained from Sigma-Aldrich (UK). Acetonitrile (ACN) and methanol (HPLC-grade) were obtained from Fisher Scientific (UK).

For cell culture media DMEM was purchased from Lonza (UK), fetal bovine serum (FBS), gentamicin (10 mg/ml), Fungizone (amphotericin B 250 μg/ml), HBSS and penicillin/streptomycin (10,000 U/ml) were all purchased from Gibco (Thermo Fischer Scientific, UK). Trypsin-EDTA solution (0.25%) was procured from Sigma-Aldrich (UK).

5.2.2   HPLC

HPLC was performed on an Agilent 1260 series (Agilent Technologies, USA), comprising a quarternary pump, Infinity VWD and autosampler. Analysis was conducted on a reversed-phase Gemini C18, 150 x 4.6 mm, 110Å, 5μm column (Phenomenex, UK). Protocols were developed, calibrated and validated for both isoniazid and rifampicin alone and in combination.

Separations were achieved using either deionised H_2O, 0.1% (v/v) TEA, 0.1% (v/v) TFA or ACN at different ratios as the mobile phase. Ascorbic acid (0.5 mg/ml) was included as an antioxidant to prevent the degradation of rifampicin [365] Isoniazid separation was performed with an isocratic mobile phase of H_2O: ACN (90:10 v/v), a flow rate of 1 ml/min and a wavelength of 254 nm. Rifampicin separation was achieved using an isocratic mobile phase of TFA: ACN (45:55 v/v), a flow rate of 1 ml/min and a wavelength of 254 nm. Separation of isoniazid and rifampicin in combination required a mobile phase of TEA: ACN delivered at a gradient (95:5 to 20:80 v/v), with a flow rate of 1 ml/min and a wavelength of 254 nm. An injection volume of 20 μl was used throughout.

HPLC method validation followed ICH guidelines [366] and involved assessment of precision through intra-day variation, accuracy by multilevel recovery studies, instrument precision, linearity and limit of detection and quantification (LOD and LOQ). Stock solutions (1 mg/ml) of each drug were prepared in mobile phase from which dilutions and subsequently two-fold serial dilutions were prepared to form a calibration curve.

5.2.3   Tablet Production

Direct compression of tablets (500 mg) at a compaction force of 22 kN (2.2 ton) was performed on an Atlas T8 automatic press (SPECAC, UK), using a 13mm round, flat faced die. Tablets were produced under ambient conditions.

5.2.4   Friability

Tablet friability was determined on 6 tablets using an F2 friability tester (Sotax, Switzerland). Tablets were placed inside the drum and rotated at 25 rpm for a total of 100 revolutions. Dust was removed pre and post testing to remove excess powder that would contribute to tablet mass. Friability was calculated and expressed as % tablet weight loss from initial tablet weight.

5.2.5   Tablet Hardness

A Tablet Hardness Tester TBF1000 (Copley Scientific, UK) was used to measure the radial crushing strength (hardness) of tablets in triplicate.

5.2.6   Dissolution Testing

API dissolution from ODTs in 900 ml biorelevant media was tested in both fasted state simulated intestinal fluid (FaSSIF) and fed state simulated intestinal fluid (FeSSIF), at pH 6.5 and 5 respectively and maintained at 37°C. An ERWEKA DT 600 USP 2 paddle apparatus (Germany) was used at a paddle speed of 50 rpm [367]. 5ml samples were

taken over 2 h, replacing with 5 ml fresh media to simulate sink conditions. API dissolution was measured using HPLC and corrected for % dose dissolved.

5.2.7   Cell Culture

Prior to seeding, cells were trypsinised (2.5 ml) from 75-cm^2 cell culture flasks (Corning, USA) on which they had been grown (80% confluence), after washing with HBSS. Caco-2 cells (passage 54-58) were seeded onto Transwell (Corning, USA) semi-permeable membrane supports (12-well, 1.12 cm^2, 0.4 µm pore size) at a density of 8x10^4 cells/cm^2. Cells were maintained in DMEM containing L-glutamine (4 mM) and glucose (4.5 mg/ml) supplemented with (v/v) 10% FBS, 1% penicillin/streptomycin, 1% NEAA, amphotericin B (0.5 µg/ml) and gentamicin (20 µg/ml). Media was changed every 2-3 days and transwells cultured at 37°C, 5% CO$_2$ for 21 days, after which transport studies were performed.

5.2.8   Transepithelial Electrical Resistance (TEER) Measurements

TEER value measurements were performed to monitor monolayer integrity using an EVOM meter (World Precision Instruments, USA). TEER values are expressed using the equation:

$$TEER\ (\Omega/cm2)\ =\ (resistance\ -\ blank\ resistance)\ x\ membrane\ surface\ area$$

5.2.9   Caco-2 Transport Studies

Caco-2 monolayers were used for transport studies between 21 and 24 days post-seeding. Drug absorption through Caco-2 monolayers was measured for isoniazid and rifampicin alone and in combination in both the apical to basolateral (A-B) and basolateral to apical (B-A) directions (n=3). Transport studies were carried out in DMEM (37°C) containing 10 mM HEPES (pH 7.4), with 0.5 ml and 1.5 ml in the A and B compartments, respectively. Samples of 100 µl were removed from the A side and 200 µl from the B side at time points over 2 h, replacing with fresh pre-warmed media (37°C) to mimic sink conditions. For mass balance, samples were taken from the donor compartments at t=0 and t=120 min.

Isoniazid was administered at a concentration of 20 µg/ml and rifampicin at a concentration of 30 µg/ml. Concentrations used were comfortably within or below previously reported well tolerated concentration ranges for both isoniazid [368, 369] and rifampicin [368, 370]. Cultures were maintained at 37°C and 5% CO_2 throughout the experiment. Samples were analysed by HPLC and apparent permeability (Papp) values were calculated using equation:

$$Papp = (dQ/dt)/(C_0 \; x \; A)$$

Where dQ/dt is the mass transfer rate of the compound from the donor to the receiver compartment, C_0 is the initial concentration in the donor chamber and A is the monolayer surface area (cm^2).

5.2.10 Clinical Trials Simulation

The population-based clinical trials simulator Simcyp (V14) (Certara, USA) was used to simulate the plasma concentration of isoniazid and rifampicin from single API and FDC formulations. Default parameter values for creating a North European Caucasian population were selected [371].

5.2.11 Compound Data

Physicochemical information for each API was collated from the literature used to develop compound files (Table 5.1). Simulations were performed using a minimal-PBPK model. Where uncertainty arose regarding the precise value of compound data parameters, parameter estimation was conducted using the Parameter Estimation Module to optimize parameter values. The ADAM model [372] was assumed for all simulations and the dissolution profile for each formulation (single and FDC) in FaSSIF and FeSSIF were utilized.

5.2.12 Clinical Studies

The optimization and validation of the PBPK model was conducted using clinical study results reported in healthy adult subjects. For isoniazid: study 1 included a total dose of

300 mg dosed to 18 healthy volunteers (18-55 years old) [373]; study 2 included a total dose of 300 mg dosed to 22 healthy volunteers [374]; study 3 included a total dose of 300 mg dosed to 20 healthy volunteers (23 ± 1.8 years old) [375]; study 4 included a total dose of 300 mg dosed to 18 healthy volunteers (36.4 ± 10.6 years old) [376]. Studies 1 and 2 were used for model development and studies 3 and 4 utilized for validation.

For rifampicin: study 1 included a total dose of 600 mg dosed to 18 healthy volunteers (18-55 years old) [373]; study 2 included a total dose of 600 mg dosed to 20 healthy volunteers (23 ± 1.8 years old) [375]; study 3 included a total dose of 600 mg dosed to 18 healthy volunteers (36.4 ± 10.6 years old) [376]; study 4 included a total dose of 600 mg dosed to 22 healthy volunteers [374]. Studies 1 and 2 were used for model development and studies 3 and 4 utilized for validation.

Raw data from published human trial plasma concentration profiles was extracted using WebPlotDigitizer 3.10 [377] and, where necessary, parameter estimation was conducted using the validation clinical datasets.

Predictions of API plasma pharmacokinetic profiles were simulated following the oral administration of a single immediate release solid dosage form of 50mg (isoniazid) and 75 mg (rifampicin) dose over a 24 hr period.

Table 5.1 Input parameter values and predicted PBPK values for simulation of pharmacokinetics of isoniazid and rifampicin.

Parameter	Isoniazid	Rifampicin
Type	Monoprotic base	Ampholyte
MW	137.1	823
LogP	-0.7	4.01
pKa	1.82	1.7,7.9
fu	0.95	0.113

	Predicted PBPK/PE	0.42 (Full PBPK)
Vss (L/kg)[a]		
B:P ratio	0.825	0.9
CLpo (L/min)	12	8.75
Peff (cm/s)	PE	2.15

MW: molecular weight; fu: plasma unbound fraction; Vss: steady-state volume of distribution; B:P ratio: blood-to-plasma ratio; Peff: human effective permeability; CLpo: oral clearance; PE: parameter estimation. [a] Vss was determined from calculation of tissue partitions coefficients within Simcyp or parameter estimated.

5.2.13 Statistical Analysis

GraphPad PRISM software version 6.01 (USA) was used for data analysis. Ordinary one-way ANOVA was used with Tukey's multiple comparisons test to analyze data for tablet characterization. Unpaired two-tailed t-test was used to determine statistical differences between data sets for pharmacokinetic parameters.

Differences between dissolution profiles of APIs in single dose (reference) and combination (test) were assessed using f_1 and f_2 difference and similarity factor testing, using the equations [346]:

$$f_1 = ([\sum_{t=1}^{n} |R_t - T_t|]/[\sum_{t=1}^{n} R_t]) * 100$$

$$f_2 = 50 * \log([1 + (1/n)\sum_{t=1}^{n} (R_t - T_t)^2]^{-0.5} * 100)$$

Where R_t and T_t are the % drug dissolved value at each time point for the reference and test product respectively and n is the number of time points.

5.3   Results and Discussion

5.3.1   ODT Development

An ODT formulation for rifampicin and isoniazid both alone and in combination was developed, with the requirement that tablets were mechanically robust whilst maintaining rapid disintegration. Round flat faced tablets (500 mg) were produced by direct compression. In order to isolate the effect of combination of APIs, the number of excipients used was kept at a minimum. The formulation consisted of API alongside Na stearyl fumerate (SSF, 0.5% w/w) as a lubricant and Pearlitol as a diluent. Compaction forces were applied at a range of 1-2 ton and the effect on ODT properties shown in Table 5.2. Hardness values were acceptable from a compaction force of 1.2 ton and above. Friability values at all compaction forces were high (1%), with tablets compressed at and below 1.2 ton not withstanding friability testing. Disintegration times at all compaction forces were within 30 s, as recommended by the FDA for ODTs [378] with no significant effect ($p > 0.05$) on disintegration with changes in compaction force.

Different concentrations of SSF or Mg stearate (MS) as lubricants were assessed for their effect on ODT properties (Table 5.3). No significant difference in tablet hardness was demonstrated when SSF concentration was altered. SSF ODT's displayed greater hardness values than MS, with the exception of SSF at 1% w/w that was not deemed significant. Increasing SSF to 1.5% w/w ensured improved lubricant ability whilst maintaining high hardness and a low disintegration time. Inclusion of MS at 1% w/w slowed disintegration when compared to all other ODTs, above the 30 s requirement ($p > 0.01$).

To combat high friability (>1%) MCC was included as a binder [160]. Addition of MCC up to 15% w/w (Table 5.4) improved hardness ($p > 0.01$) compared to other concentrations whilst lowering friability and maintaining rapid disintegration. MCC has excellent binding properties due to its plastic deformation, maximising interparticulate bonding [160] and hydrogen bond formation between adjacent molecules [162, 379], whilst mechanical interlocking has also been proposed as a mechanism [165, 380]. The high intraparticle porosity of MCC promotes rapid penetration of water through capillary action and is responsible for its ability to enhance disintegration [160, 381, 382]. Raising compaction force to 2.2 T lowered friability <1% (0.74%), maintained a low disintegration time of 22.67 ± 2.52 sec and raised hardness to 137.63 ± 2.91 N (data not shown). Formulation

composition is shown in Table 5.5 and characterisation of formulations is shown in Table 5.6.

Table 5.2 ODTs of rifampicin and isoniazid (15% and 10% w/w respectively), containing SSF (0.5% w/w) and Pearlitol Flash as a diluent. The effect on tablet properties of altering compaction force is shown (mean ± SD, n=3)

Compaction Force (T)	Hardness (N)	Disintegration Time (s)	Friability (% loss)
1	51.40 ± 0.26	19.33 ± 1.53	
1.2	68.27 ± 5.56	20.67 ± 4.16	
1.4	78.23 ± 2.96	18.33 ± 2.52	3.97
1.6	99.37 ± 5.28	21.33 ± 0.58	2.46
1.8	99.83 ± 13.67	19.67 ± 1.15	2.29
2	100.17 ± 7.97	20.33 ± 0.58	1.97

Table 5.3 FDC ODTs of rifampicin and isoniazid (15% and 10% w/w respectively), containing either MS or SSF as lubricants. The effect that changing lubricant and lubricant concentration has on ODT properties is shown (mean ± SD, n=3).

Lubricant	Hardness (N)	Disintegration Time (s)	Friability (%)
SSF 0.5% w/w	100.17 ± 7.97	20.33 ± 0.58	1.97
SSF 1% w/w	96.27 ± 6.87	18.67 ± 1.15	1.62
SSF 1.5% w/w	101.03 ± 2.35	21.67 ± 0.58	1.71
MS 0.5% w/w	82.07 ± 7.72	25.33 ± 2.52	1.61
MS 1% w/w	61.90 ± 2.55	43.67 ± 9.71	2.83

Table 5.4 Inclusion of MCC as a binder and disintegrant in the ODTs containing both rifampicin and isoniazid (15% and 10% w/w respectively), SSF (1.5% w/w) and Pearlitol diluent. MCC concentrations are given as % w/w (mean ± SD, n=3).

MCC	Hardness (N)	Disintegration Time (s)	Friability (%)
5% MCC w/w	102.03 ± 1.62	19.33 ± 1.15	1.67
10% MCC w/w	106.00 ± 3.68	20.67 ± 1.15	1.48
15% MCC w/w	119.50 ± 3.90	20.33 ± 1.15	1.04

Table 5.5 ODT formulations for individual dose and FDC ODTs. Values for APIs and excipients are given as % w/w for 500mg tablets. All formulations underwent compaction at 2.2 T with a 6 s dwell time

	Isoniazid (10%)	Rifampicin (15%)	Isoniazid + Rifampicin (10% + 15%)
	f1	f2	f3
Isoniazid	50		50
Rifampicin		75	75
Pearlitol Flash	367.5	342.5	292.5
SSF (1.5%)	7.5	7.5	7.5
MCC (15%)	75	75	75

Table 5.6 Individual and FDC ODT properties. All formulations underwent compaction at 2.2 T with a 6 s dwell time (mean ± SD, n=3)

	Hardness (N)	Porosity	Disintegration Time (s)	Friability (%)
f1	95.50 ± 1.15	0.26 ± 0.01	22.67 ± 1.53	1.10
f2	143.90 ±15.47	0.25 ± 0.01	22.67 ± 1.15	0.86
f3	151.17 ± 4.48	0.23 ± 0.01	26.67 ± 2.52	0.85

5.3.2   HPLC Protocol Validation

Linearity test solutions were prepared from stocks at six concentrations ranging from 100 to 1.5625 µg/ml. Calibration curves for both drugs alone and in combination are shown in Figure 5.5 to Figure 5.8. Validation of protocols by intraday studies for isoniazid, rifampicin and isoniazid/rifampicin combination (Table 5.7 to Table 5.9), show good method accuracy and precision. Method accuracy is demonstrated by multilevel recovery, ranging from 100 µg/ml to 6.25 µg/ml. Accurate recovery was exhibited in all

instances, ranging from 98.03 to 101.98 %. Relative standard deviation (RSD) values representing intraday precision for isoniazid, rifampicin and isoniazid/rifampicin were low, ranging from 0.51 to 2.40 %. Instrument precision, tested for by six consecutive injections of the same sample (100 µg/ml), was high, with RSD values of 0.01% in all cases. LOQ and LOD values for isoniazid and rifampicin alone were at or below 0.80 and 0.24 µg/ml, respectively. LOQ and LOD values for isoniazid in combination were even lower, whilst rifampicin in combination rifampicin showed the highest LOQ and LOD of 1.18 and 0.36 µg/ml, respectively.
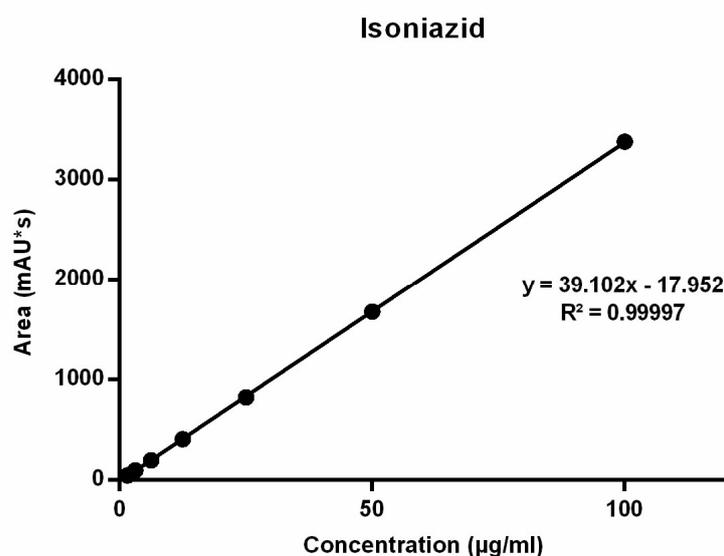
Figure 5.1 HPLC calibration curve for isoniazid, linear over a concentration range of 100 to 1.6 µg/ml (mean ± SD, n=3)

Rifampicin

$y = 31.668x - 3.7091$
$R^2 = 0.99994$
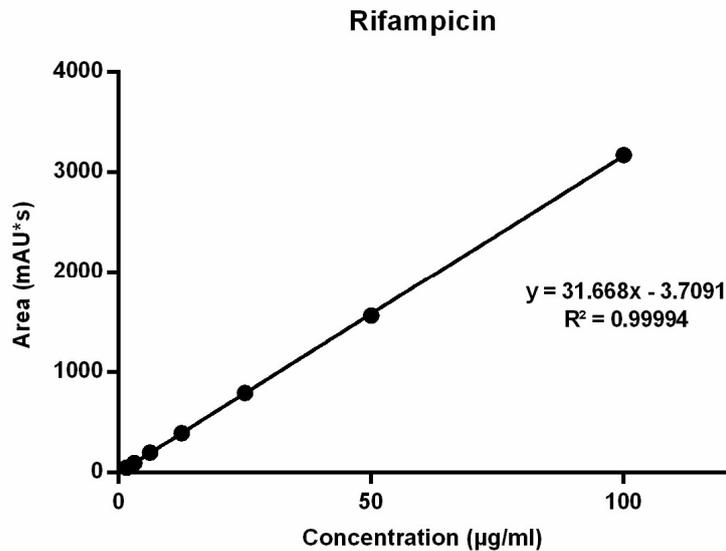
Figure 5.3 HPLC calibration curve for rifampicin, linear over a concentration range of 100 to 1.6 µg/ml (mean ± SD, n=3)

Isoniazid Combination

$y = 39.723x + 91.706$
$R^2 = 0.99996$
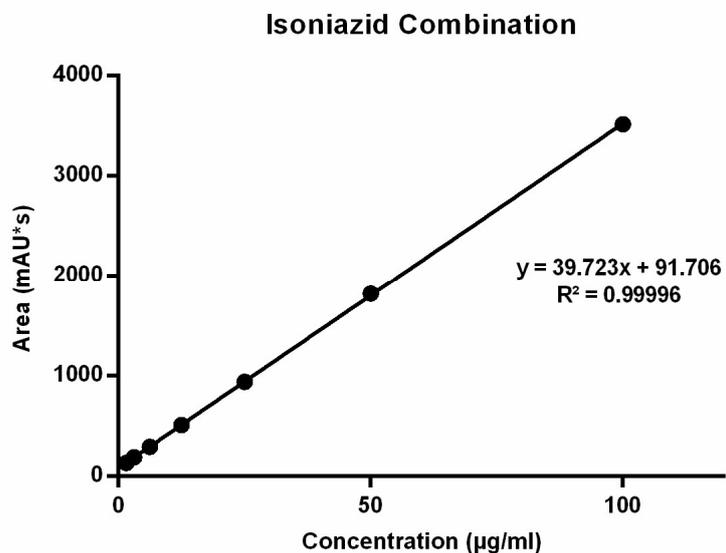
Figure 5.2 HPLC calibration curve for detection of isoniazid (50 mg) in combination with rifampicin, linear over a concentration range of 25 to 0.78 µg/ml (mean ± SD, n=3)

Rifampicin Combination

$$y = 34.309x + 33.549$$
$$R^2 = 0.99987$$
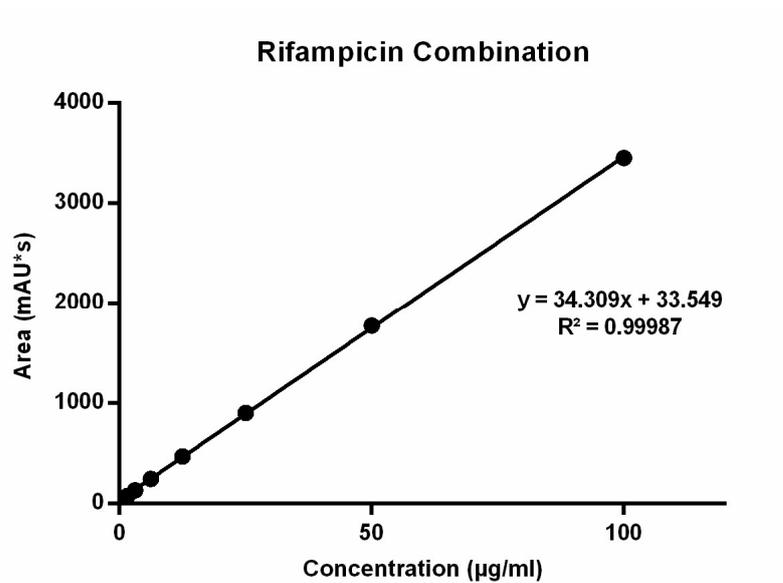
Figure 5.4 HPLC calibration curve for detection of rifampicin (75 mg) in combination with isoniazid, linear over a concentration range of 25 to 0.78 µg/ml (mean ± SD, n=3)

Table 5.7 HPLC method validation for detection of isoniazid. Data for linearity (correlation coefficient), instrument precision, accuracy (recovery), precision (% RSD), LOD and LOQ are displayed (mean ± SD, n=3)

Isoniazid conc. actual (µg/ml)	Isoniazid conc. calculated (µg/ml)	RSD (%)	Recovery (%)
100	100.15 ± 0.94	0.94	100.15 ± 0.94
50	49.87 ± 0.35	0.70	99.74 ± 0.70
25	24.69 ± 0.31	1.25	98.78 ± 1.25
12.5	12.38 ± 0.10	0.83	99.03 ± 0.83
6.25	6.25 ± 0.04	0.71	99.96 ± 0.71

Instrument precision (% RSD) = 0.08

Mean % recovery = 99.53 ± 0.60

RSD % recovery = 0.01

LOD = 0.24 µg /ml

LOQ = 0.80 µg /ml

Correlation coefficient 0.99997

Table 5.8 HPLC method validation for detection of rifampicin. Data for linearity (correlation coefficient), instrument precision, accuracy (recovery), precision (% RSD), LOD and LOQ are displayed (mean ± SD, n=3)

Rifampicin conc. actual (µg/ml)	Rifampicin conc. calculated (µg/ml)	RSD (%)	Recovery (%)
100	100.26 ± 2.40	2.40	100.26 ± 2.40
50	49.39 ± 1.12	2.24	98.78 ± 2.24
25	25.10 ± 0.53	2.11	100.42 ± 2.11
12.5	12.53 ± 0.16	1.31	100.22 ± 1.31
6.25	6.37 ± 0.15	2.32	101.98 ± 2.32

Instrument precision (% RSD) = 0.13

Mean % recovery = 100.33 ± 1.13

RSD % recovery = 0.01

LOD = 0.14 µg /ml

LOQ = 0.46 µg /ml

Correlation coefficient 0.99994

Table 5.9 HPLC method validation for simultaneous detection of isoniazid and rifampicin. Data for linearity (correlation coefficient), instrument precision, accuracy (recovery), precision (% RSD), LOD and LOQ are displayed (mean ± SD, n=3)

Conc. actual (µg/ml)	Conc. calculated (µg/ml)	RSD (%)	Recovery (%)
Isoniazid			
100	99.78 ± 1.89	1.89	99.78 ± 1.89
50	50.51 ± 0.90	1.81	101.02 ± 1.81
25	24.94 ± 0.20	0.80	99.75 ± 0.80
12.5	12.45 ± 0.15	1.19	99.61 ± 1.19
6.25	6.13 ± 0.11	1.69	98.03 ± 1.69

Instrument precision (% RSD) = 0.27

Mean % recovery = 99.64 ± 1.06

RSD % recovery = 0.01

LOD = 0.15 µg /ml

LOQ = 0.51 µg /ml

Correlation coefficient 0.99996

Rifampicin			
100	99.59 ± 1.78	1.78	99.59 ± 1.78
50	50.65 ± 0.62	1.23	101.30 ± 1.23
25	25.34 ± 0.13	0.51	101.36 ± 0.51
12.5	12.69 ± 0.14	1.13	101.52 ± 1.13
6.25	6.17 ± 0.08	1.35	98.69 ± 1.35

Instrument precision (% RSD) = 0.02

Mean % recovery = 100.49 ± 1.28

RSD % recovery = 0.01

LOD = 0.36 µg /ml

LOQ = 1.18 µg /ml

Correlation coefficient 0.99987

5.3.3   Dissolution

Dissolution of API from single and FDC ODTs was tested in FaSSIF and FeSSIF media (Figure 5.5 to Figure 5.8) and profiles were compared by f1 and f2 testing (Table 5.10). Rapid and complete isoniazid dissolution from single dose (99.2%) and FDC (100.6%) in FaSSIF was observed. Difference testing showed dissolution profiles were equivalent (f1=14.17), however similarity testing indicated difference between both profiles (f2=32.79). Despite this isoniazid dissolution exceeded 85% within 15 min. In FeSSIF, similar drug release profiles for isoniazid are again seen from both single dose and FDC formulations. Rapid dissolution, peaking at 100.12% and 101.52%, was observed in single and FDC respectively, with both formulations exceeding 85% dissolution by 5 min. Values for f_1 and f_2 testing support the similarity between single and FDC, showing no difference between the two dissolution profiles.

Rifampicin dissolution from single and FDC formulations in FaSSIF was comparable based on f_1 and f_2 testing, with complete dissolution of 100.6% from single dose, whilst dissolution from FDC peaked at 91.5%. Dissolution profiles for rifampicin from single and FDC in FeSSIF were deemed different, failing f_1 and f_2 testing. Rifampicin from single dose was rapidly released, showing >85% dissolution by 5 min, peaking at 98.26%, however in combination rifampicin release was retarded, with a maximum dissolution after 1 h of 85.32%.
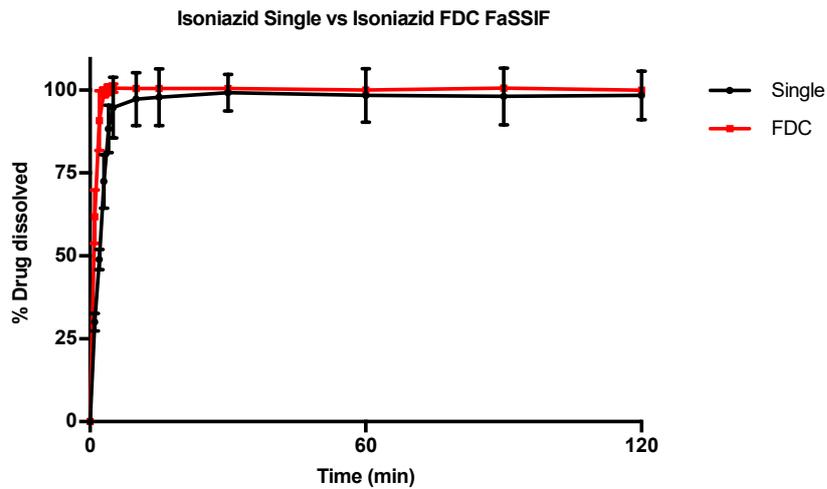
Figure 5.5 Isoniazid (50 mg) dissolution profiles of single and FDC formulations in fasted state biorelevant media (900 ml, 37°C) from 500 mg ODTs. Dissolution performed using USP 2 paddle apparatus (mean ± SD, n=3)
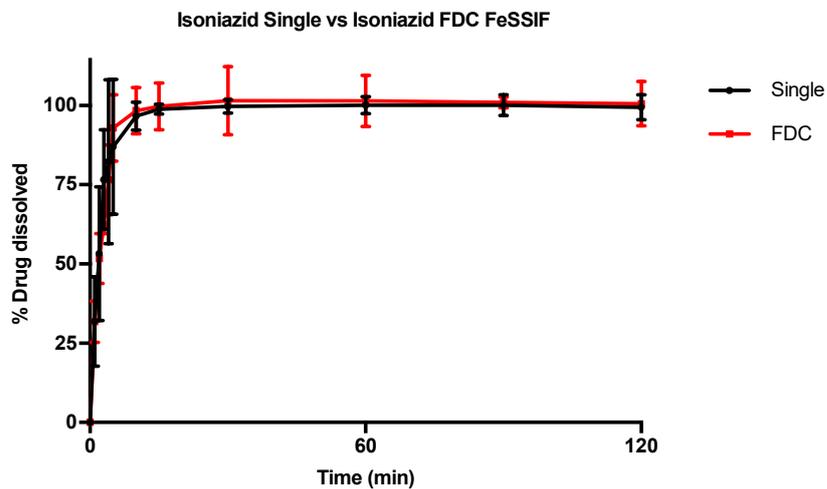
Figure 5.6 Isoniazid (50 mg) dissolution profiles of single and FDC formulations in fed state biorelevant media (900 ml, 37°C) from 500 mg ODTs. Dissolution performed using USP 2 paddle apparatus (mean ± SD, n=3)
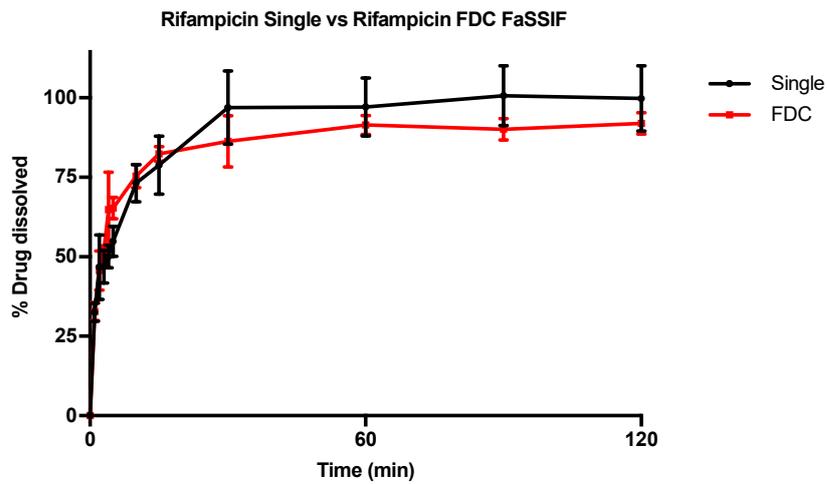
Figure 5.7 Rifampicin (75 mg) dissolution profiles of single and FDC formulations in fasted state biorelevant media (900 ml, 37°C) from 500 mg ODTs. Dissolution performed using USP 2 paddle apparatus (mean ± SD, n=3)

Figure 5.8 Rifampicin (75 mg) dissolution profiles of single and FDC formulations in fed state biorelevant media (900 ml, 37°C) from 500 mg ODTs. Dissolution performed using USP 2 paddle apparatus (mean ± SD, n=3)

Table 5.10 Comparison of dissolution profiles for each compound from single and FDC formulations in FaSSIF and FeSSIF media, by difference factor f_1 and similarity factor f_2 testing. Dissolution profiles are considered similar if the f_1 value is below 15 and the f_2 value is above 50.

Compound	Media	>85% Dissolution ≤15 min	f_1	f_2	Result
Isoniazid	FaSSIF	Yes	14.17	32.79	Pass
	FeSSIF	Yes	3.78	65.30	Pass
Rifampicin	FaSSIF	No	9.30	55.76	Pass
	FeSSIF	No	15.55	44.82	Fail

5.3.4 Permeability Studies

TEER values for Caco-2 cells over 21 days (Figure 5.9) plateau from day 18, showing a resistance of 1351.1 ± 88.6 $\Omega \cdot cm^2$ by day 21 post-seeding. Isoniazid and rifampicin transport across Caco-2 monolayers alone and in combination was measured in A-B and B-A directions. Drug transport is shown for isoniazid (Figure 5.10), rifampicin (Figure 5.11), isoniazid combination (Figure 5.12) and rifampicin combination (Figure 5.13). Papp values were calculated using the gradient of the linear portion of the curve and are summarised in Table 5.11.

Isoniazid was readily absorbed across Caco-2 monolayers from both A-B and B-A directions, exhibiting an efflux ratio of 1.18 indicating passive diffusion. Similar permeability was displayed for isoniazid in combination with rifampicin, with an efflux ratio of 1.19. Rifampicin Papp values suggested active efflux of the compound, with efflux ratio values of 4.33 and 2.61 from single and combination respectively. Active efflux of rifampicin across Caco 2 monolayers has previously been indicated [383].
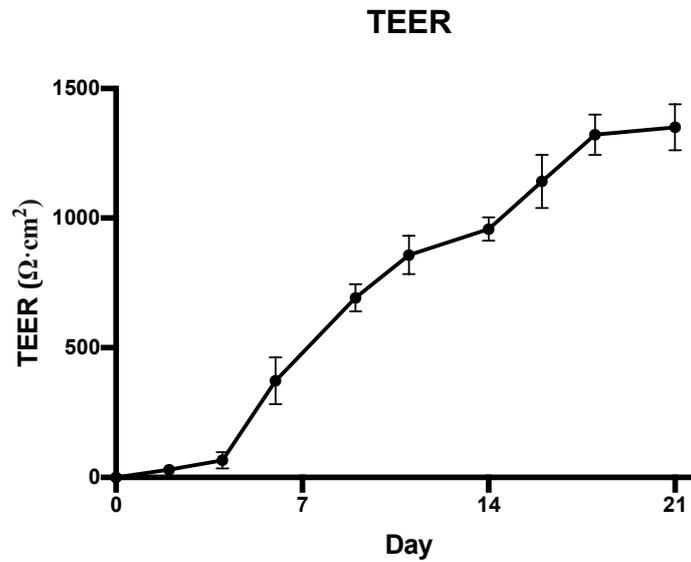
Figure 5.9 TEER values for Caco-2 monolayers grown on 12 mm Transwell inserts from days 0-21 post-seeding. Cells were seeded at a density of 8×10^4 cells/cm^2 and maintained in DMEM at 37°C and 5% CO_2 (mean ± SD, n=12)
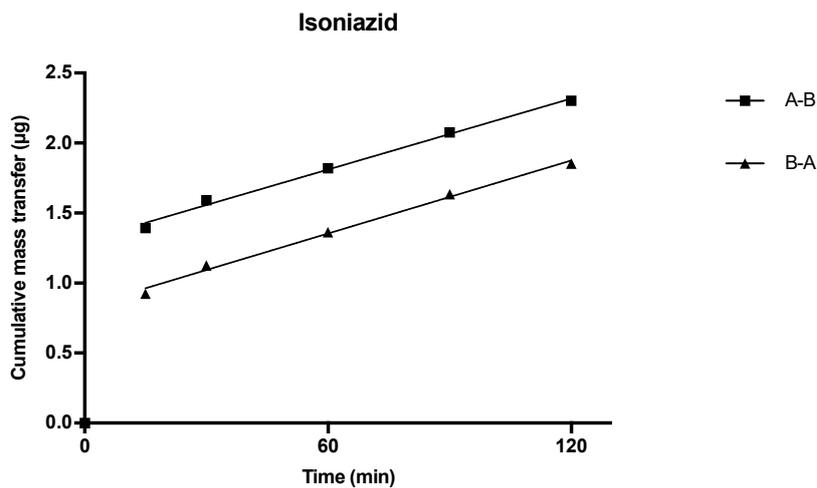
Figure 5.10 Cumulative mass transfer of isoniazid alone (20 µg/ml) across Caco-2 monolayers (pH 7.4). Papp values calculated using the gradient of the linear portion of the curve (mean ± SD, n=3)
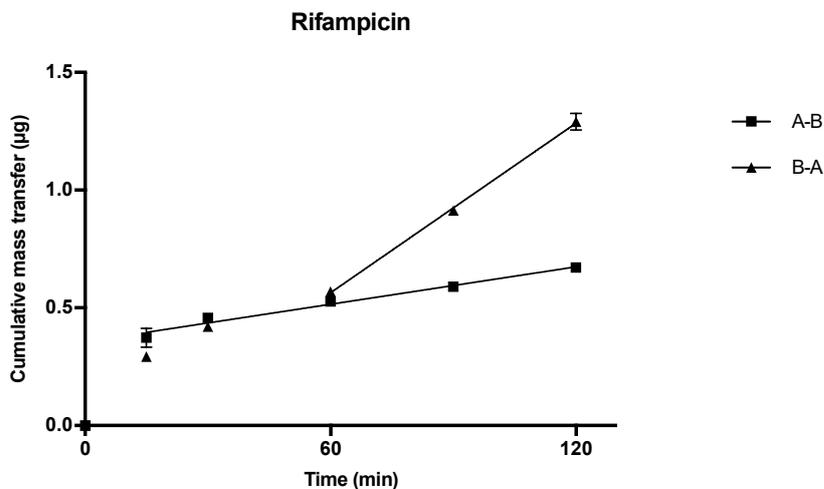
Rifampicin

Figure 5.11 Cumulative mass transfer of rifampicin alone (20 µg/ml) across Caco-2 monolayers (pH 7.4). Papp values calculated using the gradient of the linear portion of the curve (mean ± SD, n=3)

Isoniazid Combination
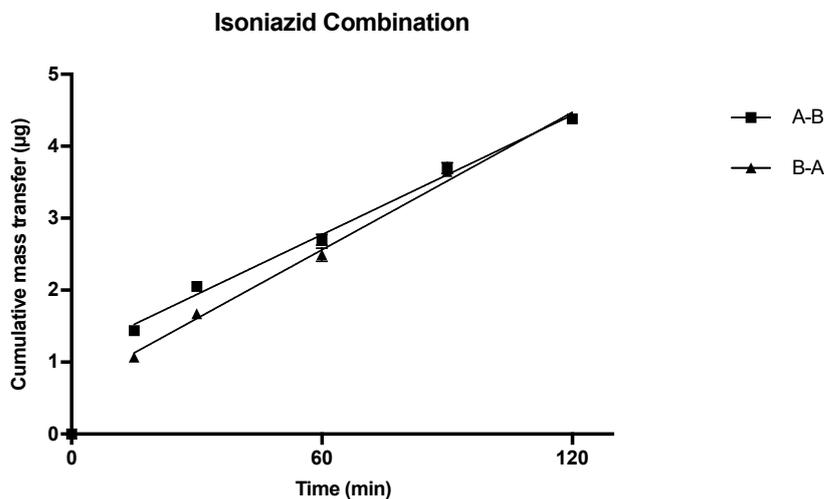
Figure 5.12 Cumulative mass transfer of isoniazid (20 µg/ml) whilst in combination with rifampicin across Caco-2 monolayers (pH 7.4). Papp values calculated using the gradient of the linear portion of the curve (mean ± SD, n=3)
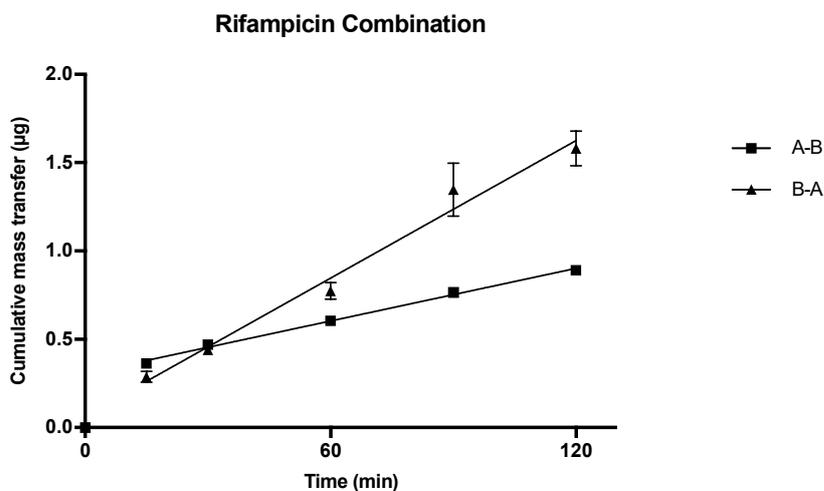
Figure 5.13 Cumulative mass transfer of rifampicin (20 µg/ml) whilst in combination with isoniazid across Caco-2 monolayers (pH 7.4). Papp values calculated using the gradient of the linear portion of the curve (mean ± SD, n=3)

Table 5.11 Papp vales for isoniazid and rifampicin alone and in combination in A-B and B-A directions across Caco-2 monolayers at pH 7.4 in both compartments (mean ± SD, n=3)

Compound	Papp 10^{-6} cm s^{-1}		Efflux Ratio
	A-B	B-A	
Isoniazid	16.37 ± 0.48	19.27 ± 0.32	1.18
Rifampicin	1.37 ± 0.12	5.95 ± 0.42	4.33
Isoniazid Combination	22.69 ± 1.21	26.98 ± 0.26	1.19
Rifampicin Combination	2.14 ± 0.19	5.58 ± 0.50	2.61

5.3.5 Clinical Trials Simulation

The initial simulation of the kinetics of isoniazid (derived from data presented in Table 5.1) were used to optimize the effective permeability (P_{eff}) and steady-state volume of distribution (V_{ss}) from clinical data sets 1 and 2 for each API. Optimized P_{eff} and V_{ss} were estimated as 10.23 $\times 10^{-4}$ cm/s and 0.63 L/kg. Default (Simcyp validated) parameters (as presented in Table 5.1) were used to simulate rifampicin kinetics.

Subsequent validation of isoniazid and rifampicin using validation data sets 3 and 4 for each API was successful and generally centred around the mean simulated profiles and within the 5th and 95th percentiles of the simulated profiles (see Figure 5.14 and Figure 5.15).
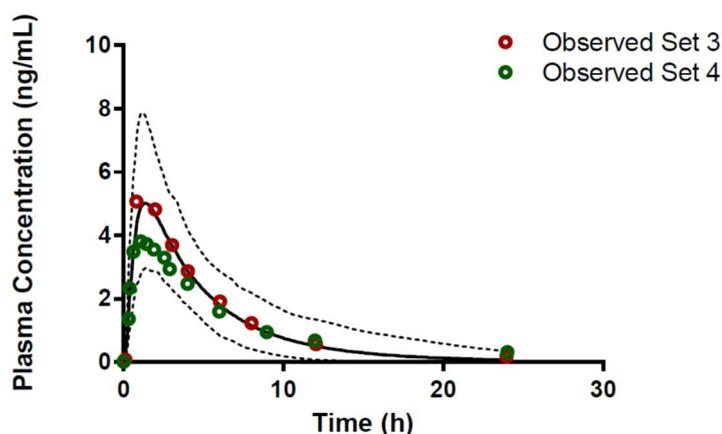
Figure 5.14 Simulated mean plasma profile after a 300 mg oral dose of isoniazid (solid black line). The corresponding observed data points are shown by red open circles. The grey lines represent the 5th and 95th percentiles for the predicted values. All simulations were performed using the minimal PBPK model.
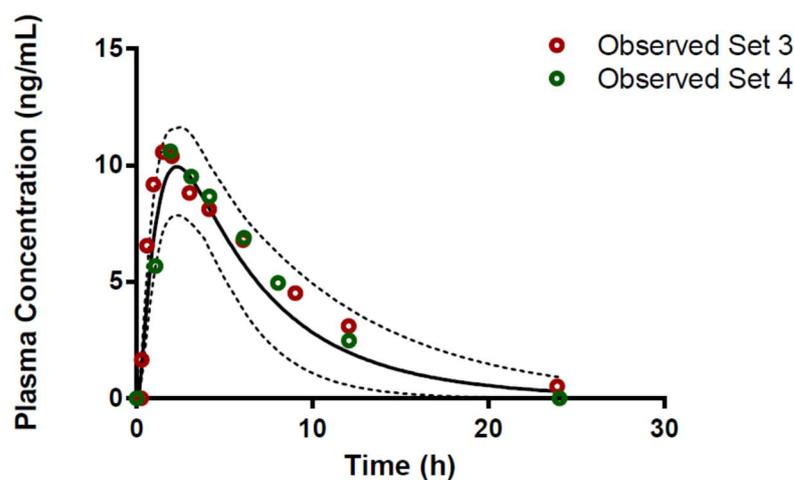
Figure 5.15 Simulated mean plasma profile after a 600 mg oral dose of rifampicin (solid black line). The corresponding observed data points are shown by red (set 3) or green (set 4) open circles. The grey lines represent the 5th and 95th percentiles for the predicted values. All simulations were performed using the minimal PBPK model.

Simulations to predict the *in vivo* performance of ODTs in healthy volunteers were used to compare the bioavailability between single and FDC formulations under fasted and fed conditions using dissolution data determined in section 5.3.3. For isoniazid the formulation state (single or combined) or dosing state (fasted or fed) had no statistically significant impact on pharmacokinetics (A and B). Isoniazid plasma concentrations reached a geometric mean C_{max} of 0.70-0.74 ng/ml in all conditions (Table 5.12), yielding a median AUC in the range of 4-4.25 ng/ml.h.

At the level of the small-intestine, predicted mean fraction dose absorbed (Fa) for isoniazid correlated with dissolution profiles, showing no significant differences between single and combination formulations, 0.98 ± 0.02 and 0.97 ± 0.03 (fasted) and 0.99 ± 0.04 and 0.96 ± 0.05 (fed), respectively.
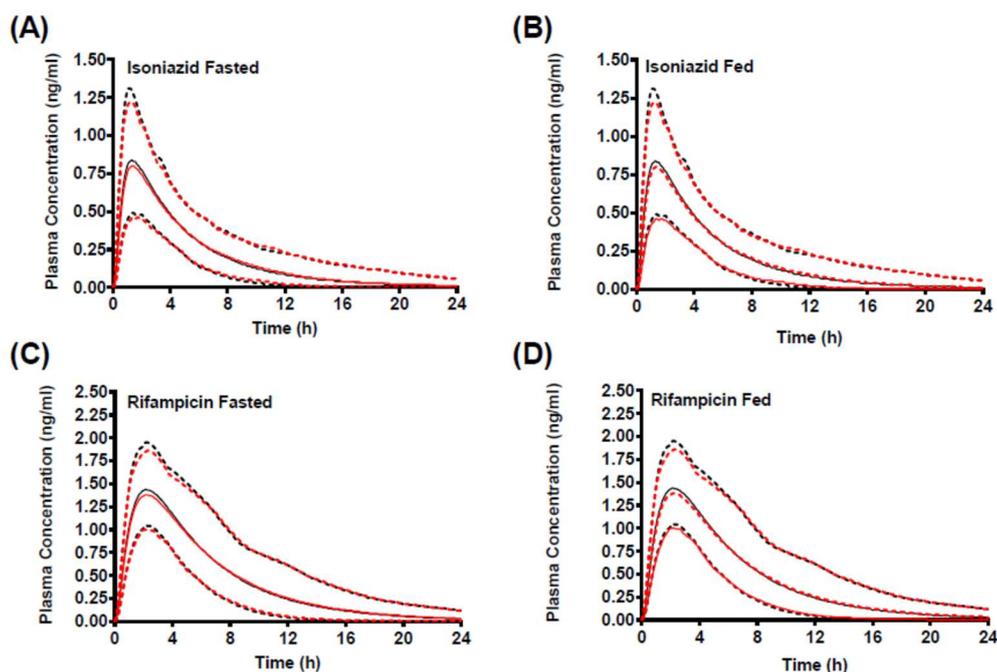
Figure 5.16 Simulated mean plasma profile after a 50 mg oral dose of isoniazid (A and B) and 75 mg oral dose of rifampicin (C and D) under fasted and fed conditions. Single API formulations indicated in black and fixed dose combination in red. Solid lines represent trial mean and dashed lines represent the 5th and 95th percentiles for the predicted values.

Fa values for rifampicin were equivalent between single and combination doses at 0.94 in fasted subjects; likewise, no difference was seen in Fa for fed subjects, with values of 0.94 for both single and combination doses. Rifampicin plasma profiles similarly showed no statistically significant difference ($p > 0.05$) in pharmacokinetic parameters between single and combination doses in fasted subjects (Figure 12C). Rifampicin plasma concentrations in combined formulations (irrespective of fasted/fed state) demonstrated higher AUCs (9.26 ng/ml.h) compared to single formulation (8.80 ng/ml.h). Furthermore, geometric mean C_{max} was generally consistent across all formulations and conditions (1.22-1.24 ng/ml) (Table 5.13) with a t_{max} of 2.56-2.38 h.

Bioavailability (F) for isoniazid in all cases was approximately 1, whilst F values for rifampicin were 0.91. This may be related to the high Fa seen with both APIs. Bioavailability for rifampicin correlates well with reported values. Rifampicin is a CYP3A4

inducer and it is likely that over a longer study period (i.e. multidose over a few weeks) F would drop to around 65-70%, as a result of increased metabolism [384].

Table 5.12 Summary of pharmacokinetic parameters for isoniazid (50 mg) under fasted and fed conditions. Geometric mean (SD) reported for C_{max} and median (range) for AUC and t_{max}

Parameters	Isoniazid Fasted		Isoniazid Fed	
	Single	Combined	Single	Combined
AUC (ng/ml.h)	4.05 (3.14-7.10)	4.24 (3.13-7.41)	4.05 (3.14-7.10)	4.24 (3.13-7.42)
C_{max} (ng/ml)	0.74 (0.13)	0.70 (0.12)	0.74 (0.13)	0.70 (0.12)
t_{max} (h)	1.48 (1.14-1.92)	1.49 (1.21-1.96)	1.48 (1.14-1.92)	1.49 (1.12-1.91)

Table 5.13 Summary of pharmacokinetic parameters for rifampicin (75 mg) under fasted and fed conditions. Geometric mean (SD) reported for C_{max} and median (range) for AUC and t_{max}

Parameters	Rifampicin Fasted		Rifampicin Fed	
	Single	Combined	Single	Combined
AUC (ng/ml.h)	8.80 (6.63-13.63)	9.26 (6.61-13.50)	8.80 (6.63-13.63)	9.26 (6.61-13.50)
C_{max} (ng/ml)	1.24 (0.18)	1.22 (0.30)	1.24 (0.18)	1.22 (0.30)
t_{max} (h)	2.38 (1.51-2.80)	2.38 (1.80-2.85)	2.38 (1.51-2.80)	2.36 (1.80-2.86)

5.4   Conclusion

ODTs demonstrated satisfactory performance for hardness, friability and disintegration. Dissolution profile assessment and comparison between single and FDC formulations of isoniazid indicated bioequivalence and this was reinforced through PBPK modelling, with no difference between pharmacokinetic parameters. Comparable bioequivalence was not assumed for rifampicin from dissolution comparison in FeSSIF, with release falling by around 15%. This observed drop in dissolution is most likely instead a result of degradation, given the complete release seen from single dose formulations and the well documented enhanced degradation of rifampicin seen in the presence of isoniazid under acidic conditions. In the absence of ascorbic acid, a perceived drop in rifampicin dissolution, due to degradation, would be seen for all rifampicin containing formulations in fact, however this is only significantly pronounced in combination with isoniazid in the more acidic FeSSIF media (pH 5).

Clinical trial simulations reported no difference in the bioavailability of isoniazid from the combination dose compared to the single dose, as predicted through dissolution profile assessment and comparison. Additionally, no food effect was seen. Interestingly, despite the retarded dissolution (degradation) from FDCs in FeSSIF, this did not result in a reduced bioavailability, with performance of FDCs in FaSSIF similarly showing bioequivalence with the single dose formulation. Furthermore, no difference in Fa values for rifampicin formulations was seen, implying that permeation across the intestinal epithelial membrane was a rate limiting factor; indeed, reclassification of rifampicin as a BCS class IV compound due to low intestinal permeability has been suggested [385], whilst the Papp values reported here indicate moderate to low permeability. Significantly, this result highlights a failure in f_1 and f_2 factor testing in this instance to predict bioequivalence, since bioavailability was not altered despite dissolution profiles being different.

For rifampicin, due to the inclusion of ascorbic acid as an antioxidant and since dissolution and degradation was not tested in simulated gastric fluid (at a lower pH), actual bioavailability values *in vivo* may differ. Regardless of this however, PBPK modelling demonstrated that the bioavailability of either drug was unaltered as a result of combination with the other, in these formulations. Rapid release isoniazid and rifampicin FDC ODTs thus may be a viable and attractive formulation prospect, whilst the framework used here could be employed in the development of more complex formulations. It should be noted that the focus for these investigations was on

preformulation and initial dosage form development and therefore stability studies were not carried out.

Chapter 6

Fixed Dose Combination Orally Disintegrating Tablets to Treat Cardiovascular Disease: Physiologically Based Pharmacokinetic Modelling to Assess Bioavailability

Chapter 6 – Fixed Dose Combination ODTs to Treat Cardiovascular Disease: Physiologically Based Pharmacokinetic Modelling to Assess Bioavailability

6.1   Introduction

Cardiovascular disease (CVD) is the leading cause of death worldwide, claiming an estimated 17.3 million lives per year, a death toll that is expected to rise to in excess of 23.6 million by 2030. Deaths from CVD accounted for 30% of global deaths in 2008, more than all forms of cancer combined [386].

CVD is multifactorial, with risk factors such as hypertension, dyslipidaemia, diabetes mellitus, smoking and obesity frequently co-existing [387]. One of the most common risk factor combinations is dyslipidaemia (elevated levels of low-density lipoprotein (LDL) and triglyceride (TG) and low levels of high-density lipoprotein (HDL)) and hypertension [388]. Studies have demonstrated the link between hypertension and metabolically associated risk factors [389]; in a retrospective study of US veterans, for example, the prevalence of CVD was commonly double that in patients exhibiting both hypertension and dyslipidaemia when compared to those with either condition alone [390]. In the UK, a 2004 analysis of the medical records of over 600,000 patients revealed a 14.7% incidence of subjects with both hypertension and dyslipidaemia [391].

Amlodipine (BCS class I [392]) is a 3rd generation dihydropyridine calcium channel blocker, a class of drug that works to lower blood pressure in hypertensive patients through relaxation of vascular smooth muscle and vessel dilation [393]. It acts by inhibiting 'slow' influx of extracellular calcium into cardiac and vascular cells via blockade of voltage-gated L-type calcium channels [394, 395]. Amlodipine's slow onset of action is responsible for a low incidence of reflex tachycardia and other vasodilator side effects when compared to other dihydropyridines, whilst its slow elimination and resultant long duration of action grants the convenience of a once-daily dosage regime [396].

Atorvastatin (BCS class II [397]), a 3-hydroxy-3-methylglutaryl coenzyme A (HMG-CoA) reductase inhibitor, is used extensively in the treatment of dyslipidaemia [398]. HMG-CoA reductase catalyses the conversion of HMG-CoA to mevalonate. Its inhibition reduces hepatocyte cholesterol levels, leading to upregulation of LDL cholesterol (LDL-C) cell surface receptors and resulting in increased clearance of LDL-C from plasma [399, 400]. Atorvastatin reportedly reduces LDL-C in hypercholesterolaemic patients by 41-61% [401], as well as reducing total cholesterol and plasma triglycerides alongside a modest increase in HDL cholesterol (HDL-C) levels [402].

Despite the substantial risk to patients suffering both dyslipidaemia and hypertension, successful treatment falls short [403]. A major reason for this is poor patient compliance, for reasons including cost, treatment regime complexity, extent of concomitant treatment and side effects [401, 404, 405]. Several clinical studies have examined the efficacy and safety of amlodipine and atorvastatin combination therapy in patients with concurrent hypertension and dyslipidaemia. Combination therapy has been shown to achieve blood pressure and LDL goals [406, 407]. The RESPOND study, which compared combination therapy with amlodipine or atorvastatin alone showed no difference in efficacy [408], whereas the AVALON study reported an increased efficacy with combination therapy over either drug alone [409]. Furthermore, when amlodipine and atorvastatin are administered in a fixed dose combination (FDC) there is no significant difference in bioavailability (based on t_{max}, C_{max} and AUC) compared to coadministered matching doses of individual amlodipine and atorvastatin tablets [410].

An amlodipine and atorvastatin FDC is therefore an attractive prospect with the view of improving patient compliance. In addition to demonstrating bioequivalence *in vivo*, in combination both amlodipine and atorvastatin allow for once-daily dosing and have no issues with tolerability [401]. Indeed, an amlodipine and atorvastatin FDC (Caduet®) was approved in 2004 as the first fixed-dose combination to treat two cardiovascular disease categories [411].

The potential to enhance therapy for patients suffering both dyslipidaemia and hypertension with an orally disintegrating FDC for amlodipine and atorvastatin is substantial. Since no change in bioavailability for amlodipine and atorvastatin from FDCs has been reported, it is expected that FDC ODTs, given their immediate disintegration and therefore rapid drug release, should show similar findings. Furthermore, the ability of ODTs to increase patient compliance due to their convenience as a dosage form, would likely enhance CVD therapy. In this work an FDC ODT for amlodipine and atorvastatin was developed and characterised. Single dose and fixed dose drug dissolution from ODTs was tested in biorelevant media, whilst drug permeability across Caco2 cell monolayers was measured for prediction of *in vivo* pharmacokinetics and bioequivalence of FDCs compared to single dose formulations, through PBPK computational modelling.

6.2   Materials and Methods

6.2.1   Materials

Amlodipine besylate (herein referred to as amlodipine) was purchased from Molekula Ltd (UK) and atorvastatin calcium (herein referred to as atorvastatin) from Chemical Point (Germany). Pearlitol Flash (mannitol-starch copolymer) was obtained from Roquette Pharma (France), with Avicel PH-102 micro-crystalline cellulose (MCC) and sodium stearyl fumerate (SSF) supplied by FMC BioPolymer (USA).

Biorelevant FaSSIF/FeSSIF/FaSSGF Instant Powder was purchased from biorelevant.com (UK). Sodium hydroxide, sodium chloride, sodium phosphate and glacial acetic acid for biorelevant media were obtained from Sigma-Aldrich (UK). Acetonitrile (ACN) and methanol (HPLC-grade) were obtained from Fisher Scientific (UK).

For cell culture media DMEM was purchased from Lonza (UK), fetal bovine serum (FBS), gentamicin (10 mg/ml), Fungizone (amphotericin B 250 µg/ml), HBSS and penicillin/streptomycin (10,000 U/ml) were all purchased from Gibco (Thermo Fischer Scientific, UK). Trypsin-EDTA solution (0.25%) was procured from Sigma-Aldrich (UK).

6.2.2   HPLC

HPLC was performed on an Agilent 1260 series (Agilent Technologies, USA), comprising a quarternary pump, Infinity VWD and autosampler. Analysis was conducted on a reversed-phase Gemini C18, 150 x 4.6 mm, 110Å, 5µm column (Phenomenex, UK). Protocols were developed, calibrated and validated for both amlodipine and atorvastatin alone and in combination.

Separations were achieved using 0.1% (v/v) TFA and ACN at different ratios as the mobile phase. Amlodipine separation was performed with an isocratic mobile phase of TFA: ACN (57.5:42.5 v/v), a flow rate of 1 ml/min and a wavelength of 360 nm. Atorvastatin separation was achieved using an isocratic mobile phase of TFA: ACN (50:50 v/v), a flow rate of 1.2 ml/min and a wavelength of 246 nm. Separation of amlodipine and atorvastatin in combination required a mobile phase of TFA: ACN delivered at a gradient (65:35 to 35:65 v/v), with a flow rate of 1.5 ml/min and a wavelength of 240 nm. An injection volume of 20 µl was used throughout.

HPLC method validation involved assessment of precision through intra-day variation, accuracy by multilevel recovery studies, instrument precision, linearity and limit of detection and quantification (LOD and LOQ). Stock solutions (1 mg/ml) of each drug were prepared (using ACN and methanol as solvents for amlodipine and atorvastatin, respectively) from which dilutions and subsequently two-fold serial dilutions were prepared to form a calibration curve.

6.2.3   Tablet Production

Direct compression of tablets (500 mg) was performed on an Atlas T8 automatic press (SPECAC, UK), using a 13mm round, flat faced die. Tablets were produced under ambient conditions.

6.2.4   Friability

Tablet friability was determined on 6 tablets using an F2 friability tester (Sotax, Switzerland). Tablets were placed inside the drum and rotated at 25 rpm for a total of 100 revolutions. Dust was removed pre and post testing to remove excess powder that would contribute to tablet mass. Friability was calculated and expressed as % tablet weight loss from initial tablet weight.

6.2.5   Tablet Hardness

A Tablet Hardness Tester TBF1000 (Copley Scientific, UK) was used to measure the radial crushing strength (hardness) of tablets in triplicate.

6.2.6   Dissolution Testing

API dissolution from ODTs in 900 ml biorelevant media was tested in both fasted state simulated intestinal fluid (FaSSIF) and fed state simulated intestinal fluid (FeSSIF), at pH 6.5 and 5 respectively and maintained at 37°C. An ERWEKA DT 600 USP 2 paddle apparatus (Germany) was used at a paddle speed of 50 rpm [367]. 5ml samples were

taken over 2 h, replacing with 5 ml fresh media to simulate sink conditions. API dissolution was measured using HPLC and corrected for % dose dissolved.

6.2.7   Cell Culture

Prior to seeding, cells were trypsinised (2.5 ml) from 75-cm^2 cell culture flasks (Corning, USA) on which they had been grown (80% confluence), after washing with HBSS. Caco-2 cells (passage 54-58) were seeded onto Transwell (Corning, USA) semi-permeable membrane supports (12-well, 1.12 cm^2, 0.4 µm pore size) at a density of 8×10^4 cells/cm^2. Cells were maintained in DMEM containing L-glutamine (4 mM) and glucose (4.5 mg/ml) supplemented with (v/v) 10% FBS, 1% penicillin/streptomycin, 1% NEAA, amphotericin B (0.5 µg/ml) and gentamicin (20 µg/ml). Media was changed every 2-3 days and transwells cultured at 37°C, 5% CO_2 for 21 days, after which transport studies were performed.

6.2.8   Transepithelial Electrical Resistance (TEER) Measurements

TEER value measurements were performed to monitor monolayer integrity using an EVOM meter (World Precision Instruments, USA). TEER values are expressed using the equation:

$$TEER\ (\Omega \cdot cm2) = (resistance - blank\ resistance)\ x\ membrane\ surface\ area\ (cm2)$$

6.2.9   Caco-2 Transport Studies

Caco-2 monolayers were used for transport studies between 21 and 24 days post-seeding. Drug absorption through Caco-2 monolayers was measured for amlodipine and atorvastatin alone and in combination in both the apical to basolateral (A-B) and basolateral to apical (B-A) directions (n=3). Transport studies were carried out in DMEM (37°C) containing 10 mM HEPES (pH 7.4), with 0.5 ml and 1.5 ml in the A and B compartments, respectively. Samples of 100 µl were removed from the A side and 200 µl from the B side at time points over 2 h, replacing with fresh pre-warmed media (37°C) to mimic sink conditions. For mass balance, samples were taken from the donor compartments at t=0 and t=120 min.

Amlodipine was administered at a concentration equivalent to 20 µg/ml (representing a dose of 5 mg in 250 ml) and atorvastatin at a concentration equivalent to 40 µg/ml (representing a dose of 10 mg in 250 ml). Cultures were maintained at 37°C and 5% CO_2 throughout the experiment. Samples were analysed by HPLC and apparent permeability (P_{app}) values were calculated using equation:

$$Papp \ = \ (dQ/dt)/(C_0 \ x \ A)$$

Where dQ/dt is the mass transfer rate of the compound from the donor to the receiver compartment, C_0 is the initial concentration in the donor chamber and A is the monolayer surface area (cm^2).

6.2.10 Clinical Trials Simulation

The population-based clinical trials simulator Simcyp (V14) (Certara, USA) was used to simulate the plasma concentration of atorvastatin and amlodipine from single API and FDC formulations. Default parameter values for creating a North European Caucasian population were selected [371].

6.2.11 Compound Data

Physicochemical information for each API was collated from the literature used to develop compound files (Table 6.1). Simulations were performed using a minimal-PBPK model. Where uncertainty arose regarding the precise value of compound data parameters, parameter estimation was conducted using the Parameter Estimation Module to optimise parameter values. The ADAM model [372] was assumed for all simulations and the dissolution profile for each formulation (single and FDC) in FaSSIF and FeSSIF were utilised.

6.2.12 Clinical Studies

The optimisation and validation of the PBPK model was conducted using clinical study results reported in healthy adult subjects. For atorvastatin: study 1 included 20 mg tablet dosed to 36 healthy volunteers (18-45 years old) [412]; study 2 included a 20 mg tablet

dosed to 24 healthy [413]; study 3 included an 80mg capsule dosed to 36 healthy subjects (20-50 years old) [414]; study 4 included 10 mg tablet dosed to 50 healthy volunteers[415]. Studies 1 and 2 were used for model development and studies 3 and 4 utilised for validation.

For amlodipine: study 1 included a 5 mg tablet dosed to 24 healthy [413]; study 2 included a 5 mg tablet dosed to 28 healthy volunteers (35.48 ± 9.52 years old) [416]; study 3 included a 10 mg tablet dosed to 24 healthy volunteers (21-29 years old) [417]; study 4 included a 10 mg tablet dosed to 35 subjects (18-46 years old) [418]. Studies 1 and 2 were used for model development and studies 3 and 4 utilised for validation.

Raw data from published human trial plasma concentration profiles was extracted using WebPlotDigitizer 3.10 [377] and, where necessary, parameter estimation was conducted using the validation clinical datasets.

Predictions of API plasma pharmacokinetic profiles were simulated following the oral administration of a single immediate release solid dosage form of 10mg (atorvastatin) and 5 mg (amlodipine) dose over a 24 hr period.

Table 6.1 Input parameter values and predicted PBPK values for simulation of pharmacokinetics of amlodipine and atorvastatin.

Parameter	Amlodipine	Atorvastatin
Type	Diprotic base	Monoprotic acid
MW	408.88	588.2
LogP	3.43 [419]	5.7
pKa	9.4,1.90 [419]	4.46
fu	0.07 [420]	0.051
Vss (L/kg)^a	Predicted PBPK/PE	Predicted PBPK/PE
B:P ratio	1	0.61
CLpo (L/min)	24.8	949
CLint$_{3A4}$^{b}	-	8.28
Peff (cm/s)	PE	PE
Jmax,$_{P-gp}$ (pmol/cm^2/min)	-	151 [421]
Km,$_{P-gp}$ (μM)	-	115 [421]
RAF$_{P-gp}$	-	PE

MW: molecular weight; fu: plasma unbound fraction; Vss: steady-state volume of distribution; B:P ratio: blood-to-plasma ratio; Peff: human effective permeability; CLpo: oral clearance; PE: parameter estimation; RAF; relative activity factor. ^{a} Vss was determined from calculation of tissue partitions coefficients within Simcyp or parameter estimated. ^{b} *In vitro* intrinsic metabolic clearance (Clint) was calculated using Simcyp Retrograde Calculator from *in vivo* oral clearance and assuming f_a=1, f_g=0.24 [422] with CYP3A4 being the predominant metabolic pathway [423].

6.2.13 Statistical Analysis

GraphPad PRISM software version 6.01 (USA) was used for data analysis. Ordinary one-way ANOVA was used with Tukey's multiple comparisons test to analyse data for tablet characterization. Unpaired two-tailed t-test was used to determine statistical differences between data sets for pharmacokinetic parameters.

Differences between dissolution profiles of APIs in single dose (reference) and combination (test) were assessed using f_1 and f_2 difference and similarity factor testing, using the equations [346]:

$$f_1 = ([\sum_{t=1}^{n} |R_t - T_t|]/[\sum_{t=1}^{n} R_t]) * 100$$

$$f_2 = 50 * \log(\{[1 + (1/n) \sum_{t=1}^{n} (R_t - T_t)^2]^{-0.5} * 100)$$

Where R_t and T_t are the % drug dissolved value at each time point for the reference and test product respectively and n is the number of time points.

6.3   Results and Discussion

6.3.1   ODT Development

ODT formulations for amlodipine and atorvastatin single and FDC ODTs were based on isoniazid and rifampicin ODTs (see section 5.3.1) and thus the formulation development is not repeated here. Formulation compositions for all amlodipine and atorvastatin ODTs are shown in Table 6.2 and characterisation is presented in Table 6.3.

Table 6.2 ODT formulations for individual dose and FDC ODTs. Values for APIs and excipients are given as % w/w for 500mg tablets. All formulations underwent compaction at 2.2 T with a 6 sec dwell time

	Amlodipine (1%)	Atorvastatin (2%)	Amlodipine + Atorvastatin (1% + 2%)
	f1	f2	f3
Amlodipine Besylate	6.95		6.95
Atorvastatin Calcium		10.85	10.85
Pearlitol Flash	410.55	406.65	399.7
SSF (1.5%)	7.5	7.5	7.5
MCC (15%)	75	75	75

Table 6.3 Individual and FDC ODT properties. All formulations underwent compaction at 2.2 T with a 6 s dwell time (mean ± SD, n=3)

	Hardness (N)	Porosity	Disintegration Time (s)	Friability (%)
f1	108.00 ± 8.35	0.23 ± 0.15	25.33 ± 3.21	0.71
f2	114.40 ± 4.10	0.25 ± 0.00	24.00 ± 3.00	1.02
f3	117.77 ± 8.97	0.24 ± 0.02	21.67 ± 1.53	0.73

6.3.2   HPLC Protocol Validation

Linearity test solutions were prepared from stocks at six concentrations ranging from 25 to 0.8 µg/ml. Calibration curves for both drugs alone and in combination are shown in Figure 6.1 to Figure 6.2. Validation of protocols by intraday studies for amlodipine, atorvastatin and amlodipine/atorvastatin combination (Table 6.4 to Table 6.6), show the methods to be accurate and precise. Method accuracy is demonstrated by multilevel recovery, ranging from 25 µg/ml to 1.5625 µg/ml. Accurate recovery was exhibited in all instances, ranging from 98.58 to 102.46 %. Relative standard deviation (RSD) values representing intraday precision for amlodipine, atorvastatin and amlodipine/atorvastatin ranged from 1.05 to 7.36 %. Instrument precision, tested for by six consecutive injections of the same sample (25 µg/ml), was high, with RSD values from 0.01 to 0.04 %. LOQ and LOD values for amlodipine and atorvastatin alone were below 0.6 and 0.2 µg/ml, respectively. LOQ and LOD values for amlodipine/atorvastatin combination were lower still, falling below 0.2 and 0.1 µg/ml, correspondingly.
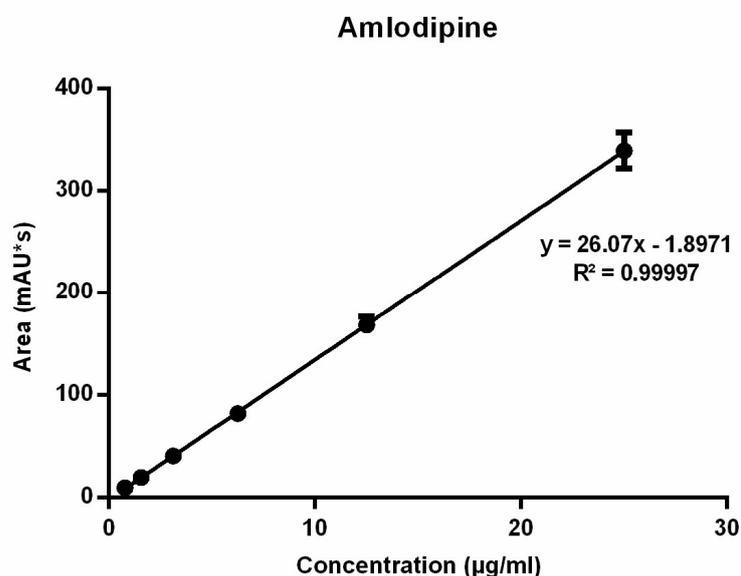
Figure 6.1 HPLC calibration curve for amlodipine besylate, linear over a concentration range of 25 to 0.8 µg/ml (n=3).
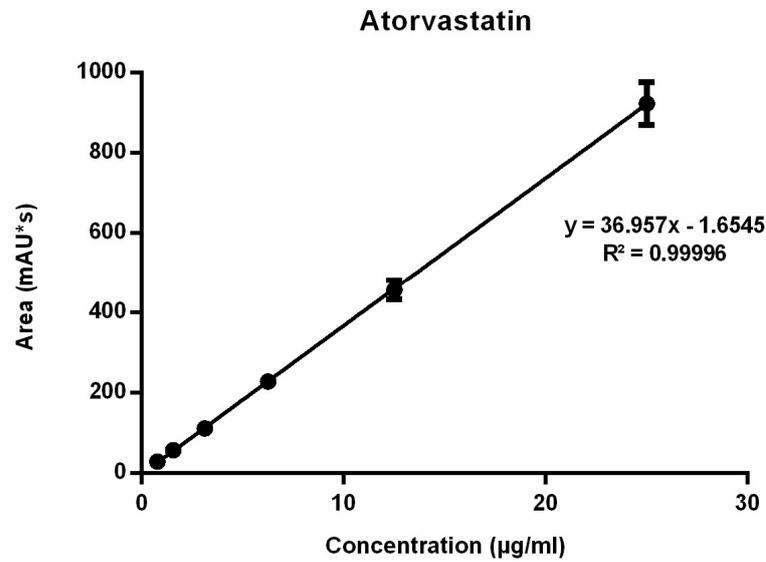
Figure 6.3 HPLC calibration curve for atorvastatin calcium, linear over a concentration range of 25 to 0.8 µg/ml (mean ± SD, n=3)
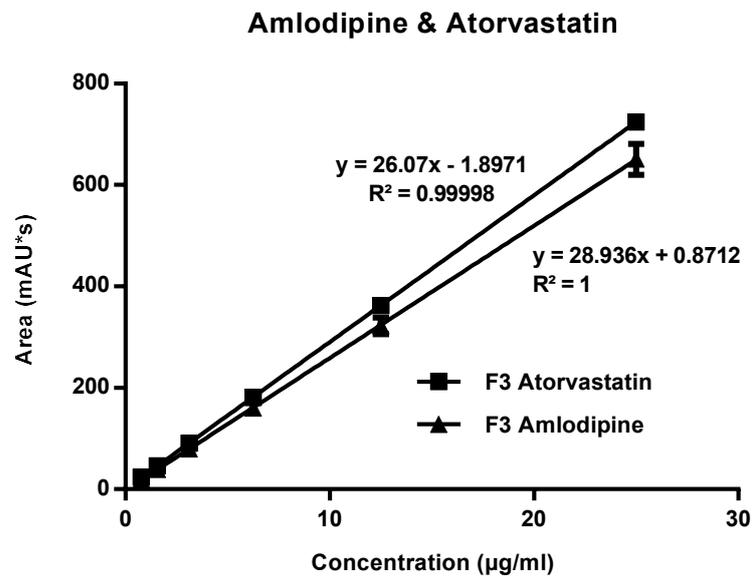
Figure 6.2 HPLC calibration curve for simultaneous detection of amlodipine besylate and atorvastatin calcium, linear over a concentration range of 25 to 0.8 µg/ml (mean ± SD, n=3)

Table 6.4 HPLC method validation for detection of amlodipine. Data for linearity (correlation coefficient), instrument precision, accuracy (recovery), precision (% RSD), LOD and LOQ are displayed (mean ± SD, n=3)

Amlodipine conc. actual (µg/mL)	Amlodipine conc. calculated (µg/mL)	RSD (%)	Recovery (%)
25	25.02 ± 1.30	5.19	100.10 ± 5.20
12.5	12.49 ± 0.57	4.59	99.95 ± 4.58
6.25	6.16 ± 0.29	4.69	98.58 ± 4.62
3.125	3.11 ± 0.13	4.13	99.54 ± 4.12
1.5625	1.59 ± 0.06	3.68	101.83 ± 3.75

Instrument precision (% RSD) = 0.02

Mean % recovery = 100.00 ± 1.18

RSD % recovery = 0.01

LOD = 0.17 µg /mL

LOQ = 0.57 µg /mL

Correlation coefficient = 0.99997

Table 6.5 HPLC method validation for detection of atorvastatin. Data for linearity (correlation coefficient), instrument precision, accuracy (recovery), precision (% RSD), LOD and LOQ are displayed (mean ± SD, n=3)

Atorvastatin conc. actual (µg/mL)	Atorvastatin conc. calculated (µg/mL)	RSD (%)	Recovery (%)
25	25.05 ± 1.44	5.76	100.19 ± 5.77
12.5	12.42 ± 0.66	5.34	99.34 ± 5.31
6.25	6.23 ± 0.38	6.08	99.72 ± 6.07
3.125	3.08 ± 0.23	7.36	98.42 ± 7.24
1.5625	1.60 ± 0.10	6.25	102.46 ± 6.40

Instrument precision (% RSD) = 0.04

Mean % recovery = 100.02 ± 1.51

RSD % recovery = 0.02

LOD = 0.12 µg /mL

LOQ = 0.40 µg /mL

Correlation coefficient = 0.99996

Table 6.6 HPLC method validation for simultaneous detection of amlodipine and atorvastatin. Data for linearity (correlation coefficient), instrument precision, accuracy (recovery), precision (% RSD), LOD and LOQ are displayed (mean ± SD, n=3)

Conc. actual (µg/mL)	Conc. calculated (µg/mL)	RSD (%)	Recovery (%)
Amlodipine			
25	25.04 ± 1.16	4.65	100.15 ± 4.65
12.5	12.43 ± 0.64	5.10	99.46 ± 5.10
6.25	6.22 ± 0.35	5.64	99.56 ± 5.64
3.125	3.12 ± 0.18	5.85	99.89 ± 5.85
1.5625	1.58 ± 0.09	6.06	100.96 ± 6.06

Instrument precision (% RSD) = 0.03

Mean % recovery = 100.01 ± 0.60

RSD % recovery = 0.01

LOD = 0.04 µg /mL

LOQ = 0.13 µg /mL

Correlation coefficient = 0.99998

Atorvastatin			
25	25.01 ± 0.26	1.05	100.03 ± 1.05
12.5	12.50 ± 0.16	1.28	99.97 ± 1.28
6.25	6.23 ± 0.14	2.17	99.72 ± 2.17
3.125	3.11 ± 0.08	2.42	99.64 ± 2.42
1.5625	1.56 ± 0.04	2.68	100.03 ± 2.68

Instrument precision (% RSD) = 0.02

Mean % recovery = 99.88 ± 0.18

RSD % recovery = 0.00

LOD = 0.05 µg /mL

LOQ = 0.17 µg /mL

Correlation coefficient = 1

6.3.3 Dissolution

Dissolution of API from formulations f1-f3 was tested in biorelevant media (Figure 6.4 to Figure 6.7). Amlodipine dissolution from single and FDC ODTs in FaSSIF was rapid, with >50% dissolution within 2 hrs. Near complete dissolution (94.9%) and complete dissolution at (101.2%) was observed in single and FDC, respectively. Amlodipine dissolution from single and FDC in FeSSIF peaked at 87.9% and 79.9%, respectively. Difference and similarity testing comparing dissolution profiles of amlodipine from single and combination formulations are shown in Table 6.7. Difference and similarity testing was used as a tool to compare dissolution profiles in order to predict bioequivalence. In fasted state media, dissolution of amlodipine from both single and FDC exceeded 85% within 15 mins, whilst f_1 and f_2 testing showed no difference between dissolution profiles. Dissolution in FeSSIF did not exceed 85% within 15 mins from either single or FDC, with dissolution profiles shown to be different based on f_1 and f_2 factors.

Atorvastatin dissolution in FaSSIF was initially rapid, although peaking at 80.0% and 89.3% for single and FDC respectively. Dissolution profiles in FeSSIF were similar to FaSSIF, with dissolution peaking at 76.9% from single and 86.2% from combination formulations. Greater atorvastatin dissolution from FDCs was not recognised by f_1 and f_2 testing (Table 6.7), with no difference observed between dissolution profiles for single and combination formulations.

Based on difference and similarity testing only amlodipine in FeSSIF failed to show similar bioequivalence, although >85% dissolution was only observed once. This would suggest that a FDC ODT would likely display similar performance *in vivo* to a single dose, although based upon current guidelines this is not assumed for BCS class II compounds. Furthermore, through development of this simple formulation to consistently deliver greater than 85% dissolution (for class I amlodipine) it may be possible to achieve biowaiver status.
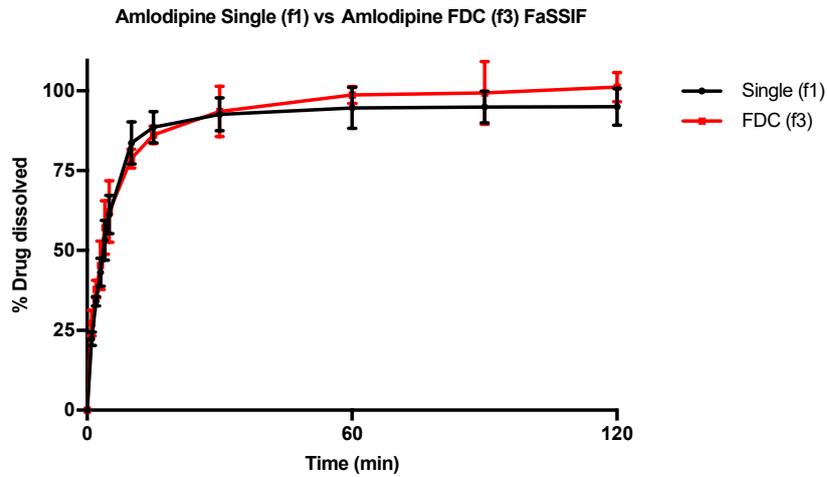
Figure 6.4 Amlodipine (5 mg) dissolution profiles of single and FDC formulations in fasted state biorelevant media (900 ml, 37°C) from 500 mg ODTs. Dissolution performed using USP 2 paddle apparatus (mean ± SD, n=3)
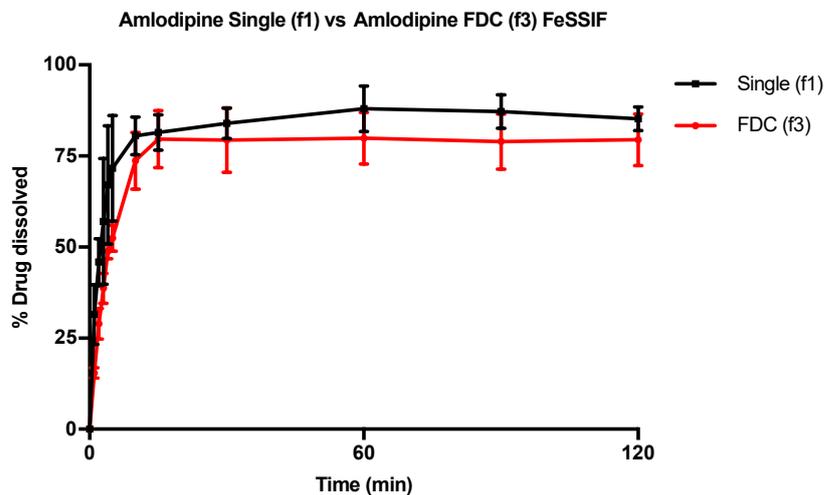
Figure 6.5 Amlodipine (5 mg) dissolution profiles of single and FDC formulations in fed state biorelevant media (900 ml, 37°C) from 500 mg ODTs. Dissolution performed using USP 2 paddle apparatus (mean ± SD, n=3)
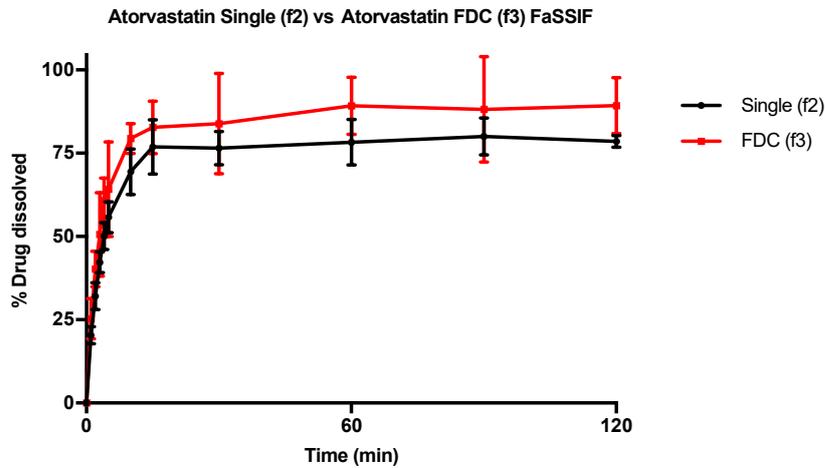
Figure 6.6 Atorvastatin (10 mg) dissolution profiles of single and FDC formulations in fasted state biorelevant media (900 ml, 37°C) from 500 mg ODTs. Dissolution performed using USP 2 paddle apparatus (mean ± SD, n=3)
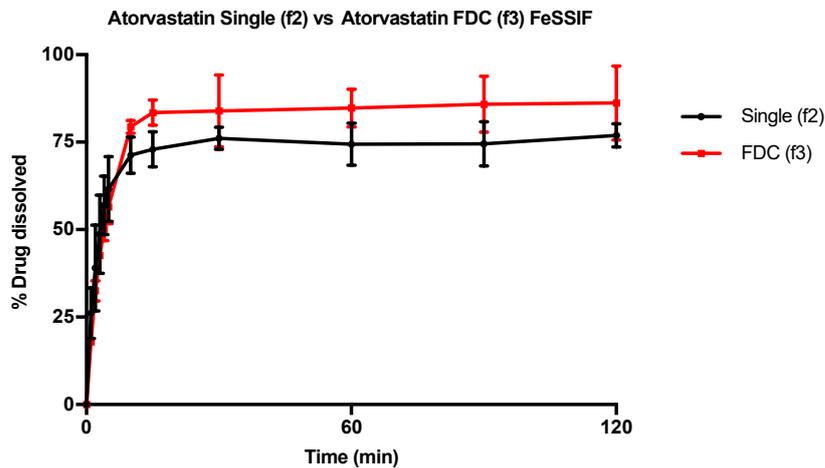
Figure 6.7 Atorvastatin (10 mg) dissolution profiles of single and FDC formulations in fed state biorelevant media (900 ml, 37°C) from 500 mg ODTs. Dissolution performed using USP 2 paddle apparatus (mean ± SD, n=3)

Table 6.7 Comparison of dissolution profiles for each compound from single and FDC formulations in FaSSIF and FeSSIF media, by difference factor f_1 and similarity factor f_2 testing. Dissolution profiles are considered similar if the f_1 value is below 15 and the f_2 value is above 50.

Compound		>85% dissolution ≤15 min	f_1	f_2	Result
Amlodipine	FaSSIF	Yes	5.08	70.80	Pass
	FeSSIF	No	15.92	45.40	Fail
Atorvastatin	FaSSIF	No	14.16	53.81	Pass
	FeSSIF	No	13.24	54.59	Pass

6.3.4   Permeability Studies

TEER values for Caco-2 cells are the same as in section 5.3.4. Amlodipine and atorvastatin transport across Caco-2 monolayers alone and in combination was measured in both A-B and B-A directions. Drug transport from A-B is shown for amlodipine (Figure 6.8), atorvastatin (Figure 6.9) and amlodipine and atorvastatin combination (Figure 6.10 and Figure 6.11, respectively). The gradient of the linear portion of the curve was used to calculate P_{app} values, summarised in Table 6.8.

P_{app} values for amlodipine closely mimic those observed by Rausl et al. [424] from both A-B and B-A. Atorvastatin P_{app} values and efflux ratio are similar to those reported by Wu et al. [425]. An efflux ratio of 1.14 for amlodipine indicates passive diffusion of the compound across Caco-2 monolayers, whereas an efflux ratio of 5.02 for atorvastatin suggests active efflux of the API in the B-A direction. Atorvastatin efflux, mediated primarily by P-glycoprotein, has been described previously in the Caco-2 model [425, 426] and other cell lines [427].

When combined with atorvastatin, P_{app} values for amlodipine decreased significantly from A-B (P<0.001) and B-A (P<0.05), although the efflux ratio remained largely unchanged at 0.96. A decrease in atorvastatin P_{app} value when in combination with

amlodipine from A-B was not significant (P>0.05) but was significant in the B-A direction (P<0.001), with the efflux ratio again maintained at a similar level.
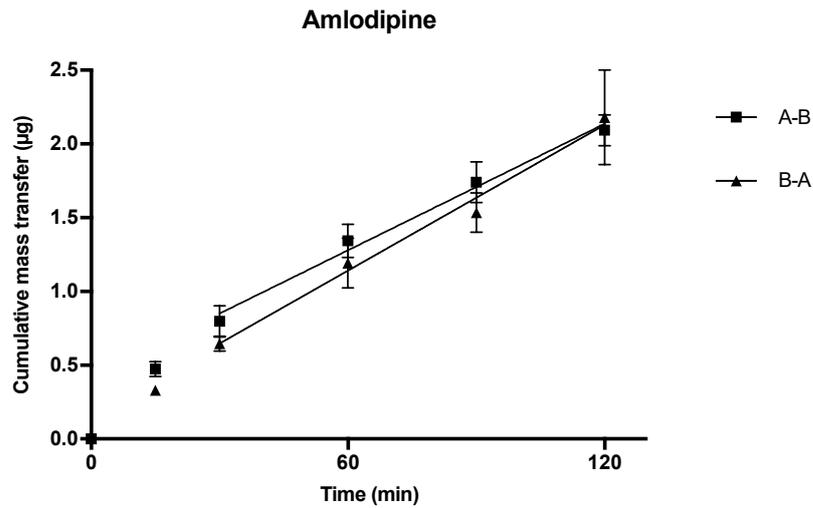
Figure 6.8 Cumulative mass transfer of amlodipine alone (20 µg/ml) across Caco-2 monolayers (pH 7.4) simulating f1. P_{app} values calculated using the gradient of the linear portion of the curve (mean ± SD, n=3)
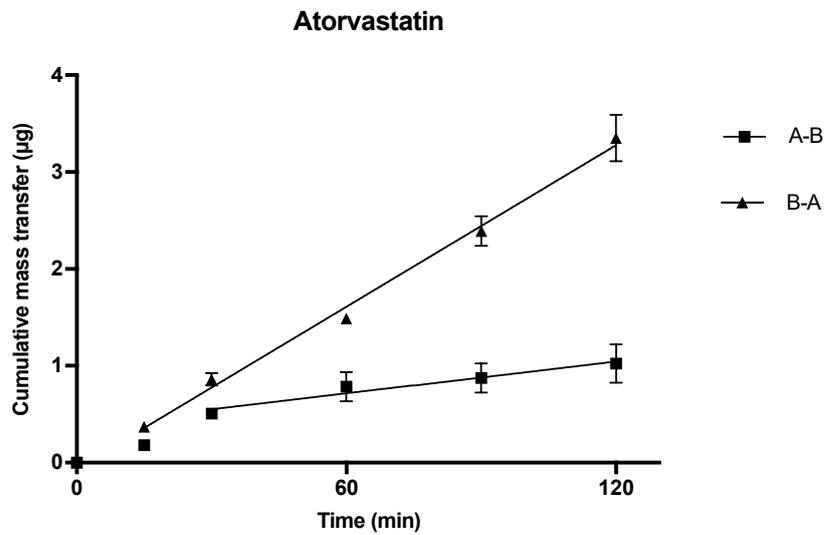
Figure 6.9 Cumulative mass transfer of atorvastatin alone (40 μg/ml) across Caco-2 monolayers (pH 7.4) simulating f2. P_{app} values calculated using the gradient of the linear portion of the curve (mean ± SD, n=3)
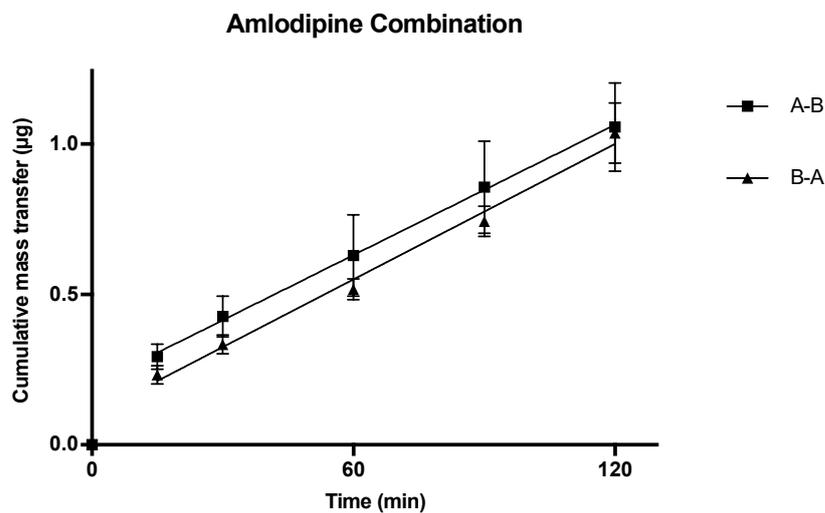
Figure 6.10 Cumulative mass transfer of amlodipine (20 μg/ml) whilst in combination with atorvastatin across Caco-2 monolayers (pH 7.4) simulating f3. P_{app} values calculated using the gradient of the linear portion of the curve (mean ± SD, n=3)
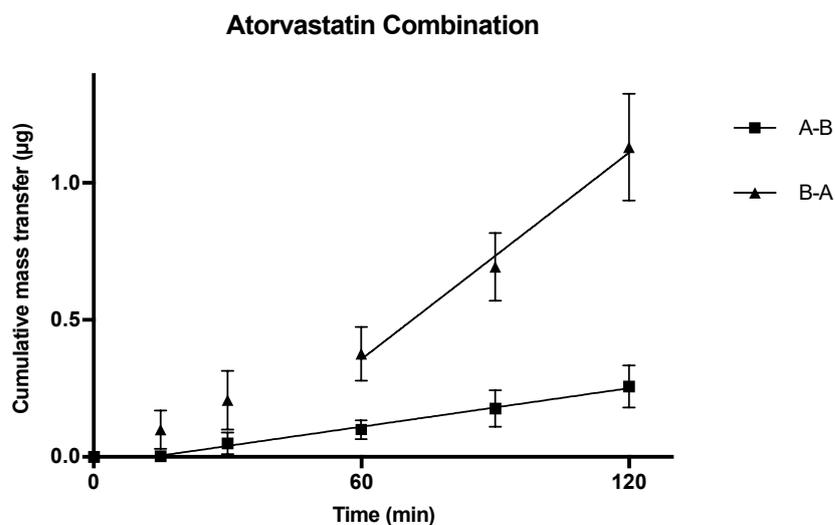
Figure 6.11 Cumulative mass transfer of atorvastatin (40 µg/ml) whilst in combination with amlodipine across Caco-2 monolayers (pH 7.4) simulating f3. P_{app} values calculated using the gradient of the linear portion of the curve (mean ± SD, n=3)

Table 6.8 P_{app} vales for amlodipine and atorvastatin alone and in combination in A-B and B-A directions across Caco-2 monolayers at pH 7.4 in both compartments (mean ± SD, n=3)

Compound	P_{app} (10^{-6} cm s^{-1})		Efflux Ratio
	A-B	B-A	
Amlodipine	8.34 ± 0.32	9.51 ± 1.70	1.14
Atorvastatin	2.03 ± 0.96	10.18 ± 0.71	5.02
Amlodipine Combination	5.40 ± 0.48	5.18 ± 0.29	0.96
Atorvastatin Combination	0.87 ± 0.18	4.59 ± 0.44	5.29

6.3.5   Clinical Trials Simulation

The initial simulation of the kinetics of amlodipine and atorvastatin (derived from data presented in Table 6.1) were used to optimise the P_{eff} and V_{ss} from clinical data sets 1 and 2 for each API. Optimised P_{eff} and V_{ss} were estimated as 1.35 x10^{-4} cm/s and 6.12

x10^{-4} cm/s for amlodipine and 13.78 l/kg and 4.78 l/kg for atorvastatin, respectively. Furthermore, a RAF$_{P-gp}$ of 8.7 was estimated to account for atorvastatin efflux (P-glycoprotein) [421, 425] contribution within the small-intestine.

Subsequent validation of atorvastatin and amlodipine using validation data sets 3 and 4 for each API was successful and generally centred around the mean simulated profiles and within the 5th and 95th percentiles of the simulated profiles (see Figure 6.12 and Figure 6.13).
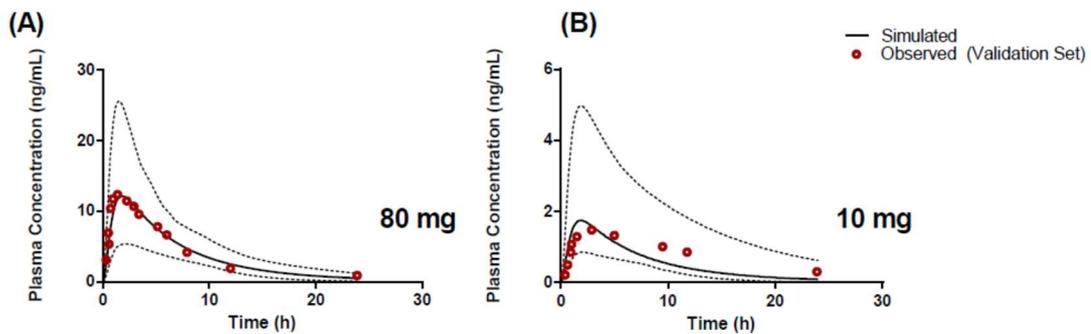
Figure 6.12 Simulated mean plasma profile after a: (a) 80 mg and (b) 10 mg oral dose of atorvastatin (solid black line). The corresponding observed data points are shown by red open circles. The grey lines represent the 5th and 95th percentiles for the predicted values. All simulations were performed using the minimal PBPK model.
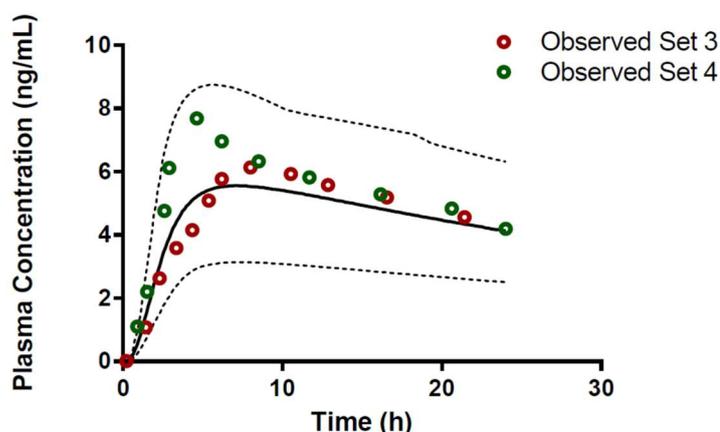
Figure 6.13 Simulated mean plasma profile after a 10 mg oral dose of amlodipine (solid black line). The corresponding observed data points are shown by red (set 3) or green (set 4) open circles. The grey lines represent the 5th and 95th percentiles for the predicted values. All simulations were performed using the minimal PBPK model.

Simulations to predict the *in vivo* performance of ODTs in healthy volunteers were used to compare the bioavailability between single and FDC formulations under fasted and fed conditions using dissolution data determined in section 6.3.3. For amlodipine the formulation state (single or combined) or dosing state (fasted or fed) had no statistically significant impact on pharmacokinetics (Figure 6.14 A and B). Amlodipine plasma concentrations reached a geometric mean C_{max} of 2.4-2.93 ng/ml in all conditions (Table 6.9), yielding a median AUC in the range of 53-60 ng/ml.h.

Fed state subjects exhibited a longer median t_{max} from 7.12 h to 8.12 h in single dose and 7.45 to 8.46 h in combination dose profiles. This increased t_{max} in fed subjects is likely a result of delayed gastric emptying and subsequent release of drug into the duodenum [428] and has been reported previously for amlodipine [429].

At the level of the small-intestine, predicted mean fraction dose absorbed (fa) for amlodipine correlated with dissolution profiles, showing significantly different (p<0.0001) values between single and combination formulations, 0.92 ± 0.05 and 0.95 ± 0.04 (fasted) and 0.91 ± 0.04 and 0.85 ± 0.05 (fed), respectively.

Atorvastatin plasma profiles similarly showed no statistically significant difference ($p > 0.05$) in pharmacokinetic parameters (Table 6.10) between single and combination doses in fasted subjects (Figure 6.14 C). Atorvastatin plasma concentration increased rapidly after dosing with a median t_{max} of 2.25 h in fasted and 2.56 h in fed states with a similar geometric mean C_{max} of 1.6-1.7 ng/ml and similar AUC (~16-17 ng/ml.h) for fasted states. However, under fed conditions there was a significant ($p < 0.05$) increase in C_{max} for both single (2.66 ng/ml) and combined (2.96 ng/ml) doses, with an associated increase in the AUC ($p < 0.0001$). Differences between single and combination doses in fed subjects were not statistically significant.

Table 6.9 Summary of pharmacokinetic parameters for amlodipine (5 mg) under fasted and fed conditions. Geometric mean (SD) reported for C_{max} and median (range) for AUC and t_{max}

Parameters	Amlodipine Fasted		Amlodipine Fed	
	Single	Combined	Single	Combined
AUC (ng/ml.h)	53.42 (32.12-75.69)	55.12 (30.12-74.11)	60.11 (42.75-81.94)	55.36 (35.69-78.91)
C_{max} (ng/ml)	2.45 (1.15)	2.57 (1.23)	2.87 (1.67)	2.89 (1.17)
t_{max} (h)	7.12 (5.92-8.21)	7.45 (5.21-9.72)	8.12 (6.96-9.54)	8.46 (7.95-9.87)

Table 6.10 Summary of pharmacokinetic parameters for atorvastatin (10 mg) under fasted and fed conditions. Geometric mean (SD) reported for C_{max} and median (range) for AUC and t_{max}

Parameters	Atorvastatin Fasted		Atorvastatin Fed	
	Single	Combined	Single	Combined
AUC (ng/ml.h)	16.24 (2.78-64.45)	17.15 (3.04-62.99)	25.77 (5.47-75.17)	29.46 (6.73-87.72)
C_{max} (ng/ml)	1.61 (1.27)	1.72 (1.31)	2.66 (1.80)	2.96 (1.97)
t_{max} (h)	2.25 (1.51-7.86)	2.28 (1.45-5.31)	2.56 (1.45-5.25)	2.71 (1.45-5.72)

Identical mean fraction dose absorbed (fa) between single and combination formulations were seen for atorvastatin under fasted state (0.91 ± 0.07). However, under fed conditions fa was lower (p<0.0001) for single compared to combination, at 0.81 ± 0.11 and 0.91 ± 0.09, respectively. It may be prudent to assume that the enhanced AUC and C_{max} for atorvastatin may be due to a positive food effect, given its BCS class II status and therefore lipophilic nature [430, 431]. However, the impact of fasted/fed status on the fa identified that the absorption across the gut lumen is delayed for both single and combination formulations (Figure 6.15 A). As the cumulative fraction dose absorbed is a reflection of events along the entire small-intestine lumen the impact of food may delay the absorption of atorvastatin into the intestinal enterocytes. However, when considering the mass of dosed atorvastatin within the stomach (10 mg) (Figure 6.15 B) significantly greater quantities of atorvastatin remain undissolved under fed conditions for a longer period of time.

When considered in the context of dissolution and taking the duodenum as an exemplar, the estimated dissolution rates within the duodenum under fasted states are significantly faster than that under fed state, which results in a significantly larger duodenal luminal C_{max} (17972 ng/ml) compared to the fed state (5002 ng/ml) (Figure 6.15 C, upper panels). This suggests that the differences between fasted and fed plasma concentrations are a result of changes in the dissolution process of the solid dosage form, otherwise uncaptured when considering the f_1 and f_2 tests, due to the dynamic and mechanistic nature of the ADAM-PBPK model.

As a result of this reduced dissolution under fed states, the absorption rate of atorvastatin in the duodenum is higher under fasted states with a maximal rate of 3.05 mg/h compared to 1.77 mg/h under fed states, both at 0.28 h (Figure 6.15 C, lower left panel). A consequence of this is a lower overall atorvastatin concentration within the enterocytes and potentially reduced gut metabolic clearance *ab orally* (Figure 6.15 C, lower right panel). Whilst the fa is relatively invariable *ab orally* for fasted or fed conditions (Figure 6.16 A), simulations confirmed a noticeable decrease in the fraction of drug metabolised within the enterocytes is observed under all fed conditions (Figure 6.16 B). Atorvastatin possesses a low oral bioavailability (F < 10%) and this is primarily a function of its high first pass metabolism. Under fed conditions this decrease in regional *ab oral* fraction of dose metabolised would result in an increased overall oral bioavailability ($F_{oral}=f_a x f_g x f_h$) and is therefore primary cause of the increased C_{max} observed under fed conditions for both single and combined formulations.

When considering the physical process of drug absorption, it is important to conceptualise the small-intestine and associated distribution of metabolic enzymes *ab orally*. With this in mind, CYP3A4 expression would be greatest duodenally and decrease longitudinally *ab orally* [432, 433]. As a result of this, the delayed absorption of drug across the gut wall (as a result of reduced dissolution) under fed states would result in a longer residency of solid (undissolved) drug in the proximal small intestine lumen, which would be susceptible to transit along the gut lumen until dissolution was complete, resulting in absorption of atorvastatin more distally.
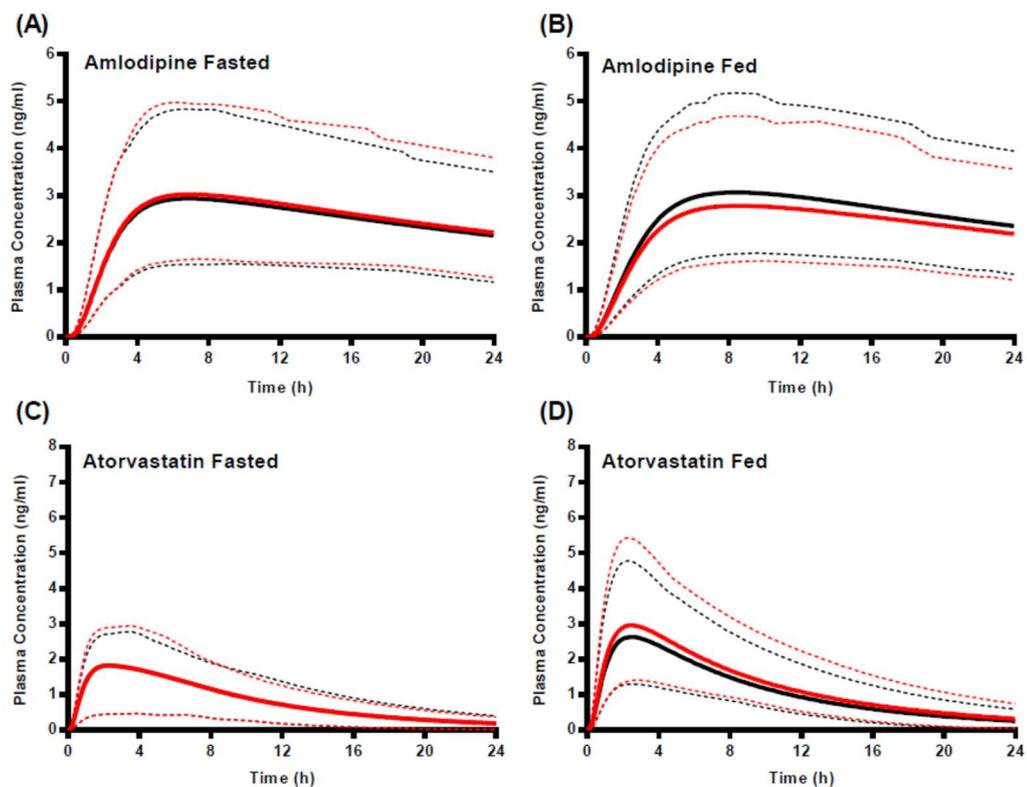
Figure 6.14 Simulated mean plasma profile after a 5 mg oral dose of amlodipine (A and B) and 10 mg oral dose of atorvastatin (C and D) under fasted and fed conditions. Single API formulations indicated in black and fixed dose combinations in red. Solid lines represent trial mean and dashed lines represent the 5th and 95th percentiles for the predicted values. All simulations were performed using the minimal PBPK model.
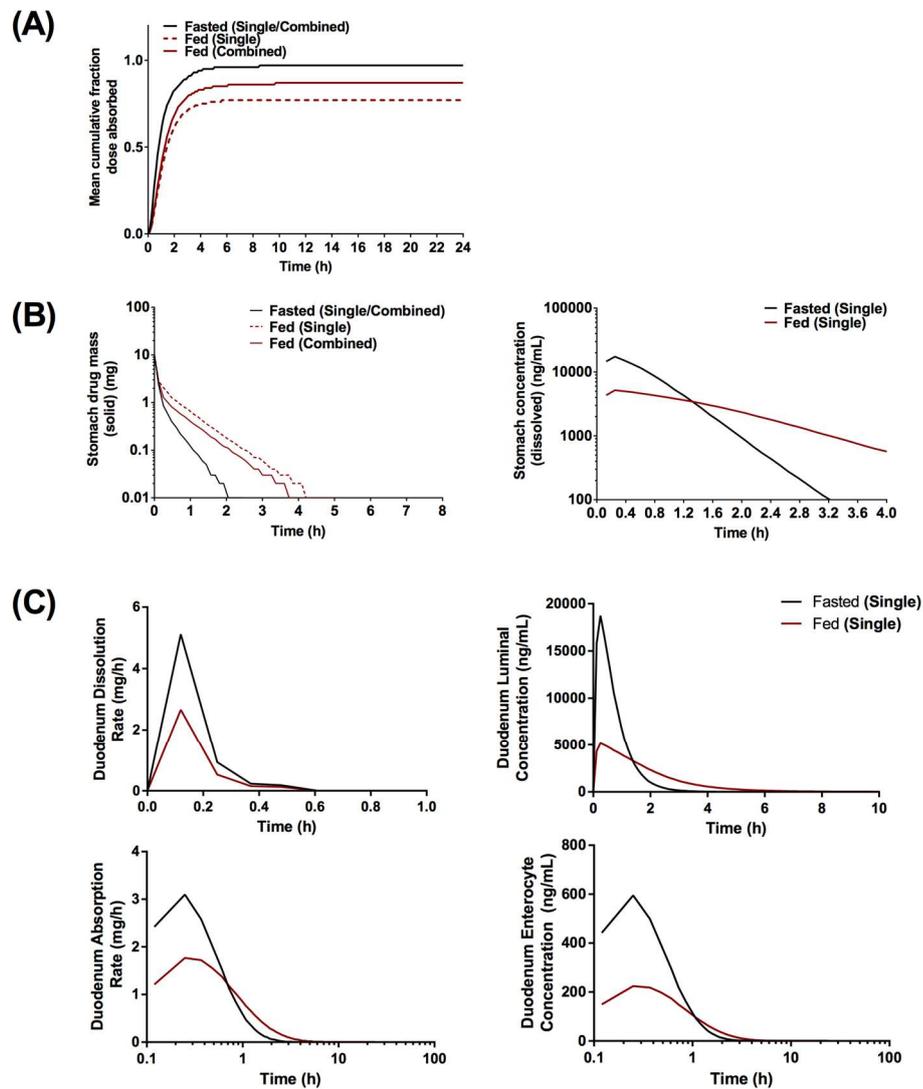
Figure 6.15 (A) Mean cumulative fraction dose absorbed; (B) Mean solid drug mass in the stomach (left panel) and mean dissolved stomach drug concentration (right panel); (C) duodenal dissolution rate (upper left panel), duodenal luminal concentration (upper right panel), duodenal absorption rate (lower left panel) and duodenal enterocyte concentration (lower right panel). Black solid line represents fasted (single/combined), red solid line represents fed (single) and red dashed line represents fed (combined) formulations.
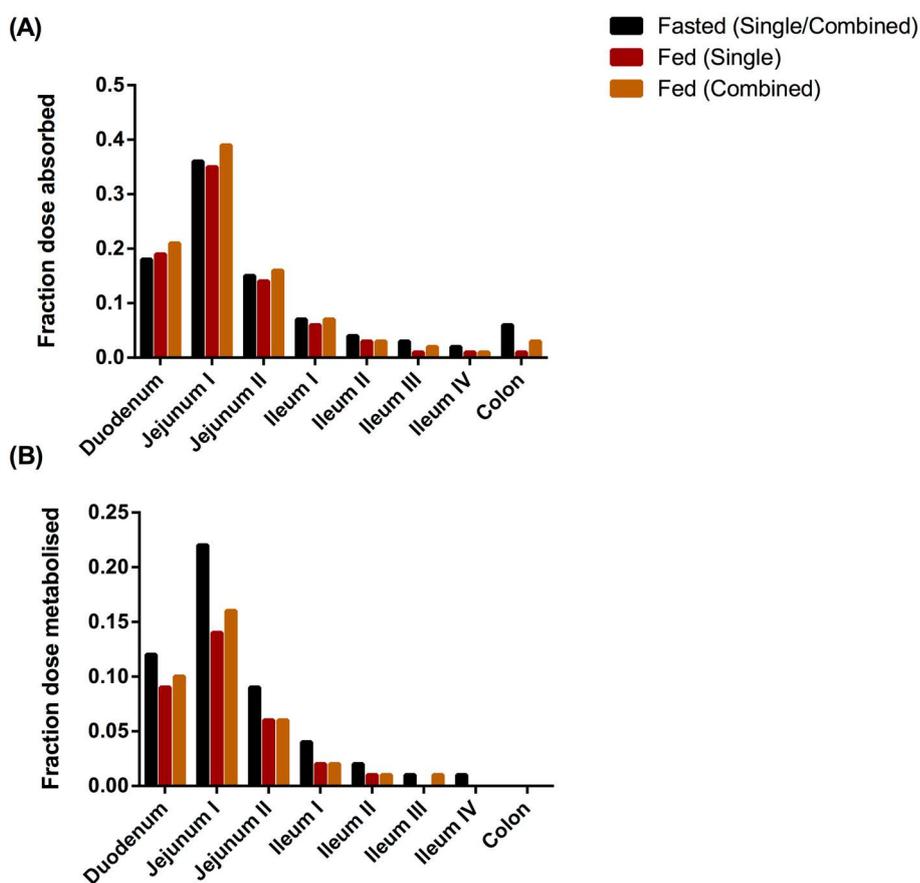
Figure 6.16 *Ab oral* regional distribution of (A) median fraction dose absorbed and (B) median fraction dose metabolised for atorvastatin. Black bars represent fasted (single/combined) formulations, red bars represent fed (single) formulations and orange bars represent fed (combined) formulations.

Atorvastatin is a BCS Class 2 compound where solubility/dissolution is the rate limiting step for absorption, coupled with often high metabolism. The oral bioavailability of atorvastatin is relatively low, indicating significant metabolic clearance [434]. Fed state often results in slower gastric emptying and the presence of food alters luminal composition through an increase in bile salts. Indeed, post-prandial changes can often contribute to an increased bioavailability of many class 2 compounds. A review by Gu *et al* [430] compared food effects on 92 sets of clinical data and demonstrated that 71% of BCS Class II compounds resulted in an enhancement of bioavailability following meals.

Although dissolution studies in FaSSIF and FeSSIF are useful, the mechanistic nature of the ADAM model, coupled with a detailed *ab oral* consideration of geometric, physiological and biochemical variations allows a greater understanding of the role of small-intestine physiology on the process of oral drug absorption; an understanding that would otherwise not be captured in *in vitro* dissolution studies or subsequent statistical analysis (i.e. f_1 and f_2 testing).

6.4 Conclusion

An ODT formulation was developed and characterised, demonstrating acceptable performance for hardness, friability and disintegration time and was subsequently used for formulation of low dose ODTs for amlodipine and atorvastatin, alone and in FDC. Clinical trial simulations using an ADAM-PBPK model were able to predict the *in vivo* pharmacokinetics of amlodipine and atorvastatin for comparison of the performance of FDCs against single dose formulations. *In vitro* dissolution data was incorporated to more accurately model the performance of the developed formulation and P_{app} values to model intestinal absorption.

Dissolution profiles showed no differences based on f_1 and f_2 testing between FDC and single dose formulations, with the exception of amlodipine in FeSSIF. All FDC formulations were shown to be bioequivalent based on clinical trial simulations in fasted and fed subjects (AUC, C_{max} and t_{max}), despite the failure of amlodipine in FeSSIF based on f_1 and f_2, adding incentive for the use of *in silico* simulation. Furthermore, the demonstration of bioequivalence through f_1 and f_2 and PBPK simulation for atorvastatin, a class II compound, adds weight to the argument for the applicability of class II inclusion in biowaiver applications, ideally in combination with PBPK modelling. Atorvastatin enjoyed a greater C_{max} and AUC in the fed state, due to an extended transit along the gut lumen as a result of poor dissolution. The attenuating expression of CYP3A4 distally along the gut meant that less atorvastatin was thus metabolised in the fed state. This food effect on the pharmacokinetic parameters for atorvastatin was not evident from *in vitro* investigation alone, further demonstrating the power and applicability of mechanistic PBPK modelling.

Chapter 7

Conclusions and Future Work

7.1 Conclusions

Oral delivery is the most widely utilised delivery route and owes its popularity to its non-invasiveness and general ease of administration. A host of different oral drug delivery systems have been developed, each with their own strengths and limitations, however the directly compressed tablet remains the most favoured. For the patient, directly compressed tablets benefit from good stability under storage, transportability and simplicity, whilst they are attractive for manufacturers due to the low costs and complexity involved in production. Despite their wide acceptance many consumers, particularly paediatrics, suffer from dysphagia, a difficulty in swallowing, and are only able to swallow tablets with the aid of water. This difficulty results in problems with patient compliance and has driven the development of novel dosage forms such as ODTs, that eliminate the need for swallowing by disintegrating rapidly within the mouth.

ODTs offer all the benefits of conventional tablets and several more, such as their applicability to dysphagia sufferers, accessibility, good mouth-feel, no risk of choking or asphyxiation, rapid absorption and potential for improved bioavailability. For manufacturers, ODTs provide new business opportunities including product differentiation, promotion, patent extension and life cycle management. In addition to achieving good mouth feel and taste, the major challenge in formulation of a directly compressed ODT is balancing rapid disintegration whilst maintaining robust mechanical properties, thus avoiding the need for specialised packaging. Careful selection of functional excipients, processing techniques and process parameters make this possible. Achieving this means that high drug loading is often not feasible, particularly for APIs that show poor water solubility and poor compactability.

Polymeric film coating of tablets is widely embraced to impart tablets with desirable aesthetic and functional properties. Aqueous polymeric suspensions or solutions are increasingly favoured over organic solvent based, due to concerns over safety and escalating costs, although offer additional challenges such as the requirement for greater drying efficiency. Coating of ODTs has not been explored, and is unattractive due to the stresses that the coating process conveys on mechanically weak cores.

FDC formulations are recommended for management of disease states where a combination of APIs with synergistic or additive effects are included in a single formulation. Like ODTs, they also improve compliance by simplifying therapy and can result in improvements in efficacy. Paediatric populations are poorly provided for with safe and appropriate child friendly formulations, due to a historic lack of consideration for physiological and behavioural differences between adults and children and the ethical

issues regarding paediatric clinical trials. Paediatric formulation development is encouraged and incentivised by bodies such as the FDA and EMA, whilst the development of FDCs at paediatric relevant doses is recommended by the WHO. Currently, no FDC ODT combinations are available on the market.

The principal aim of this thesis is to investigate and engineer solutions to formulate ODTs for high dose drugs and study the applicability of ODTs for FDC formulations.

Flucloxacillin sodium was chosen as a model API that would present high dose challenges for an ODT. Initial work involved identifying excipients commonly used in and suitable for compressed ODTs. This involved formulation of a placebo ODT that was also used to investigate the impact of process parameters on key tablet properties. Increasing compaction force expectedly improved mechanical properties including tablet hardness and friability, whilst slowing disintegration. Indications of powder fragmentation under high compaction forces were attributed to fragmentation of crospovidone with subsequent Heckel analysis. Heckel analysis also signified fragmentation of mannitol at low compaction force, showing a very high out-of-die mean yield pressure, which resulted in unacceptable tablet friability. Optimisation of crospovidone concentration was also performed to enhance disintegration further.

Inclusion of flucloxacillin at 250 mg resulted in tablets with unacceptable properties and despite experimentation with different excipients, dose was lowered to 125 mg for further development. Different disintegrants and disintegrant combinations were also examined, although it was concluded that crospovidone alone was preferable. Blending alteration was shown to have an effect on resultant ODT properties, although any drop in disintegration was also met with a drop in tablet hardness and increased friability. The inclusion of MCC as a binder to overcome the major limitation of the formulation, namely poor mechanical properties, was successful and revealed that an MCC: mannitol ratio of 2:1 was optimal. Further development of the formulation is necessary to achieve the desired properties.

Aqueous polymeric film coating of ODTs to overcome high friability was investigated and was shown to reduce friability to an acceptable level. Increase in tablet hardness of film coated ODTs was also demonstrated. The high attrition of tablets during the fluidised bed coating process meant that coating was counterintuitive and led to the development of a novel stationary coating technique. Briefly, tablets were held stationary under vacuum on a perforated platform within the spray zone. Redirection of heated air from below the tablet bed over the tablet surface allowed for satisfactory film formation, where previously poor drying resulted in over-wetting and poor adhesion of the coating to the

tablet core. A post-coating curing step resulted in tablets that displayed hardness values as high as double that of uncoated cores. This novel technique was successfully applied as a proof of concept, although is not without its own limitations, primarily the requirement to manually invert the tablet during coating and issues over drying efficiency.

With a view to investigate and improve the coating process and address the difficulty in evaporation of water from aqueous coating solutions, optimisation of the size of droplets produced through atomisation was studied. A DOE approach was used where CPPs including atomisation pressure, coating solution concentration and solution flow rate were used to model the atomisation process. Optimisation revealed the process parameters required to produce droplets of a desired VMD within the range of 20-70 µm. This was used to investigate the effect of droplet size on film coat quality and characteristics. To visualise the coating on a micro-scale and evaluate its morphology, two non-invasive imaging techniques, CLSM and XµCT were employed. This was the first study of its kind to directly evaluate the impact droplet size had on film quality through imaging of the coat, providing both qualitative and quantitative information. Imaging showed that smaller droplets produced thinner, less porous coats that were more uniform and homogenous. Information on the atomisation process and droplet size optimisation gleamed from this study will aid in future development of stationary coating techniques, since smaller droplets evaporate more rapidly.

The applicability of ODTs for FDC formulations to provide a highly convenient dosage form in the interests of patient compliance, was investigated using model APIs for two disease states. Amlodipine and atorvastatin at low doses for the treatment of CVD and isoniazid and rifampicin at high drug loading for tuberculosis therapy were investigated, with all doses at paediatrically relevant levels. An ODT formulation showing acceptable tablet properties was developed, where the number of excipients was kept at a minimum in the interests of complexity. Dissolution of API from single and combination doses was tested in biorelevant media to mimic *in vivo* performance as closely as possible. FDA recommended bioequivalence testing was used to compare dissolution profiles, to examine whether API combination resulted in altered dissolution. No differences were seen between single and FDC formulation, with the exception of rifampicin release in FeSSIF. To examine bioequivalence in much greater detail, PBPK modelling was used to simulate healthy adult clinical trials *in silico*. Modelling included dissolution and Caco-2 permeability data. Prediction of *in vivo* pharmacokinetics showed no differences in bioavailability between single and combination doses, highlighting the shortcomings of dissolution profile comparison in the case of rifampicin. Although no differences were

reported between single and combination, a positive food effect was shown for atorvastatin, with greater oral bioavailability as a result of reduced CYP3A4 metabolism within enterocytes.

7.2 Future Work

Flucloxacillin ODT development showed promise in achieving acceptable properties and holds substantial scope for future development. The use of SSF as a lubricant with greater water solubility and different grades of crospovidone are such examples, that have been touched upon in preliminary work. The use of compaction forces below 1 ton should also be explored. The use of granulated flucloxacillin in future work should allow for this. Taste masking is another important area for future development and ultimately would prevent any successful formulation if this could not be achieved. Preliminary work into this involving dry coating of flucloxacillin with sweeteners and flavours, shows potentially tremendous promise and would also likely improve flow properties further.

Development of the novel stationary film coating technique could ultimately provide a means to successfully formulate high dose ODTs with poor compactability. Indeed, this technology would not need to be limited to ODTs. An overhaul in the technique design is necessary to overcome the predominant limitation, namely the need for manual inversion of tablets mid process. Further optimisation of drying is also required. This may in part be aided through reduction of droplet size, the means to which is possible due to the work involving DOE optimisation of the atomisation process.

Although PBPK modelling was able to predict bioavailability in adults, this was not demonstrated in children. Modelling in simulated paediatric populations would be the next step and may be achieved through the use of further *in silico* techniques and adjustment of CYP activity using published data for enzyme expression levels, for example.

References

1.   Food, U., *Drug Administration (2000) Guidance for industry. E11 clinical investigation of medicinal products in the pediatric population*. 2010.

2.   Drakulich, A., *European Requirements for Pediatric Formulations.* 2009.

3.   Zisowsky, J., A. Krause, and J. Dingemanse, *Drug development for pediatric populations: regulatory aspects.* Pharmaceutics, 2010. **2**(4): p. 364-388.

4.   Roberts, R., et al., *Pediatric drug labeling: Improving the safety and efficacy of pediatric therapies.* JAMA, 2003. **290**(7): p. 905-911.

5.   Congress, U., *Pediatric Research Equity Act of 2003.* Public law, 2003. **108**(155): p. 117.

6.   FDA, *Guidance for Industry Pediatric Study Plans: Content of and Process for Submitting Initial Pediatric Study Plans and Amended Pediatric Study Plans.* 2013.

7.   Temeck, J., *FDA and EMEA: Pediatric Regulatory Processes.—2009.* Available on http://www.fda.gov/downloads/AdvisoryCommittees/CommitteesMeetingMaterials/Drugs/OncologicDrugsAdvisoryCommittee/UCM197964.pdf.

8.   Breitkreutz, J., *European perspectives on pediatric formulations.* Clin Ther, 2008. **30**(11): p. 2146-54.

9.   Fabiano, V., C. Mameli, and G.V. Zuccotti, *Paediatric pharmacology: Remember the excipients.* Pharmacological Research, 2011. **63**(5): p. 362-365.

10.   Nahata, M.C., *Safety of "inert" additives or excipients in paediatric medicines.* Archives of Disease in Childhood-Fetal and Neonatal Edition, 2009. **94**(6): p. F392-F393.

11.   van Riet-Nales, D.A., et al., *The EMA quality guideline on the pharmaceutical development of medicines for paediatric use.* International journal of pharmaceutics, 2012. **435**(2): p. 132-134.

12.   Walsh, J., *Excipients for the Formulation of Medicines for Children.* European Industrial Pharmacy, 2012(13).

13.   Kearns, G.L., et al., *Developmental pharmacology—drug disposition, action, and therapy in infants and children.* New England Journal of Medicine, 2003. **349**(12): p. 1157-1167.

14.   Ivanovska, V., et al., *Pediatric drug formulations: a review of challenges and progress.* Pediatrics, 2014. **134**(2): p. 361-372.

15.   Nunn, T. and J. Williams, *Formulation of medicines for children.* British Journal of Clinical Pharmacology, 2005. **59**(6): p. 674-676.

16.   Matsui, D., *Current issues in pediatric medication adherence.* Pediatric Drugs, 2007. **9**(5): p. 283-288.

17.   Cram, A., et al., *Challenges of developing palatable oral paediatric formulations.* International journal of pharmaceutics, 2009. **365**(1): p. 1-3.

18.   Thomson, S.A., et al., *Minitablets: New Modality to Deliver Medicines to Preschool-Aged Children.* Pediatrics, 2009. **123**(2): p. e235-e238.

19. AlHusban, F.A., et al., *Recent patents and trends in orally disintegrating tablets.* Recent Pat Drug Deliv Formul, 2010. **4**(3): p. 178-97.

20. Stoltenberg, I., G. Winzenburg, and J. Breitkreutz, *Solid oral dosage forms for children-Formulations, excipients and acceptance issues.* J Appl Ther Res, 2011. **7**: p. 141-146.

21. Porter, S.C., *Novel drug delivery: Review of recent trends with oral solid dosage forms.* American Pharmaceutical Review, 2001. **4**: p. 28-36.

22. Ahmed, I.S. and M.H. Aboul-Einien, *In vitro and in vivo evaluation of a fast-disintegrating lyophilized dry emulsion tablet containing griseofulvin.* European Journal of Pharmaceutical Sciences, 2007. **32**(1): p. 58-68.

23. Seager, H., *Drug-delivery Products and the Zydis Fast-dissolving Dosage Form*.* Journal of Pharmacy and Pharmacology, 1998. **50**(4): p. 375-382.

24. Thakur, R.R. and M. Kashi, *An unlimited scope for novel formulations as orally disintegrating systems: Present and future prospects.* 2011.

25. Biradar, S., S. Bhagavati, and I. Kuppasad, *Fast dissolving drug delivery systems: a brief overview.* The internet journal of pharmacology, 2006. **4**(2): p. 26-30.

26. Pfister, W. and T. Ghosh, *Orally Disintegrating Tablets: Products, Technologies and Development issues.* Pharm Tech, 2005: p. 136-150.

27. Deshmukh, V., *A Mouth Dissolving Drug Delivery system.* Int. J. Pharmatech Research, 2012: p. 412-421.

28. Dutta, S. and P.K. De, *Formulation of fast disintegrating tablets.* Int J Drug Formulation & Research, 2011. **201**(2): p. 1.

29. Brown, D., *Orally disintegrating tablets-taste over speed.* Drug Del Tech, 2003. **3**(6): p. 58-61.

30. Liew, K., K. Peh, and Y. Tan, *Orally disintegrating dosage forms: breakthrough solution for non-compliance.* International Journal of Pharmacy and Pharmaceutical Sciences, 2013. **5**: p. 4-8.

31. Hirani, J.J., D.A. Rathod, and K.R. Vadalia, *Orally disintegrating tablets: A review.* Tropical Journal of Pharmaceutical Research, 2009. **8**(2).

32. Sudhir Bharawaj*, V.J.S.S.R.C.J. and J. Suman, *Orally Disintegrating Tablets: A Review.* Drug Invention Today, 2010. **2**(1): p. 81-88.

33. Velmurugan, S. and S. Vinushitha, *Oral disintegrating tablets: An overview.* Int. J. Chem. Pharm. Sci, 2010. **1**: p. 1-12.

34. Fu, Y., et al., *Orally fast disintegrating tablets: developments, technologies, taste-masking and clinical studies.* Critical Reviews™ in Therapeutic Drug Carrier Systems, 2004. **21**(6).

35. Dobetti, L., *Fast-melting tablets: Developments and technologies.* Pharm Technol Eur, 2000. **12**(9): p. 32-42.

36.   Wagh, M.A., et al., *Techniques used in orally disintegrating drug delivery system.* International journal of drug delivery, 2011. **2**(2).

37.   Shukla, D., et al., *Mouth dissolving tablets I: An overview of formulation technology.* Sci Pharm, 2009. **77**(2): p. 309-326.

38.   Kaur, T., et al., *Mouth dissolving tablets: a novel approach to drug delivery.* Int J Curr Pharm Res, 2011. **3**(1): p. 1-7.

39.   Goel, H., et al., *Orally disintegrating systems: innovations in formulation and technology.* Recent Pat Drug Deliv Formul, 2008. **2**(3): p. 258-74.

40.   Manivannan, R., *Oral disintegrating tablets: A future compaction.* Drug Invention Today, 2009. **1**(1).

41.   Pahwa, R., et al., *Orally disintegrating tablets-Friendly to pediatrics and geriatrics.* Archives of applied science research, 2010. **2**(2): p. 35-48.

42.   Bandari, S., et al., *Orodispersible tablets: An overview.* Asian journal of pharmaceutics, 2008. **2**(1): p. 2.

43.   Randale, S.A., et al., *Rapidly disintegrating tablets containing taste masked metoclopramide hydrochloride prepared by extrusion-precipitation method.* Chemical and Pharmaceutical Bulletin, 2010. **58**(4): p. 443-448.

44.   Badgujar, B. and A. Mundada, *The technologies used for developing orally disintegrating tablets: a review.* 2011.

45.   Tousey, M., *The granulation process 101. Basic technologies for tablet making. 2002*.

46.   Aulton, M., *Aulton's Pharmaceutics: The Design and Manufacture of Medicines* Third ed, ed. M. Aulton. 2007: Churchill Livingstone Elsevier.

47.   Patel, R., M. Patel, and A. Suthar, *Spray drying technology: an overview.* Indian Journal of Science and Technology, 2009. **2**(10): p. 44-47.

48.   Al-khattawi, A. and A.R. Mohammed, *Compressed orally disintegrating tablets: excipients evolution and formulation strategies.* Expert Opinion on Drug Delivery. **0**(0): p. 1-13.

49.   Gonnissen, Y., J.P. Remon, and C. Vervaet, *Development of directly compressible powders via co-spray drying.* Eur J Pharm Biopharm, 2007. **67**(1): p. 220-6.

50.   Nagar, P., et al., *Orally disintegrating tablets: formulation, preparation techniques and evaluation.* Journal of Applied Pharmaceutical Science, 2011. **1**(04): p. 35-45.

51.   Lagoviyer, Y., et al., *Means for creating a mass having structural integrity*. 2002, Google Patents.

52.   Jacob, S., et al., *Novel co-processed excipients of mannitol and microcrystalline cellulose for preparing fast dissolving tablets of glipizide.* Indian Journal of Pharmaceutical Sciences, 2007. **69**(5): p. 633.

53. Armstrong, N.A. and L.P. Palfrey, *The Effect of Machine Speed on the Consolidation of 4 Directly Compressible Tablet Diluents.* Journal of Pharmacy and Pharmacology, 1989. **41**(3): p. 149-151.

54. Bi, Y.X., et al., *Evaluation of Rapidly Disintegrating Tablets Prepared by a Direct Compression Method.* Drug Development and Industrial Pharmacy, 1999. **25**(5): p. 571-581.

55. Fukami, J., et al., *Development of fast disintegrating compressed tablets using amino acid as disintegration accelerator: evaluation of wetting and disintegration of tablet on the basis of surface free energy.* Chem Pharm Bull (Tokyo), 2005. **53**(12): p. 1536-9.

56. Shangraw, R., A. Mitrevej, and M. Shah, *A new era of tablet disintegrants.* Pharm Technol, 1980. **4**(10): p. 49-57.

57. Caramella, C., et al., *Disintegrants in Solid Dosage Forms.* Drug Development and Industrial Pharmacy, 1990. **16**(17): p. 2561-2577.

58. Malke, S., S. Shidhaye, and V. Kadam, *Formulation and evaluation of oxcarbazepine fast dissolve tablets.* Indian journal of Pharmaceutical sciences, 2007. **69**(2): p. 211.

59. Wehling, F., S. Schuehle, and N. Madamala, *Effervescent dosage form with microparticles*. 1993, Google Patents.

60. Parkash, V., et al., *Fast disintegrating tablets: Opportunity in drug delivery system.* J Adv Pharm Technol Res, 2011. **2**(4): p. 223-35.

61. Khankari, R.K., et al., *Rapidly dissolving robust dosage form*. 2000, Google Patents.

62. Cousin, G., E. Bruna, and E. Gendrot, *Rapidly disintegratable multiparticular tablet*. 1995, Google Patents.

63. Mizumoto, T., Y. Masuda, and M. Fukui, *Intrabuccally dissolving compressed moldings and production process thereof*. 1996, Google Patents.

64. Cole, G., et al., *Pharmaceutical coating technology.* 1995.

65. Parmar, K., et al., *An overview: Aqueous film coating technology on tablets.* International Journal of Pharmaceutical and Chemical Sciences, 2012. **1**(3): p. 994-1001.

66. Bharadia, P. and V.M. Pandya, *A Review on Aqueous Film Coating Technology.* Innovative Publication, 2014.

67. Basu, A., A. De, and S. Dey, *Techniques of Tablet Coating: Concepts and Advancements: A Comprehensive Review.* Research & Reviews: Journal of Pharmacy and Pharmaceutical Sciences, 2013. **2**(4).

68. Grodowska, K. and A. Parczewski, *Organic solvents in the pharmaceutical industry.* Acta Pol Pharm, 2010. **67**(1): p. 3-12.

69. Jimenez-Gonzalez, C., D.J.C. Constable, and C.S. Ponder, *Evaluating the "Greenness" of chemical processes and products in the pharmaceutical industry- a green metrics primer.* Chemical Society Reviews, 2012. **41**(4): p. 1485-1498.

70. Rane, S. and V. Kale, *Evaluation of modified Guar Gum as film coating material.* Int J of Chem Tech Res, 2009. **1**(2): p. 180-2.

71. Bechard, S., O. Quraishi, and E. Kwong, *Film coating: effect of titanium dioxide concentration and film thickness on the photostability of nifedipine.* International journal of pharmaceutics, 1992. **87**(1): p. 133-139.

72. Felton, L. and G. Timmins, *A nondestructive technique to determine the rate of oxygen permeation into solid dosage forms.* Pharmaceutical development and technology, 2006. **11**(1): p. 141-147.

73. Cerea, M., et al., *A novel powder coating process for attaining taste masking and moisture protective films applied to tablets.* International journal of pharmaceutics, 2004. **279**(1): p. 127-139.

74. Keraliya, R.A., et al., *Osmotic drug delivery system as a part of modified release dosage form.* ISRN pharmaceutics, 2012. **2012**.

75. Telenti, A., et al., *Detection of rifampicin-resistance mutations in Mycobacterium tuberculosis.* The Lancet, 1993. **341**(8846): p. 647-651.

76. Dumouchel, C., *On the experimental investigation on primary atomization of liquid streams.* Experiments in fluids, 2008. **45**(3): p. 371-422.

77. Fraser, R., N. Dombrowski, and J. Routley, *The atomization of a liquid sheet by an impinging air stream.* Chemical Engineering Science, 1963. **18**(6): p. 339-353.

78. Felton, L.A., *Mechanisms of polymeric film formation.* Int J Pharm, 2013.

79. Felton, L.A. and S.C. Porter, *An update on pharmaceutical film coating for drug delivery.* Expert opinion on drug delivery, 2013. **10**(4): p. 421-435.

80. Bauer, K.H., et al., *Coated pharmaceutical dosage forms.* Medpharm Scientific, Stuttgart, 1998: p. 63-119.

81. Donbrow, M., *Microcapsules and nanoparticles in medicine and pharmacy.* 1991: CRC press.

82. Florence, A.T. and D. Attwood, *Physicochemical Principles of Pharmacy: In Manufacture, Formulation and Clinical Use.* 2015: Pharmaceutical Press.

83. Toschkoff, G. and J.G. Khinast, *Mathematical modeling of the coating process.* International journal of pharmaceutics, 2013. **457**(2): p. 407-422.

84. Levina, M.C., Charles R., *The Effect of Core Design and Formulation on the Quality of Film Coated Tablets.* Pharmaceutical Technology Europe, 2005. **17**(4): p. 29-37.

85. Sauer, D., et al., *Dry powder coating of pharmaceuticals: a review.* International journal of pharmaceutics, 2013. **457**(2): p. 488-502.

86. Felton, L.A., *Characterization of coating systems.* AAPS PharmSciTech, 2007. **8**(4): p. 258-266.

87. Gaur, P.K., et al., *Film Coating Technology: Past, Present and Future.* Journal of Pharmaceutical Sciences and Pharmacology, 2014. **1**(1): p. 57-67.

88. Singh, R.K., et al., *Dry coating method using magnetically assisted impaction in a randomly turbulent fluidized bed.* KONA Powder and Particle Journal, 1997. **15**(0): p. 121-131.

89. Bhattacharjee, S., et al., *Solventless Coating for Tablet: A Technical Review.* 2016.

90. Singh, P., et al., *Estimation of coating time in the magnetically assisted impaction coating process.* Powder technology, 2001. **121**(2): p. 159-167.

91. Achanta, A., et al., *Development of hot melt coating methods.* Drug development and industrial pharmacy, 2008.

92. Jannin, V. and Y. Cuppok, *Hot-melt coating with lipid excipients.* International journal of pharmaceutics, 2013. **457**(2): p. 480-487.

93. Augsburger, L.L. and S.W. Hoag, *Pharmaceutical dosage forms-tablets*. 2016: CRC Press.

94. Meyer, R.J. and A.S. Hussain, *Awareness Topic: Mitigating the risks of ethanol induced dose dumping from oral sustained/controlled release dosage forms.* 2005.

95. Fadda, H.M., M.A. Mohamed, and A.W. Basit, *Impairment of the in vitro drug release behaviour of oral modified release preparations in the presence of alcohol.* International journal of pharmaceutics, 2008. **360**(1): p. 171-176.

96. Ho, L., et al., *Analysis of sustained-release tablet film coats using terahertz pulsed imaging.* Journal of Controlled release, 2007. **119**(3): p. 253-261.

97. Sadeghi, F., J.L. Ford, and A. Rajabi-Siahboomi, *The influence of drug type on the release profiles from Surelease-coated pellets.* International journal of pharmaceutics, 2003. **254**(2): p. 123-135.

98. Freire, C., et al., *Influence of the coating formulation on enzymatic digestibility and drug release from 5-aminosalicylic acid pellets coated with mixtures of high-amylose starch and Surelease intended for colon-specific drug delivery.* Drug Dev Ind Pharm, 2010. **36**(2): p. 161-72.

99. Ensslin, S., et al., *Modulating pH-independent release from coated pellets: effect of coating composition on solubilization processes and drug release.* European Journal of Pharmaceutics and Biopharmaceutics, 2009. **72**(1): p. 111-118.

100. Sadeghi, F., et al., *Study of drug release from pellets coated with Surelease containing hydroxypropylmethylcellulose.* Drug development and industrial pharmacy, 2001. **27**(5): p. 419-430.

101. Ramakrishna, N. and B. Mishra, *Plasticizer effect and comparative evaluation of cellulose acetate and ethylcellulose–HPMC combination coatings as*

semipermeable membranes for oral osmotic pumps of naproxen sodium. Drug development and industrial pharmacy, 2002. **28**(4): p. 403-412.

102. Fallingborg, J., *Intraluminal pH of the human gastrointestinal tract.* Danish medical bulletin, 1999. **46**(3): p. 183-196.

103. Uchegbu, I.F. and A.G. Schatzlein, *Polymers in drug delivery*. 2006: CRC Press.

104. Amighi, K. and A. Möes, *Influence of plasticizer concentration and storage conditions on the drug release rate from Eudragit® RS30D film-coated sustained-release theophylline pellets.* European journal of pharmaceutics and biopharmaceutics, 1996. **42**(1): p. 29-35.

105. Wu, T., et al., *Studies of the drug permeability and mechanical properties of free films prepared by cellulose acetate pseudolatex coating system.* Drug development and industrial pharmacy, 2000. **26**(1): p. 95-102.

106. Felton, L.A. and J.W. McGinity, *Influence of plasticizers on the adhesive properties of an acrylic resin copolymer to hydrophilic and hydrophobic tablet compacts.* International journal of pharmaceutics, 1997. **154**(2): p. 167-178.

107. Wu, C. and J.W. McGinity, *Influence of ibuprofen as a solid-state plasticizer in Eudragit® RS 30 D on the physicochemical properties of coated beads.* AAPS PharmSciTech, 2001. **2**(4): p. 35-43.

108. Fassihi, R., et al., *Potential use of magnesium stearate and talc as dissolution retardants in the development of controlled drug delivery systems.* Pharmazeutische Industrie, 1994. **56**(6): p. 579-583.

109. Nimkulrat, S., et al., *Influence of selected surfactants on the tackiness of acrylic polymer films.* International journal of pharmaceutics, 2004. **287**(1): p. 27-37.

110. Felton, L.A., T. Austin-Forbes, and T.A. Moore, *Influence of surfactants in aqueous-based polymeric dispersions on the thermomechanical and adhesive properties of acrylic films.* Drug development and industrial pharmacy, 2000. **26**(2): p. 205-210.

111. Felton, L.A. and J.W. McGinity, *Influence of insoluble excipients on film coating systems.* Drug development and industrial pharmacy, 2002. **28**(3): p. 225-243.

112. McGinity, J., *Aqueous polymeric coatings for pharmaceutical dosage forms*. 2008: Informa healthcare.

113. Shenfield, G.M., *Fixed combination drug therapy.* Drugs, 1982. **23**(6): p. 462-480.

114. Kararli TT, S.K., Bossart J, *Fixed-dose combination products—a review.* Drug Development and Delivery. **14**(2): p. 32-35.

115. Wofford, J.L., *History of fixed-dose combination therapy for hypertension.* Archives of internal medicine, 1997. **157**(9): p. 1044-1044.

116. Bangalore, S., et al., *Fixed-dose combinations improve medication compliance: a meta-analysis.* The American journal of medicine, 2007. **120**(8): p. 713-719.

117. Li, F., J. Lu, and X. Ma, *CPY3A4-mediated Lopinavir Bioactivation and its Inhibition by Ritonavir.* Drug Metabolism and Disposition, 2012. **40**(1): p. 18-24.

118. Kota, J., P.S. Ayalavajjala, and R. Sivasubramanian, *Development of Orally Administered Fixed Dose Combination (FDC) Products: Pharmacokinetic and Biopharmaceutical Considerations.* International journal of pharmaceutical sciences and research, 2015. **6**(8): p. 3161.

119. Hao, J., R. Rodriguez-Monguio, and E. Seoane-Vazquez, *Fixed-dose combination drug approvals, patents and market exclusivities compared to single active ingredient pharmaceuticals.* PloS one, 2015. **10**(10): p. e0140708.

120. Gadzhanova, S., J. Ilomäki, and E.E. Roughead, *Antihypertensive use before and after initiation of fixed-dose combination products in Australia: a retrospective study.* International journal of clinical pharmacy, 2013. **35**(4): p. 613-620.

121. Bain, K.T., et al., *Discontinuing Medications: A Novel Approach for Revising the Prescribing Stage of the Medication-Use Process.* Journal of the American Geriatrics Society, 2008. **56**(10): p. 1946-1952.

122. WHO, *Guidelines for registration of fixed-dose combination medicinal products. Annex 5*. 2005: World Health Organization.

123. WHO. *Fixed-dose combinations for HIV/AIDS, tuberculosis and malaria*. 2003. World Health Organization.

124. Hillgren, K.M., A. Kato, and R.T. Borchardt, *In vitro systems for studying intestinal drug absorption.* Medicinal research reviews, 1995. **15**(2): p. 83-109.

125. Lipinski, C.A., et al., *Experimental and computational approaches to estimate solubility and permeability in drug discovery and development settings.* Adv Drug Deliv Rev, 2001. **46**(1-3): p. 3-26.

126. Kubinyi, H., *Lipophilicity and biological acitivity. Drug transport and drug distribution in model systems and in biological systems.* Arzneimittel-Forschung, 1978. **29**(8): p. 1067-1080.

127. Nagar, S. and K. Korzekwa, *Commentary: nonspecific protein binding versus membrane partitioning: it is not just semantics.* Drug Metabolism and Disposition, 2012. **40**(9): p. 1649-1652.

128. Hogben, C.A.M., et al., *On the mechanism of intestinal absorption of drugs.* Journal of Pharmacology and Experimental Therapeutics, 1959. **125**(4): p. 275-282.

129. Ehrhardt, C. and K.-J. Kim, *Drug absorption studies: in situ, in vitro and in silico models*. 2007: Springer Science & Business Media.

130. Menard, S., N. Cerf-Bensussan, and M. Heyman, *Multiple facets of intestinal permeability and epithelial handling of dietary antigens.* Mucosal immunology, 2010. **3**(3): p. 247-259.

131. Boroujerdi, M., *Pharmacokinetics and Toxicokinetics*. 2015: CRC Press.

132. Bareford, L.M. and P.W. Swaan, *Endocytic mechanisms for targeted drug delivery.* Advanced drug delivery reviews, 2007. **59**(8): p. 748-758.

133.	Buckley, S.T., et al., *In vitro models to evaluate the permeability of poorly soluble drug entities: challenges and perspectives.* European Journal of Pharmaceutical Sciences, 2012. **45**(3): p. 235-250.

134.	Sun, H., et al., *The Caco-2 cell monolayer: usefulness and limitations.* Expert opinion on drug metabolism & toxicology, 2008. **4**(4): p. 395-411.

135.	Peng, Y., et al., *Applications of a 7-day Caco-2 cell model in drug discovery and development.* European Journal of Pharmaceutical Sciences, 2014. **56**: p. 120-130.

136.	Hunter, J., et al., *Functional expression of P-glycoprotein in apical membranes of human intestinal Caco-2 cells. Kinetics of vinblastine secretion and interaction with modulators.* Journal of Biological Chemistry, 1993. **268**(20): p. 14991-14997.

137.	Kessel, M. and F. Frank, *A better prescription for drug-development financing.* Nature biotechnology, 2007. **25**(8): p. 859-866.

138.	Badhan, R.K.S., *Physiologically Based Pharmacokinetic Modelling in Drug Delivery.* Computational Pharmaceutics: Application of Molecular Modeling in Drug Delivery, 2015: p. 263.

139.	Alavijeh, M. and A. Palmer, *The pivotal role of drug metabolism and pharmacokinetics in the discovery and development of new medicines.* IDrugs: the investigational drugs journal, 2004. **7**(8): p. 755-763.

140.	Rostami-Hodjegan, A., I. Tamai, and K.S. Pang, *Physiologically based pharmacokinetic (PBPK) modeling: it is here to stay!* Biopharmaceutics & drug disposition, 2012. **33**(2): p. 47-50.

141.	Aarons, L., *Physiologically based pharmacokinetic modelling: a sound mechanistic basis is needed.* British journal of clinical pharmacology, 2005. **60**(6): p. 581-583.

142.	Gabrielsson, J. and D. Weiner, *Pharmacokinetic and pharmacodynamic data analysis: concepts and applications*. Vol. 1. 2001: CRC Press.

143.	Teorell, T., *Kinetics of distribution of substances administered to the body, I: The extravascular modes of administration.* Archives internationales de pharmacodynamie et de therapie, 1937. **57**: p. 205-225.

144.	Bischoff, K., et al., *Methotrexate pharmacokinetics.* Journal of pharmaceutical sciences, 1971. **60**(8): p. 1128-1133.

145.	Huang, S.M. and M. Rowland, *The role of physiologically based pharmacokinetic modeling in regulatory review.* Clinical Pharmacology & Therapeutics, 2012. **91**(3): p. 542-549.

146.	Wu, B., *Use of physiologically based pharmacokinetic models to evaluate the impact of intestinal glucuronide hydrolysis on the pharmacokinetics of aglycone.* Journal of pharmaceutical sciences, 2012. **101**(3): p. 1281-1301.

147.	Lyons, M.A., et al., *A physiologically based pharmacokinetic model of rifampin in mice.* Antimicrobial agents and chemotherapy, 2013. **57**(4): p. 1763-1771.

148. Rowland, M., C. Peck, and G. Tucker, *Physiologically-based pharmacokinetics in drug development and regulatory science.* Annual review of pharmacology and toxicology, 2011. **51**: p. 45-73.

149. Sutherland, R., E. Croydon, and G. Rolinson, *Flucloxacillin, a new isoxazolyl penicillin, compared with oxacillin, cloxacillin, and dicloxacillin.* British medical journal, 1970. **4**(5733): p. 455.

150. Barza, M. and R.T. Scheife, *Drug therapy reviews: Antimicrobial spectrum, pharmacology and therapeutic use of antibiotics--part 4: aminoglycosides.* American Journal of Health-System Pharmacy, 1977. **34**(7): p. 723-737.

151. Mainardi, J.L., et al., *Evolution of peptidoglycan biosynthesis under the selective pressure of antibiotics in Gram-positive bacteria.* FEMS microbiology reviews, 2008. **32**(2): p. 386-408.

152. Lynn, B., *Recent work on parenteral penicillins.* Journal of Hospital Pharmacy, 2002. **29**: p. 183-94.

153. Committee, J.F. and R.P.S.o.G. Britain, *British national formulary (bnf)*. Vol. 64. 2012: Pharmaceutical Press.

154. Baguley, D., et al., *Prescribing for children–taste and palatability affect adherence to antibiotics: a review.* Archives of disease in childhood, 2012. **97**(3): p. 293-297.

155. Gohel, M.C. and P.D. Jogani, *A review of co-processed directly compressible excipients.* J Pharm Pharm Sci, 2005. **8**(1): p. 76-93.

156. Bolhuis, G.K., E.G. Rexwinkel, and K. Zuurman, *Polyols as filler-binders for disintegrating tablets prepared by direct compaction.* Drug Dev Ind Pharm, 2009. **35**(6): p. 671-7.

157. Yoshinari, T., et al., *The improved compaction properties of mannitol after a moisture-induced polymorphic transition.* International Journal of Pharmaceutics, 2003. **258**(1–2): p. 121-131.

158. Rowe, R.C., et al., *Handbook of pharmaceutical excipients*. Vol. 6. 2009: Pharmaceutical press London.

159. Ferrari, F., et al., *Investigation on bonding and disintegration properties of pharmaceutical materials.* International journal of pharmaceutics, 1996. **136**(1): p. 71-79.

160. Thoorens, G., et al., *Microcrystalline cellulose, a direct compression binder in a quality by design environment—A review.* International Journal of Pharmaceutics, 2014. **473**(1–2): p. 64-72.

161. Hwang, R.-c. and G.R. Peck, *A systematic evaluation of the compression and tablet characteristics of various types of microcrystalline cellulose.* Pharmaceutical technology, 2001. **25**(3): p. 112-132.

162. Saigal, N., et al., *Microcrystalline cellulose as a versatile excipient in drug research.* Journal of Young Pharmacists, 2009. **1**(1): p. 6.

163. Zhang, Y., Y. Law, and S. Chakrabarti, *Physical properties and compact analysis of commonly used direct compression binders.* aaps Pharmscitech, 2003. **4**(4): p. 489-499.

164. Picker-Freyer, K.M., *An insight into the process of tablet formation of microcrystalline cellulose.* Journal of Thermal Analysis and Calorimetry, 2007. **89**(3): p. 745-748.

165. Al-Khattawi, A., et al., *Evidence-based nanoscopic and molecular framework for excipient functionality in compressed orally disintegrating tablets.* PloS one, 2014. **9**(7): p. e101369.

166. Bagul, U.S., et al., *Current status of tablet disintegrants: A review.* Retrieved March, 2006. **5**: p. 2011.

167. Kumar, V., M. de la Luz Reus-Medina, and D. Yang, *Preparation, characterization, and tabletting properties of a new cellulose-based pharmaceutical aid.* International journal of pharmaceutics, 2002. **235**(1): p. 129-140.

168. Mohamed, M.B., et al., *Pharmaceutical applications of crospovidone: a review.*

169. Kornblum, S.S. and S.B. Stoopak, *A new tablet disintegrating agent: Cross-linked polyvinylpyrrolidone.* Journal of pharmaceutical sciences, 1973. **62**(1): p. 43-49.

170. Gordon, M.S. and Z.T. Chowhan, *Effect of tablet solubility and hygroscopicity on disintegrant efficiency in direct compression tablets in terms of dissolution.* J Pharm Sci, 1987. **76**(12): p. 907-9.

171. Rudnic, E., et al., *Studies of the utility of cross linked polyvinlpolypyrrolidine as a tablet disintegrant.* Drug development and industrial pharmacy, 1980. **6**(3): p. 291-309.

172. Maschke, A., et al. *Effect of Crospovidone Particle Size on Tablet Properties Prepared via Wet Granulation*. in *PBP World Meeting*. 2008. Barcelona, Spain.

173. Kumar, P. and R. Nirmala, *Fundamental Aspects of Superdisintegrants: A Concise Review.* Journal of Global Pharma Technology, 2012. **4**: p. 1-12.

174. Mangal, M., et al., *Superdisintegrants: An Updated Review.* Int. J. Pharm. Pharm. Sci. Research, 2012.

175. Pharmacopoeia, B. and B.P. Commission, *Vol. I, II, III.* IV and, 2012. **154**: p. 156.

176. Carr, R.L., *Evaluating flow properties of solids.* Chem. Eng, 1965. **72**(2): p. 163-168.

177. Hausner, H., *Friction conditions in a mass of metal powder*. 1967, Polytechnic Inst. of Brooklyn. Univ. of California, Los Angeles.

178. Sangekar, S.A., M. Sarli, and P.R. Sheth, *Effect of moisture on physical characteristics of tablets prepared from direct compression excipients.* J Pharm Sci, 1972. **61**(6): p. 939-44.

179. Rees, J.E. and P.J. Rue, *Time-dependent deformation of some direct compression excipients.* J Pharm Pharmacol, 1978. **30**(10): p. 601-7.

180. Odeku, O.A. and O.A. Itiola, *Evaluation of Khaya Gum as a Binder in a Paracetamol Tablet Formulation.* Pharmacy and Pharmacology Communications, 1998. **4**(4): p. 183-188.

181. Research, F.C.f.D.E.a., *Guidance for industry: orally disintegrating tablets.* 2008.

182. Chandrasekhar, R., et al., *The role of formulation excipients in the development of lyophilised fast-disintegrating tablets.* European Journal of Pharmaceutics and Biopharmaceutics, 2009. **72**(1): p. 119-129.

183. Nelson, D., R. Wu, and K. Wymbs, *Effects of Magnesium Stearate on Tablet Properties.*

184. Sun, C. and D.J. Grant, *Compaction properties of L-lysine salts.* Pharm Res, 2001. **18**(3): p. 281-6.

185. Elshaer, A., P. Hanson, and A.R. Mohammed, *A systematic and mechanistic evaluation of aspartic acid as filler for directly compressed tablets containing trimethoprim and trimethoprim aspartate.* Eur J Pharm Biopharm, 2012.

186. Jain, S., *Mechanical properties of powders for compaction and tableting: an overview.* Pharmaceutical Science & Technology Today, 1999. **2**(1): p. 20-31.

187. Fichtner, F., et al., *Effect of preparation method on compactability of paracetamol granules and agglomerates.* International Journal of Pharmaceutics, 2007. **336**(1): p. 148-158.

188. Rasenack, N. and B.W. Müller, *Crystal habit and tableting behavior.* International Journal of Pharmaceutics, 2002. **244**(1–2): p. 45-57.

189. Riippi, M., et al., *The effect of compression force on surface structure, crushing strength, friability and disintegration time of erythromycin acistrate tablets.* European Journal of Pharmaceutics and Biopharmaceutics, 1998. **46**(3): p. 339-345.

190. Sun, C. and D.J. Grant, *Influence of elastic deformation of particles on Heckel analysis.* Pharmaceutical development and technology, 2001. **6**(2): p. 193-200.

191. Mattsson, S., *Pharmaceutical binders and their function in directly compressed tablets.* 2000.

192. Brater, C., *The United States Pharmacopoeia (USP 29)/National Formulary (NF 24).* The United States Pharmacopeial Convention, Rockville, USA, 2006.

193. Okuda, Y., et al., *A new formulation for orally disintegrating tablets using a suspension spray-coating method.* International Journal of Pharmaceutics, 2009. **382**(1–2): p. 80-87.

194. Eriksson, M. and G. Alderborn, *The effect of particle fragmentation and deformation on the interparticulate bond formation process during powder compaction.* Pharmaceutical research, 1995. **12**(7): p. 1031-1039.

195. Westermarck, S., et al., *Pore structure and surface area of mannitol powder, granules and tablets determined with mercury porosimetry and nitrogen adsorption.* Eur J Pharm Biopharm, 1998. **46**(1): p. 61-8.

196.   Ho, R., et al., *Effect of milling on particle shape and surface energy heterogeneity of needle-shaped crystals.* Pharmaceutical research, 2012. **29**(10): p. 2806-2816.

197.   Koner, J.S., et al., *A holistic multi evidence approach to study the fragmentation behaviour of crystalline mannitol.* Scientific reports, 2015. **5**.

198.   Nakanishi, S., et al., *Evaluation of the physicochemical characteristics of crospovidone that influence solid dispersion preparation.* International Journal of Pharmaceutics, 2011. **413**(1–2): p. 119-125.

199.   Patil, S.L. and M.A. Shivnikar, *Formulations and Technology of Fast Disintegrating Tablets: A Review.* Journal of Pharmaceutical and Biomedical Sciences (JPBMS), 2011. **9**(09).

200.   Szakonyi, G. and R. Zelkó, *Water content determination of superdisintegrants by means of ATR-FTIR spectroscopy.* Journal of Pharmaceutical and Biomedical Analysis, 2012. **63**(0): p. 106-111.

201.   Schulz, M., B. Fussnegger, and R. Bodmeier, *Adsorption of carbamazepine onto crospovidone to prevent drug recrystallization.* International Journal of Pharmaceutics, 2010. **391**(1–2): p. 169-176.

202.   Lerk, C.F., G.K. Bolhuis, and A.H. de Boer, *Effect of microcrystalline cellulose on liquid penetration in and disintegration of directly compressed tablets.* J Pharm Sci, 1979. **68**(2): p. 205-11.

203.   Sun, C.C., *Setting the bar for powder flow properties in successful high speed tableting.* Powder Technology, 2010. **201**(1): p. 106-108.

204.   Alderborn, G. and C. Nystrom, *Pharmaceutical powder compaction technology.* 1996.

205.   Steckel, H. and N. Bolzen, *Alternative sugars as potential carriers for dry powder inhalations.* International journal of pharmaceutics, 2004. **270**(1): p. 297-306.

206.   Kavitha, P., et al., *Formulation and evaluation of flucloxacillin sodium dispersible tablets.* Int J Pharm, 2010. **1**(3): p. 41-44.

207.   Abdelbary, A., A.H. Elshafeey, and G. Zidan, *Comparative effects of different cellulosic-based directly compressed orodispersable tablets on oral bioavailability of famotidine.* Carbohydrate Polymers, 2009. **77**(4): p. 799-806.

208.   Gosai, A.R., S.B. Patil, and K.K. Sawant, *Formulation and Evaluation of Oro Dispersible Tablets of Ondansetron Hydrochloride by Direct Compression using Superdisintegrants.* International Journal of Pharmaceutical Sciences and Nanotechnology, 2008. **1**(1): p. 106-11.

209.   Patil, C. and S. Das, *Effect of various superdisintegrants on the drug release profile and disintegration time of Lamotrigine orally disintegrating tablets.* Afr J Pharm Pharmacol, 2011. **5**(1): p. 76-82.

210.   Swamy, P., et al., *Orodispersible tablets of meloxicam using disintegrant blends for improved efficacy.* Indian journal of pharmaceutical sciences, 2007. **69**(6): p. 836.

211. Rangole, U.S., P. Kawtikwar, and D. Sakarkar, *Formulation and in-vitro evaluation of rapidly disintegrating tablets using hydrochlorothiazide as a model drug.* Research journal of pharma and tech, 2008. **1**(4): p. 349-352.

212. Carter, J., *The role of disintegrants in solid oral dosage manufacturing.* Carter Pharmaceutical Consulting Inc, 2002. **6**.

213. Battu, S.K., et al., *Formulation and evaluation of rapidly disintegrating fenoverine tablets: effect of superdisintegrants.* Drug Dev Ind Pharm, 2007. **33**(11): p. 1225-32.

214. Jeong, S.H., et al., *Material properties for making fast dissolving tablets by a compression method.* Journal of Materials Chemistry, 2008. **18**(30): p. 3527-3535.

215. Bolhuis, G.K., K. Zuurman, and G.H.P. te Wierik, *Improvement of dissolution of poorly soluble drugs by solid deposition on a super disintegrant. II. The choice of super disintegrants and effect of granulation.* European Journal of Pharmaceutical Sciences, 1997. **5**(2): p. 63-69.

216. Setty, C.M., et al., *Development of fast dispersible aceclofenac tablets: effect of functionality of superdisintegrants.* Indian journal of pharmaceutical sciences, 2008. **70**(2): p. 180.

217. Late, S.G., Y.-Y. Yu, and A.K. Banga, *Effects of disintegration-promoting agent, lubricants and moisture treatment on optimized fast disintegrating tablets.* International Journal of Pharmaceutics, 2009. **365**(1–2): p. 4-11.

218. Ganderton, D., *The effect of distribution of magnesium stearate on the penetration of a tablet by water.* Journal of Pharmacy and Pharmacology, 1969. **21**(S1): p. 9S-18S.

219. Jones, D., *Pharmaceutics - Dosage Form and Design.* Pharmaceutical Press, 2008.

220. Qiu, Y., et al., *Developing solid oral dosage forms: pharmaceutical theory & practice*. 2009: Academic Press.

221. Stern, P.W., *Effects of film coatings on tablet hardness.* J Pharm Sci, 1976. **65**(9): p. 1291-5.

222. Fell, J., R. Rowe, and J. Newton, *The mechanical strength of film-coated tablets.* Journal of Pharmacy and Pharmacology, 1979. **31**(1): p. 69-72.

223. Kolter, K., *Kollicoat IR®—innovation in instant release film coating.* BASF ExAct, 2002. **8**: p. 4-5.

224. Siepmann, F., et al., *How to adjust desired drug release patterns from ethylcellulose-coated dosage forms.* Journal of Controlled Release, 2007. **119**(2): p. 182-189.

225. Wilson, K.E. and E. Crossman, *The influence of tablet shape and pan speed on intra-tablet film coating uniformity.* Drug Development and Industrial Pharmacy, 1997. **23**(12): p. 1239-1243.

226. Ketterhagen, W.R., *Modeling the motion and orientation of various pharmaceutical tablet shapes in a film coating pan using DEM.* International journal of pharmaceutics, 2011. **409**(1): p. 137-149.

227. Robinson, R.L., et al., *Soft, convex shaped chewable tablets having reduced friability.* 2001, Google Patents.

228. Rosen, M.J. and J.T. Kunjappu, *Surfactants and interfacial phenomena.* 2012: John Wiley & Sons.

229. Rai, P.R., A. Tiwary, and V. Rana, *Superior disintegrating properties of calcium cross-linked Cassia fistula gum derivatives for fast dissolving tablets.* Carbohydrate Polymers, 2012. **87**(2): p. 1098-1104.

230. Heng, P.W., L.S. Wan, and T.S. Ang, *Role of surfactant on drug release from tablets.* Drug Development and Industrial Pharmacy, 1990. **16**(6): p. 951-962.

231. Felton, L.A. and J.W. McGinity, *Adhesion of polymeric films to pharmaceutical solids.* European Journal of Pharmaceutics and Biopharmaceutics, 1999. **47**(1): p. 3-14.

232. Strickley, R.G., *Solubilizing excipients in oral and injectable formulations.* Pharmaceutical research, 2004. **21**(2): p. 201-230.

233. Griffin, W.C., *Classification of surface-active agents by "HLB".* J. Soc. Cosmet. Chem., 1949(1): p. 311–326.

234. Gordon, M., et al., *Osmotic and stimulant laxatives for the management of childhood constipation.* The Cochrane Library, 2016.

235. Leonard, T.W., et al., *Promoting absorption of drugs in humans using medium-chain fatty acid-based solid dosage forms: GIPET™.* Expert opinion on drug delivery, 2006. **3**(5): p. 685-692.

236. Lanigan, R. and T. Yamarik, *Final report on the safety assessment of PEG-6,-8, and-20 sorbitan beeswax.* International journal of toxicology, 2000. **20**: p. 27-38.

237. Fiume, Z., *Final report on the safety assessment of Lecithin and Hydrogenated Lecithin.* Int J Toxicol, 2001. **20 Suppl 1**: p. 21-45.

238. Rangel-Yagui, C.O., A. Pessoa Jr, and L.C. Tavares, *Micellar solubilization of drugs.* J Pharm Pharm Sci, 2005. **8**(2): p. 147-163.

239. Seedher, N. and M. Kanojia, *Micellar solubilization of some poorly soluble antidiabetic drugs: a technical note.* AAPS PharmSciTech, 2008. **9**(2): p. 431-436.

240. Mukerjee, P. and K.J. Mysels, *A Re-evaluation of the Spectral Change Method of Determining Critical Micelle Concentration1.* Journal of the American Chemical Society, 1955. **77**(11): p. 2937-2943.

241. Patist, A., et al., *On the measurement of critical micelle concentrations of pure and technical-grade nonionic surfactants.* Journal of Surfactants and Detergents, 2000. **3**(1): p. 53-58.

242. Limaye, S., et al., *An allergic reaction to erythropoietin secondary to polysorbate hypersensitivity.* Journal of allergy and clinical immunology, 2002. **110**(3): p. 530.

243. Rey, L. and J.C. May, *Freeze-drying/lyophilization of pharmaceutical and biological products*. 2010: CRC Press.

244. Ke, W.T., et al., *Physical characterizations of microemulsion systems using tocopheryl polyethylene glycol 1000 succinate (TPGS) as a surfactant for the oral delivery of protein drugs.* J Control Release, 2005. **102**(2): p. 489-507.

245. Mexal, J., et al., *Oxygen availability in polyethylene glycol solutions and its implications in plant-water relations.* Plant Physiology, 1975. **55**(1): p. 20-24.

246. Nema, N., N. Singh, and A. Pandey, *The Supramicellar Solutions of Polymeric Surfactant (PEG 400) for the Determination of Poorly Soluble Antifungal Drug.* Chemistry, 2010. **19**(2).

247. Roy, A., et al., *Effects of plasticizers and surfactants on the film forming properties of hydroxypropyl methylcellulose for the coating of diclofenac sodium tablets.* Saudi Pharmaceutical Journal, 2009. **17**(3): p. 233-241.

248. Leuenberger, H., *The compressibility and compactibility of powder systems.* International Journal of Pharmaceutics, 1982. **12**(1): p. 41-55.

249. Gentis, N.D. and G. Betz, *Compressibility of binary powder formulations: Investigation and evaluation with compaction equations.* Journal of pharmaceutical sciences, 2012. **101**(2): p. 777-793.

250. McLaughlin, R., S. Banbury, and K. Crowley, *Orally disintegrating tablets: the effect of recent FDA guidance on ODT technologies and applications.* 2009.

251. Ruotsalainen, M., et al., *A novel technique for imaging film coating defects in the film-core interface and surface of coated tablets.* European Journal of Pharmaceutics and Biopharmaceutics, 2003. **56**(3): p. 381-388.

252. Jhansi Rani, M., et al., *Formulation and Evaluation of Acetaminophen and Diphenhydramine HCl Rapid Release Gelcaps.* World Journal of Pharmacy and Pharmaceutical Sciences, 2016. **5**(7): p. 1534-1555.

253. Barot, B.S., et al., *Compactibility improvement of metformin hydrochloride by crystallization technique.* Advanced Powder Technology, 2012. **23**(6): p. 814-823.

254. Kumar, V., *Direct compression metformin hydrochloride tablets*. 2000, Google Patents.

255. Nokhodchi, A., O. Amire, and M. Jelvehgari, *Physico-mechanical and dissolution behaviours of ibuprofen crystals crystallized in the presence of various additives.* Daru: journal of Faculty of Pharmacy, Tehran University of Medical Sciences, 2010. **18**(2): p. 74.

256. Faruki, M.Z., E. Razzaque, and M.A. Bhuiyan, *Improvement of Solubility of badly water soluble drug (Ibuprofen) by using Surfactants and Carriers.* International Journal of Pharmaceutical Sciences and Research, 2013. **4**(4): p. 1569.

257. Cheng, C.-L., et al., *Biowaiver extension potential to BCS Class III high solubility-low permeability drugs: bridging evidence for metformin immediate-release tablet.* European Journal of Pharmaceutical Sciences, 2004. **22**(4): p. 297-304.

258. Park, J.H., et al., *An alternative to the USP disintegration test for orally disintegrating tablets.* Pharmaceutical Technology, 2008. **32**(8).

259. Hede, P.D., P. Bach, and A.D. Jensen, *Two-fluid spray atomisation and pneumatic nozzles for fluid bed coating/agglomeration purposes: A review.* Chemical Engineering Science, 2008. **63**(14): p. 3821-3842.

260. Mansour, A. and N. Chigier, *Disintegration of liquid sheets.* Physics of Fluids A: Fluid Dynamics (1989-1993), 1990. **2**(5): p. 706-719.

261. Rizkalla, A. and A. Lefebvre, *The influence of air and liquid properties on airblast atomization.* Journal of Fluids Engineering, 1975. **97**(3): p. 316-320.

262. Lewis, H., et al., *Atomization of liquids in high velocity gas streams.* Industrial & Engineering Chemistry, 1948. **40**(1): p. 67-74.

263. Kemp, I.C., et al., *Experimental study of spray drying and atomization with a two-fluid nozzle to produce inhalable particles.* Drying Technology, 2013. **31**(8): p. 930-941.

264. Thybo, P., et al., *Droplet size measurements for spray dryer scale-up.* Pharmaceutical development and technology, 2008. **13**(2): p. 93-104.

265. Rambali, B., L. Baert, and D.L. Massart, *Using experimental design to optimize the process parameters in fluidized bed granulation on a semi-full scale.* Int J Pharm, 2001. **220**(1-2): p. 149-60.

266. Prpich, A., et al., *Drug product modeling predictions for scale-up of tablet film coating—a quality by design approach.* Computers & chemical engineering, 2010. **34**(7): p. 1092-1097.

267. Roy, S., *Quality by design: A holistic concept of building quality in pharmaceuticals.* International Journal of Pharmaceutical and Biomedical Research, 2012. **3**(2): p. 100-108.

268. Aliseda, A., et al., *Atomization of viscous and non-newtonian liquids by a coaxial, high-speed gas jet. Experiments and droplet size modeling.* International Journal of Multiphase Flow, 2008. **34**(2): p. 161-175.

269. Sander, A. and T. Penović, *Droplet Size Distribution Obtained by Atomization with Two-Fluid Nozzles in a Spray Dryer.* Chemical Engineering & Technology, 2014. **37**(12): p. 2073-2084.

270. Schmidt, D.P., et al., *Pressure-swirl atomization in the near field*. 1999, SAE Technical Paper.

271. Jiang, D.-J., et al., *Modeling atomization of a round water jet by a high-speed annular air jet based on the self-similarity of droplet breakup.* Chemical Engineering Research and Design, 2012. **90**(2): p. 185-192.

272. Funada, T., D. Joseph, and S. Yamashita, *Stability of a liquid jet into incompressible gases and liquids.* International journal of multiphase flow, 2004. **30**(11): p. 1279-1310.

273. Marmottant, P. and E. Villermaux, *On spray formation.* Journal of fluid mechanics, 2004. **498**: p. 73-111.

274. Mansour, A. and N. Chigier, *Air-blast atomization of non-Newtonian liquids.* Journal of Non-Newtonian Fluid Mechanics, 1995. **58**(2): p. 161-194.

275. Lorck, C.A., et al., *Influence of process parameters on sustained-release theophylline pellets coated with aqueous polymer dispersions and organic solvent-based polymer solutions.* European journal of pharmaceutics and biopharmaceutics, 1997. **43**(2): p. 149-157.

276. Christensen, F.N. and P. Bertelsen, *Qualitative description of the Wurster-based fluid-bed coating process.* Drug development and industrial pharmacy, 1997. **23**(5): p. 451-463.

277. Lecomte, F., et al., *Polymer blends used for the coating of multiparticulates: comparison of aqueous and organic coating techniques.* Pharmaceutical research, 2004. **21**(5): p. 882-890.

278. Hemati, M., et al., *Fluidized bed coating and granulation: influence of process-related variables and physicochemical properties on the growth kinetics.* Powder Technology, 2003. **130**(1–3): p. 18-34.

279. Lasheras, J., E. Villermaux, and E. Hopfinger, *Break-up and atomization of a round water jet by a high-speed annular air jet.* Journal of Fluid Mechanics, 1998. **357**: p. 351-379.

280. Aulton, M.E. and A.M. Twitchell, *Solution properties and atomization in film coating.* Pharmaceutical Coating Technology. London, UK: Taylor & Francis, 1995: p. 65-117.

281. Saleh, K., R. Cherif, and M. Hemati, *An experimental study of fluidized-bed coating: influence of operating conditions on growth rate and mechanism.* Advanced Powder Technology, 1999. **10**(3): p. 255-277.

282. Gaunø, M.H., et al., *Evaluation of droplet size distributions using univariate and multivariate approaches.* Pharmaceutical development and technology, 2013. **18**(4): p. 926-934.

283. Lefebvre, A.H., *Airblast atomization.* Progress in Energy and Combustion Science, 1980. **6**(3): p. 233-261.

284. Aguilar, G., et al., *Theoretical and experimental analysis of droplet diameter, temperature, and evaporation rate evolution in cryogenic sprays.* International Journal of Heat and Mass Transfer, 2001. **44**(17): p. 3201-3211.

285. Ranz, W. and W. Marshall, *Evaporation from drops.* Chem. Eng. Prog, 1952. **48**(3): p. 141-146.

286. Wang, J., et al., *An evaluation of process parameters to improve coating efficiency of an active tablet film-coating process.* International Journal of Pharmaceutics, 2012. **427**(2): p. 163-169.

287. Pandey, P., D.S. Bindra, and L.A. Felton, *Influence of Process Parameters on Tablet Bed Microenvironmental Factors During Pan Coating.* AAPS PharmSciTech, 2014. **15**(2): p. 296-305.

288. Schmidt, P.C. and C.J. Rubensdörfer, *Evaluation of Ludipress as a "Multipurpose Excipeent" for Direct Compression: Part I: Powder Characteristics and Tableting Properties.* Drug development and industrial pharmacy, 1994. **20**(18): p. 2899-2925.

289. Missaghi, S. and R. Fassihi, *A novel approach in the assessment of polymeric film formation and film adhesion on different pharmaceutical solid substrates.* AAPS PharmSciTech, 2004. **5**(2): p. 32-39.

290. Depypere, F., et al., *Quantification of microparticle coating quality by confocal laser scanning microscopy (CLSM).* European Journal of Pharmaceutics and Biopharmaceutics, 2009. **73**(1): p. 179-186.

291. Ozeki, Y., et al., *Comparison of the compression characteristics between new one-step dry-coated tablets (OSDRC) and dry-coated tablets (DC).* International journal of pharmaceutics, 2003. **259**(1): p. 69-77.

292. Perfetti, G., et al., *X-ray micro tomography and image analysis as complementary methods for morphological characterization and coating thickness measurement of coated particles.* Advanced Powder Technology, 2010. **21**(6): p. 663-675.

293. Russe, I.-S., et al., *Validation of Terahertz Coating Thickness Measurements Using X-ray Microtomography.* Molecular Pharmaceutics, 2012. **9**(12): p. 3551-3559.

294. Suyari, M. and A. Lefebvre, *Drop-Size Measurements in Air-Assist Swirl Atomizer Sprays.* NASA-Levis Research Center, Cleveland, 1986.

295. Hildebrand, T. and P. Rüegsegger, *A new method for the model-independent assessment of thickness in three-dimensional images.* Journal of Microscopy, 1997. **185**(1): p. 67-75.

296. Beaulieu, L., A. Rutenberg, and J. Dahn, *Measuring thickness changes in thin films due to chemical reaction by monitoring the surface roughness with in situ atomic force microscopy.* Microscopy and Microanalysis, 2002. **8**(05): p. 422-428.

297. Péan, S., http://www.samuelpean.com/heatmap-histogram/.

298. Ginebra, M., et al., *Mechanical performance of acrylic bone cements containing different radiopacifying agents.* Biomaterials, 2002. **23**(8): p. 1873-1882.

299. Coomaraswamy, K.S., P.J. Lumley, and M.P. Hofmann, *Effect of bismuth oxide radioopacifier content on the material properties of an endodontic Portland cement–based (MTA-like) system.* Journal of Endodontics, 2007. **33**(3): p. 295-298.

300. Daniel, T.M., *The history of tuberculosis.* Respiratory medicine, 2006. **100**(11): p. 1862-1870.

301. WHO, *Global tuberculosis report*. 2015: World Health Organization.

302. Porth, C., *Alterations in respiratory function: respiratory tract infections, neoplasms, and childhood disorders.* Porth CM, Kunert MP. Pathophysiology: Concepts of Altered Health States. Philadelphia, PA: Lippincott Williams & Wilkins, 2002: p. 615-619.

303. Knechel, N.A., *Tuberculosis: pathophysiology, clinical features, and diagnosis.* Critical care nurse, 2009. **29**(2): p. 34-43.

304. Sharma, S. and A. Mohan, *Extrapulmonary tuberculosis.* Indian Journal of Medical Research, 2004. **120**(4): p. 316.

305. Jensen, P.A., et al., *Guidelines for preventing the transmission of Mycobacterium tuberculosis in health-care settings, 2005.* 2005: US Department of Health and Human Services, Public Health Service, Centers for Disease Control and Prevention.

306. Frieden, T.R., et al., *Tuberculosis.* The Lancet, 2003. **362**(9387): p. 887-899.

307. WHO, *Tuberculosis. Fact sheet N 104. Updated October 2015*. 2016: World Health Organization.

308. Sutherland, I., *The ten-year incidence of clinical tuberculosis following "conversion" in 2550 individuals aged 14 to 19 years.* TSRU Progress Report (KNCV, The Hague, Netherlands), 1968.

309. Maher, D., *The natural history of Mycobacterium tuberculosis infection in adults.* Tuberculosis: A comprehensive clinical reference, 2009: p. 129-132.

310. Dheda, K., C.E. Barry 3rd, and G. Maartens, *Tuberculosis.* The Lancet. **387**(10024): p. 1211-1226.

311. Li, Y.-j., M. Petrofsky, and L.E. Bermudez, *Mycobacterium tuberculosis uptake by recipient host macrophages is influenced by environmental conditions in the granuloma of the infectious individual and is associated with impaired production of interleukin-12 and tumor necrosis factor alpha.* Infection and immunity, 2002. **70**(11): p. 6223-6230.

312. Smith, I., *Mycobacterium tuberculosis pathogenesis and molecular determinants of virulence.* Clinical microbiology reviews, 2003. **16**(3): p. 463-496.

313. Feja, K. and L. Saiman, *Tuberculosis in children.* Clinics in chest medicine, 2005. **26**(2): p. 295-312.

314. Ward, H., et al., *Extent of pulmonary tuberculosis in patients diagnosed by active compared to passive case finding.* The International Journal of Tuberculosis and Lung Disease, 2004. **8**(5): p. 593-597.

315. Peto, H.M., et al., *Epidemiology of extrapulmonary tuberculosis in the United States, 1993–2006.* Clinical Infectious Diseases, 2009. **49**(9): p. 1350-1357.

316. Golden, M.P. and H.R. Vikram, *Extrapulmonary tuberculosis: an overview.* Am Fam Physician, 2005. **72**(9): p. 1761-8.

317. Lönnroth, K., et al., *Drivers of tuberculosis epidemics: the role of risk factors and social determinants.* Social science & medicine, 2009. **68**(12): p. 2240-2246.

318. Narasimhan, P., et al., *Risk factors for tuberculosis.* Pulmonary medicine, 2013. **2013**.

319. Corbett, E.L., et al., *The growing burden of tuberculosis: global trends and interactions with the HIV epidemic.* Archives of internal medicine, 2003. **163**(9): p. 1009-1021.

320. Lahey, T., et al., *Recurrent tuberculosis risk among HIV-infected adults in Tanzania with prior active tuberculosis.* Clinical infectious diseases, 2013. **56**(1): p. 151-158.

321. Cegielski, J. and D. McMurray, *The relationship between malnutrition and tuberculosis: evidence from studies in humans and experimental animals.* The international journal of tuberculosis and lung disease, 2004. **8**(3): p. 286-298.

322. Chandra, R.K. and S. Kumari, *Nutrition and immunity: an overview.* The Journal of nutrition, 1994. **124**(8 Suppl): p. 1433S-1435S.

323. Muniyandi, M., et al., *The prevalence of tuberculosis in different economic strata: a community survey from South India [Short Communication].* The International Journal of Tuberculosis and Lung Disease, 2007. **11**(9): p. 1042-1045.

324. Marais, B. and P. Donald, *The natural history of tuberculosis infection and disease in children.* 2009.

325. WHO, *19th WHO Model List of Essential Medicines*. 2015: World Health Organization.

326. WHO, *19th WHO Model List of Essential Medicines for Children*. 2015: World Health Organization.

327. WHO, *General notes on Biopharmaceutics Classification System (BCS)-based biowaiver applications*. Accessed November. Vol. 23. 2009: World Health Organization. 2009.

328. Colón-Useche, S., et al., *Investigating the discriminatory power of BCS-biowaiver in vitro methodology to detect bioavailability differences between immediate release products containing a class I drug.* Molecular pharmaceutics, 2015. **12**(9): p. 3167-3174.

329. Metcalfe, C., et al., *The tuberculosis prodrug isoniazid bound to activating peroxidases.* Journal of Biological Chemistry, 2008. **283**(10): p. 6193-6200.

330. Somoskovi, A., L.M. Parsons, and M. Salfinger, *The molecular basis of resistance to isoniazid, rifampin, and pyrazinamide in Mycobacterium tuberculosis.* Respiratory research, 2001. **2**(3): p. 1.

331. Timmins, G.S. and V. Deretic, *Mechanisms of action of isoniazid.* Molecular microbiology, 2006. **62**(5): p. 1220-1227.

332. Jena, L., et al., *Computational approach to understanding the mechanism of action of isoniazid, an anti-TB drug.* International journal of mycobacteriology, 2014. **3**(4): p. 276-282.

333. Becker, C., et al., *Biowaiver monographs for immediate release solid oral dosage forms: Rifampicin.* Journal of pharmaceutical sciences, 2009. **98**(7): p. 2252-2267.

334. WHO, *Biopharmaceutics Classification System (BCS)-based biowaiver applications: Anti-tuberculosis medicines. Accessed November 20, 2009*. 2009: World Health Organization.

335. Hartmann, G., et al., *The specific inhibition of the DNA-directed RNA synthesis by rifamycin.* Biochimica et Biophysica Acta (BBA)-Nucleic Acids and Protein Synthesis, 1967. **145**(3): p. 843-844.

336. Campbell, E.A., et al., *Structural mechanism for rifampicin inhibition of bacterial RNA polymerase.* Cell, 2001. **104**(6): p. 901-912.

337. Gohel, M.C. and K.G. Sarvaiya, *A novel solid dosage form of rifampicin and isoniazid with improved functionality.* AAPS PharmSciTech, 2007. **8**(3): p. E133-E139.

338. Sankar, R., N. Sharda, and S. Singh, *Behavior of decomposition of rifampicin in the presence of isoniazid in the pH range 1–3.* Drug development and industrial pharmacy, 2003. **29**(7): p. 733-738.

339. SINGH, S., et al., *Degradation of rifampicin, isoniazid and pyrazinamide from prepared mixtures and marketed single and combination products under acid conditions.* Pharmacy and Pharmacology Communications, 2000. **6**(11): p. 491-494.

340. WHO, *Treatment of tuberculosis: guidelines*. 2010: World Health Organization.

341. Gallardo, C.R., et al., *Fixed-dose combinations of drugs versus single-drug formulations for treating pulmonary tuberculosis.* The Cochrane Library, 2016.

342. WHO, *Guidance for national tuberculosis programmes on the management of tuberculosis in children*. 2014: World Health Organization.

343. Albanna, A.S., et al., *Fixed-dose combination antituberculosis therapy: a systematic review and meta-analysis.* European Respiratory Journal, 2013. **42**(3): p. 721-732.

344. Use, C.f.M.P.f.H. and C.f.M.P.f.H. Use, *Guideline on the investigation of bioequivalence.* European Medicines Agency (EMA), London, 2010.

345. Food and D. Administration, *Guidance for industry: bioavailability and bioequivalence studies submitted in NDAs or INDs–General Considerations.* Rockville, MD: Food and Drug Administration, 2014.

346. FDA, U., *Guidance for Industry: Dissolution testing of immediate-release solid oral dosage forms.* Food and Drug Administration, Center for Drug Evaluation and Research (CDER), 1997.

347. WHO, *Annex 7: Multisource (generic) pharmaceutical productsguidelines on registration requirements to establish interchangeability.* WHO technical report series, 2006(937).

348. Yang, S.-G., *Biowaiver extension potential and IVIVC for BCS Class II drugs by formulation design: Case study for cyclosporine self-microemulsifying formulation.* Archives of pharmacal research, 2010. **33**(11): p. 1835-1842.

349. Tubic-Grozdanis, M., M.B. Bolger, and P. Langguth, *Application of gastrointestinal simulation for extensions for biowaivers of highly permeable compounds.* The AAPS journal, 2008. **10**(1): p. 213-226.

350. Bois, F.Y., M. Jamei, and H.J. Clewell, *PBPK modelling of inter-individual variability in the pharmacokinetics of environmental chemicals.* Toxicology, 2010. **278**(3): p. 256-267.

351. Zhao, P., et al., *Applications of physiologically based pharmacokinetic (PBPK) modeling and simulation during regulatory review.* Clinical Pharmacology & Therapeutics, 2011. **89**(2): p. 259-267.

352. Kostewicz, E.S., et al., *PBPK models for the prediction of in vivo performance of oral dosage forms.* European Journal of Pharmaceutical Sciences, 2014. **57**: p. 300-321.

353. Jamei, M., et al., *Population-based mechanistic prediction of oral drug absorption.* The AAPS journal, 2009. **11**(2): p. 225-237.

354. Lukacova, V., W.S. Woltosz, and M.B. Bolger, *Prediction of modified release pharmacokinetics and pharmacodynamics from in vitro, immediate release, and intravenous data.* The AAPS journal, 2009. **11**(2): p. 323-334.

355. Kesisoglou, F. and A. Mitra, *Application of absorption modeling in rational design of drug product under quality-by-design paradigm.* The AAPS journal, 2015. **17**(5): p. 1224-1236.

356. Crison, J.R., et al., *Biowaiver approach for biopharmaceutics classification system class 3 compound metformin hydrochloride using in silico modeling.* Journal of pharmaceutical sciences, 2012. **101**(5): p. 1773-1782.

357. Mitra, A., F. Kesisoglou, and P. Dogterom, *Application of absorption modeling to predict bioequivalence outcome of two batches of etoricoxib tablets.* AAPS PharmSciTech, 2015. **16**(1): p. 76-84.

358. Ke, A., et al., *A PBPK Model to Predict Disposition of CYP3A-Metabolized Drugs in Pregnant Women: Verification and Discerning the Site of CYP3A Induction.* CPT: pharmacometrics & systems pharmacology, 2012. **1**(9): p. 1-10.

359. Party, W., *Reflection paper: formulations of choice for the paediatric population.* EMEA, London, 2006.

360. Singh, M., et al., *An overview on fast disintegrating sublingual tablets.* International Journal of Drug Delivery, 2012. **4**(4): p. 407.

361. Freedman, S.B., et al., *Oral ondansetron for gastroenteritis in a pediatric emergency department.* New England Journal of Medicine, 2006. **354**(16): p. 1698-1705.

362. Blonde, L. and Z.T. San Juan, *Fixed-dose combinations for treatment of type 2 diabetes mellitus.* Advances in therapy, 2012. **29**(1): p. 1-13.

363. Connor, J., *Effect of fixed-dose combination (FDC) medications on adherence and treatment outcomes*, in *Fixed-dose combinations for HIV/AIDS, tuberculosis and malaria*. 2003. p. 119.

364. Pan, F., M.E. Chernew, and A.M. Fendrick, *Impact of fixed-dose combination drugs on adherence to prescription medications.* Journal of general internal medicine, 2008. **23**(5): p. 611-614.

365. Conte, J.E., E. Lin, and E. Zurlinden, *Liquid chromatographic determination of rifampin in human plasma, bronchoalveolar lavage fluid, and alveolar cells.* Journal of chromatographic science, 2000. **38**(2): p. 72-76.

366. Guideline, I.H.T., *Validation of analytical procedures: text and methodology.* Q2 (R1), 2005. **1**.

367. Klancke, J., *Dissolution testing of orally disintegrating tablets.* Dissolution technologies, 2003. **10**(2): p. 6-9.

368. Ranaldi, G., K. Islam, and Y. Sambuy, *Epithelial cells in culture as a model for the intestinal transport of antimicrobial agents.* Antimicrobial agents and chemotherapy, 1992. **36**(7): p. 1374-1381.

369. A Nkabinde, L., et al., *Permeation of PLGA nanoparticles across different in vitro models.* Current drug delivery, 2012. **9**(6): p. 617-627.

370. Gonçalves, J.E., et al., *Effect of pH, mucin and bovine serum on rifampicin permeability through Caco-2 cells.* Biopharmaceutics & drug disposition, 2012. **33**(6): p. 316-323.

371. Howgate, E.M., et al., *Prediction of in vivo drug clearance from in vitro data. I: impact of inter-individual variability.* Xenobiotica, 2006. **36**(6): p. 473-97.

372. Jamei, M., et al., *Population-based mechanistic prediction of oral drug absorption.* Aaps j, 2009. **11**(2): p. 225-37.

373. Hao, L.H., et al., *Comparative bioavailability of rifampicin and isoniazid in fixed-dose combinations and single-drug formulations.* The International Journal of Tuberculosis and Lung Disease, 2014. **18**(12): p. 1505-1512.

374. Agrawal, S., et al., *Comparative bioavailability of rifampicin, isoniazid and pyrazinamide from a four drug fixed dose combination with separate formulations at the same dose levels.* International Journal of Pharmaceutics, 2004. **276**(1–2): p. 41-49.

375. Milán-Segovia, R.C., et al., *Relative bioavailability of isoniazid in a fixed-dose combination product in healthy Mexican subjects.* The International Journal of Tuberculosis and Lung Disease, 2014. **18**(1): p. 49-54.

376. Xu, J., et al., *Oral Bioavailability of Rifampicin, Isoniazid, Ethambutol, and Pyrazinamide in a 4-Drug Fixed-Dose Combination Compared With the Separate Formulations in Healthy Chinese Male Volunteers.* Clinical Therapeutics, 2013. **35**(2): p. 161-168.

377. Rohatgi, A., *WebPlotDigitizer 3.10.* See http://arohatgi. info/WebPlotDigitizer, 2016.

378. Food and D. Administration, *Guidance for industry: orally disintegrating tablets. 2008*.

379. Millili, G.P., R.J. Wigent, and J.B. Schwartz, *Differences in the mechanical strength of dried microcrystalline cellulose pellets are not due to significant changes in the degree of hydrogen bonding.* Pharmaceutical development and technology, 1996. **1**(3): p. 239-249.

380. Westermarck, S., et al., *Microcrystalline cellulose and its microstructure in pharmaceutical processing.* European journal of pharmaceutics and biopharmaceutics, 1999. **48**(3): p. 199-206.

381. Jivraj, M., L.G. Martini, and C.M. Thomson, *An overview of the different excipients useful for the direct compression of tablets.* Pharmaceutical Science & Technology Today, 2000. **3**(2): p. 58-63.

382. Doelker, E., *Comparative compaction properties of various microcrystalline cellulose types and generic products.* Drug development and industrial pharmacy, 1993. **19**(17-18): p. 2399-2471.

383. Lakshminarayana, S.B., et al., *Comprehensive physicochemical, pharmacokinetic and activity profiling of anti-TB agents.* Journal of Antimicrobial Chemotherapy, 2015. **70**(3): p. 857-867.

384. Loos, U., et al., *Pharmacokinetics of oral and intravenous rifampicin during chronic administration.* Klinische Wochenschrift, 1985. **63**(23): p. 1205-1211.

385. Mariappan, T. and S. Singh, *Positioning of rifampicin in the biopharmaceutics classification system (BCS).* Clinical Research and Regulatory Affairs, 2006. **23**(1): p. 1-10.

386. Mozaffarian, D., et al., *Heart Disease and Stroke Statistics—2015 Update: A Report From the American Heart Association.* Circulation, 2015. **131**(4): p. e29-e322.

387. Ivanovic, B. and M. Tadic, *Fixed Combination of Amlodipine/Atorvastatin From Mechanisms to Trials.* Journal of cardiovascular pharmacology and therapeutics, 2013. **18**(6): p. 544-549.

388. Curran, M.P., *Amlodipine/Atorvastatin.* Drugs, 2010. **70**(2): p. 191-213.

389. Kannel, W.B., *Risk stratification in hypertension: new insights from the Framingham Study.* Am J Hypertens, 2000. **13**(1 Pt 2): p. 3s-10s.

390. Johnson, M.L., et al., *Prevalence of comorbid hypertension and dyslipidemia and associated cardiovascular disease.* heart disease (CHD), 2004. **2**: p. 3.

391. Williams, B., et al., *The prevalence and management of patients with co-existing hypertension and hypercholesterolaemia in the UK.* 2004.

392. WHO, *WHO expert committee on specifications for pharmaceutical preparations. Fortieth report.* World Health Organization technical report series, 2006. **937**: p. 1.

393. McKeage, K. and M.A. Siddiqui, *Amlodipine/atorvastatin fixed-dose combination: a review of its use in the prevention of cardiovascular disease and in the treatment of hypertension and dyslipidemia.* Am J Cardiovasc Drugs, 2008. **8**(1): p. 51-67.

394. Murdoch, D. and R.C. Heel, *Amlodipine.* Drugs, 1991. **41**(3): p. 478-505.

395. Kass, R.S., J.P. Arena, and D. DiManno, *Block of heart calcium channels by amlodipine: influence of drug charge on blocking activity.* Journal of cardiovascular pharmacology, 1988. **12**: p. S45&hyhen.

396. Van Zwieten, P., *Amlodipine: an overview of its pharmacodynamic and pharmacokinetic properties.* Clinical cardiology, 1994. **17**(9 Suppl 3): p. III3-6.

397. Amidon, G.L., et al., *A theoretical basis for a biopharmaceutic drug classification: the correlation of in vitro drug product dissolution and in vivo bioavailability.* Pharmaceutical research, 1995. **12**(3): p. 413-420.

398. Lau, W.C., et al., *Atorvastatin reduces the ability of clopidogrel to inhibit platelet aggregation a new drug–drug interaction.* Circulation, 2003. **107**(1): p. 32-37.

399. Croom, K.F. and G.L. Plosker, *Atorvastatin.* Drugs, 2005. **65**(1): p. 137-152.

400. Malhotra, H.S. and K.L. Goa, *Atorvastatin.* Drugs, 2001. **61**(12): p. 1835-1881.

401. Devabhaktuni, M. and S. Bangalore, *Fixed combination of amlodipine and atorvastatin in cardiovascular risk management: patient perspectives.* Vasc Health Risk Manag, 2009. **5**(1): p. 377-87.

402. de Haan, W., et al., *Atorvastatin increases HDL cholesterol by reducing CETP expression in cholesterol-fed APOE*3-Leiden.CETP mice.* Atherosclerosis, 2008. **197**(1): p. 57-63.

403. Pettitt, D., et al. *The Impact of Concurrent Dyslipidemia and Diabetes on Hypertension Management and Goal Attainment.* in *Journal of General Internal Medicine.* 2003. Blackwell Publishing Inc 350 Main St, Malden, MA 02148 USA.

404. Insull, W., *The problem of compliance to cholesterol altering therapy.* Journal of internal medicine, 1997. **241**(4): p. 317-325.

405. Chapman, R.H., et al., *Predictors of adherence with antihypertensive and lipid-lowering therapy.* Archives of internal Medicine, 2005. **165**(10): p. 1147-1152.

406. Hobbs, F.R., et al., *Can combining different risk interventions into a single formulation contribute to improved cardiovascular disease risk reduction? Rationale and design for an international, open-label program to assess the effectiveness of a single pill (amlodipine/atorvastatin) to attain recommended target levels for blood pressure and lipids (The JEWEL Program).* International journal of cardiology, 2006. **110**(2): p. 242-250.

407. Flack, J.M., et al. *Improved attainment of blood pressure and cholesterol goals using single-pill amlodipine/atorvastatin in African Americans: the CAPABLE trial.* in *Mayo Clinic Proceedings.* 2008. Elsevier.

408. Preston, R.A., et al., *A Randomized, Placebo-Controlled Trial to Evaluate the Efficacy, Safety, and Pharmacodynamic Interaction of Coadministered Amlodipine and Atorvastatin in 1660 Patients With Concomitant Hypertension and Dyslipidemia: The Respond Trial.* The Journal of Clinical Pharmacology, 2007. **47**(12): p. 1555-1569.

409. Messerli, F.H., et al., *Efficacy and safety of coadministered amlodipine and atorvastatin in patients with hypertension and dyslipidemia: results of the AVALON trial.* The Journal of Clinical Hypertension, 2006. **8**(8): p. 571-583.

410. Chung, M., et al., *Bioavailability of amlodipine besylate/atorvastatin calcium combination tablet.* The Journal of Clinical Pharmacology, 2006. **46**(9): p. 1030-1037.

411. Glass, G., *Cardiovascular combinations.* Nat Rev Drug Discov, 2004. **3**(9): p. 731-732.

412. Patiño-Rodríguez, O., et al., *Absence of a significant pharmacokinetic interaction between atorvastatin and fenofibrate: a randomized, crossover, study of a fixed-dose formulation in healthy Mexican subjects.* Frontiers in Pharmacology, 2015. **6**(4).

413. Yang, Y., et al., *High-throughput salting-out-assisted liquid–liquid extraction for the simultaneous determination of atorvastatin, ortho-hydroxyatorvastatin, and para-hydroxyatorvastatin in human plasma using ultrafast liquid chromatography with tandem mass spectrometry.* Journal of Separation Science, 2015. **38**(6): p. 1026-1034.

414. Patiño-Rodríguez, O., et al., *Pharmacokinetic non-interaction analysis in a fixed-dose formulation in combination of atorvastatin and ezetimibe.* Frontiers in Pharmacology, 2014. **5**(261).

415. Zhou, Y., et al., *Development and validation of a liquid chromatography–tandem mass spectrometry method for simultaneous determination of amlodipine, atorvastatin and its metabolites ortho-hydroxy atorvastatin and para-hydroxy atorvastatin in human plasma and its application in a bioequivalence study.* Journal of Pharmaceutical and Biomedical Analysis, 2013. **83**: p. 101-107.

416. Noemi Santos-Caballero, L.M.B.-G., Jose Carlos Aguilar-Carrasco, Miriam del Carmen Carrasco-Portugal and Francisco Javier Flores-Murrieta,, *Evaluation of the Possible Pharmacokinetic Interaction Between Amlodipine, Losartan and Hydrochlorothiazide in Mexican Healthy Volunteers.* International Journal of Pharmacology, 2016(12): p. 101-107.

417. Lv, C.-M., et al., *Determination of Amlodipine in Human Plasma by LC-MS/MS and Its Bioequivalence Study in Healthy Chinese Subjects.* Pharmacology & Pharmacy, 2013. **Vol.04No.02**: p. 10.

418. Mascoli V, K.U., Bapuji AT, Wang R, Damle B, *Pharmacokinetics of a Novel Orodispersible Tablet of Amlodipine in Healthy Subjects.* Journal of Bioequivalence and Bioavailability, 2013(5): p. 76-79.

419. Zhou, D., et al., *Simulation and Prediction of the Drug-Drug Interaction Potential of Naloxegol by Physiologically Based Pharmacokinetic Modeling.* CPT: Pharmacometrics & Systems Pharmacology, 2016. **5**(5): p. 250-257.

420. Pharmacy, U.o.W.S.o. *Drug Interaction Database Program*. Available from: http://www.druginteractioninfo.org/.

421. Watanabe, T., et al., *Physiologically Based Pharmacokinetic Modeling to Predict Transporter-Mediated Clearance and Distribution of Pravastatin in Humans.* Journal of Pharmacology and Experimental Therapeutics, 2009. **328**(2): p. 652-662.

422. Gertz, M., et al., *Prediction of human intestinal first-pass metabolism of 25 CYP3A substrates from in vitro clearance and permeability data.* Drug Metab Dispos, 2010. **38**(7): p. 1147-58.

423. Park, J.E., et al., *Contribution of cytochrome P450 3A4 and 3A5 to the metabolism of atorvastatin.* Xenobiotica, 2008. **38**(9): p. 1240-51.

424. Raušl, D., et al., *Intestinal permeability and excretion into bile control the arrival of amlodipine into the systemic circulation after oral administration.* Journal of pharmacy and pharmacology, 2006. **58**(6): p. 827-836.

425. Wu, X., L.R. Whitfield, and B.H. Stewart, *Atorvastatin transport in the Caco-2 cell model: contributions of P-glycoprotein and the proton-monocarboxylic acid co-transporter.* Pharmaceutical research, 2000. **17**(2): p. 209-215.

426. Li, J., et al., *Use of transporter knockdown Caco-2 cells to investigate the in vitro efflux of statin drugs.* Drug Metabolism and Disposition, 2011. **39**(7): p. 1196-1202.

427. Hochman, J.H., et al., *Interactions of human P-glycoprotein with simvastatin, simvastatin acid, and atorvastatin.* Pharmaceutical research, 2004. **21**(9): p. 1686-1691.

428. Food and D. Administration, *Guidance for industry: food-effect bioavailability and fed bioequivalence studies.* Food and Drug Administration, Rockville, MD, 2002.

429. Lv, C., et al., *The Influence of Food on the Pharmacokinetics of Amlodipine and Losartan after Single-Dose of its Compound Tablets in Healthy Chinese Subjects.* Drug Res (Stuttg), 2014. **64**(05): p. 229-235.

430. Gu, C.-H., et al., *Predicting effect of food on extent of drug absorption based on physicochemical properties.* Pharmaceutical research, 2007. **24**(6): p. 1118-1130.

431. Lentz, K.A., *Current methods for predicting human food effect.* The AAPS journal, 2008. **10**(2): p. 282-288.

432. Paine, M.F., et al., *Characterization of interintestinal and intraintestinal variations in human CYP3A-dependent metabolism.* J Pharmacol Exp Ther, 1997. **283**(3): p. 1552-62.

433. Badhan, R., et al., *Methodology for development of a physiological model incorporating CYP3A and P-glycoprotein for the prediction of intestinal drug absorption.* Journal of pharmaceutical sciences, 2009. **98**(6): p. 2180-2197.

434. Lennernas, H., *Clinical pharmacokinetics of atorvastatin.* Clin Pharmacokinet, 2003. **42**(13): p. 1141-60.